Impact of TCS08 and TCS09 on the pathophysiology of *Streptococcus pneumoniae*

I n a u g u r a l d i s s e r t a t i o n

zur

Erlangung des akademischen Grades eines

Doktors der Naturwissenschaften (Dr. rer. nat.)

der

Mathematisch-Naturwissenschaftlichen Fakultät

der

Universität Greifswald

vorgelegt von

Stephanie Hirschmann

Greifswald, 31. Mai 2021

Dekan:	Herr Prof. Dr. Gerald Kerth
1. Gutachter:	Herr Prof. Dr. Sven Hammerschmidt
2. Gutachter:	Herr Prof. Dr. Jan Maarten van Dijl
Tag der Promotion:	21.09.2021

„Doch Forschung strebt und ringt, ermüdend nie,
Nach dem Gesetz, dem Grund, Warum und Wie.“

Johann Wolfgang von Goethe

CONTENTS

1. Zusammenfassung

Streptococcus pneumoniae kolonisiert in einem Teil der Bevölkerung asymptomatisch den Nasenrachenraum, kann aber auch als bakterieller Erreger mit hohem Virulenzpotential seine ökologische Nische verlassen und sich in Lunge und Blut ausbreiten. Dabei müssen sich Pneumokokken an sich wechselnde externe Umweltbedingungen, wie Nährstoffverfügbarkeit, Temperatur oder Sauerstoffgehalt, anpassen. Die Weiterleitung dieser Umgebungsparameter in das Zellinnere der Bakterien erfolgt über den Prozess der Signaltransduktion, welcher letztendlich in einer kontrollierten differentiellen Genexpression mündet. Die häufigste verwendete Strategie zur Signaltransduktion ist die Nutzung von Zwei-Komponenten-Regulationssystemen (TCS), bestehend aus einer membrangebundenen Histidinkinase als Sensor und einem zytoplasmatischen Regulatorprotein, dem sogenannten „response regulator“, der an die Promotorregion der Zielgene bindet und die Genexpression steuert.

Der Fokus dieser Arbeit liegt auf den Zwei-Komponenten-Regulationssystemen TCS08 und TCS09, deren regulatorische Funktion und Einfluss auf den Phänotyp und die Pathophysiologie von *S. pneumoniae* in zwei unterschiedlichen Serotypen (Serotyp 2: D39 und Serotyp 4: TIGR4) untersucht wurden. Dazu wurden Einzel- (Δ*rr08*/Δ*rr09* bzw. Δ*hk08*/Δ*hk09*) und Doppelmutanten (Δ*tcs08* bzw. Δ*tcs09*) mit Hilfe der Insertions-Deletions-Mutagenese konstruiert.

Zunächst konnte mittels RNA-Sequenzierung in einer vergleichenden Transkriptomanalyse zwischen *tcs09*-Mutanten und dem parentalen Wildtyp D39, insbesondere bei Abwesenheit der HK09, eine verstärkte Expression des *aga*-Operons, welches in Verbindung zum Galaktosemetabolismus steht, und eine verringerte Expression des Regulators AgaR beobachtet werden. Interessanterweise zeigten bekapselte und unbekapselte *hk09*-Mutanten in D39 signifikante Wachstumsdefekte, wenn Galaktose als Kohlenhydratquelle eingesetzt wurde. Mittels Elektronenmikroskopie wurden morphologische Veränderungen wie die erhöhte Anzahl an Membranvesikeln und Zellwanddegradation der unbekapselten *hk09*- und *tcs09*-Mutanten und eine erhöhte Kapselproduktion der bekapselten *hk09*- und *tcs09*-Mutanten in D39 aufgezeigt. Die bekapselten *hk09*- und *tcs09*-Mutanten sowie die bekapselte *rr09*-Mutante zeigten außerdem eine veränderte Koloniemorphologie. Dabei bildete die Mutante D39Δ*hk09* nur opaque Kolonien, während D39Δ*rr09* und D39Δ*tcs09* vermehrt transparente Kolonien bildeten. In einem Triton X-100 induzierten Autolysetest und in Gegenwart von oxidativem Stress konnte ein negativer Einfluss der morphologischen Veränderungen von D39Δ*cps*Δ*hk09* und D39Δ*cps*Δ*tcs09* auf deren Überlebensfähigkeit

gezeigt werden. Zusammenfassend wurde beobachtet, dass das TCS09 in *S. pneumoniae* D39 für dessen Fitness durch Regulation des Kohlenhydratstoffwechsels wichtig ist. Über weitere Regulationsmechanismen wird dabei indirekt die Zellwandintegrität und die Menge an Kapselpolysaccharid beeinflusst, was sich letztendlich auf die Stresstoleranz auswirkt.

In einer zweiten Studie wurde das Virulenzpotential von TCS09 im Pneumokokkenstamm TIGR4 untersucht. *In vitro* Wachstumsanalysen in einem Komplexmedium zeigten keinen Effekt der TCS09-Deletion auf die Fitness der Pneumokokken. Im Gegensatz dazu konnte unter Verwendung der Disaccharide Lactose und Saccharose als Kohlenstoffquellen im chemisch definierten Medium eine verlängerte Lag-Phase der *tcs09*-Mutanten beobachtet werden. Mittels Immunblots wurde die Abundanz wichtiger Virulenzfaktoren von *S. pneumoniae* untersucht. Lediglich für RrgB, dem Strukturprotein des Pilus Typ 1, konnte eine verminderte Proteinmenge in der *hk09*-Mutante festgestellt werden. Zur Untersuchung der bakteriellen Morphologie wurden Feldemissions-Rasterelektronenmikroskopie und Transmissionselektronenmikroskopie Aufnahmen erstellt. Diese morphologischen Analysen zeigten keinen Einfluss der TCS09-Deletion auf das Erscheinungsbild der Pneumokokken. Zellkulturbasierte Infektionsversuche offenbarten keine veränderte Anheftung der *tcs09*-Mutanten an Lungenepithelzellen. Dagegen konnte eine signifikant erhöhte Tötungsrate der Mutante TIGR4Δ*cps*Δ*tcs09* nach Aufnahme durch Makrophagen gezeigt werden. Abschließende experimentelle Maus-Infektionsmodelle der akuten Pneumonie und der systemischen Infektion zeigten keine verringerte Virulenz der *tcs09*-Mutanten. Eine *in vivo* Koinfektion mit dem biolumineszierenden Wildtyp und einer Mutante zur genaueren Analyse des Virulenzverhaltens der *tcs09*-Mutanten verdeutlichte eine signifikant geringere bakterielle Last von TIGR4*lux*Δ*hk09* und TIGR4*lux*Δ*tcs09* im Vergleich zum Wildtyp. Insbesondere in den Lungen, Blut und Gehirn war die Anzahl der Mutanten nach 48 h verringert. Zusammenfassend kann festgestellt werden, dass das TCS09 in TIGR4 eine wichtige Rolle bei der Verbreitung im Wirt durch Aufrechterhaltung der bakteriellen Fitness hat.

In der dritten Studie wurde der Einfluss des TCS08 auf die Genexpression sowie auf metabolische und pathophysiologische Prozesse analysiert. Mittels Microarray und qPCR wurde insbesondere eine differentielle Genexpression in der *hk08*-Mutante von TIGR4 festgestellt. Dabei zeigten sich eine verringerte Expression der Cellobiose spezifischen Phosphotransferasesysteme, sowie eine verstärkte Expression des *fab*-Operons, des *arc*-Operons und des *psa*-Operons. Diese Operons kodieren für Proteine, die in der Fettsäurebiosynthese, im Arginin-Katabolismus bzw. für die Manganaufnahme notwendig sind. Des Weiteren wurde eine verringerte Expression des Pilus Typ 1 in TIGR4Δ*cps*Δ*tcs08* und eine erhöhte Expression von PavB in TIGR4Δ*cps*Δ*hk08* entdeckt. Diese differentiellen

Expressionen wurden durch Immunblots und Oberflächenlokalisationsstudien bestätigt. Mittels einer *in silico* Analyse wurde in der Promoterregion von *pavB* ein SaeR-like Bindungsmotiv identifiziert. Der Einfluss des TCS08 auf die Virulenz von Pneumokokken wurde *in vivo* unter Verwendung des akuten Pneumonie- und Sepsismodells untersucht. Diese Modelle zeigten einen stammabhängigen Effekt der einzelnen TCS08 Mutationen zwischen D39 und TIGR4 Pneumokokken. Während der Verlust der HK08 oder des TCS08 in D39 zu einer Abschwächung der Virulenz im Pneumoniemodell führte, war in TIGR4 der Verlust der RR08 dafür verantwortlich. Dagegen förderte der Verlust der HK08 in TIGR4 eine erhöhte Virulenz im Pneumonie- und Sepsismodell. Insgesamt zeigen diese Daten, dass das TCS08 ebenfalls an der bakteriellen Fitness während der Wirtskolonisierung beteiligt ist.

2. Summary

Streptococcus pneumoniae colonizes asymptomatically the upper respiratory tract as a commensal, but has also a high virulence potential and can leave this ecological niche, thereby spreading to the lungs and blood. During this process, pneumococci must adapt to changing external environmental conditions and parameters such as nutrient availability, temperature, or oxygen levels. The transmission of these signals into the bacterial cell interior occurs via the process of signal transduction, which ultimately results in controlled differential gene expression. The most commonly strategy for signal transduction is the use of two-component regulatory systems (TCS), consisting of a membrane-bound histidine kinase as a sensor and a cytoplasmic response regulator that binds to the promoter region of its target genes and interferes with gene expression.

In this study the regulatory impact and influence of the TCS08 and TCS09 on the phenotype and pathophysiology of *S. pneumoniae* were investigated using two different serotypes (serotype 2: D39 and serotype 4: TIGR4). For all functional assays, single (Δ*rr08*/Δ*rr09* or Δ*hk08*/Δ*hk09*) and double (Δ*tcs08* or Δ*tcs09*) mutants that were constructed by insertion-deletion mutagenesis, were applied.

In the first study a comparative transcriptome analysis using RNA-sequencing was conducted with our *tcs09*-mutants and the parental wild-type D39. The data indicated upregulation of the *aga* operon, which is related to galactose metabolism, and downregulation of the regulator AgaR, particularly in the absence of HK09. Interestingly, encapsulated and nonencapsulated *hk09*-mutants in D39 showed significant growth defects when galactose was used as sole carbohydrate source. Electron microscopy revealed morphological changes such as an increased number of membrane vesicles and cell wall degradation for the nonencapsulated *hk09*- and *tcs09*-mutants of strain D39. An increased capsule production was indicated for the encapsulated *hk09*- and *tcs09*-mutants in D39. The latter two mutants as well as the encapsulated *rr09*-mutant also showed altered colony morphology. While D39Δ*hk09* formed only opaque colonies, the mutants D39Δ*rr09* and D39Δ*tcs09* showed increased numbers of transparent colonies. In a Triton X-100 induced autolysis assay and in the presence of oxidative stress, a negative effect of the morphological changes of D39Δ*cps*Δ*hk09* and D39Δ*cps*Δ*tcs09* on their survivability was demonstrated. In conclusion, we observed that TCS09 in *S. pneumoniae* D39 is important for its fitness through regulation of carbohydrate metabolism. This indirectly influences cell wall integrity and capsular polysaccharide amount via other regulatory mechanisms, which ultimately affects stress tolerance.

In a second study, we investigated the virulence potential of TCS09 in pneumococcal strain TIGR4. *In vitro* growth analyses in complex medium showed no effect after loss of function of TCS09 on pneumococcal fitness. In contrast, using the disaccharides lactose and sucrose in chemically defined medium, an extended lag phase of *tcs09*-mutants was monitored. To assess changes of virulence factor expression, immunoblots were applied to demonstrate the abundance of various essential virulence factors of *S. pneumoniae*. The results revealed a decreased amount for RrgB, which is the backbone pilus component of type 1 pili, in the *hk09*-mutant. Field emission scanning electron microscopy and transmission electron microscopy images were applied to study alterations of the bacterial cell shape. The illustrations by FESEM and TEM showed no effect of TCS09-deletion on pneumococcal cell morphology. Cell culture-based infection analyses revealed a similar adhesion capacity of the parental strain and isogenic mutants to lung epithelial cells. However, phagocytosis assays indicated a significantly increased killing rate of intracellular TIGR4Δ*cps*Δ*tcs09*, when compared to the isogenic parental strain. In experimental mouse infection models of acute pneumonia and systemic infection the *tcs09*-mutants were not attenuated. However, to decipher in more detail differences between the wild-type and *tcs09*-mutants, *in vivo* co-infection were performed, which highlighted a significantly lower bacterial load of TIGR4*lux*Δ*hk09* and TIGR4*lux*Δ*tcs09* especially in the lungs, blood, and brain after 48 h. In conclusion, the TCS09 in TIGR4 is necessary for maintaining metabolic fitness, which in turn contributes to dissemination in the host.

In the third study, the influence of TCS08 on gene expression and metabolic and pathophysiological processes of *S. pneumoniae* was analyzed. In particular, differential gene expression in the *hk08*-mutant of TIGR4 was detected using microarray and qPCR. The transcriptome analysis revealed a downregulation of cellobiose specific phosphotransferase systems as well as an upregulation of the *fab* operon, *arc* operon, and *psa* operon. These operons encode proteins involved in fatty acid biosynthesis, arginine catabolism, and manganese uptake, respectively. Furthermore, we measured a downregulation of pilus 1 genes in TIGR4Δ*cps*Δ*tcs08* and an increased expression of *pavB* in TIGR4Δ*cps*Δ*hk08*. These data were confirmed by immunoblotting and surface localization studies. Using *in silico* analysis, a SaeR-like binding motif was identified in the promoter region of *pavB*. Furthermore, the impact of TCS08 on pneumococcal virulence was investigated *in vivo* using the acute pneumonia and sepsis models. These models showed a strain-dependent effect of the single TCS08 component deletions between D39 and TIGR4 pneumococci. Whereas loss of HK08 or TCS08 in D39 attenuated the mutants in the pneumonia model, loss of RR08 in TIGR4 was responsible for a similar effect. In contrast, loss of HK08 in TIGR4 promoted

increased virulence in the pneumonia and sepsis model. Overall, these data indicate that TCS08 is involved as key player in bacterial fitness during host colonization.

3. Introduction

"It is time to close the book on infectious diseases and declare the war against pestilence won." (William H. Stewart, U.S. health official surgeon general 1967 or 1969) [1]. This statement clearly shows how much infectious diseases were underestimated in the middle of the last century. Rarely has a medical dogma been so quickly reduced to absurdity, considering that several hundred new infectious diseases have emerged or been discovered in the period from 1940 to 2021. The incidence of emerging infectious diseases has been increased since 1940 and reached its preliminary maximum in the 1980s [2] until the ongoing COVID-19 pandemic in December 2019 occurred. By far the most common are viral and bacterial infections, but fungal infections, infections caused by protozoa or worms also occur millions of times worldwide, whereas prion diseases are much rarer in humans. Some diseases are endemic only in certain regions e.g., tropical diseases usually occur only in warmer climates and some infectious diseases such as influenza accumulate seasonally. Major epidemics occur at intervals of years and decades like the black plague and when worldwide spread happens it might cause a pandemic. In 2016 lower respiratory infections caused about 2.3 million deaths worldwide, with *Streptococcus pneumoniae* (*S. pneumoniae*) being the leading cause [3].

3.1. Historical background and characteristics of the pathogen *Streptococcus pneumoniae*

The genus *Streptococcus* was first described in 1880 by Theodor Billroth. Only one year later, in 1881, *Streptococcus pneumoniae* was isolated from the saliva of rabbits and a child who died of rabies, cultivated and characterized as a separate species within the genus *Streptococcus* by the two scientists George Miller Sternberg and Louis Pasteur [4,5]. Later this bacterium was recognized as a major cause of pneumonia. First, the microorganism was termed "pneumococcus" and later in 1920 "*Diplococcus pneumoniae*" [6], before renamed in 1974 as *Streptococcus pneumoniae* because of its characteristic chain formation in liquid medium [7]. Taxonomically, together with the genera *Lactococcus* and *Lactovum*, they form the family *Streptococcaceae*, class *Bacilli*, phylum *Firmicutes* and belong to the order *Lactobacillales*. *S. pneumoniae* is a close relative to *Streptococcus mitis* as shown in a phylogenetic study [8]. In 1928 the physician Frederick Griffith discovered bacterial transformation in pneumococci after observing that capsule formation information is transferable between encapsulated and nonencapsulated pneumococci due to natural competence [9]. Later, in 1944, Avery, MacLeod and McCarty were able to clearly identify DNA as the transforming principle and element of the genetic material [10,11]. Pneumococci

are encapsulated, Gram-positive, ovoid to lanceolate shaped, α-hemolytic, facultative anaerobic, oxidase- and catalase-negative, sporeless and non-motile bacteria that morphologically belong to the group of diplococci meaning they are mainly found in pairs [12]. In α-hemolytic streptococci, a green area is formed around its colonies on blood agar plates due to incomplete degradation of the hemoglobin of erythrocytes in the medium. Fe^{2+} ions of the heme groups are oxidized to Fe^{3+} by secretion of hydrogen peroxide resulting in methemoglobin, which absorbs light in the green color spectrum [13]. Since 1919, this property of *S. pneumoniae* is used for diagnostic purposes.

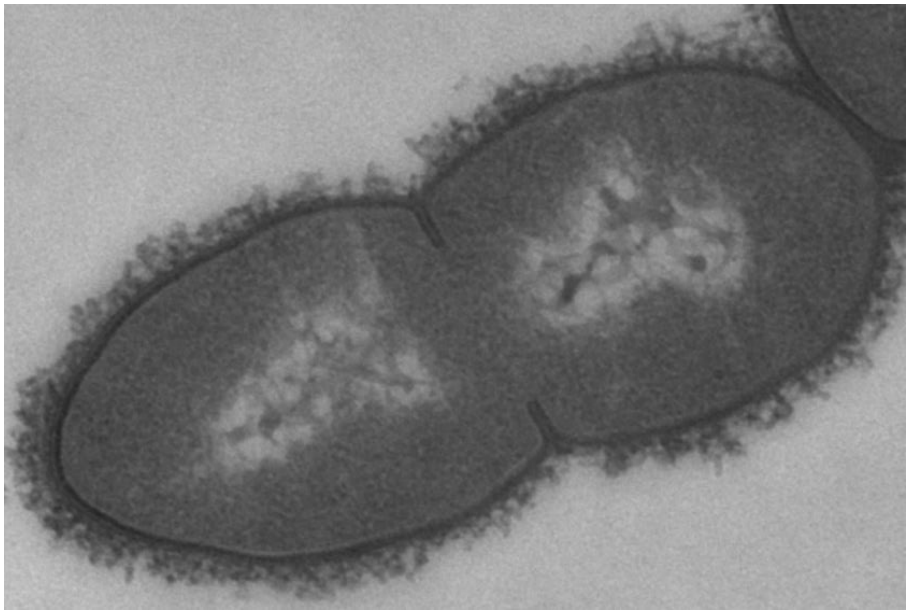

Figure 1: Transmission electron microscopy image of *S. pneumoniae* D39. Typically ovoid to lanceolate shaped pneumococcal cells found in pairs surrounded by capsule structures (own photo recording).

The natural competence allows pneumococci to take up foreign DNA from the environment, which permits their genome to be highly variable at approximately 2.0 - 2.2 Mbp depending on the strain [14,15]. This natural competence has also the disadvantage for the host, namely *S. pneumoniae* acquires antimicrobial resistance and virulence factor genes via horizontal gene transfer [16-19]. This high genomic variability is further supported by recombination and random mutation, with recombination frequency being 10-fold higher than mutation frequency [20]. In 2001, almost at the same time, the whole genome sequence of three *S. pneumoniae* strains, TIGR4 (serotype 4) [15], R6 (nonencapsulated derivative of D39, serotype 2) [14] and G54 (serotype 19F) [21], were published. Six years later, the D39 genome was sequenced and R6 was corrected in the same procedure [22]. Depending on the gene conservation the genome can be classified as core genome, supercore genome, flexible genome and/or the supragenome [16,18]. The supercore genome includes 303 genes and the core genome additional 461 genes [18], but between the individual strains and

serotypes, the genetic variance can be up to 10% [23]. Compared to other published genomes, there are many insertions, transposons and repetitive elements, which can account for up ~5% of the genome [15]. Pathogenicity islands, pseudogenes and regulators are present in different strains with different levels of conservation [24]. Thirteen regions of diversity (RDs) were identified in the genome, 8 of which contribute to virulence [25]. Furthermore, plasmids occur in small numbers in pneumococci and mostly they are very similar to pDP1, a 3 kb plasmid found in D39 [26]. Due to the high variability in chemical composition of capsular polysaccharides, 98 different serotypes with different potentials in disease, virulence, prevalence and drug resistance can currently be distinguished [27-30]. In contrast to the encapsulated strains (s-form; “smooth”) showing colonies with a slimy surface, the nonencapsulated phenotype (r-form; “rough”) having lackluster colonies, are in general avirulent (up to 10^7-fold less virulent than their encapsulated counterparts in the mouse infection model) [31,32].

3.2. Epidemiology, Infection route and Pathogenesis

According to statistics, pneumococci are one of the most common agents of community-acquired pneumonia (CAP) in adults [33]. The mortality rate of this disease still averages 10% to 30% depending on age despite decades of research and the development of improved vaccines and new antibiotics [34,35]. The constant mortality rate can be attributed to the increasing number of resistant or multidrug-resistant pneumococcal strains [36]. WHO estimates that 1.6 million people die annually from pneumococcal infections including the deaths of 826,000 children under the age of five; most of them living in developing countries [37]. Before PCV7 vaccine introduction in 2001, the incidence of invasive pneumococcal disease (IPD) in children younger than 2 years of age ranged ~ 44.4 per 100,000 per year in Europe [38]. A 69% decrease in IPD cases in children under 2 years, 32% in adults in the age between 20 – 39 years, 8% in adults of 40 – 64 years and 18% in adults older than 65 years was demonstrated after the introduction of PCV7 and the resulting herd immunity [39].

Typically, pneumococci are transmitted via aerosols and acquired via the nasopharynx [40-42]. Carriers and vectors of pneumococci are mainly children in the first six years of life (50%) depending on genetic background, socioeconomic status and geographical location with decreasing probability to 3% - 5% in adulthood [43,44]. This number increases again (0% - 39%) in adults aged 60 years and older and/or having a weaker immune system [45]. In exceptional cases, simultaneous colonization by up to three serotypes occurs, which are repeatedly replaced by new ones [46,47]. However, in most cases one isolate dominates and persists for weeks in the nasal and pharyngeal cavities of the healthy asymptomatic host. During co-colonization, horizontal gene transfer, which is promoted by natural competence in

pneumococci, occurs frequently with different strains exchanging DNA segments [47]. *S. pneumoniae* colonizes its natural habitat, the mucosa of the human upper respiratory tract (URT), the nasopharynx, as an asymptomatic commensal without clinical outcome [36,48]. However, pneumococci disturb the defense mechanism and thus contribute to a higher risk of infection, and may become pathogenic. Different factors are of great importance for the development and course of an invasive pneumococcal infection such as the serotype of the pathogen, the constitution of the host and so-called virulence factors [49]. At high risk are immunocompromised individuals (e.g., people living with HIV), young children in the first two years of life, elderly patients over 65 years of age and people after a previous viral infection [36,50]. Viral infections, for example by the influenza A virus, favor a subsequent infection with *S. pneumoniae* as the immune system is weakened and receptors for pneumococcal adherence are exposed. Such a secondary infection, often also referred to as superinfection, is the cause of an increased mortality rate after an influenza infection [51]. For further dissemination in the host and the spread to normally sterile areas, the pathogen must leave its biological niche. Different strategies play an important role in the establishment in the host and spread of *S. pneumoniae*:

1. Resistance of elimination by mucus and ciliary clearance, by lysis of respiratory epithelial cells [52,53].
2. Evasion of the immune system especially through lysis of immune cells [54], inhibition of opsonization by capsule expression [55] and IgA cleavage [56].
3. Successful adhesion to the mucosal host cell surface or receptors or the extracellular matrix (ECM; thrombospondin-1, fibronectin, vitronectin) via surface exposed pneumococcal adhesins [57-60].
4. Transcytosis through host cells [61] and gaining access to the blood or brain via crossing the blood-brain barrier [62]. Internalization of pneumococci occurs with an extremely low frequency, and if, this is mostly receptor-mediated [63] or integrin-determined [59] and associated with tight binding to host cells.

If pneumococci spread to sterile host compartments they cause diseases ranging from mild local infections such as otitis media and sinusitis, to severe diseases including pneumonia, septicemia, and meningitis [36,40,50]. In the blood stream, pneumococci can lodge in erythrocytes to avoid detection by neutrophils, contributing to bacterial spread and increased risk of severe diseases [64]. Pneumococci can grow planktonically as mono-, diplo- or polycocci, but also sessile in biofilms. Biofilm formation also appears to play an important role in colonization of the nasopharynx [65], with altered protein profiles between the two

growth types [66]. However, the exact reasons why colonization leads to life-threatening diseases in certain people, while most show no symptoms at all are not yet fully understood.

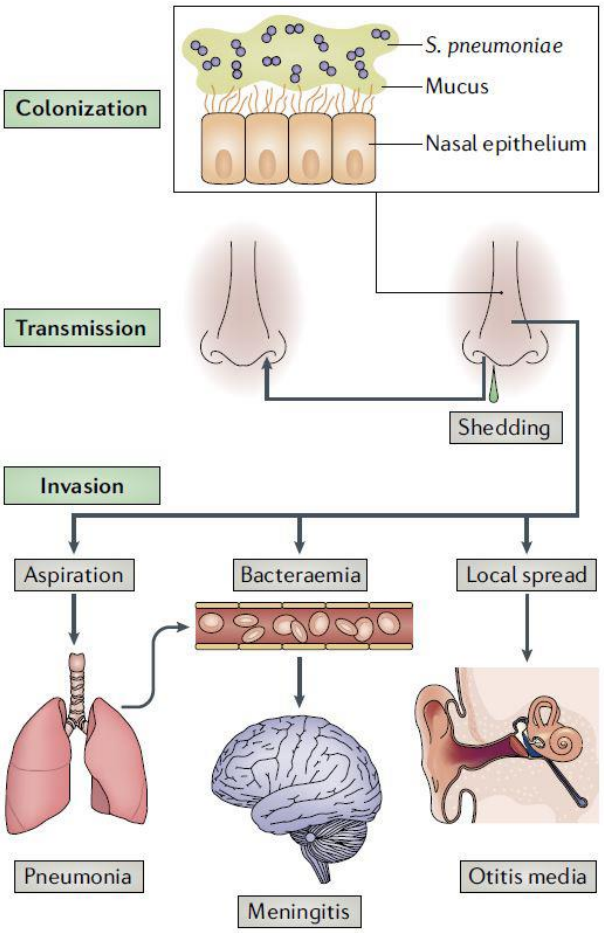

Figure 2: Schematic representation of *S. pneumoniae* pathogenic route. As colonizing the mucosa of the upper respiratory tract, pneumococci can be transmitted in nasal secretions to other individuals and may cause mild local infections as well as invasive disease [67].

3.3. Diagnostics and Therapy

Pneumococci can be detected microscopically and culturally in appropriate test specimens (blood, bronchial secretions, cerebrospinal fluid). These α-hemolytic bacteria exhibit a green area around their colonies on blood agar plates and they are optochin-sensitive, although optochin resistance has been observed [68]. Serological typing can be conducted with antibodies specifically directed against the capsular polysaccharides (CPS) in the so-called Neufeld test or “Quellung” reaction [69]. An alternative method for serotyping *S. pneumoniae* is the multiplex PCR, a PCR approach that is applied to detect more than one genomic segment in organisms [70]. Using this method sequence differences of the individual pneumococcal capsule locus can be detected using specific primers targeting this locus [70-72].

Current therapy for pneumococcal infection consists of prophylactic vaccination and antibiotic treatment. Worldwide, penicillins belonging to the group of β-lactam antibiotics are the

antibiotics of choice for the treatment of pneumococcal infections [73]. Further, the pathogen can be controlled with other antibiotics such as cefotaxime [74], chloramphenicol or fluoroquinolone [75]. In parts of the world where these medications are used to treat tuberculosis, resistance has been described [76]. Rifampin and vancomycin are available as reserve antibiotic for penicillin-resistant pneumococcal strains, but the misuse of antibiotics in the world are leading to an increasing prevalence of multiple antibiotic resistance [73,77]. Due to natural competence, the development of antibiotic resistance in pneumococci is further promoted [40,78]. For these reasons, the use of preventive vaccines is more appropriate to address infections caused by pneumococci.

3.3.1. Vaccination

Two pneumococcal vaccine types are available as either polysaccharide vaccines or conjugate vaccines. The polysaccharide vaccine, used in persons aged 65 years and individuals with immunocompromising conditions [79], is a mixture of the capsular polysaccharides of the 23 most clinically important serotypes (PPV23, Pneumo®23 or Pneumovax®23) and covers all serotypes responsible for 90% of diseases caused by pneumococci in the USA and Europe. It is directed against serotypes 1, 2, 3, 4, 5, 6B, 7F, 8, 9N, 9V, 10A, 11A, 12F, 14, 15B, 17F, 18C, 19A, 19F, 20, 22F, 23F and 33F [80]. However, the polysaccharide vaccine is not sufficiently effective in infants and young children under two years and also has weakness in long-term efficacy in adults [81,82]. Children of this age cannot develop immunologic memory (no generation of memory B cells) due to the absence of a T-cell-dependent immune response [82,83]. In this regard, the many different and only marginally immunogenic serotypes of the capsule pose a major challenge [82]. This led to the introduction of a new heptavalent conjugate vaccine (PCV7; predominant serotypes: 4, 6B, 9V, 14, 18C, 19F and 23F) called Prevnar® in USA in early 2000, which is intended for young children [36,39]. Conjugate vaccines provoke a significantly more robust immune response in children by recruiting T_h2 cells, which enable switching of the type and production of B lymphocytes for immunological memory [82,84]. More than 37,000 infants have been vaccinated in clinical trials in the USA and these studies have demonstrated the efficacy of the new vaccine in the selected target group [85]. It became immediately apparent that the number of invasive pneumococcal diseases, caused by serotypes included in the vaccine PCV7, in children under five years of age was declining in Germany and the USA [82,86]. However, this increases colonization and infections of other highly virulent serotypes, not covered by PCV7. This phenomenon, known as serotype replacement, is reflected, for example, in the rise of type 19A, which accounts for 50% of all isolated serotypes in children in the United States in 2007 and 2008 [34,87]. Because of a persistent risk of infection with serotypes not covered by PCV7, the PCVs have been continuously improved and extended

until the establishment of the 10-valent conjugate vaccine PCV10 (Synflorix) and the 13-valent conjugate vaccine PCV13 (Prevnar 13®) [88]. The approved conjugate vaccines contain the conjugated capsular antigens of either ten (PCV10: 1, 4, 5, 6B, 7F, 9V, 14, 18C, 19F and 23F) or thirteen clinically relevant serotypes (PCV13: 1, 3, 4, 5, 6A, 6B, 7F, 9V, 14, 18C, 19A, 19F and 23F) coupled to an immunogenic strong antigen as carrier. In Synflorix, 8 capsule antigens are conjugated to protein D of non-typeable *Haemophilus influenzae*, 18C to a tetanus toxoid carrier protein of *Clostridium tetani* and 19F to a diphtheria toxoid [89]. PCV7 and PCV13 are chemically coupled by reductive amination to the nontoxic form of the diphtheria toxin CRM197 from *Corynebacterium diphtheriae* to form glycoconjugates [82,88]. Aluminium orthophosphate is added to all vaccines as an adjuvant to enhance immune response [90].

Vaccination against pneumococci is recommended for all children after their second birthday and for persons with increased health risk for severe pneumococcal disease [91]. Because pneumococcal vaccines do not cover all of the approximately 98 pathogenic pneumococcal serotypes and no mucosal immunity is provoked, these types of vaccines do not provide complete protection from infections, carrier status or even herd immunity [82]. Due to the increasing antibiotic resistance of bacteria and the risk of so-called serotype replacement by non-vaccine serotypes (NVT) in the population, which means a colonization of ecological host compartments with serotypes not covered by the PCV, new vaccines against a broader spectrum of pneumococci are currently being sought [36,82,92,93]. In this regard, promising candidates for vaccines that can be used in a serotype-independent manner are the widely distributed and highly conserved pneumococcal virulence factors [19].

3.4. Morphological characteristics of *S. pneumoniae*

3.4.1. Capsule

The capsule, the outer envelope of all virulent pneumococci, was isolated in 1917 [94], but since only proteins were known to be immunogens, it was assumed that the capsule was also composed of proteins. In the 1920s, it was explored that the capsule is composed of polysaccharides and thus was discovered to be the first antigen that is not a protein [95,96]. These polysaccharides are repetitive sequences of e.g., galactose, glucose, rhamnose, ribitol, and glucuronic acid, linked by glycosidic bonds and depending on the serotype, they may contain various acetyl- and phosphoryl groups, di/trideoxyhexoses, amino sugars and cholines [97-99]. Except for serotype 3, the capsule is covalently linked in all serotypes to the peptidoglycan (PGN) of the cell wall [100]. With the polysaccharide capsule, the pathogen possesses an important virulence factor in pneumococcal colonization [32], transmission [101] and virulence [29,102]. The different serotypes vary both in their ability to resist phagocytosis

and in eliciting a human immune response [97,103]. Capsules prevent complement-mediated opsonophagocytosis by impairing binding of the opsonin iC3b (alternative complement cascade) and immunoglobulins to the surface of pneumococci, so that only encapsulated pneumococci are virulent [53,55,104]. Furthermore, the capsule serves to escape binding by neutrophil extracellular traps (NETs) [105] and to confer resistance to spontaneous or antibiotic-induced autolysis [106]. The negative charge of the capsule counteracts mucus-mediated export from the nasopharynx via electrostatic repulsion, which facilitates penetration into the glycocalyx layer of the respiratory epithelium and contacting receptors there [107]. The layer thickness of the CPS can vary between 200 – 400 nm [108], but capsule thickness is not necessarily proportional to virulence [109]. For example, serotypes 3 and 37 produce very thick capsules, but only serotype 3 is highly virulent to humans and laboratory animals [110,111]. The amount of CPS may be reduced upon contact with respiratory epithelial cells [112], improving adhesion to host cells and increasing invasiveness [113]. This is necessary because surface-associated proteins involved in adherence and virulence otherwise remain masked, making it to an important mechanism for successful nasopharyngeal colonization [114]. To date, 98 serotypes [27-30] of CPS have been described, differing firstly in their molecular capsule composition and secondly in the *cps* operon [29,30,115]. Changes in the *cps* locus can be on single nucleotide level or entire genes can be replaced or deleted [116,117].

3.4.2. Cell wall

As a Gram-positive pathogen, pneumococci have only a cytoplasmic cell membrane with a peptidoglycan layer covering the phospholipid layer. The PGN is a thick murein sacculus often simply called cell wall. The cell wall serves to shape and stabilize the cell and counteracts the turgor prevailing in the cell [118]. Although it has often been conceived as an inert structure, it is in fact a highly dynamic and tightly regulated macromolecule that is continuously assembled and disassembled to ensure cell growth and division [119,120]. As a Gram-positive bacterium of the *Firmicutes* phylum, the cell wall of pneumococci is a mesh-like network mainly composed of a heteropolymer peptidoglycan layer of i) *N*-acetylglucosamine (Glc*N*Ac); ii) *N*-acetylmuramic acid (Mur*N*Ac); iii) teichoic acids; iv) phosphorylcholine; and v) tethered peptides of alanine, glutamate and lysine [121-124]. The sugars built an alternating structure with β-1,4-glycosidic bonds (Glc*N*Ac-(β1,4)-Mur*N*Ac) and the pentapeptide L-Ala-D-iGln-L-Lys-D-Ala-D-Ala attaches via the lactyl residue to Mur*N*Ac. While the basic repeating structure of the disaccharide is present in all bacterial peptidoglycan layers, the oligopeptides differ between bacterial species [125]. The biosynthesis of the PGN network is a complex process and requires the involvement of more

than 20 proteins from different protein families, including penicillin-binding proteins (PBPs) and choline-binding proteins (CBP) [126,127]. The biosynthesis reactions are catalyzed in the cytoplasm (synthesis of peptidoglycan precursor molecules), at the inner side (synthesis of lipid-coupled intermediates), and the outer side (polymerization of Glc*N*Ac-(β1,4)-Mur*N*Ac-L-Ala-D-iGln-L-Lys-D-Ala-D-Ala fragments) of the plasma membrane [128-131]. Whereas earlier models assumed the existence of two strictly separate processes for realizing septal and peripheral growth, recent data suggest the existence of a single, finely regulated machinery [132]. Peptidoglycan biosynthesis can be divided into eight steps [129-131,133]:

Cytoplasmic steps [128,129]:

1. Synthesis of UDP (uridine diphosphate)-*N*-acetylglucosamine (UDP-Glc*N*Ac) and UDP-*N*-acetylmuramic acid (UDP-Mur*N*Ac).
2. Addition of amino acids (AS) L-alanine, D-glutamate, L-lysine, D-alanine-D-alanine to UDP-Mur*N*Ac in an ATP-dependent manner, while terminal D-alanines are attached together as a dipeptide.

Intracellular membrane steps [129,130]:

3. Cleavage of UMP (uridine monophosphate) from UDP-Mur*N*Ac-pentapeptide and binding to a lipid carrier in the cell membrane.
4. Binding of UDP-Glc*N*Ac to UDP-Mur*N*Ac-pentapeptide, UDP is cleaved followed by amidation of the α-carboxyl group of D-glutamate, the second amino acid of the pentapeptide, to D-isoglutamine (D-iGln) [134].
5. Direction outward of sugar moieties (completed precursor) across the cytoplasmic membrane by flipping the lipid carrier [135].

Extracellular membrane/cell wall steps catalyzed by penicillin-binding proteins [129-131]:

6. Attachment of the completed precursor to the preexisting cell wall. This leads to an elongation of the peptidoglycan scaffold.
7. Cross-linkage of individual murein strands via interpeptide bridge. In this process, the fifth D-alanine of the pentapeptide is cleaved off and at the same time a new bond with another pentapeptide chain on the fourth D-alanine is generated. This process is called transpeptidation and is carried out by transpeptidases such as D,D-carboxypeptidase (DacA) and L,D-carboxypeptidase (DacB) [119,120].
8. Return of the lipid carrier to the intracellular space to bind a new UDP-Mur*N*Ac molecule and start a new synthesis cycle.

The peptides and N-acetylglycans of the cell wall are subject to various modifications, especially acetylations and deacetylations. One example is the O-acetylation of the C_6-OH of

Mur*N*Ac, which serves, among other things, to bind wall teichoic acids [121,124] as well as various capsule polysaccharides [100,136]. The aforementioned modifications as well as branches in the peptides network of the cell wall are frequently associated with the formation of resistance to lysozyme and various antibiotics [137].

3.5. The metabolism of *S. pneumoniae*

Metabolism includes all biochemical processes in an organism that result in the uptake, transport, transformation and degradation of substances. All these processes are necessary for the maintenance of life. Pneumococci depend on the nutrients that are available in the respective host compartment and can be taken up as well as catabolized. Genome analysis revealed the absence of the tricarboxylic acid (TCA) cycle and electron transport chain (aerobic and anaerobic respiration) enzymes [14]. Pneumococci have various transporter systems for carbohydrate, amino acid, vitamins and metal ion uptake [14,15,138-142]. For the important cofactors iron, zinc, and manganese *S. pneumoniae* encodes several ABC transporters (ATP binding cassette transporters) (for iron: **Piu**, **Pit** and **Pia**, which is the dominant one; for manganese: **PsaBCA** and for zinc: **AdcCBA** and **AdcAII**) to maintain oxidative stress response and virulence [140,143-147]. Under iron limiting conditions, pneumococci showed morphological defects as a disturbed cell division and an altered expression of proteins involved in cell division underlining the necessity of iron uptake [148].

3.5.1. Carbohydrate metabolism

Since pneumococci belong to the lactic acid bacteria, they are only capable of fermentative energy metabolism and thus depend on carbohydrates for optimal growth. Genome analyses showed that *S. pneumoniae* possesses numerous affine and specific transporters for carbohydrates and amino acids. Over 30% of the transporters of pneumococci are transporters for carbohydrates, which is an unusually high percentage among prokaryotes [149]. In the *S. pneumoniae* genome, 21 PTS (phosphotransferase system), 7 ABC transporters, one channel protein and one secondary transporter have been identified [139]. Compared to ABC transporters, PTSs are significantly more energy efficient, as they phosphorylate their substrate already during transport. *In vitro* pneumococci can take up at least 32 different carbohydrates (e.g., glucose, galactose, sucrose and lactose) into the cell. Under *in vitro* conditions pneumococci prefer glucose, however, this sugar is not available in the human URT [139,149]. In the URT the bacteria settle on a mucin layer consisting of glycoproteins (macromolecules composed of a central protein chain and long, complex oligosaccharides) [150]. In general, these subunits represent the only carbohydrate source for pneumococci in the respiratory tract. With the help of exoenzymes, such as

hydrolases, hyaluronidase, neuraminidases (NanA, NanB, NanC), α-galactosidase (AgaN), β-galactosidase (BgaC), and N-acetylglucosaminidase (StrH), *S. pneumoniae* can release monosaccharides from the present host polymeric structure, transport and utilize them in the bacterial cell [151-153]. In the blood, glucose is present as a carbon and energy source for pneumococci [154]. Sugars such as glucose and sucrose are metabolized via glycolysis (Embden-Meyerhof-Parnas (EMP) pathway) [155], whereas pentoses, such as ribose, are theoretically introduced into glycolysis via the pentose phosphate pathway (PPP) [15]. A metabolomics study analyzing the intracellular metabolic profile confirmed the high glycolytic activity of *S. pneumoniae* [156]. Galactose and lactose are first metabolized in two different pathways, the tagatose-6-phosphate and the Leloir pathway, and enter later the glycolysis pathway [155,157,158]. Finally, all carbohydrates are oxidized to pyruvate, which is subsequently converted to lactate by lactate dehydrogenase. During this process pneumococci regenerates NADH to NAD^+ [155]. Streptococci are able to metabolize sugars homo- and heterofermentatively to regenerate spent reduction equivalents (NADH/NAD+) and thus energy [159]. Under glucose-limited conditions and induction of heterofermentative growth, additional end products may also be formed, such as formate, acetate and ethanol [160]. In the presence of galactose, the pyruvate dehydrogenase converts pyruvate to acetyl-CoA and recycles NAD^+, but more than 50% of pyruvate is cleaved by the pyruvate formate lyase (Pfl). Two enzymes, pyruvate formate lyase activating enzyme (PflA) and pyruvate formate lyase (PflB) are required for a functional Pfl catalyzing the reaction of pyruvate to acetyl-CoA and formate [161,162]. Metabolic proteins play an important role in virulence. Mutations in the *pflA* and *pflB* genes attenuate the virulence of pneumococci, as mice infected intranasally with *pflA*- and *pflB*-mutants survived longer than mice infected with the wild-type. Bacteremia also developed later in mice infected with the mutants [161]. Pneumococcal metabolism is controlled by global regulators, such as CodY [163], or the catabolite control protein CcpA [164].

3.6. Pneumococcal virulence factors

S. pneumoniae preferentially colonizes the mucosal epithelium of the URT as commensal. Only when the pneumococcus overcomes this natural barrier the bacterium causes invasive, life-threatening diseases. Pathogenicity is the fundamental ability of infectious agents to cause disease in specific organisms and can occur through molecular mimicry [165], attachment to the extracellular matrix or host cells or modulation of the host immune system [166]. Virulence factors play an important role in pathogenesis and promote the growth as well as the spread, invasion and survival of microorganisms within a host organism [15,53]. The role of pneumococcal virulence factors in the pathophysiology and their in part multiple functions have not yet been comprehensively elucidated. Virulence factors

are produced depending on the stage of infection and may be present in a surface-associated manner or secreted [167-169]. Multiple genes encoding virulence factors are sometimes grouped into pathogenicity islands (PAIs), which can be transferred to other strains via horizontal gene transfer [170]. Virulence factor expression is regulated in response to the environment and host immunological response by a wide variety of mechanisms; they can be achieved at the transcriptional level with thermosensors [171], riboswitches [172] and non-coding RNAs [173] or via promoter regulation using stand-alone regulators or two-component regulatory systems (TCS) [174,175].

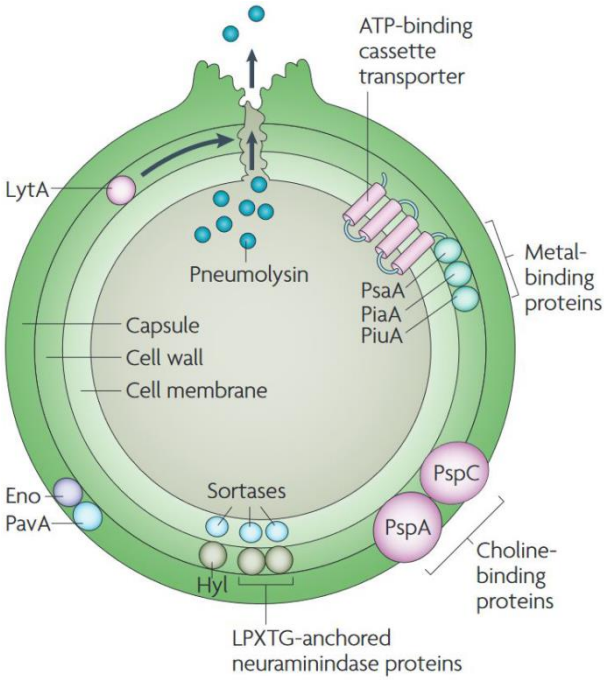

Figure 3: Schematic representation of *S. pneumoniae* virulence factors. A number of virulence factors are necessary for the viability of the pneumococcus. Illustrated pneumococcal virulence factors include: the capsule; the cell wall; choline-binding proteins; pneumococcal surface proteins A and C (PspA and PspC); the LPXTG-anchored neuraminidase proteins; hyaluronate lyase (Hyl); pneumococcal adhesion and virulence A (PavA); enolase (Eno); pneumolysin; autolysin A (LytA); and the metal-binding proteins pneumococcal surface antigen A (PsaA), pneumococcal iron acquisition A (PiaA) and pneumococcal iron uptake A (PiuA) [168].

3.6.1. Surface proteins

Pneumococci possess diverse surface-anchored or surface-associated proteins that act as virulence factors. Four classes of proteins can be distinguished depending on the surface-anchoring motif: choline-binding proteins, lipoproteins anchored to the membrane via a lipobox motif, surface proteins anchored to the cell wall via cleavage of the LPxTG motif by a transpeptidase called sortase and the non-classical surface proteins (NCSP), also called moonlighting proteins [142,167,168,176]. These various surface proteins are especially required for pneumococci to attach to eukaryotic host cells and to maintain pneumococcal

fitness. These proteins target host structures such as components of the host cell membrane, the ECM or body fluids. Among the adhesins expressed by pneumococci are the MSCRAMMs (microbial surface components recognizing adhesive matrix molecules), which are encoded in the core genome for the majority of pneumococcal strains. MSCRAMMs are able to mediate initial attachment of bacteria to the ECM components of host cell tissue or sequester ECM proteins [177,178]. The ECM, a three-dimensional network, consists of collagenous and non-collagenous glycoproteins [179]. *S. pneumoniae* can utilize ECM proteins as molecular bridge to link to integrins and finally manipulate host cell signal transduction cascades for internalization. Integrins are glycoproteins that mediate a dynamic link between the ECM and the intracellular actin cytoskeleton [180]. In this regard, a single bacterial MSCRAMM can recognize and bind a specific or several ECM proteins and, conversely, several MSCRAMMs can bind the same ECM protein, increasing the efficiency of the interaction [60,178]. The human thrombospondin-1 (TSP-1), a matricellular protein, can recognize surface exposed structures of pneumococci and other Gram-positive bacteria, facilitating bacterial adherence [178,181-184]. In addition to TSP-1, pneumococci also bind to ECM proteins such as fibronectin [57,58], fibrinogen and vitronectin [59], as well as lactoferrin [185], a mucosal iron transport protein and plasminogen, a serum protein [186]. Additionally, tight junctions are broken by diverse virulence factors, which leads to a leaky epithelium and thus functional impairment [187].

3.6.1.1. Choline-binding proteins

In pneumococci, 13 – 16 CBPs have been identified to date, of which PspA [188], PspC [189] and some cell wall hydrolases such as LytA, LytB [190], LytC [191] and CbpF [192], in particular contribute to adhesion, cell wall physiology and virulence [167,168,193]. These proteins are non-covalently bound via C-terminal repeats (3 - 18 choline-binding domains, 20 conserved AS each) to the phosphorylcholine of lipoteichoic and wall teichoic acids of the cell [193-197]. Additionally, they have a signal peptide and a variable N-terminus [196]. An important representative is **PspA**, which prevents complement-mediated opsonization by interfering with the accumulation of C3 opsonin [198]. Furthermore, PspA has been described to bind human lactoferrin, an iron-binding protein, and thus inhibit the bactericidal effect of apolactoferrin [185,199]. **PspC** binds to factor H [200], plasminogen [201], TSP-1 [181], vitronectin [202] and interacts directly with the secretory component (SC) of pIgR [63,203,204] leading to increased adherence to host cells. The interaction with the pIgR induces the transcytosis pathway, which actually transports IgA from the basolateral to the apical cell side, proceeding backwards. As a result, pneumococci are transported from the apical to the basolateral side and thus into deeper tissue layers [204-206]. Due to binding of factor H, PspC enables immune evasion of pneumococci [207]. The autolysins **LytA** and **LytB** are

important in normal growth by cleaving the amide bond between alanine and muramic acid in the cell wall as well as during nutrient deficiency or antibiotic stress [208,209]. They facilitate the release of other virulence factors (e.g., proinflammatory peptidoglycan and pneumolysin) localized in the cytoplasm [210].

3.6.1.2. Sortase-anchored proteins

The *S. pneumoniae* genome contains up to 18 sortase-anchored proteins [176]. These surface proteins possess a conserved C-terminal leucine-proline-any AS (x)-threonine-glycine (LPxTG) motif, followed by an uncharged domain with hydrophobic properties [211]. This is usually followed by several amino acid residues with a positive charge [212]. The specific LPxTG sequence is recognized by a membrane-bound sortase (SrtA), leading to the cleavage of the bond between threonine (T) and glycine (G) resulting in a covalent link of the carboxyl group of threonine to the amino group of a pentaglycine of the cell wall peptidoglycan [213-215]. SrtA plays a significant role in adhesion to nasopharyngeal cells [216] and colonization of host cells [217], as well as in the development of pneumonia and bacteremia [218]. LPxTG proteins include hyaluronidases (**Hyl**) [219], hydrolases (**BgaA**) [220], neuraminidases (**NanA**) [221], proteases (**IgA1 protease**) [222] and plasminogen and fibronectin binding proteins (**PfbA**) [223]. They cleave human glycoproteins, glycolipids and oligosaccharides on the host cell surface and thus may play a role in unmasking receptors for attachment [220,224]. Sortase-anchored proteins have a major role in pneumococcal adhesion and interaction with ECM proteins [225]. An important member of this group is **PavB**, which with its variable number of repetitive SSURE (streptococcal surface repeat) sequence peptides interacts with fibronectin and plasminogen to increase bacterial adherence to host cells in the early phase of colonization [226-228]. The SSURE domains of PavB exhibit high homology among themselves and are also highly conserved among pneumococcal strains [228]. They can be divided into three sections: i) the first domain consists of 150 amino acids, is highly conserved between the strains, but differs from the core SSURE and the last SSURE; ii) the core SSURE consists of 152 amino acids and, depending on the strain, 2 – 7 of these identical sequences; iii) the last SSURE is truncated, consists only of 136 amino acids and is also highly conserved between the strains. Accordingly, the size of the mature protein varies considerably in the serotypes [226]. PavB has been shown to contribute to pneumococcal colonization of the nasopharynx and to transmigration to the lungs [226]. Many of the **pili** proteins regulated by TCS08 are also considered to be sortase-anchored proteins [229]. Pili, hair-like structures on the pneumococcal surface, are produced by only about 20% of clinical isolates and confer additional adhesive properties facilitating colonization of epithelial cells in the URT. The pili

protruding from the capsule initially allow attachment to cellular receptors and ECM proteins like fibronectin over a longer distance [230-232].

3.6.1.3. Lipoproteins

However, the largest group of surface proteins are the lipoproteins, which are found, among others, as substrate-binding components of ABC transporters for nutrient transport and bacterial fitness. These multifunctional proteins play a role in signal transduction [142], adhesion [233], oxidative stress response [234], antibiotic resistance mechanisms [235] and extracellular protein folding [236]. Thus, lipoproteins possess important functions or properties in virulence, such as colonization [236], invasion [237] and immune evasion [238]. Thirty-seven lipoproteins have now been classified in serotype 2 and 4 pneumococci on the basis of the lipobox motif [142,239]. They are synthesized in the cytoplasm as a preprolipoprotein containing a signal peptide and an N-terminal conserved lipobox ($(LVI)_{-3}(ASTVI)_{-2}(GAS)_{-1}C_{+1}$)) [233], which allows covalent binding of the lipoprotein to the outer side of the phospholipid bilayer [240,241]. The preprolipoprotein is lipidated by a diacylglyceryltransferase (Lgt), which adds a diacylglyceryl residue to the thiol group of the conserved cysteine in the lipobox. The covalent binding to the cell membrane is mediated by diacylglyceryl moieties. Finally, the signal peptide is cleaved by lipoprotein-specific signal peptidase (Lsp) [241]. A unique highly conserved two-pathway system (**CcdA-Etrx-MsrAB2 (CEM) system**) responsible for extracellular oxidative stress resistance partially consists of lipoproteins and is located upstream of the TCS09. As commensal of the human respiratory tract, pneumococci are constantly exposed to reactive oxygen species (ROS). In particular, the amino acids cysteine and methionine are susceptible to oxidative stress and can be oxidized, leading to the conformational change of a protein and its activation or inactivation [242]. The extracellular CEM system, which repairs surface proteins by restoring them to their reduced state, was characterized in 2013 [234]. The CEM operon is highly conserved in *S. pneumoniae*, consists of three genes encoding the integral membrane protein CcdA1, the extracellular thioredoxin-like lipoprotein Etrx1, and the membrane-anchored methionine sulfoxide reductase MsrAB2. The integral membrane proteins CcdA1 and CcdA2 receive electrons from cytoplasmic thioredoxin A (TrxA) after they are transferred to TrxB from the NADH pool of the cell. Subsequently, electrons are transferred to the surface-localized proteins Etrx1 and Etrx2, then to the reductase MsrAB2, which leads to reduction of the single domains MsrA and MsrB. By possessing an additional long and flexible domain, MsrAB2 can most likely reach domains of oxidized proteins on the surface, which then allows their reduction. Thus, the oxidation of methionine to methionine sulfoxide can be reversed and the corresponding proteins repaired [234]. Another example is **PsaA**, which was initially hypothesized to be an adhesin in early publication because of the

pleiotropic effect [243]. Later analyses showed that it is an extracellular metal-binding component of a manganese PsaBCA ABC transporter [146,147]. However, binding of PsaA to E-cadherin has been shown later, but the function of this interaction has not been assessed further [244]. Complete deletion of the *psaA* gene has been shown to abolish or reduce the virulence of *S. pneumoniae* in murine bacteremia and colonization models [245,246]. Further important transporters are **AliA**, **AmiA**, and **AliB**, which participate in oligopeptide transport [247,248] and the iron uptake transporters **PiaA** and **PiuA** [140].

3.6.1.4. Moonlighting proteins

Moonlighting proteins lack a signal peptide and membrane-anchoring motif [176]. These proteins are mostly intracellular proteins essential for metabolism that are bound on the surface by reassociation [249], where they play a role in host-pathogen interactions [167]. They interact with human ECM proteins, especially plasminogen [186] and fibronectin, and enable pneumococci to migrate through the epithelium [57,58]. This group includes several glycolytic enzymes such as enolase [186,249], glyceraldehyde-3-phosphate dehydrogenase (**GAPDH**) [250] and phosphoglycerate kinase (**PGK**) [251] as well as the pneumococcal adherence and virulence factor A (**PavA**) [57,58,227]. Moreover, they can also inhibit the complement system by binding C4b-binding protein [252] and affecting the membrane attack complex formation [253].

3.7. Regulation

Living cells rely on sensing and interpreting external signals as an adaptive mechanism against changes in their environment such as oxygen, temperature and pH. This process is known as signal transduction and allows the cell to react immediately and appropriately to specific alterations in their habitat. Similarly, cellular mechanisms such as osmoregulation, photosynthesis, chemotaxis, sporulation and antibiotic production can be regulated [254]. In pathogenic bacteria, gene regulation plays an important role in the conquest of the host and the penetration of new host niches with changing environmental parameters, as virulence factors can be activated in this process [255]. As a consequence, bacteria evolved cellular regulatory mechanisms consisting of specialized sensor proteins, proteins activating or repressing gene expression [256], and chemical signal molecules [257]. *S. pneumoniae* utilizes quorum sensing (QS) systems, stand-alone regulators, non-coding RNAs (ncRNAs) and two-component regulatory systems for sensing and responding to the environment [174,175]. A comprehensive bioinformatics analysis revealed a high conservation of regulatory genes of 25 pneumococcal strains differing in phylogenetic lineages and serotype [19].

3.7.1. Quorum sensing

The regulation of various physiological processes in bacteria often occurs via a quite ancient system, the so-called quorum sensing [258-260]. The phenomenon of the QS systems was first described by scientists Nealson, Platt and Woodland Hastings, when they studied bioluminescence in the marine bioluminescent bacterium *Aliivibrio fischeri* [261]. Quorum sensing is the ability of unicellular organisms to measure the cell density of the population of their own species and the complexity of the community via chemical communication using highly specific signal molecules [262]. These signaling molecules, called autoinducers (AIs), are generally freely diffusing, amphiphilic molecules that are continuously produced and emitted into the environment in small quantities by the bacteria. In Gram-negative bacteria, AIs are predominantly low molecular weight compounds (N-acyl homoserine lactone; AHL), while in Gram-positive bacteria they are linear or cyclic oligopeptides (autoinducing peptide; AIP) [262,263]. AHLs usually do not need additional processing, whereas the very heterogeneous group of AIPs, including the competence stimulating peptide (CSP) of *S. pneumoniae*, are synthesized as prepropeptide and activated during transport [263-265]. At a sufficiently high threshold concentration of the released AIs, they can be sensed by the surrounding bacteria via cell-specific receptors, which receive now information about population density and community complexity leading to an altered phenotype of the population [264]. AHL and AIP can either bind directly to cytosolic transcription factors to initiate or inhibit transcription or they use TCSs as signal transduction [262,264,266]. The triggered positive feedback of the signaling molecules induces mostly their own synthesis [267]. Bacteria can communicate simultaneously in complex environments via different QS systems with different autoinducers and adapt to the situation at hand [268,269] e.g., ensure population survival [270], gain advantages over competitors [271], bioluminescence [261], biofilm formation [272], secretion of antibiotics [273], pathogenicity factors [274], sporulation [275], infection of plants [276] and eukaryotic host [277], nitrogen fixation [278] and to open up new suitable ecological niches [279].

In *S. pneumoniae* the natural ability to take up free DNA from the environment into the cytoplasm (competence; transformation) for genetic modification is regulated by a QS. Bacteria can thus undergo new metabolic pathways or gain new virulence genes [280]. Plasmids as well as DNA cleaved fragments in linearized form can be taken up [281]. In this process the *comAB* and *comCDE* operons, encoding among others the TCS12 (**ComDE**), are of crucial importance [282-285]. Transcription of *comC*, located upstream of TCS12 [286], generates the CSP first as a 44 AS long pro-peptide, which is processed into an active molecule (C-terminal 17 AS) [282] and secreted into the extracellular space by the ABC transporter ComAB [287]. The histidine kinase (HK) ComD registers the level of accumulated CSP [285] and after exceeding a certain threshold due to high cell density, the response

regulator (RR) ComE is phosphorylated via ComD [282] and activates transcription of early *com* genes, such as *comCDE*, *comAB*, *comX* and *comW* [288-290]. ComX, encoded by two identical genes, acts as an alternative sigma factor and initiates, as already ComE, transcription of genes necessary for DNA uptake and recombination [289]. ComW is a positive regulator that assists in the assembly of ComX and RNA polymerase and protects ComX from proteolysis [290,291]. Finally, pneumococci take up free fragments of DNA or larger DNA segments through surface-associated DNA-binding proteins.

Pneumococci are able to form biofilms during infection, as shown in first studies using otitis media models [292]. An important QS during biofilm formation is the wide distributed **LuxS**, which induces increased iron uptake and regulates LytA and Ply expression. D39Δ*luxS* mutants demonstrated a reduced expression of the Fe^{3+} transporter PiuA, leading to a lower concentration of intracellular Fe^{3+} and weaker biofilm formation [293,294]. After intranasal infection of mice, a *luxS*-mutant was less able to translocate from the nasopharynx to the lungs or blood, which was further supported by using a co-infection sepsis mouse model, in which the *luxS*-mutant was outcompeted by the wild-type [295]. Furthermore, LuxS is associated with a downregulation of competence [296].

A QS system that regulates a lantibiotic biosynthesis gene cluster, is the **TprA/PhrA**. This QS gives pneumococci the ability to scavenge sugars from the host mucin and to outcompete neighboring bacteria in the nasopharynx. The autoinducer PhrA is exported by the Sec secretion system and imported via AmiC, an oligopeptide permease. Lanthionine containing antimicrobial peptides are higher expressed when pneumococci are at high density in galactose instead of glucose containing environment, as it is the case in the nasopharynx [297].

3.7.2. Stand-alone regulators

Stand-alone regulators possess a dual role by recognizing specific signals and binding to a specific target to modulate gene expression [298]. These regulators have an important role in metabolism and virulence and are classified into different families. Most of the stand-alone regulators harbor a helix-turn-helix (HTH) DNA binding motif [299].

CodY is a highly conserved global transcriptional repressor of low G+C content Gram-positive bacteria that has been particularly extensively studied in *Bacillus subtilis* [300] and *Lactococcus lactis* [301]. Mainly genes of carbon and nitrogen metabolism including genes for the synthesis of branched-chain amino acids or peptides as well as carbohydrate uptake are repressed [302]. CodY regulates transcription by binding as dimer [303] to a 15 bp AT-rich DNA sequence whose consensus sequence 5'-AATTTTCWGAAAATT-3' has already been identified in *L. lactis* as well as in *S. pneumoniae* [163,304]. Microarray analyses showed that 47 genes, predominantly of amino acid metabolism, were differentially expressed in a *codY*-

mutant. The overexpression of 43 genes confirmed the assumption that CodY acts mainly as a repressor of transcription. In experimental mouse models, CodY is necessary for colonization as also shown by diminishes adherence to nasopharyngeal cells *in vitro* [163].

Another regulator involved in carbon transport and metabolism is the catabolite control protein A (**CcpA**) [164,305]. CcpA controls expression of transcriptional regulatory proteins, amino acid transporters, and virulence factors like the capsule [306]. CcpA recognizes and binds to the cre site (catabolite responsive element), a highly degenerate pseudo-palindrome sequence 5'-WTGNNARCGNWWWCAW-3' (R = G/A, W = A/T, N = variable) [307,308]. In TIGR4, 275 out of 2087 genes (13%) with putative cre sites were identified, many of them are involved in carbohydrate transport and metabolism [309].

Important stand-alone regulators essential for pneumococcal amino acid metabolism are ArgR2 and GlnR. Interestingly, the **ArgR2** regulator is expressed in TIGR4, but not in D39. *S. pneumoniae* is auxotrophic for arginine and ArgR2 is involved in arginine metabolism regulation by inducing the expression of the arginine deiminase system (ADS) *arcABCDT*. In a mouse co-infection model, a deficiency of ArgR2 in TIGR4 led to an increased outgrowth of the mutant compared to the wild-type, probably due to increased fitness [310]. Two further ArgR-type regulators that are involved in arginine metabolism regulation are ArgR1 and AhrC, which target the amino acids transport genes *artPQ*, *abpA*, *abpB*, and *aapA* and the arginine biosynthesis gene *argGH* [311].

Glutamine/glutamate metabolism is regulated by the glutamine-dependent regulator **GlnR**. The amino acids glutamine and glutamate serve as the main nitrogen source for *S. pneumoniae* [312] and their uptake occurs via ABC transporters [313]. Ten percent of the transporter genes in pneumococcal strain R6 encode glutamine transporters [14]. GlnR regulates the expression of *glnRA*, *glnHPQ*, *zwf* and *gdhA*, and in presence of high levels of glutamine, glutamate and ammonium, GlnR represses gene expression [314]. The regulation of GlnR is dependent on GlnA, however, the mechanism is still unclear. It might be that conformational changes or multimerization by GlnA on GlnR occurs, increasing the DNA binding affinity [314]. A GlnR-deficient mutant shows no significant effect on virulence during adherence, pneumonia, and sepsis [312].

The "redox sensing" regulator **Rex** or homologs were found in most Gram-positive bacteria [315], such as *Staphylococcus aureus* [316], *Listeria monocytogenes* [317] and *S. pneumoniae* [318]. Structure analysis in *Thermus aquaticus* revealed a homodimer whose subunits consist of a C-terminal NAD(H)-binding domain with a rossman fold and an N-terminal DNA-binding domain with winged HTH motif linked by α-helices [319]. The coenzyme nicotinamide adenine dinucleotide (NAD^+ (oxidized form), $NADH/H^+$ (reduced form)) plays an important role in various redox reactions of metabolism [320]. Both coenzymes can bind competitively to Rex, thereby affecting the affinity of Rex to the target

sequence. NADH acts as an allosteric inhibitor for Rex, whose binding modifies the nicotinamide binding pocket [315]. If the Rex interaction domain binds NADH, it promotes ordering into a closed hairpin motif leading to a conformational change and inactivation of the DNA binding domain [321]. NAD^+ increases the binding of Rex to the regulated gene [316] but requires a 5 – 20,000-fold higher concentration to displace NADH and thus regenerate the active conformation [321]. Rex detects alterations in redox balance by changes in the NADH:NAD^+ ratio rather than via the NADH concentration per se [315]. In Gram-positive bacteria, Rex has been shown to influence carbon metabolism such as glycolysis [322], energy metabolism [322], fermentation [316], hydrogen production [323], reduction of sulfate/sulfide [324] and NAD(P)H biogenesis [318]. Genes to which Rex binds are often identified to encode NAD(P)H-dependent enzymes such as NADH dehydrogenase or lactate dehydrogenase [325]. Although Rex acts as a repressor in most cases, there are assumptions that Rex can act also as an activator [326]. To date, nearly no published studies of the Rex regulator in *S. pneumonia*e are available. Microarray studies in response to NADH characterized Rex as transcriptional repressor of *gapN*, *fba*, *pncB*, *adhB2*, *gap* and *adhE*, all involved in niacin transport and biosynthesis. As DNA binding site 5′-TTGTKAWAAWWTTCACAA-3′ (W = A/T; K = G/T) was revealed [318].

3.7.3. Non-coding RNA

Non-coding RNA refers to all RNA molecules that are transcribed from the DNA as RNA but are not translated into proteins like mRNA [327]. Instead, they are essential members of the regulatory network in bacteria [328]. Non-coding RNAs can be divided into different classes, small RNAs (sRNA) form the largest set [329]. These sRNAs can, among others, bind messenger RNA (mRNA) alone [330] or together with chaperon proteins at posttranscriptional level leading to repression of mRNA translation [331]. Recently, over 170 sRNAs were detected in *S. pneumoniae* TIGR4 [332,333] and 112 in D39 by transcriptomic studies [334]. A strain specific sRNA repertoire was observed, which probably contributes to strain-specific virulence [334]. However, nearly no information are available about the biological function of sRNAs. Some sRNAs are regulated by pneumococcal TCSs e.g., CiaR controls the expression of 5 sRNAs, designed as csRNAs [335]. These csRNAs control DNA competence by binding of a minimum of 3 csRNAs the CSP precursor *comC* RNA [336]. A virulence study assessed 15 sRNA mutants for their role in pneumonia, sepsis and meningitis after intranasal challenge of mice. All 15 sRNA mutants were able to cause bacteremia without differences, but survival in the bloodstream was attenuated in 8 sRNA mutants indicating reduced bacterial fitness. In an additional approach, pathogenesis was investigated by Tn-seq fitness determination. Twenty-eight transposon mutants in the lungs, 26 in the

nasopharynx and 18 in the blood were predicted to have a role in bacterial fitness in these specific niches [333].

3.7.4. Two-component regulatory system

Phosphotransfer mediated intracellular signaling pathways are widely used in many organisms to process environmental stimuli. Many eukaryotic signaling cascades involve protein kinases that autophosphorylate or phosphorylate other proteins at specific serine, threonine or tyrosine residues and thus regulate protein expression [337]. In bacteria, external stimuli are usually processed by a family of proteins called TCS allowing them to adapt to a wide range of environments, stresses, and growth conditions [338,339]. TCSs are ancient and evolutionarily conserved, common in Gram-negative, Gram-positive bacteria, archaea, plants, and lower eukaryotes, but have not yet been detected in vertebrates [340]. The number of TCS varies widely in the bacterial kingdom [341], with an average of about 20 TCS [342]. It ranges from zero TCS in *Mycoplasma genitalium* [343] to 272 TCS in *Myxococcus xanthus* [344]. TCS are known to regulate virulence factors important for pathogenicity in many bacterial strains [174,255,345,346].

In bacteria, a TCS consists of a transmembrane protein (histidine kinase, HK) that functions as sensor, and a corresponding cytoplasmic protein (response regulator, RR) controlling gene expression and influencing biological processes [338]. A typical HK has an N-terminal periplasmic domain that is anchored to the cell membrane with one or more transmembrane (TM) domains and functions as a receptor domain. This domain is of variable structure making it possible to respond to many different environmental signals. The cytoplasmic C-terminal part of a HK is important for signal transduction, has histidine kinase activity and is responsible for catalyzing the phosphorylation reaction [254]. The cytoplasmic kinase domain is highly conserved and divided into two distinct functional subdomains A and B. Subdomain A contains the histidine residue essential for ATP-dependent autophosphorylation and is referred to as the H-box, which represents the dimerization domain [254,339,347]. In subdomain B, 4 highly conserved sequence motifs (N, G1, F and G2) have been described by comparative analysis of different kinase domains, which are involved in ATP binding and hydrolysis in different ways [339]. Sequence comparisons of the functional kinase domain allow classification of HKs [348], however, functional aspects of kinases are disregarded in this classification, which is why another classification is more appropriate. HKs have then been classified into three major groups based on their sensor domain structure, membrane topology and known signal perception: i) HKs sensing signals in the periplasm or extracellular space; ii) HKs with absent extracellular sensor domain; iii) HKs, which are soluble cytoplasmic proteins or may be membrane-anchored and sense only intracellular signals [349,350]. HKs are generally found as dimers with one HK monomer

catalyzing the phosphorylation of the conserved histidine residue of a second monomer [254,351]. The RR can also be subdivided into two principal domains, the N-terminal conserved regulatory receiver (REC) domain and the variable C-terminal effector domain containing DNA-binding motifs, leading to transcriptional control and regulation of different types of output [339,340]. The regulatory domain contains a conserved aspartate residue, interacts with the phosphorylated HK, catalyzes autophosphorylation and regulates the activity of its associated effector domain in a phosphorylation-dependent manner.

The classical signaling cascade is initiated by the reception of an appropriate environmental signal via the periplasmic sensor domain of the HK. The kinase domain of the HK is activated, followed by an ATP-dependent trans- or cis-autophosphorylation reaction in the dimer [352]. The histidine is thus turned into the pentavalent phosphointermediate phosphoimidazole that can act as a phosphoryl group donor and this results in a conformational change of the HK. Further, the RR catalyzes the transfer of the high-energy phosphoryl group from the histidine residue to the aspartate of its own REC domain (autophosphorylation). The highly conserved acidic aspartate residues coordinate a magnesium ion that is essential for phosphoryl transfer, corresponding to an S_N2 reaction [339]. This causes a conformational change in the RR resulting in the activation of the output effector domain, exposing its active site leading to promotor binding [353,354]. This in turn generates a suitable adaptive response to the signal but the triggered effects of phosphotransfer are versatile and specific to each TCS [355]. The direct or indirect aim is always to achieve a particular level of RR phosphorylation to specify the generated response. The phosphoryl group is finally released as inorganic phosphate by the autophosphatase activity of RRs that determines the duration of the phosphorylated state. Often, auxiliary proteins accelerate the dephosphorylation of the RR and in addition to phosphotransfer many sensor kinases have phosphatase activity on their RR. Both activities can be regulated directly by the stimulus or indirectly by interaction with auxiliary proteins [339].

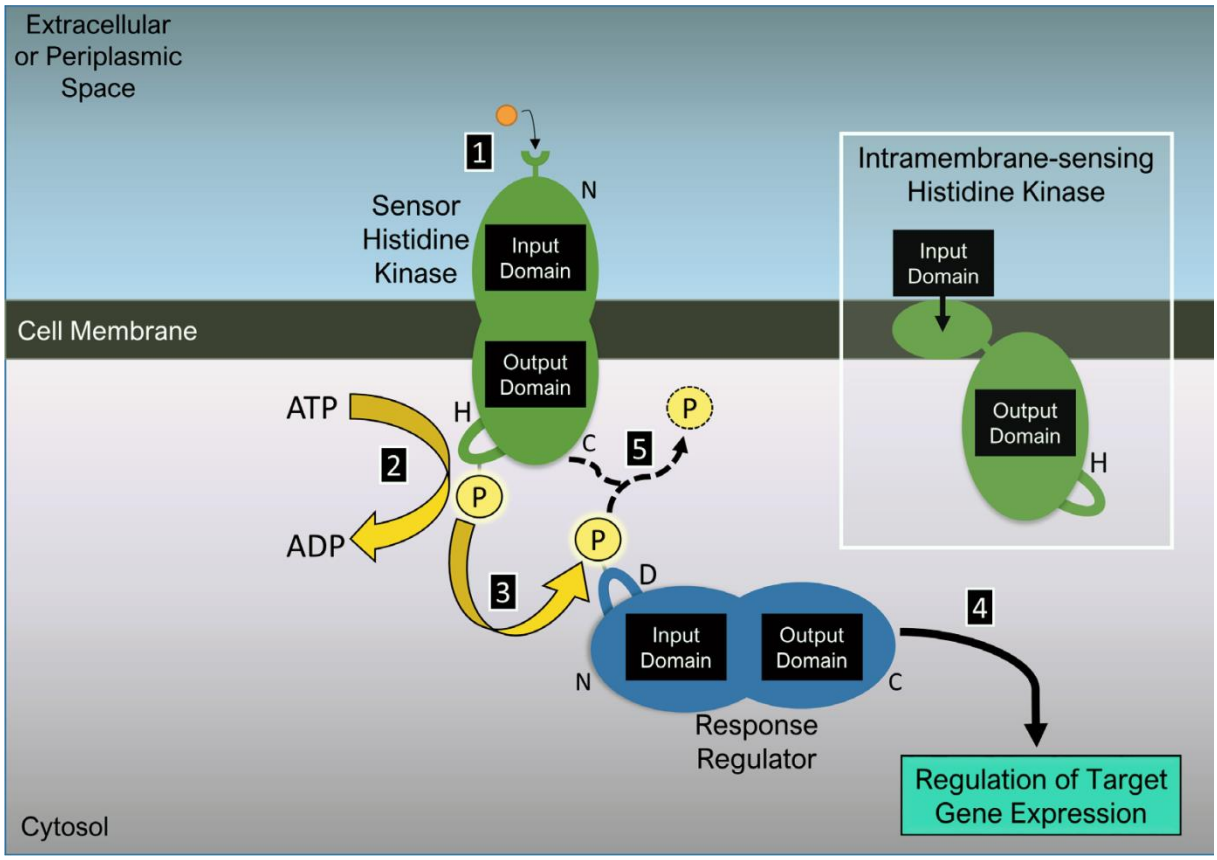

Figure 4: Schematically representation of signal transduction of a bacterial two-component regulatory system

After detecting a specific external stimulus (orange) by the N-terminal periplasmic domain (input domain) of the HK (green) (**1**), the cytoplasmic kinase domain (output domain) hydrolyzes cellular ATP for autophosphorylation of its conserved histidine residue (**2**). The phosphate group (yellow) will be transferred to an aspartate residue of the regulatory receiver domain (input domain) of the corresponding cytosolic RR (blue) (**3**). Finally, the C-terminal effector domain (output domain) is activated leading to controlled gene expression, by binding upstream at the promotor region of target genes (**4**). HK can also function as phosphatase by removing the bound phosphate of the RR (**5**). Inset to right: intramembrane HK with absent extracellular sensor domain [356].

In general, a HK is specific to its cognate RR, however, crosstalk between different TCSs in the bacterial cell can also occur [338,357]. One can only speak of a real “crosstalk”, if the TCSs affected by the crosstalk would function completely independently of each other [338]. Via crosstalk multiple responses to an external factor can also be generated or a strong response can be generated by multiple weaker stimuli [338,358]. However, phosphorylation is less pronounced than in related TCS pairs and prevented by the bifunctionality of many HKs [339,359,360]. The actual extent of the influence of crosstalk *in vivo* has not yet been clarified as the dephosphorylation character of HKs complicates the study of this complex system. Branched pathways refer to branched signaling pathways that can only together elicit the desired response. In the first model “one to many” there is only one HK, but it phosphorylates not just one RR but several e.g., to generate a more extensive response to

the external stimulus [338,361]. In the second model “many to one”, multiple HKs are required to phosphorylate one RR in sufficient quantity [338].

The majority of RRs are subdivided into different “types” or subfamilies based on their structure in the DNA binding domain. These subfamilies have been named after representative members. RRs of the OmpR, NarL, LytR and YesN types represent 58% of all RRs [362]. The effector domain of **OmpR**-type regulators contains a winged “helix-turn-helix” motif (three α-helices followed by a β-sheet) [363,364]. OmpR-type RRs often bind to direct sequence repeats, in which the nucleotide sequence is variable, but so is the number of sequence repeats and the number of bases separating the sequence repeats [363]. *S. pneumoniae* encodes 8 OmpR-type RR: RR01, RR02, RR04, RR05, RR06, RR08, RR10 and RR14 [174,340]. The effector domain of **NarL**-type regulators contains a “helix-turn-helix” motif [362] and NarL regulators control nitrate and nitrite regulated gene expression [365]. RR03 and RR11 are classified as NarL regulators in pneumococci [174]. In *S. pneumoniae*, RR12 and RR13 belong to the **LytR**-type of RRs [174]. Structure analysis of RR12 revealed a series of β-sheets and short α-helices in the DNA binding domain [366]. The **YesN** family, a poorly studied group of RRs in *S. pneumoniae*, presents an HTH_AraC output domain [362].

3.7.4.1. TCS in *Streptococcus pneumoniae*

For successful colonization of the URT *S. pneumoniae* has evolved TCSs and adapted their use to the host compartments. In pneumococci, 13 HK and 13 RR working in pairs plus one orphan RR were identified via genomic analyses [174,340,367]. Their genes also exist paired in an operon, with the *rr* gene usually upstream of the *hk* gene [340]. The coding sequence of these proteins overlaps or is characterized by no more than 11 bp spacing [340]. Similar to other human pathogenic bacteria, some of the TCSs are associated with the virulent properties of the pathogen *S. pneumoniae* [345]. Insertional mutagenesis was used to delete each of the 13 *rr* genes to investigate the regulatory role of these transcription factors. All viable mutants were further characterized in terms of their growth *in vitro*, competence and virulence. Two *rr* genes (*rr02* and *rr13*) could not be inactivated, which is indicative that they regulate essential cellular functions [340]. Virulence studies conducted to assess the role of TCSs demonstrated that 7 TCSs and the orphan RR influence bacterial growth and virulence in a mouse respiratory tract infection model [367]. Pneumococcal TCSs are associated with regulation of different processes such as: i) competence and fratricide (TCS02 (WalRK/VicRK/YycFG), 03 (LiaSR), 05 (CiaRH) and 12 (ComDE)), ii) bacteriocin production (TCS05, 12 and 13 (BlpRH)), iii) virulence factor expression (TCS02, 03, 05, 06 (CbpRS), 08, 09 (ZmpRS) and 10 (VncRS)), iv) response to antibiotic and cell wall perturbations (TCS02, 03, 05 and 11), v) environmental stress (TCS01 (SirRH), 04 (PnpRS), 05, 12 and RR14 (RitR)) and vi) nutrients uptake (TCS04, 05, 07, 08, 09, 12 and RR14) [174,368].

Initial large screening approaches revealed an important role of the **TCS01** (SirRH) during virulence and lung infection [367,369]. Recently, the TCS01 was shown to increase pneumococcal survival in pneumocytes after an influenza A infection by transcription of genes involved in stress response [368]. One essential RR for *S. pneumoniae* is VicR (**RR02**) [340,367], which makes it difficult to assess its role in regulation. A successful approach to study RR02 includes its overexpression [370] or alternatively, the constitutive expression of its regulated gene *pcsB*, which is involved in murein biosynthesis [371,372]. An altered expression of RR02 leads therefore to defects in cell wall synthesis and cell separation [373]. RR02 further regulates the expression of genes in fatty acid biosynthesis [370] and PspA [372]. LiaSR (**TCS03**) of TIGR4 is involved in virulence as deletion of HK03 causes increased survival of intranasally infected mice [374]. In the same study, the association of TCS03 with pili regulation was revealed, as the RR03 binds directly to the *rlrA* promoter [374]. Furthermore, TCS03 responds to cell envelope stress elicited by murein hydrolase during autolysis and fratricide [375]. A vancomycin dependent activation has also been shown [376]. The **TCS04** (PnpRS) showed a clear growth defect *in vitro* and during pneumonia model of infection [367], but no attenuation during bacteremia [340]. It is one of the pneumococcal TCS having a strain specific role during virulence and gene expression [377]. RR04 controls the expression of two phosphate transporters Pst1 and Pst2 [378] and the manganese ABC transporter PsaBCA [377], to support oxidative stress response and virulence [377]. The first TCS described and characterized in *S. pneumoniae* was **TCS05** (CiaRH) [379], which belongs to the EnvZ/OmpR family [340] and is linked to the efficient colonization of pneumococci as well as the oxidative stress response [380,381]. Among others, it regulates the expression of HtrA, a heat-induced surface–associated serine protease with proteolytic activity and chaperone function [380]. Upon loss of the CiaRH operon, there is an up to 1000-fold decrease in the number of bacteria colonizing the nasopharynx and a 25-fold decrease in HtrA expression. Because absence of the HtrA gene causes only an up to 10-fold decrease in nasopharyngeal colonization, CiaRH is thought to regulate other factors as well [380]. Moreover, TCS05 is essential for bacterial aggregation in biofilms [382]. CiaRH is associated with the repression of competence by three mechanisms: i) HtrA digests the CSPs in pneumococci [383]; ii) CiaR controls expression of five sRNAs regulating the CSP precursor coding gene *comC* on post-transcriptional level [336] and iii) repression of *comCDE* operon [384]. The important role of **TCS06** (CbpRS) for virulence was already shown [367] and confirmed with decreased *in vitro* adherence to nasopharyngeal and lung epithelial cells [385]. In an acute pneumonia mouse model, opposite effects of *hk06*-and *rr06*-mutants could be observed as the colony forming units (CFU) of *rr06*-mutants was higher in nasopharynx, lung and blood compared to the wild-type and *hk09*-mutant [385]. Important adhesins like PspC [385], PspA [386] and pili [374] are regulated by the

pneumococcal TCS06, which support its role as an important player during host colonization. It was hypothesized that RR06 activates *pspC* transcription in its nonphosphorylated form [386]. **TCS07** (YesMN) is involved in virulence in pneumonia mouse models [367,369,387]. Recently the regulon of TCS07 was identified in D39, all regulated genes of known function are involved in host glycan and carbohydrate metabolism. In *S. pneumoniae*, glycan scavenging is a major source of vital carbon in niches depleted of free sugars, thus linking the virulence and the TCS07 regulon. A *tcs07*-mutant is incapable of growing on or responding to the glycan model protein fetuin, suggesting that the TCS07 recognizes a complex structure in the glycan [388]. Only a few contrary information are found for **TCS10** (VncRS) as it is possibly involved in vancomycin tolerance [389-391] and pili regulation [391]. Another least studied TCS is the **TCS11**, which is upregulated during vancomycin stress [376]. Very extensively the **TCS12** ComDE has been studied, which has been implicated in genetic competence in response to CSP as discussed [282,286]. TCS12 regulates directly ~ 20 early competence genes [289] and indirectly ~ 80 late competence genes by the expression of the early competence genes *comX* and *comW* [289,291,392-394]. Early studies revealed an increased survival of infected mice by blocking TCS12 [395]. BlpRH (**TCS13**), belonging to the QS of pneumococci, is induced by the autoinducible peptide BlpC [396]. Interestingly, this TCS also responds to BlpC of cocolonizing strains [397]. It controls bacteriocin [396] and immunity peptide production, which play an important role for inter- and intrastrain competition [398] and colonization [399]. TCS12 and TCS13 have similar amino acid sequences leading to possible regulation of the same genes [284]. The orphan **RR14** RitR in *S. pneumoniae* suppresses iron transport and obtains an important role during lung infection [400] and oxidative stress [401]. Interestingly, crystal structure studies revealed no conserved aspartate residue in the REC domain, but an asparagine residue [402]. Since RitR has no pair HK, it is probably phosphorylated by StkP and dephosphorylated by PhpP in its DNA binding domain, giving a new regulatory link between RR and kinases and phosphatases [403].

The special focus of this study lies on TCS08 and TCS09. The HK08 of **TCS08**, an intramembrane histidine kinase with short extracellular loop, is probably required in response to membrane disturbances [349,404]. TCS08 is involved in pneumococcal colonization and fitness by regulating the virulence factors PavB, the *rlrA* islet (Pilus-1) and the cellobiose metabolism. To study the TCS08 regulon, the first transcriptional profiles of *S. pneumoniae* R6 *tcs08*-mutants were analyzed using microarrays. The most downregulated genes of the *hk08*-mutant were *spr_0276* - *spr_0282*, encoding a cellobiose PTS. Growth experiments on cellobiose with *tcs08*-mutants clearly showed a growth defect of the *hk08*-mutant suggesting that TCS08 must be involved in the catabolism of cellobiose [405]. In 2009, the relationship between TCS08 and pili synthesis was investigated in encapsulated serotype 4 pneumococci

(TIGR4). For this purpose, single and double mutants (Δ*rr08*, Δ*hk08*, Δ*tcs08*) were used and the expression of the *rlrA* genes encoding the pili was examined. They showed that *rlrA* expression is upregulated in the Δ*rr08*-mutant and more significant in the late-logarithmic phase. In the Δ*tcs08*-mutant, there was a dramatic increase in adherence to human lung epithelial cells (A549) in the late-logarithmic growth phase. Thus, this study confirmed that the TCS08 of TIGR4 influences the growth-phase-dependent expression of PI-1 components [406]. A link between phase variation and TCS08 was already established as RR08 is significantly differentially expressed in opaque variants and transparent variants [407].

TCS09 is among the pneumococcal TCS whose function and target genes are still incomplete described. The HK09 belongs to the histidine protein kinase class 08 [348] and is characterized by a relatively long contiguous extracellular domain, while its cognate RR09 is part of the YesN subgroup containing an HTH_ARAC DNA binding domain [355]. Initially, it was suggested that TCS09 regulates the expression of the virulence factor ZmpB, but follow up studies were unable to reproduce and confirm this [408,409]. A previous study suggested that the function of TCS09 is connected to metabolism [410] and virulence [411] in a strain dependent manner. Various PTS genes involved in carbon transport were found to be downregulated in an RR09-deficient strain D39, while only three PTS genes (lactose, trehalose and galactitol) showed a similar effect in TIGR4Δ*rr09* [410]. Strain D39 (serotype 2) pneumococci showed a complete avirulent phenotype in the absence of RR09, however, this phenotype was not observed for a serotype 3 and 4 *S. pneumoniae rr09* knock out mutant in a sepsis and acute pneumonia mouse infection model [369,411]. The different outcome of loss of function of RR09 in pneumococci is intriguing, but the reasons for the strain specific effects are unknown and require further evaluation. A recent study showed that the switch between opaque (O) and transparent (T) variants of pneumococci is regulated by 5 RRs. Pneumococci deficient in RR06, RR08, RR09, RR11 or RR14 produced significantly more T- than O-colonies [412]. Furthermore, it was shown that RR06, RR08, RR09 and RR11, respectively, modify the direction of the DNA inversion reaction in the *hsdS* genes (DNA methyltransferases) catalyzed by the tyrosine recombinase PsrA [413], which leads to a higher number of opaque variants [412]. Thus, TCS09 seems to play an important role in fitness and in phase variation, which could have a significant impact on virulence.

3.7.4.2. Why is it of crucial importance to study two-component regulatory systems?

The large number of serotypes poses a major challenge, especially since pneumococci have the capacity for serotype switching through their natural competence [414]. Accordingly, a vaccine should be developed that induces protection independently of the serotype, is based

on T-cell-dependent protein antigens, and is immunologically remembered, even in children. TCSs could also contribute to vaccine development as they have a crucial influence in bacterial response to changing external host stimuli during their course of infection [415,416]. Since TCSs are not found in vertebrates, they may play an important role in the development of new agents against the pathogen [340]. If one focuses on the specific regions of the individual TCSs during production, the drug can be used in a species- and organism-specific manner. Inhibitors of TCSs have been known as antimicrobial agents for some time and may represent a suitable target for combating pathogenic bacteria [417,418]. Several pneumococcal TCSs have been shown to be associated with pathogen growth, survival, and virulence [340,367], but not all TCSs and their regulatory networks in pneumococci are characterized and need further research.

The focus of this study was on the less characterized TCS08 and TCS09. The aim was to identify potential target genes and to characterize their specific role on pneumococcal phenotype, pathophysiology and virulence. For a comprehensive understanding of each component of the TCS08 and TCS09, single (Δ*rr08*, Δ*rr09*, Δ*hk08* or Δ*hk09*) and double mutants (Δ*tcs08* or Δ*tcs09*) were constructed in *S. pneumoniae* D39 and TIGR4.

In the first study, the role of TCS09 on the pathophysiology of *S. pneumoniae* D39 was explored by transcriptome analysis (RNA-seq). The TCS09 in D39 was phenotypically characterized by performing growth analysis in chemically defined medium with different carbon sources. Field emission scanning electron microscopy and transmission electron microscopy were used to study the cell morphology as well as the capsule structure of *tcs09*-mutants. Capsule visualization results were confirmed by flow cytometric analysis and a phase variation approach. Likewise, the autolysis and oxidative stress behavior of the *tcs09*-mutants were investigated.

In the second part of this thesis, the impact of TCS09 on the pathophysiology and virulence of *S. pneumoniae* TIGR4 was reported by *in vitro* adherence and phagocytosis assays and finally by *in vivo* mouse infection assays using the acute pneumonia, septicemia and co-infection model. Further, the abundance of important pneumococcal proteins participating in virulence and bacterial fitness was determined.

Finally, in the third study, pneumococcal TCS08 specific role in fitness, gene expression and virulence was analyzed in *S. pneumoniae* D39 and TIGR4. Possible target genes were identified using microarray and confirmed on protein level by immunoblot and surface abundance assay. The potential impact of TCS08 on virulence was elucidated in experimental acute pneumonia and sepsis infection models.

4. Publications

4.1. Publication 1

The Two-Component System 09 Regulates Pneumococcal Carbohydrate Metabolism and Capsule Expression

4.2. Publication 2

The two-component system 09 of Streptococcus pneumoniae is important for metabolic fitness and resistance during dissemination in the host

4.3. Publication 3

Pneumococcal Metabolic Adaptation and Colonization Are Regulated by the Two-Component Regulatory System 08

4.1. Publication 1

The Two-Component System 09 Regulates Pneumococcal Carbohydrate Metabolism and Capsule Expression

Stephanie Hirschmann, Alejandro Gómez-Mejia, Ulrike Mäder, Julia Karsunke, Dominik Driesch, Manfred Rohde, Susanne Häussler, Gerhard Burchhardt and Sven Hammerschmidt

Published in the journal Microorganisms, 2021 Feb 24;9(3):468.
doi: 10.3390/microorganisms9030468

microorganisms

MDPI

Article

The Two-Component System 09 Regulates Pneumococcal Carbohydrate Metabolism and Capsule Expression

Stephanie Hirschmann [1], Alejandro Gómez-Mejia [1], Ulrike Mäder [2], Julia Karsunke [1], Dominik Driesch [3], Manfred Rohde [4], Susanne Häussler [5], Gerhard Burchhardt [1] and Sven Hammerschmidt [1,*]

[1] Department of Molecular Genetics and Infection Biology, Interfaculty Institute for Genetics and Functional Genomics, Center for Functional Genomics of Microbes, University of Greifswald, 17487 Greifswald, Germany; hirschmans@uni-greifswald.de (S.H.); alejandro.gomezmejia@usz.ch (A.G.-M.); julia.karsunke@gmx.de (J.K.); gerhard.burchhardt@uni-greifswald.de (G.B.)
[2] Department of Functional Genomics, Interfaculty Institute for Genetics and Functional Genomics, Center for Functional Genomics of Microbes, University Medicine Greifswald, 17475 Greifswald, Germany; ulrike.maeder@uni-greifswald.de
[3] BioControl Jena GmbH, 07745 Jena, Germany; dominik.driesch@biocontrol-jena.com
[4] Central Facility for Microscopy, Helmholtz Centre for Infection Research, 38124 Braunschweig, Germany; manfred.rohde@helmholtz-hzi.de
[5] Department of Molecular Bacteriology, Helmholtz Centre for Infection Research, 38124 Braunschweig, Germany; susanne.haeussler@helmholtz-hzi.de
* Correspondence: sven.hammerschmidt@uni-greifswald.de

check for updates

Citation: Hirschmann, S.; Gómez-Mejia, A.; Mäder, U.; Karsunke, J.; Driesch, D.; Rohde, M.; Häussler, S.; Burchhardt, G.; Hammerschmidt, S. The Two-Component System 09 Regulates Pneumococcal Carbohydrate Metabolism and Capsule Expression. *Microorganisms* **2021**, *9*, 468. https://doi.org/10.3390/microorganisms9030468

Academic Editor: Jane Turton

Received: 1 January 2021
Accepted: 22 February 2021
Published: 24 February 2021

Publisher's Note: MDPI stays neutral with regard to jurisdictional claims in published maps and institutional affiliations.

Abstract: *Streptococcus pneumoniae* two-component regulatory systems (TCSs) are important systems that perceive and respond to various host environmental stimuli. In this study, we have explored the role of TCS09 on gene expression and phenotypic alterations in *S. pneumoniae* D39. Our comparative transcriptomic analyses identified 67 differently expressed genes in total. Among those, *agaR* and the *aga* operon involved in galactose metabolism showed the highest changes. Intriguingly, the encapsulated and nonencapsulated *hk09*-mutants showed significant growth defects under nutrient-defined conditions, in particular with galactose as a carbon source. Phenotypic analyses revealed alterations in the morphology of the nonencapsulated *hk09*- and *tcs09*-mutants, whereas the encapsulated *hk09*- and *tcs09*-mutants produced higher amounts of capsule. Interestingly, the encapsulated D39Δ*hk09* showed only the opaque colony morphology, while the D39Δ*rr09*- and D39Δ*tcs09*-mutants had a higher proportion of transparent variants. The phenotypic variations of D39Δ*cps*Δ*hk09* and D39Δ*cps*Δ*tcs09* are in accordance with their higher numbers of outer membrane vesicles, higher sensitivity against Triton X-100 induced autolysis, and lower resistance against oxidative stress. In conclusion, these results indicate the importance of TCS09 for pneumococcal metabolic fitness and resistance against oxidative stress by regulating the carbohydrate metabolism and thereby, most likely indirectly, the cell wall integrity and amount of capsular polysaccharide.

Keywords: *Streptococcus pneumoniae*; two-component system 09; carbohydrate metabolism; capsule

1. Introduction

Living cells rely on sensing and interpreting external signals as an adaptive mechanism against changes in their environment such as oxygen, temperature, and pH. This process is known as signal transduction and allows the cell to react immediately and appropriately to specific alterations in their habitat. One of the main signaling mechanisms used by bacteria are the two-component regulatory systems (TCSs). In bacteria, a TCS consists of a transmembrane protein (histidine kinase (HK)) that functions as a sensor and a corresponding cytoplasmic protein (response regulator (RR)) controlling gene expression. The HK can react to external and internal signals by binding a phosphate group to a conserved histidine residue (autophosphorylation) [1]. In general, a histidine kinase is

specific to its cognate response regulator; however, crosstalk between different TCSs in the bacterial cell can also occur [2].

For successful colonization of the upper respiratory tract, *Streptococcus pneumoniae* (pneumococci) have evolved TCSs and adapted their use to the host compartments. In pneumococci, 13 histidine kinases and 13 response regulators working in pairs plus one orphan response regulator were identified [3–5]. Virulence studies conducted to assess the role of TCSs indicated that 7 TCSs and the orphan response regulator influence bacterial growth and virulence in a mouse respiratory tract infection model [4]. Pneumococcal TCSs are associated with regulation of different processes such as competence and fratricide (TCS02 (WalRK/VicRK/YycFG), 03, 05 (CiaRH), and 12 (ComDE)), bacteriocin production (TCS05, 12, and 13 (BlpRH)), virulence factor expression (TCS02, 03, 05, 06 (CbpRS), 08, 09 (ZmpRS), and 10 (VncRS)), response to antibiotic and cell wall perturbations (TCS02, 03, 05, and 11), environmental stress (TCS01 (SirRH); TCS04 (PnpRS), 05, and 12; and RR14 (RitR)) and nutrients uptake (TCS04, 05, 07, 08, 09, and 12 and RR14) [5,6]. We have shown previously that TCS08 is involved in pneumococcal colonization by regulating the virulence factors PavB, the *rlrA* islet (Pilus-1), and the cellobiose metabolism. Moreover, the TCS08 effect on regulatory processes including colonization is strain-dependent, as shown in a murine model when comparing *S. pneumoniae* strains TIGR4 and D39 [7]. Recently, TCS01 (SirRH) was shown to increase pneumococcal survival in pneumocytes after influenza An infection by transcription of genes involved stress response [6].

TCS09 is among the pneumococcal TCSs whose function and target genes are still unknown. The histidine kinase 09 belongs to the histidine protein kinase class 08 [8], while its cognate RR09 is part of the YesN subgroup containing an HTH_ARAC DNA binding domain [9–11]. Initially, it was suggested that TCS09 regulates the expression of the virulence factor ZmpB, but follow up studies were unable to reproduce and confirm this [12–15]. A previous study suggested that the function of TCS09 is connected to metabolism and virulence [15,16]. Using microarray analysis, it was reported that pneumococcal gene regulation by TCS09 is strain-dependent and that TCS09 plays a role in metabolic processes. Various PTS genes involved in carbon transport were found to be downregulated in an RR09-deficient strain D39, while only three PTS genes (lactose, trehalose, and galactitol) showed a similar effect in TIGR4Δ*rr09* [15]. A strain-specific effect of RR09 deficiency was reported with respect to virulence. Strain D39 (serotype 2) pneumococci showed a complete avirulent phenotype in the absence of RR09; however, this phenotype was not observed for a serotype 3 and 4 *S. pneumoniae rr09* knock out mutant in a sepsis and acute pneumonia mouse infection model [16]. The different outcome of loss of function of RR09 in pneumococci is intriguing, but the reasons for the strain specific effects are unknown and require further evaluation. A recent study showed that the switch between opaque (O) and transparent (T) variants of pneumococci is regulated by five response regulators. Pneumococci deficient in RR06, RR09, RR11, or RR14 produced significantly more T than O colonies. Furthermore, it was shown that RR06, RR08, RR09, and RR11, respectively, modify the direction of the DNA inversion reaction in the *hsdS* genes (DNA methyltransferases) catalyzed by the tyrosine recombinase PsrA, which leads to a higher number of opaque variants [17,18]. Thus, TCS09 seems to play an important role in fitness and in phase variation, which could have a significant impact on virulence. In this study, we have explored the role of TCS09 on the pathophysiology of *S. pneumoniae* by transcriptome analysis (RNA-seq) of strain D39 employing mutants deficient for the response regulator (Δ*rr09*), the histidine kinase (Δ*hk09*), and both TCS09 components (Δ*tcs09*). Our data suggest potential target genes for the TCS09 of D39 that are involved in capsule modulation and fine-tuning of the metabolism but not virulence.

2. Materials and Methods

2.1. Bacterial Strains and Culture Conditions

Encapsulated and nonencapsulated (Δ*cps*) *Streptococcus pneumoniae* serotype 2 (D39) parental strains and isogenic *tcs09*-mutants (Table 1) were used in this study. Pneumococci

grown on blood agar plates (Oxoid, Wesel, Germany) with appropriate antibiotics were inoculated in chemically-defined medium (CDM) $RPMI_{modi}$ (RPMI1640: GE Healthcare; $RPMI_{modi}$: [19]) supplemented with 1% *w/v* glucose or galactose or Todd Hewitt Broth (Roth) supplemented with 0.5% yeast extract and cultivated at 37 °C without agitation up to middle logarithmic phase (OD_{600nm} 0.6). *Escherichia coli* DH5α was used as a host strain for recombinant plasmids for *rr09*, *hk09*, and *tcs09* mutagenesis and cultivated at 37 °C on LB agar or liquid culture with 200 µg/mL erythromycin and 120 rpm agitation.

Table 1. *S. pneumoniae* wild-type strains and mutants used in this study.

Strain	Capsule Type	Resistance	Knockout Genes	Reference
D39	2	-	-	[20]
D39Δ*rr09*	2	erythromycin	*spd_0574*	This study
D39Δ*hk09*	2	erythromycin	*spd_0575*	This study
D39Δ*tcs09*	2	erythromycin	*spd_0574*, *spd_0575*	This study
D39Δ*cps*	2	kanamycin	*spd_0312–spd_0333*	[21]
D39Δ*cps*Δ*rr09*	2	kanamycin, erythromycin	*spd_0312–spd_0333*, *spd_0574*	This study
D39Δ*cps*Δ*hk09*	2	kanamycin, erythromycin	*spd_0312–spd_0333*, *spd_0575*	This study
D39Δ*cps*Δ*tcs09*	2	kanamycin, erythromycin	*spd_0312–spd_0333 spd_0574*, *spd_0575*	This study

2.2. Molecular Biological Techniques

Chromosomal DNA isolation from pneumococci was performed using phenol-chloroform methodology. In brief, bacteria were cultivated in THY and harvested by centrifugation. The pellet was resuspended in TES buffer and treated with lysozyme, pronase E, RNase A, and N-lauryl sarcosine. Finally, phenol and phenol:chloroform:isoamyl alcohol (25:24:1 ratio) were used to separate the DNA. The resulting DNA was washed with 96% ethanol and stored in Tris-EDTA buffer at −20 °C until further experimentation. DNA regions for mutant generation were amplified by PCR, and the oligonucleotides used (Eurofins MWG, Ebersberg, Germany) are listed in Table 2. PCR products were purified using the Zymoclean Gel DNA Recovery Kit (Zymo Research, Freiburg, Germany), and plasmid DNA (Table 3) was isolated using the Wizard® Plus SV Minipreps DNA Purification System (Promega). The T4 DNA ligase and restriction enzymes were purchased from Thermo Fisher Scientific and New England Biolabs and used according to the manufacturer's instructions. Transformation of *E. coli* with recombinant plasmids was conducted with calcium chloride competent cells. Transformants were selected on LB agar containing 5 µg/mL erythromycin, and plasmids sequences were verified by DNA sequencing (Eurofins MWG, Ebersberg, Germany).

2.3. Generation of Pneumococcal Mutants

Pneumococcal Δ*rr09* (*spd_0574*; SPD_RS03105), Δ*hk09* (*spd_0575*; SPD_RS03110), and Δ*tcs09*, lacking the *rr09* and *hk09* mutants, were constructed by insertion-deletion mutagenesis (Figure S1). Transformation of *S. pneumoniae* D39 using the constructed plasmids was performed in the presence of competence-stimulating peptide CSP1, as described [7]. Transformants were selected on blood agar plates containing 5 µg/mL erythromycin, and all mutants were confirmed on the molecular level by colony PCR and RNA-sequencing.

To generate RR09-deficient pneumococci, the gene *spd_0574* with 600 bp flanking regions upstream and downstream was PCR amplified with primers 1122/1123. The resulting 2049 bp DNA fragment was ligated via TA cloning into vector pGXT [22] and transformed into competent *E. coli* DH5α. To delete the *rr09* gene, the recombinant plasmid pGXT_*rr09* was used as a template for an inverse PCR with primers 1124/1232, which have an incorporated *Hin*dIII restriction site. The PCR product was ligated with the erm^R cassette amplified with primers 105/106 (pGXTΔ*rr09*::erm^R) and transformed into competent *E. coli* DH5α.

Table 2. Primers used for mutagenesis.

No.	Primer	Sequence 5′-3′	Restriction Site
100	MC-Erm-R	CCCGGGGAAATTTTGATATCGAT**AAGCTT**GAATTCCCGTA GGCGCTAGGGACCTC	*Hin*dIII
105	Erm Forw	GATGATGATGATCCCGGGTACC**AAGCTT**GAATTCACGG TTCGTGTTCGTGCTG	*Hin*dIII
106	Erm rev	AGTGAGTGAGTCCCGGGCTCGAG**AAGCTT**GAATTCGTAGG CGCTAGGGACCTC	*Hin*dIII
1122	*rr09*_Start Forw	CAGAACGAGCTTTCTCAAACC	
1123	*rr09*_End Rev	GCCTCCATTTTGCTAGACGA	
1124	*rr09*_End Forw	CTCACTG**AAGCTT**GAGATCGCAGAGAAGGTTGG	*Hin*dIII
1125	*rr09*_Start Rev	ATCATC**GCTAGC**GTAGGCTGCTACATTGACC	*Nhe*I
1126	*hk09*_Start Forw	GGTCAATGTAGCAGCCTACGA	
1127	*hk09*_End Rev	CGCACCTCCGATTAATTTTG	
1128	*hk09*_End Forw	CTCACTG**AAGCTT**CGATCAACGGCTCAAACTTC	*Hin*dIII
1129	*hk09*_Start Rev	ATCATC**GCTAGC**CAACCAGAGCTAGGAGAA	*Nhe*I
1232	*rr09*_sr_fw *Hin*dIII	ATCATC**AAGCTT**GTAGGCTGCTACATTGACC	*Hin*dIII
1234	*Nhe_erm* f	GCTT**GCTAGC**GACGGTTCGTGTTCGTGCTG	*Nhe*I

Restriction sites are shown in bold.

Table 3. Plasmids used for mutagenesis.

Plasmids	Properties	Source
pGXT	pGEM-T Easy backbone, linker region with toxic gene *ccdB* (Flanked by two *Xcm*I sites), TA cloning vector (3047 bp), Amp^R, Pt7, *lacZ*	[22]
pGSP72N	pSP72 derivative, *Hin*dIII restriction site eliminated, generation of a *Nhe*I restriction site	This study
pSP72	Cloning vector (2462 bp), Amp^R	Promega
pGXTΔ*rr09*::erm^R	pGXT derivative vector with the subcloned 5′ and 3′-end homolog fragments of *spd_0574* interrupted by *ermB* resistance gene cassette for mutagenesis	This study
pGSP72NΔ*hk09*::erm^R	pGSP72N derivative vector with the subcloned 5′ and 3′-end homolog fragments of *spd_0575* interrupted by *ermB* resistance gene cassette for mutagenesis	This study
pSP72Δ*tcs09*::erm^R	pSP72 derivative vector with the subcloned 5′ end homolog fragment of *spd_0574* and 3′ end homolog fragment of *spd_0575* interrupted by *ermB* resistance gene cassette for mutagenesis	This study

For the construction of the vector pGSP72NΔ*hk09*::erm^R, the 3′ flanking region of *spd_0575* was amplified using primers 1127/1128. The erythromycin resistance gene cassette (erm^R) was amplified with primers 1234 and 100. These two DNA fragments were digested with the restriction enzyme *Hin*dIII and ligated, and amplified by PCR with primers 1234/1127. This PCR product was ligated into *Eco*RV linearized vector pGSP72N (this study) and transformed into competent *E. coli* DH5α resulting in pGSP72N_erm^R-3′*hk09*. The 5′ flanking region of the gene *spd_0575* was amplified with primers 1126/1129 and digested with *Nhe*I. This DNA fragment was ligated with *Nhe*I and *Sma*I cleaved vector pGSP72N_erm^R-3′*hk09*, and the ligation product was transformed into competent *E. coli* DH5α cells.

To produce the mutagenesis plasmid pSP72Δ*tcs09*::erm^R, the 5′ flanking region of *spd_0574* and the 3′ flanking region of *spd_0575* were amplified by PCR using primers

1122/1125 and 1128/1127. The obtained PCR fragments were digested with *Nhe*I (5′-*spd_0574*) and *Hin*dIII (3′-*spd_0575*), respectively, and genetically fused with a similarly digested erythromycin resistance gene (erm^R), which was amplified with the primers 1234 and 106. A PCR reaction using the three PCR products with primers 1122 and 1127 was conducted to obtain a mutated *spd_0574* DNA region. This DNA fragment was ligated into vector pSP72 (Promega), which was linearized with *Eco*RV. The genes downstream (or upstream) of the genes knocked-out by the insertion-depletion strategy are continuously expressed, and their expression level is not changed. This is clearly shown in the RNA-seq data (log_2-fold change RNA expression pattern) (Table S1).

2.4. RNA Purification

Pneumococcal strain D39 and isogenic Δ*rr09*-, Δ*hk09*-, and Δ*tcs09*-mutants were cultivated in glucose supplemented $RPMI_{modi}$ up to an OD_{600nm} of 0.6. Ice cold killing buffer (20 mM Tris HCl pH 7.5, 5 mM $MgCl_2$, 20 mM NaN_3) was added to the bacterial cultures and centrifuged for 10 min at 3200× *g* at 4 °C. The supernatant was removed and the bacterial pellets were immediately frozen in liquid nitrogen and stored at −80 °C. For total RNA extraction, the samples were treated with acidic phenol-chloroform and subjected to TURBO™ DNase (2 U/reaction; Invitrogen, Carlsba, CA, USA) digestion to remove genomic DNA. The RNA was purified using RNA cleanup and concentration kit (Norgen Biotek Corp., Thorold, ON, Canada). The RNA quality was controlled with Agilent 2100 Bioanalyzer (Figure S2), and the amount of RNA was measured using a NanoDrop ND-1000 spectrophotometer (Peqlab). Four replicates were prepared per strain and mutant.

2.5. RNA-Sequencing

Libraries for transcriptomics were generated according to Shishkin et al., 2015 and Bhattacharyya et al., 2019 [23,24]. Briefly, 1 µg of total RNA was fragmented in 150–350 bp, and phosphate groups at the 3′ and 5′ end were removed using FastAP (Thermo Scientific). A further DNA digestion step with the TURBO™ DNase (Invitrogen, Carlsba, CA, USA) was carried out. The fragmented RNA was purified with RNA Clean XP Beads following ligation of phosphorylated barcoded DNA adapters (L01–L32; Table S2) to the fragmented RNA by a T4 RNA ligase (NEB) with final column-based (RNA clean & concentrator-25, purchased from Zymo Research) purification of the ligated RNA. The rRNA was removed with the RiboZero Kit, and RNA was purified again with the RNA Clean XP Beads. A reverse transcription to cDNA with the two primers AR2 and 3Tr3 (Table S3) was performed and followed by subsequent removal of the untranscribed RNA using RNA Clean XP Beads. The purified cDNA was enriched by PCR using primers P5 and X01 (Table S3), while a second DNA adapter was added. The cDNA was then purified again with Clean XP Beads. Sequencing on NovaSeq 6000 (Illumina, San Diego, CA, USA) followed in paired-end mode with 50 cycles. Fastq files were assessed for sequence quality using FastQC (version 0.11.5), and an index from the genome from the file NC_008533 (D39) was created with bowtie2 (version 2.3.4.3). The mapping of the reads to the index was also performed with bowtie2. Reads were counted and assigned to the corresponding genome using function featureCounts of R package Rsubread (version 2.2.2). Contrasts were calculated using R package DESeq2 (version 1.28.1). R version 3.4.4 was used. To analyze the differential gene expression of the mutants vs. wild-type (referred as control), DESeq2 (version 1.18.1) was used. A log_2 fold change threshold was set to 1 and an adjusted p-value cutoff of 0.05. Heatmaps were created using ClustVis [25].

2.6. Quantitative Real-Time PCR (qPCR)

Isolated RNA was transcribed in cDNA using Superscript III reverse transcriptase (Thermofisher, Waltham, MA, USA) and random hexamer primers (BioRad, Hercules, CA, USA) according the instructions of the manufacturer. A StepOnePlus thermocycler (Applied Biosystems, Foster City, CA, USA) and the iTaq Universal SYBR Green Supermix

(BioRad) were used for quantitative real-time PCR. Enolase (*spd_1012*) was used as a reference gene and to correct for sample variation regarding, for example, reverse transcriptase efficiency. The enolase gene expression was not significantly changed in the mutants, as indicated by RNA-seq (Table S1). The *agaR* (*spd_0064*), *gadV* (*spd_0066*), *celA* (*spd_0277*), *eng* (*spd_0335*), and *spd_1588* genes were used as targets (Primer list Table 4). The qPCR conditions using 20 ng/µL cDNA as a template were as followed: initial denaturation at 95 °C for 2 min, denaturation at 95 °C for 15 s, primer annealing at 60 °C for 30 s, and extension at 72 °C for 30 s for 40 cycles with a final melting curve step for quality control. Differential gene expression was calculated by the Pfaffl method [26].

Table 4. Primers used for qPCR.

Target Gene	Primer	Sequence 5′→3′
enolase (*spd_1012*)	*eno*RT_F *eno*RT_R	CGGACGTGGTATGGTTCCA TAGCCAATGATAGCTTCAGCA
agaR (*spd_0064*)	qPCR *agaR* Forward qPCR *agaR* Reverse	TCATTTCAATGTACGATGTCAG GTTTGCGTGCACGTGAAACG
gadV (*spd_0066*)	qPCR *gadV* Forward qPCR *gadV* Reverse	ACGACGAAGTTGTCAACAACG GAGACGTTGGCTATCGTATTT
celA (*spd_0277*)	qPCR *celA* Forward qPCR *celA* Reverse	ATGTTATGACTGCTGGTCGTC CCATTTCAGCAAAAAGTGCTAT
eng (*spd_0335*)	qPCR *eng* Forward qPCR *eng* Reverse	GTCCGGTTCTTGCAGATAGC CCACCTTAGGCGCTTCAAAA
spd_1588	qPCR *spd_1588* Forward qPCR *spd_1588* Reverse	GTATTCATCTACTTAGCTGGAG ACATCACAACTAAAATGGATAATA

2.7. Field Emission Scanning Electron Microscopy (FESEM)

Bacteria were cultivated in CDM with glucose as a carbon source until OD_{600nm} 0.6 at 37 °C. After centrifugation, the encapsulated strains were fixed with precooled 2.5% glutardialdehyde, 2% paraformaldehyde, 0.075% ruthenium red, and 75 mM L-lysine acetate salt in cacodylate buffer on ice for 20 min (Lysine-ruthenium-red (LRR) fixation) and washed with cacodylate buffer containing 0.075% ruthenium red. Subsequently, in a second fixation step, the sediment was resuspended with precooled fixing solution (without L-lysine acetate salt) and incubated on ice for 2 h. After washing three times with cacodylate buffer and 0.075% ruthenium red, the samples were dissolved in 1% osmium solution (containing ruthenium red) and incubated at room temperature for 1 h. Finally, the sediment was washed twice with HEPES buffer. Nonencapsulated strains were fixed with 2% glutardialdehyde and 5% paraformaldehyde.

Bacterial aliquots were placed on cover slips, fixed with 1% glutaraldehyde, washed with TE buffer, and dehydrated in a graded series of acetone (10, 30, 50, 70, 90, and 100%) on ice for 10 min for each step. Critical-point drying of the samples was performed with liquid CO_2 (CPD 30, Bal-Tec, Pfäffikon, Switzerland). Subsequently, the dried samples were covered with palladium-gold film by sputter coating (SCD 500, Bal-Tec) before examination in a field emission scanning electron microscope (Zeiss Merlin, Jena, Germany) using the HESE2 Everhart Thornley SE detector and the in-lens SE detector in a 75:25 ratio at an acceleration voltage of 5 kV.

2.8. Transmission Electron Microscopy (TEM)

For TEM, the fixed bacteria were mixed with an equal volume of 2% water agar, solidified, and cut into small cubes. This was followed by dehydration in a graded series of ethanol (10, 30, and 50%) on ice. Subsequently, nonencapsulated strains were incubated in 70% ethanol containing 2% uranyl acetate overnight at 7 °C, whereas LRR fixed samples were incubated in 70% ethanol without uranyl acetate. Afterwards, all samples were dehydrated with 90% and 100% ethanol and infiltrated with aromatic acrylic resin LRWhite

(London resin company, London, UK) by applying, firstly, 1 part 100% ethanol and 1 part LRWhite overnight and, secondly, 1 part ethanol and 2 parts LRWhite for 24 h on ice. Pure LRWhite was added with two exchanges within 2 days. Finally, samples were placed in gelatin capsules and filled with pure LRWhite resin. LRWhite resin was polymerized for 2–4 days at 50 °C. Ultrathin sections were cut and counterstained for 3 min with 4% aqueous uranyl acetate. Samples were examined in a Zeiss TEM 910 transmission electron microscope at an acceleration voltage of 80 kV and at calibrated magnifications.

2.9. Flow Cytometric Analysis of Capsular Polysaccharide Abundance

The relative abundance of the capsular polysaccharide (CPS) of *S. pneumoniae* D39 and isogenic mutants was measured by flow cytometry, as described [27]. Briefly, pneumococci were grown in CDM with glucose as a carbon source to a final OD_{600nm} 0.6. After sedimentation and resuspension in PBS 2×10^8, CFU pneumococci were incubated for 45 min with specific anti-serotype 2 antibodies (Staten Serum Institute, Copenhagen, Denmark) at 4 °C. Pneumococci were washed with PBS, and bound primary antibodies were labelled with Alexa Fluor 488 conjugated anti-rabbit antibodies (abcam) at 4 °C. Pneumococci were finally fixed with 1% paraformaldehyde, and the fluorescence intensity was analyzed by flow cytometry using a FACS Calibur (BD Biosciences, Heidelberg, Germany). The forward and sideward scatter dot plots were used to detect fluorescent pneumococci. A gating region was set to exclude cell debris and larger bacteria aggregates. At least 50,000 pneumococci (events) were analyzed. The geometric mean fluorescence intensity multiplied by the percentage of bacteria in complex with fluorescent labelled bacteria was calculated and used as a relative value for the capsule amount.

2.10. Visualization of Pneumococcal Colony Phase Variation

Pneumococcal strain D39 and isogenic mutants were cultivated in CDM at 37 °C until the mid-logarithmic phase (OD_{600nm} 0.6). Afterwards, 200 CFU per strain and mutant were plated on Tryptic Soy Agar (TSA) plates containing 1,000,000 U catalase. The plates were incubated at 5% CO_2 at 37 °C for 16 h. The colonies were evaluated for their opacity under oblique transmitted light using a Leica M125 C dissecting microscope and LAS X software.

2.11. Autolysis Assay with Triton X-100

The autolysis assay was conducted, as described [28]. In brief, pneumococci grown in CDM were adjusted to an OD_{600nm} of 1 in a solution of PBS in the presence of 0.01% or 0.005% Triton X-100 or in the control reaction, in the absence of Triton X-100. The samples were incubated at 37 °C and 5% CO_2, and the absorbance (OD_{600nm}) was measured every 10 min using a spectrophotometer to quantify cell lysis.

2.12. Hydrogen Peroxide Toxicity Test

Pneumococci were cultivated until the mid-logarithmic phase (OD_{600nm} 0.6) in CDM at 37 °C without agitation. Next, 10 mL cultures ($n = 3$ per strain) were prepared with a final concentration of 0, 5, or 10 mM hydrogen peroxide. The samples were incubated at 37 °C for 30 min. Subsequently, serial dilutions were prepared, plated on blood agar plates, and CFU were counted after 20 h incubation at 37 °C and 5% CO_2.

2.13. Statistical Analysis

Unless stated otherwise, all the data collected in this study are presented as mean of at least three independent experiments with standard deviation ±SD. The results were statistically evaluated using a two-way ANOVA or the unpaired two-side student's *t*-test (GraphPad Prism 5.01). A p-value < 0.05 was considered as statistically significant.

3. Results

3.1. HK09 of TCS09 Is Essential for Optimal Growth Of Pneumococci under Defined In Vitro Conditions

To investigate the impact of TCS09 on pneumococcal fitness and physiology in a chemically-defined medium (CDM), we cultivated RR09-, HK09-, and TCS09-deficient pneumococci and their isogenic parental strains D39 and D39Δ*cps* in a CDM with glucose or galactose as a carbon source [19]. The growth kinetics of nonencapsulated mutant strains deficient for RR09, HK09, or the complete TCS09 in CDM with glucose as carbon source were similar to the isogenic parental nonencapsulated strain D39Δ*cps* (Figure 1). In contrast, the encapsulated mutant D39Δ*hk09* showed a significantly ($p < 0.001$) longer generation time (g = 129 min) and final bacterial cell density, as indicated by a lower optical density at 600 nm when compared to the encapsulated wild-type strain D39 (g = 79 min) (Figure 1B). The D39Δ*tcs09*-mutant had only a slightly increased generation time (g = 107 min) compared to wild-type D39 (Figure 1C). When we used galactose as a carbon source, encapsulated pneumococci showed an extended lag phase compared to the cultures with glucose as a carbon source (Figure 1G–I). In galactose containing CDM, loss of HK09 substantially decelerated the growth (2.1 fold longer generation time) of encapsulated pneumococci, while the loss of TCS09 had only a minor effect (1.2 fold) (Figure 1H,I and Table 5). Interestingly, the nonencapsulated *hk09*- and *tcs09*-mutants were not able to grow in galactose supplemented CDM (Figure 1K,L and Table 5). Thus, under heterofermentative growth conditions, the deficiency of HK09 or the complete TCS09 in the encapsulated strain significantly decelerate growth (Figure 1H,I) and lead to a loss of growth in the nonencapsulated strains. Additionally, encapsulated and nonencapsulated D39 parental strains and their isogenic *tcs09*-mutants were cultured in THY, where no growth defects of the *tcs09*-mutants were observed (data not shown). Taken together, loss of HK09 or the complete TCS09 in *S. pneumoniae* significantly affects pneumococcal growth kinetics depending on the carbon source available under nutrient defined conditions.

Table 5. Characteristic growth parameters of strains D39, D39Δ*cps*, and isogenic mutants.

Strain	Growth Rate [h^{-1}]	Max OD_{600nm}	Generation Time ± SD [min]
glucose			
D39	0.5252	1.199	79.3 ± 4.3
D39Δ*rr09*	0.5503	1.125	75.7 ± 2.6
D39Δ*hk09*	0.3226	0.943	128.7 ± 8.4
D39Δ*tcs09*	0.3859	1.173	107.3 ± 11.2
D39Δ*cps*	0.3224	0.910	135.3 ± 36.8
D39Δ*cps*Δ*rr09*	0.3296	0.927	135.8 ± 46.3
D39Δ*cps*Δ*hk09*	0.3804	0.900	114.3 ± 35.6
D39Δ*cps*Δ*tcs09*	0.3664	0.880	114.5 ± 14.4
galactose			
D39	0.3174	1.436	131.2 ± 4.5
D39Δ*rr09*	0.3546	1.313	117.4 ± 3.4
D39Δ*hk09*	0.1878	0.909	277.4 ± 148.3
D39Δ*tcs09*	0.2611	1.002	160.3 ± 14.4
D39Δ*cps*	0.4614	1.073	90.1 ± 5.1
D39Δ*cps*Δ*rr09*	0.5917	1.027	70.2 ± 1.9
D39Δ*cps*Δ*hk09*	0.2830	0.251	148.6 ± 17.9
D39Δ*cps*Δ*tcs09*	0.2779	0.241	149.7 ± 5.2

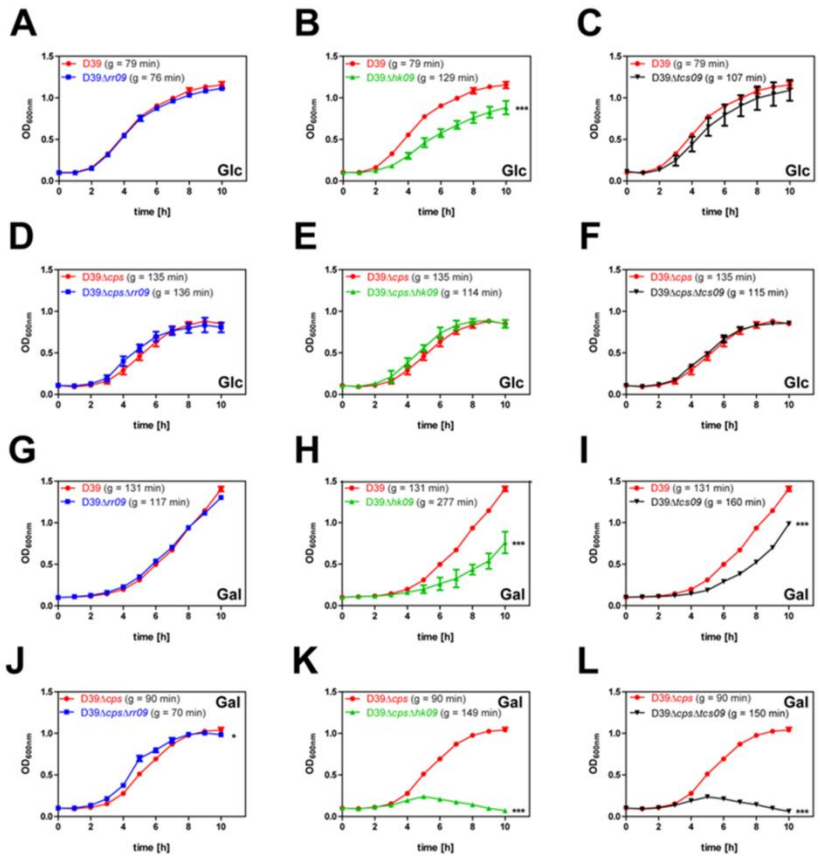

Figure 1. Growth kinetics of RR09-, HK09-, and TCS09-deficient D39 pneumococci and parental strains under defined nutrient resources. The parental strains D39 or D39Δ*cps* and their isogenic Δ*rr09*-, Δ*hk09*-, and Δ*tcs09*-mutants were cultivated in a chemically-defined medium (CDM) with glucose or galactose as a carbon source at 37 °C under microaerophilic conditions. (**A**–**F**) Growth behavior with glucose as a carbon source. (**G**–**L**) Growth kinetics with galactose as the sole carbon source. Results are presented as the mean ± SD for three independent experiments. The mean value of the generation time of the respective strain is given in brackets. A two-way ANOVA proved a significance with *p*-value * < 0.05 and *** < 0.001 relative to the parental pneumococcal strain. g: generation time.

3.2. Analysis of the D39 Transcriptome under In Vitro Conditions

To assess the effects of the TCS09 components on the transcriptome level under nutrient defined conditions, we cultured the encapsulated *S. pneumoniae* D39 and isogenic mutants in glucose supplemented CDM and isolated total RNA from pneumococci collected in the exponential growth phase (OD_{600nm} 0.6). We performed RNA-seq analysis using four biological replicates per strain and assessed the overall variance in gene expression by means of Principal Component Analysis (PCA) (Figure 2A). Interestingly, only the samples obtained from D39Δ*hk09* were clearly separated from those of the wild-type D39 and other mutants. The respective biological replicates grouped together, except for the D39Δ*tcs09* samples, where two replicates clustered together with the wild-type and Δ*rr09* samples, and two replicates were separated from all other samples. Our further analysis revealed that in the two deviant samples of D39Δ*tcs09*, especially genes belonging to the competence cluster of *S. pneumoniae*, were highly upregulated (Table S1 and Figure S3).

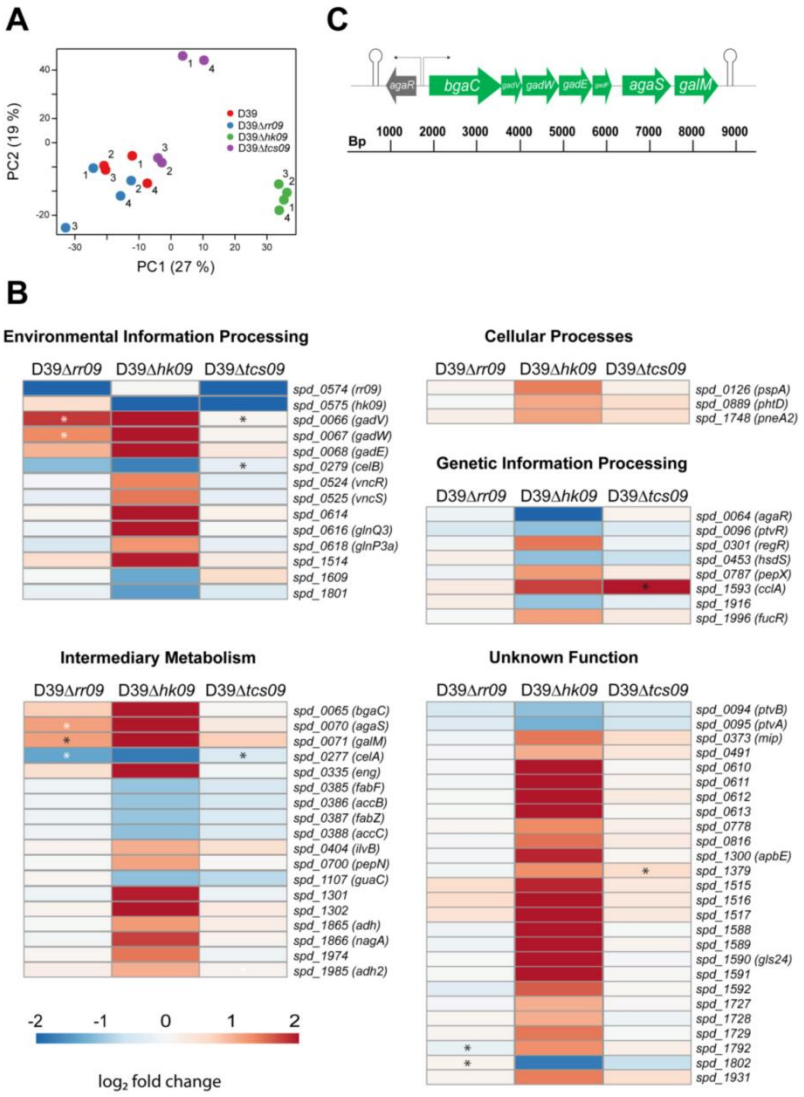

Figure 2. Expression profile of two-component regulatory system 09 mutants. (**A**) Principal component analysis (PCA) of all *S. pneumoniae* samples with color codes. (**B**) Heat maps showing genes with altered expression compared to the wild-type strain D39. Red boxes show upregulation and blue boxes show downregulation in gene expression. The heat maps are divided into different functional categories. The boxes represent the average $\log_2$ fold change values of four replicates of each strain. A black asterisk (*) means that the coefficient of variation (CV) values of the corresponding gene in the strain replicates is > 1.5 x interquartile range (IQR). White stars indicate a significantly different expression pattern. All presented genes in D39Δ*hk09* are significantly changed. Heat maps showing the $\log_2$ fold changes in individual replicates of D39Δ*rr09*, D39Δ*hk09*, and D39Δ*tcs09* are depicted in Figure S5. (**C**) Genomic organization of the *aga* operon in *S. pneumoniae* D39. Genes within the *aga* operon are shown in green, and the gene encoding AgaR is upstream of the *aga* operon and shown in grey. The large and filled arrows represent their relative gene size and orientation in the genome. Transcriptional start sites are indicated with thin arrows and terminators with lollypops. Schematic representation was designed according to information from the Pneumobrowser (https://veeninglab.com/pneumobrowse visited on 19 September 2020).

For the analysis of differential gene expression in the mutants compared to the wild-type $\log_2$ expression levels < −1 and > 1 and an adjusted p-value < 0.05 were considered significant. Because we observed a heterogenous transcriptome between the replicates of D39Δ*tcs09*, the coefficient of variation (CV) values of the individual genes in all strains were determined for all strains, and genes with values > 1.5 x interquartile range (IQR) were not considered for further analysis and are displayed in the heat maps with black asterisks (Figures 2B and S5). According to the specified criteria, a total of 67 protein encoding genes showed significant differences in expression between one of the three mutants and the D39 wild-type. Four genes in D39Δ*rr09*, 67 genes in D39Δ*hk09*, and 0 genes in D39Δ*tcs09* were differentially regulated compared to the wild-type D39 (Figures 2B and S4, Table S1). Most of these genes encode proteins with functions in intermediary metabolism (18 genes), environmental information processing (12 genes), and genetic information processing (8 genes) (Figure 2B and Table S1). The highest change in mRNA level within the category of transporters was detected for the PTS encoding *aga* operon *gadVWEF* (galactosamine-specific PTSBCDA component), which was upregulated in the *rr09*- (fold change: 2.2–3.4) and *hk09*-mutants (fold change: 20.2–38.6). In addition, *bgaC*, *agaS*, and *galM*, all involved in galactose metabolism and located in the same operon as *gadVWEF*, exhibited similarly increased mRNA levels in the *rr09*- and *hk09*-mutants as *gadVWEF*. Notably, in the HK09 deficient encapsulated D39 mutant, the mRNA level of *agaR* (*spd_0064*), which is a transcriptional regulator of the GntR family and acts as repressor of the *aga* operon [29], was strongly downregulated (fold change: 17.5). AgaR, also referred to as CpsR, is also suggested to be involved in capsule expression regulation [30]. The only major virulence factors contributing to host-pathogen interactions we found to be significantly upregulated on the mRNA level in the *tcs09*-mutants of D39 were *pspA* (*spd_0126*) and *phtD* (*spd_0889*) in D39Δ*hk09*. Moreover, we identified a number of genes coding for proteins with unknown function that were differentially expressed (Figure 2B, Figure S5 and Table S1).

3.3. HK09 Regulates Capsule Expression and Carbohydrate Metabolism

To study the effects of *tcs09*-deletion on the pneumococcal genes involved in metabolic processes, capsule regulation, and competence, we used qPCR to validate the findings of the RNA-seq analysis. For qPCR, we repeated the isolation of RNA from D39 wild-type bacteria and isogenic *tcs09*-mutants grown in CDM with glucose as a carbon source. For the Δ*rr09*-mutant, we observed a 2.3 fold increase of mRNA expression of *spd_1588*, a hypothetical protein, whereas *agaR*, *gadV* (galactose metabolism), *celA* (cellobiose metabolism), and *eng* (unclassified carbohydrate metabolism) expression was unaffected compared to the wild-type (Figure 3A). In D39Δ*hk09*, we determined significant upregulation of *gadV* (44.1 fold), *eng* (93.4 fold), and *spd_1588* (23.5 fold) and a significant downregulation of *agaR* (8.8 fold) (Figure 3A). These results are in agreement with our RNA-seq analysis, which showed similar fold changes. Additionally, qPCR with the Δ*tcs09*-mutant revealed higher expression of *spd_1588* (2.2 fold) (Figure 3A). Because the RNA-seq data showed an inconsistent gene expression of the competence cluster in D39Δ*tcs09*, we analyzed the expression of four competence genes by qPCR. Importantly, the qPCR results indicated no significant effect of TCS09 deletion in the regulation of the competence genes (Figure 3B).

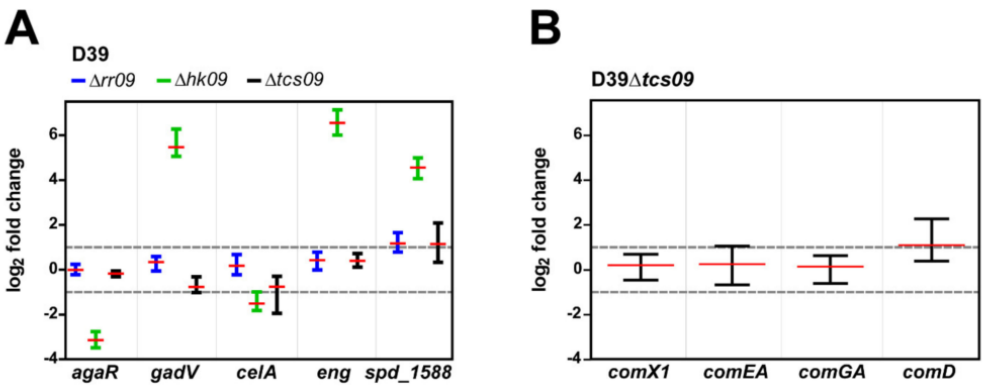

Figure 3. Differential gene expression in *S. pneumoniae* D39 and isogenic *tcs09*-mutants using qPCR. Pneumococci were grown in CDM with glucose to OD_{600nm} of 0.6; the RNA was isolated and reverse transcribed into cDNA. As indicated by dotted lines, log_2 fold changes < −1 and > 1 were set as significant for differential gene expression. (**A**) Differential gene expression of *agaR*, *gadV*, *celA*, *eng*, and *spd_1588*. (**B**) Differential gene expression of the competence genes *comX1*, *comEA*, *comGA*, and *comD*. The log_2 fold changes of differential gene expression in four replicates and their means are presented.

3.4. Phenotypic Characterization of TCS09-Deficient Pneumococci

Expression of *agaR* was significantly downregulated in the *hk09*-mutant, and mutants deficient for HK09 showed an altered growth behavior (Figure 1) as well as an upregulation of the genes involved in metabolic processes (Figures 2 and 3). We therefore analyzed our set of parental D39 strains and isogenic mutants cultured to mid-exponential phase for changes in the cell morphology and amount of CPS. Our field emission scanning electron microscopy (FESEM) suggested differences in the surface complexity of the capsular polysaccharide layer of D39Δ*rr09* and D39Δ*tcs09*. The Δ*rr09*- and Δ*tcs09*-mutants consist of two different populations showing a high variation in their roughness phenotype. Interestingly, the *hk09*-mutant presented a thicker CPS compared to its parental strain and cognate mutants (Figure 4A). As a control, the nonencapsulated D39 mutant was used, which showed a clear surface roughness in comparison to its isogenic encapsulated wild-type strain D39 (Figure 4A). In the nonencapsulated strains, a high number of cell ends of D39Δ*cps*Δ*hk09* and D39Δ*cps*Δ*tcs09* looked swollen and wrinkly (Figure 4A). The cellular surface of the swollen ends had a morphology that was clearly distinct from that of the smooth surface of wild-type or RR09-deficient D39Δ*cps* pneumococci (Figure 4A). Additionally, small outer membrane vesicles (white arrows), probably due to cell wall degradation or alterations in peptidoglycan, were detectable on the surface of all strains with a higher proportion for the *hk09*- and *tcs09*-mutants.

In addition, we applied transmission electron microscopy (TEM) to compare cell morphology, amount of CPS, and intracellular appearance of the *tcs09*-mutants with their D39 wild-types. Our ultrathin sections of *S. pneumoniae* D39Δ*rr09* suggested a detachment of CPS and a lower capsule density on the cell surface. In contrast, D39Δ*tcs09* presented a cell population with a variation in the amount of surface CPS (Figure 4B). This phenomenon was not detectable for D39Δ*hk09*; instead, this strain exhibited a thicker capsule layer than the wild-type or its cognate mutants (Figure 4B). Further analysis of the *rr09*-mutant of D39 revealed a less dense cytoplasm, probably due to less proteins and ribosome accumulation (Figure 4B). Additionally, the cytoplasm of all *tcs09*-mutants of the nonencapsulated strains exhibit some distinct white small areas in the bacterial cytoplasm, but these seemed not to be vesicles due to a missing membrane, and no contact to the cytoplasmic membrane is detectable (Figure 4B). All pneumococcal membranes and cell walls appeared to be intact, indicating that complete deletion of the TCS09 system did not have a deleterious effect on the cell surface structure of the *S. pneumoniae* strains (Figure 4B).

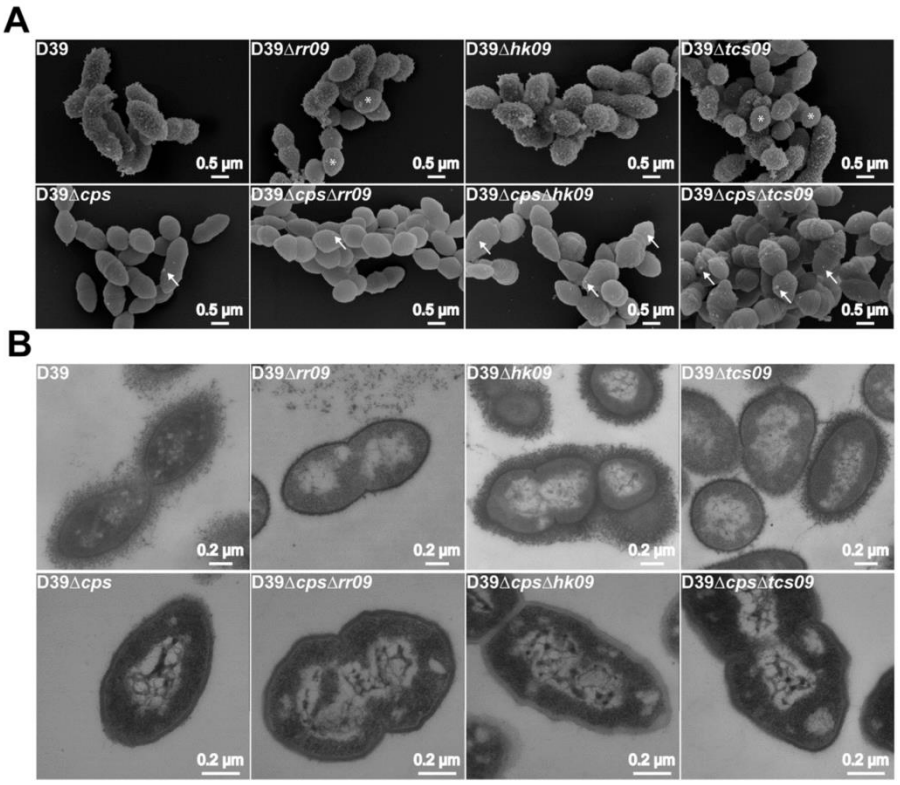

Figure 4. Influence of pneumococcal *tcs09*-mutations on pneumococcal cell morphology and capsule. (**A**) The pneumococcal cell morphology and capsular polysaccharide layer of D39, D39Δ*cps*, and their isogenic *rr09*-, *hk09*-, and *tcs09*-mutants illustrated by field emission scanning electron microscopy (FESEM). The white bars correspond to 500 nm. White arrows indicate outer membrane vesicles and white stars indicate cells with lower capsule amount. (**B**) TEM illustration of pneumococcal cell morphology and capsular polysaccharide layer. The white bars correspond to 200 nm.

3.5. Impact of TCS09 on the CPS Amount on the Pneumococcal Surface

Our CPS illustration of pneumococcal *tcs09* regulatory mutants by FESEM and TEM suggested different amounts of CPS compared to the isogenic D39 wild-type. Therefore, we assessed and quantified the relative amount of CPS linked to the pneumococcal surface by flow-cytometry (Figure 5). The CPS of D39 was detected using a serotype 2 antiserum and secondary Alexa conjugated antibody. The fluorescence intensity of the labeled pneumococci was quantified by flow cytometry. As control, the nonencapsulated D39Δ*cps* strain was used, and D39Δ*cps* revealed a significantly lower fluorescence signal compared to the encapsulated D39 strain (Figure 5). Our measurements indicated that a high proportion (99.7% of D39, 91.3% of D39Δ*rr09*, 99.8% of D39Δ*hk09*, and 98.6% of D39Δ*tcs09*) of pneumococci were fluorescent and, hence, were positive for CPS (Figure S6). Importantly, the histograms (Figure 5A) and the relative quantification of CPS (Figure 5B) indicated that pneumococci deficient in HK09 or the complete TCS09 had, at least proportionally, a significantly higher capsule amount compared to the wild-type D39. Interestingly, the *rr09*- and *tcs09*-mutants showed heterogeneous populations regarding the CPS expression. A minor proportion shows low levels of fluorescence intensity, indicating low amounts of CPS, while a higher proportion showed a high fluorescence intensity, indicating a high amount

of CPS (Figure 5). Immediately at time point 0, the population of the *rr09*-mutant could be divided into a lower capsule expressing population and a wild-type like population (Figures 5 and S6). For the *tcs09*-mutant, which is deficient in RR09 and HK09, a similar effect was observed, but it was less pronounced compared to D39Δ*rr09* (Figures 5A and S6). Furthermore, capsule detachment was investigated in mutants resuspended in PBS over a period of 60 min. The flow cytometric analyses showed that the proportion of low CPS expressing pneumococci of D39Δ*rr09* and D39Δ*tcs09* remained constant, suggesting that the reduced amount of CPS in these strains is not caused by CPS shearing during sample preparation (Figure 5B). Taken together, our relative quantification of the CPS confirmed the electron microscopic data and indicates that TCS09 contributes to pneumococcal CPS expression.

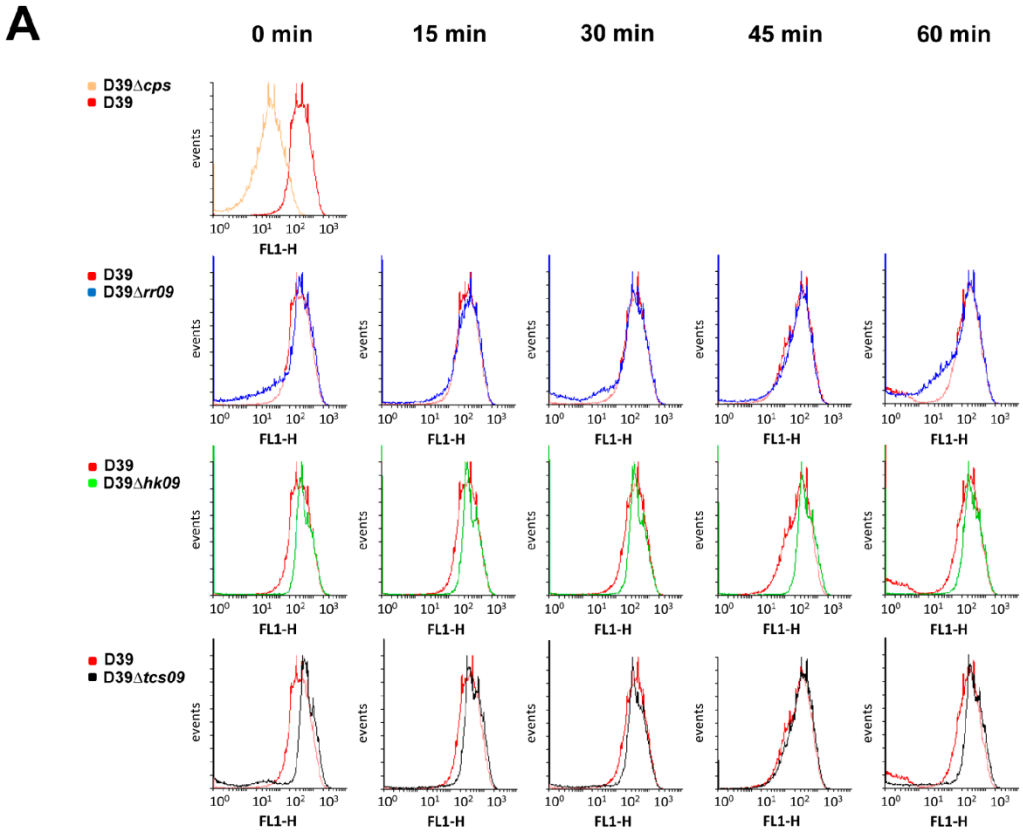

Figure 5. *Cont.*

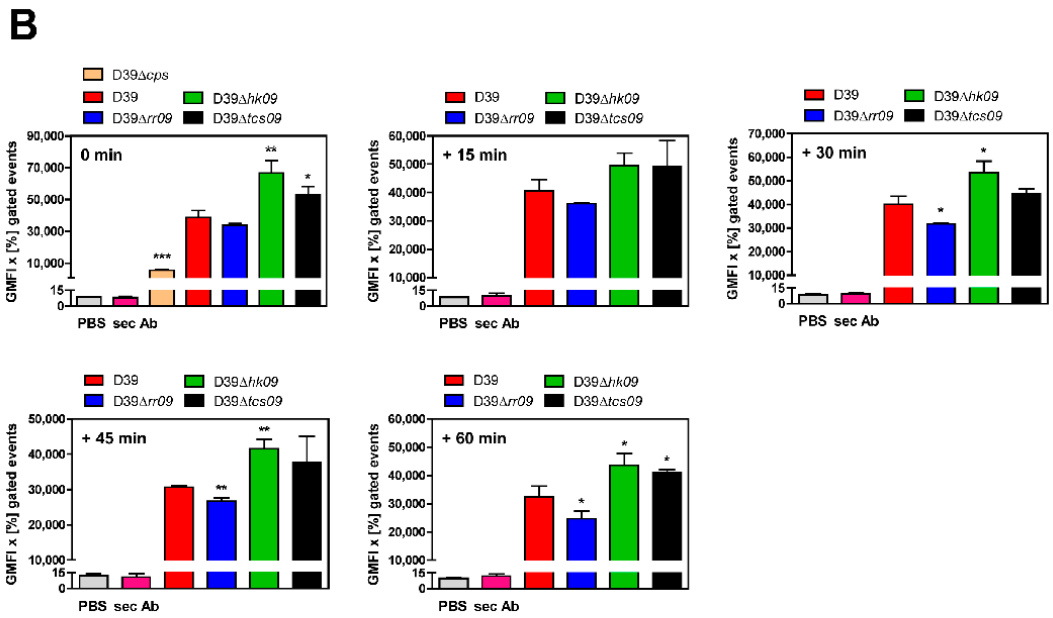

Figure 5. Abundance of surface exposed capsule in *S. pneumoniae* D39 and its isogenic *tcs09*-mutants measured via flow cytometry. The capsule expression of pneumococci was investigated via flow cytometry over a period of time of 60 min. For the analysis, 2×10^8 bacteria of D39Δ*cps*, the D39 wild-type, and its isogenic Δ*rr09*-, Δ*hk09*-, and Δ*tcs09*-mutants cultured in CDM with glucose were used. To analyze capsule detachment, pneumococci were resuspended in PBS over 15–60 min before capsule detection. (**A**) An increase of the fluorescence intensity (FL-1 H channel) in the histograms shows a higher capsule expression of the pneumococci. (**B**) Shown are the calculated geometric mean fluorescence intensities (GMFI) x [%] gated events. Results are presented as the mean ± SD for three independent experiments. An independent student's t-test proved a significance with *p*-values * < 0.05, ** < 0.01, and *** < 0.001 relative to the parental pneumococcal strain D39.

3.6. Impact of TCS09 on Pneumococcal Phase Variation

We further analyzed the mutants for their change of colony opacity phenotype. *S. pneumoniae* D39 and isogenic mutants were plated out on TSA plates supplemented with catalase, and single colonies were observed under oblique transmitted light. Opaque colonies are typically of convex elevation compared to transparent colonies, which have a central dent, as shown in Figure 6A. Most of the D39Δ*rr09* and D39Δ*tcs09* colonies appeared smaller and transparent (74% and 65%, respectively) compared to the opaque wild-type D39 colonies (Figure 6). Interestingly, the D39Δ*hk09* mutant showed the same opaque phenotype as the isogenic wild-type strain D39 (Figure 6). These observations are in agreement with our findings regarding the CPS amount, as indicated by electron microscopy and flow cytometry.

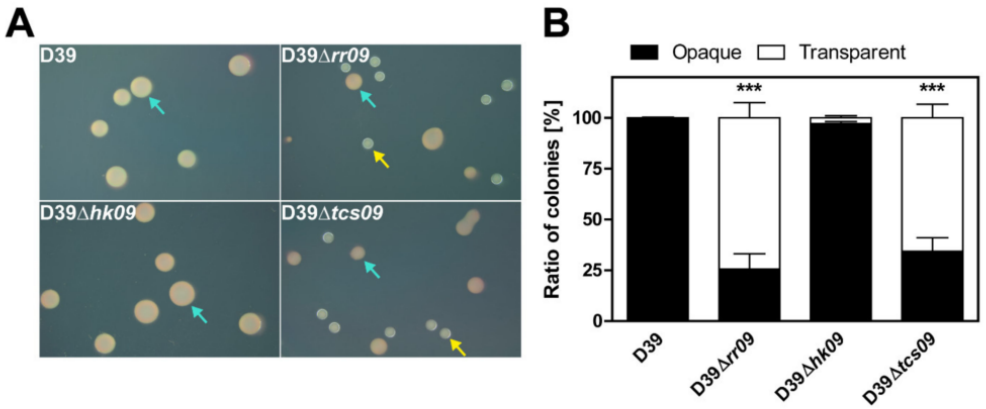

Figure 6. Colony morphology of opaque (O) and transparent (T) variants of *S. pneumoniae* D39 and isogenic *tcs09*-mutants. (**A**) Transparent (yellow arrow) and opaque (turquoise arrow) colonies of D39 and isogenic mutants plated on tryptic soy agar supplemented with catalase. (**B**) Percentage distribution of O and T colonies in D39 and isogenic mutants. Images were taken under oblique transmitted illumination using a Leica M125 C dissecting microscope and LAS X software. Results are presented as the mean ± SD for three independent experiments. An independent student's *t*-test proved a significance with *p*-value *** < 0.001 relative to the parental pneumococcal strain D39.

3.7. Autolysis Assay with Triton X-100

Our FESEM studies suggested alterations in the cell morphology and cell wall integrity in D39Δ*cps*Δ*hk09* and D39Δ*cps*Δ*tcs09* (Figure 4A). Thus, we hypothesized that these bacterial cells lyse faster under stress conditions. To accelerate or induce pneumococcal cell lysis, Triton X-100 was used at a low concentration to study the impact of TCS09 on pneumococcal stability and autolysis. Triton X-100 is a non-ionic detergent with a polar head group disrupting the hydrogen bonds in lipid bilayers. The integrity of the lipid membrane is disrupted, which ultimately leads to cell lysis. Pneumococci were cultured in CDM until OD_{600nm} 0.6 and resuspended in PBS containing Triton X-100 at a final concentration of 0.005% or 0.01%. Control samples were incubated in PBS without Triton X-100. The results show the survival rate given as a normalized percentage (%) by taking the initial OD at time 0 as 100% (Figure 7). In general, we monitored that the nonencapsulated D39 strain lysed faster than the encapsulated strains within the same time period (Figure 7). The autolysis assay with D39Δ*cps* and its isogenic *tcs09*-mutants showed that the HK09- and the TCS09-deficient mutants exhibited an increased Triton X-100 induced autolysis rate compared to the parental strain D39Δ*cps*. After 50 min, 50% of D39Δ*cps*Δ*hk09* and D39Δ*cps*Δ*tcs09* showed lysis, while for D39Δ*cps* this was the case only after 70 min. In the same period of time, only 15% of the RR09-deficient pneumococci presented lysis (Figure 7A). A significant dose-dependent effect was not observed. When we tested the lysis of the encapsulated strains, D39Δ*tcs09* exhibited an autolysis rate of 50% in 1 h, when pneumococci are exposed to 0.01% Triton X-100, which is significantly different to the wild-type and other mutants showing an autolysis rate of 20%. After 80 min and in the presence of 0.01% Triton X-100, the Δ*rr09*-mutant of D39 started to lyse faster than the wild-type D39 (Figure 7B). In conclusion, a higher autolysis rate compared to isogenic parental strains is indicated for D39Δ*cps*Δ*hk09*, D39Δ*cps*Δ*tcs09*, D39Δ*tcs09*, and partially for D39Δ*rr09*.

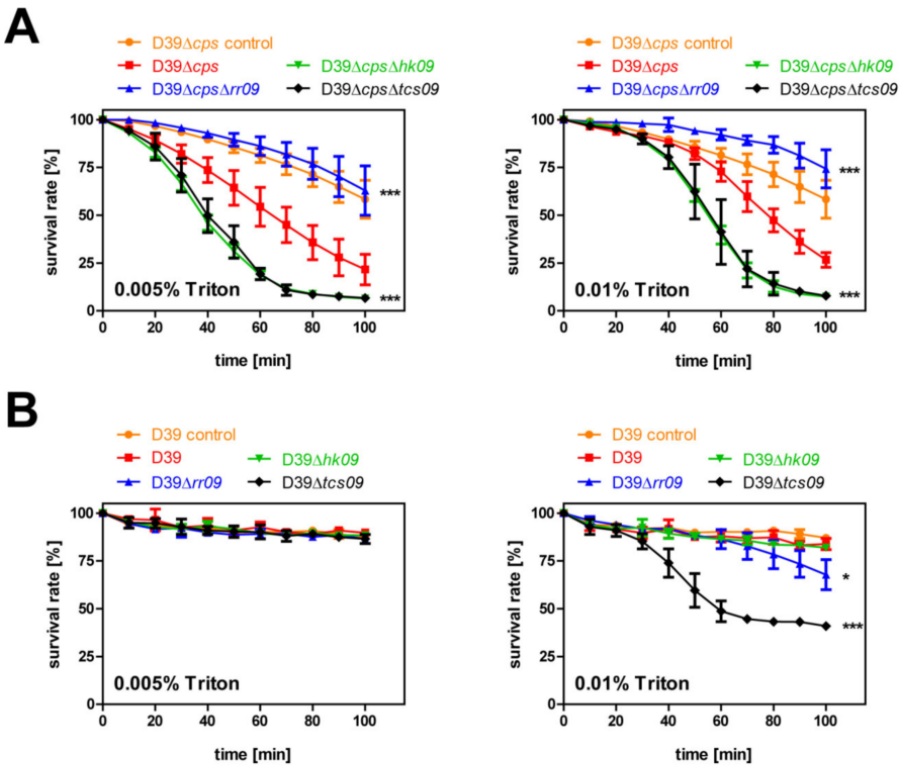

Figure 7. Effect of TCS09 in stability and autolysis in *S. pneumoniae*. The pneumococcal parental strains D39Δ*cps* or D39 and their isogenic mutants Δ*rr09*, Δ*hk09*, and Δ*tcs09* were cultivated in CDM until an OD_{600nm} 0.6, resuspended in PBS, and treated with Triton X-100. (**A**) Survival rate of nonencapsulated D39Δ*cps* and *tcs09*-mutant strains. (**B**) Percentage of survived encapsulated D39 and *tcs09*-mutant strains. Results are presented as the mean ± SD of the normalized percentage for three independent experiments. A two-way ANOVA proved a significance with a *p*-value * < 0.05 and *** < 0.001 relative to the parental pneumococcal strain.

3.8. Impact of TCS09 on Resistance against Oxidative Stress

To assess the sensitivity of *tcs09*-mutants against oxidative stress, we investigated pneumococcal survival in the presence of exogenous hydrogen peroxide resembling oxidative stress conditions. Reactive oxygen species (ROS), such as hydrogen peroxide, can diffuse in a limited manner through the lipid bilayer of a cell membrane and cause oxidation of DNA, proteins, and membrane lipids, resulting in the accumulation of irreversible oxidative damages and cell lysis [31–34]. Because *hk09*- and *tcs09*-mutants showed alterations of the cell wall (Figure 4A), hydrogen peroxide might diffuse easier into the cell and cause cell damage and lysis. D39, D39Δ*cps*, and its isogenic *tcs09*-mutants were cultivated in CDM to an OD_{600nm} of 0.6, and oxidative stress conditions were created by adding different hydrogen peroxide concentrations (5 and 10 mM). No significant difference between the encapsulated wild-type and *tcs09*-mutant strains were observed when exposed to different concentrations of hydrogen peroxide (Figure 8A). However, we detected a significant difference between D39Δ*cps* and the isogenic D39Δ*cps*Δ*hk09* as well as with D39Δ*cps*Δ*tcs09* mutants, with a dose-dependent lower survival rate for the mutants. In contrast, the RR09-deficient mutant D39Δ*cps*Δ*rr09* showed a similar resistance to oxidative stress conditions induced by hydrogen peroxide as the parental strain D39Δ*cps*

(Figure 8B). These data are in accordance to the higher sensitivity of the D39Δ*cps*Δ*hk09* and D39Δ*cps*Δ*tcs09* mutants for Triton X-100.

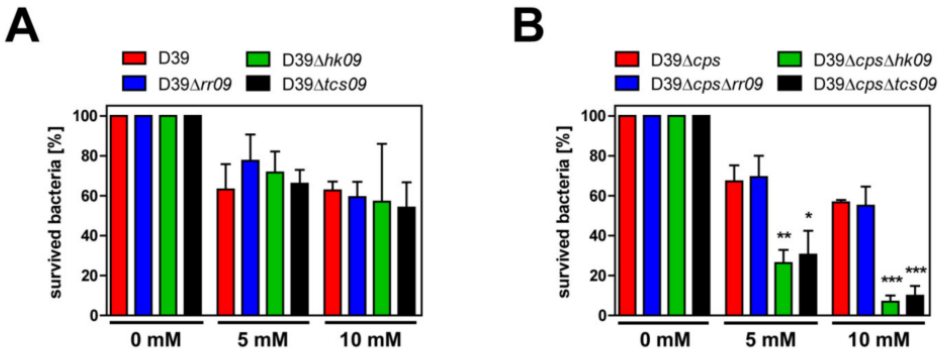

Figure 8. Resistance of pneumococcal *tcs09*-mutants against oxidative stress. Survivability of the *S. pneumoniae* strain D39, D39Δ*cps*, and its isogenic *rr09*-, *hk09*-, and *tcs09*-mutants under oxidative stress conditions. Pneumococci were cultured in CDM up to an OD_{600nm} of 0.6, and incubation with different H_2O_2 concentrations was performed for 30 min at 37 °C. The number of CFU were determined by plating a dilution series on blood agar. (**A**) Survival rate of encapsulated D39 and *tcs09*-mutant strains. (**B**) Percentage of survived bacteria of nonencapsulated D39Δ*cps* and *tcs09*-mutant strains. The measured values, presented as normalized percentage, are shown as mean ± SD of three independently performed experiments. An independent student's *t*-test proved a significance with a *p*-value * < 0.05, ** < 0.01, and *** < 0.001 relative to the parental pneumococcal strain D39Δ*cps*.

4. Discussion

Pneumococci are extracellular human opportunistic bacteria colonizing, mostly symptomless, the upper respiratory tract. However, these pathobionts are also capable of causing severe lung infections, septicemia, and meningitis [35–37]. The host compartments encountered by pneumococci during their extracellular fate differ significantly with respect to nutrient availability, physiological conditions, and immune defense factors. Bacteria sense their environment via TCS, and the induced outside-inside signaling allows the adaptation to specific physiological conditions via altered gene expression. This in turn endows the bacterium, e.g., with a higher abundance of specific fitness factors or a modified set of virulence factors that enable bacterial growth and survival in various ecological host niches [12,27,38–40]. Among the set of pneumococcal TCS, TCS09 has been previously suggested to be involved in fitness adaptation. TCS09 is also referred to as ZmpRS because initial studies suggested a regulation of the virulence factor ZmpB, which could not be confirmed in follow up studies [12,13,15,16]. Further studies showed that TCS09 regulates in a strain-specific manner pneumococcal virulence and metabolic processes. However, these studies have mostly compared the wild-type with the RR09 deficient isogenic mutant [15–17].

Initially, we compared the growth and transcriptomes of *S. pneumoniae* serotype 2 strain D39 mutants deficient for RR09, HK09, or the complete TCS09 with the isogenic wild-type D39 to comprehensively characterize the physiological role of the pneumococcal TCS09. Our growth experiments under nutrient defined conditions in a CDM with glucose as the sole carbon source showed similar growth kinetics and generation time for wild-type D39 and its isogenic mutants D39Δ*rr09* and D39Δ*tcs09*. The generation time of the nonencapsulated D39Δ*cps* and its isogenic mutants was also similar, albeit the overall growth was slower compared to the wild-type D39 (Figure 1A–F). In contrast, a significant decelerated growth was monitored for the D39Δ*hk09* mutant compared to the D39 wild-type strain (Figure 1B). The growth defects of mutants were even more pronounced when we used galactose as a carbon source (Figure 1G–L). The loss of function of HK09 and

both TCS09 components resulted in a significant growth defect when compared to the wild-type D39. When we tested the nonencapsulated mutants, the deficiency of HK09 and the complete TCS09 regulatory unit impaired growth in the CDM with galactose as a carbon source (Figure 1K,L). Interestingly, the generation time of the nonencapsulated D39Δ*cps* is shorter compared to the encapsulated wild-type in CDM with galactose as a carbon source. Pneumococci are strictly fermentative human pathogens relying on carbohydrate metabolism to generate energy for growth [41–45]. When we compared the growth kinetics of encapsulated pneumococci in the context of the carbon source used, galactose slowed down pneumococcal growth but leads to a higher optical density, at least in D39 and the isogenic *rr09*-mutant. Notable, pneumococci ferment glucose homofermentatively with the main products lactate and acetate, while the fermentation with galactose is heterofermentative with mixed-acid products, and lactate is not produced [42,46,47]. Our results with a lower growth rate with galactose as a carbon source are in accordance with a previous study, which further showed the importance of the lactate dehydrogenase for the pyruvate metabolism of pneumococci [47]. Galactose is a constituent of mucin in the human nasopharynx and is imported by several ATP binding cassette (ABC) transporters and PTSs (*gadVWEF*, *spd_0088–spd_0090*, *manNML*, and *spd_0559–spd_0561*). Intracellular galactose or galactoseamine is metabolized by the tagatose pathway. The genes encoding enzymes of this pathway (*lacABCD*, *lacT*, *lacF-2*, *lacE-2*, and *lacG-2*) are higher expressed in the presence of galactose [46,48,49]. It has to be mentioned that *lacD* in D39v is annotated as a pseudogene according to PneumoBrowse (https://veeninglab.com/pneumobrowse, accessed on 16 November 2020) [49]. Additionally, galactose can be further metabolized in the Leloir pathway (*galM*, *galE-1*, *galE-2*, *galT-2* and *galK*) [41,42].

The observed growth defects correlated with our RNA-seq based transcriptome analysis. We successfully identified differential expression of 67 protein encoding genes when wild-type and mutant pneumococci were cultivated in glucose-containing CDM. The most significantly regulated genes were found in the mutant D39Δ*hk09* (Figure 2B). Comparisons of the transcriptome data (Figure 2B) and qPCR data (Figure 3A) between the D39 wild-type and Δ*hk09*-mutant revealed in each an elevated expression of genes involved in carbohydrate metabolism, especially of genes contributing to galactose metabolism (*spd_0065–spd_0071*). As mentioned above, these genes are organized in a single transcriptional unit, the *aga* operon (Figure 2C). This operon contains an exo-β-galactosidase (*bgaC*), the PTS *gadVWEF* involved in galactoseamine transport, a sugar isomerase (*agaS*), and an aldose 1-epimerase (*galM*) [29]. According to the study by Afzal et al., the promotor region of this operon exhibits an *agaR* binding motif (5′-ATAATTAATATAACAACAAA-3′). In an *agaR*-mutant, the *aga*-operon was upregulated, whereas no other operons were significantly changed [29]. Intriguingly, one of the significantly downregulated genes (17.5-fold) under our growth conditions in D39Δ*hk09* was *agaR* (*spd_0064*) (Figure 2B). Regulation of *agaR* was verified by qPCR, showing an 8.8-fold down-regulation (Figure 3A). The upregulation of the *aga* operon in the *hk09*-mutant fits perfectly with the downregulation of *agaR*, which acts as a repressor of the operon (Figures 2B and 3A). AgaR is a GntR family regulator, which is further suggested to be involved in capsular polysaccharide biosynthesis. AgaR (referred to as CpsR in [29]) was described to interact directly with the *cps* promotor and to control negatively the *cps* gene transcription [30]. However, our transcriptome data did not support this finding, because we could not measure a lower expression of the *cps*-operon. BgaC, a non-classical surface protein, has a sugar specific hydrolysis activity for Galβ1-3-GlcNAc moiety of oligosaccharides, a known receptor for pneumococcal attachment [50,51]. The cleavage releases galactose that can now be imported and used in further metabolic processes. A deficiency of BgaC enhances pneumococcal adherence to epithelial cells and therefore it can be responsible for the release of *S. pneumoniae* from the host cell surface, so that pneumococci can now perform transcellular migration [51].

Two replicates of the D39Δ*tcs09* mutant showed increased expression of competence genes in the RNA-seq analysis, most probably indicating higher extracellular levels of the competence-stimulating peptide (CSP) and concomitant activation of the ComE and ComX

regulons. Because of the almost identical growth of the four replicates, this observation was hard to explain but did not seem to be directly linked to TCS09 deficiency. Accordingly, qPCR-based analysis of independently generated samples confirmed that competence gene expression in D39Δ*tcs09* cultures is consistent and comparable to the D39 wild-type.

For D39Δ*rr09*, we measured only a significant upregulation for the *gadVW and agaS* gene expression, which could not be confirmed by qPCR (Figures 2B and 3). In accordance with the qPCR, the *rr09*-mutant did not show any regulation of *agaR*, which suggests a direct role of RR09 on transcription of this operon (Figure 2B). An earlier performed microarray-based transcriptome analysis with D39Δ*rr09* cultivated in complex media such as Todd Hewitt Broth supplement with yeast (THY) or brain-heart infusion (BHI) demonstrated a significant down-regulation of *gadVWEF* gene expression [15]. However, because these results are not in accordance with our findings, we hypothesize that the main reasons for these contradicting results are the use of different culture media. Our RNA-seq based transcriptome analyses were done with pneumococci cultured in CDM containing a defined carbon source and mix of nutrients, while lacking peptides, lipids, polymers, and growth factors. In CDM cultured pneumococci, especially genes in amino acid metabolism, are upregulated compared to pneumococcal THY cultures [43,44,52]. Both, THY and BHI, are complex media, and pneumococcal growth is faster and relies, in addition to the carbon source, on the uptake of the oligopeptides present in these media [27,42–44,52]. Thus, the selection of the culture medium or especially the availability of nutrients in the host can influence the gene regulation. These findings are not surprising considering the versatile adaptation of pneumococci to its different host compartments during colonization, dissemination in the blood, or other invasive infections such as meningitis [27,38,39,52].

Although we could not demonstrate a direct role of RR09 on expression of virulence factors, another previous study described an avirulent phenotype of the D39Δ*rr09* mutant in murine models of intraperitoneal, intranasal, and intravenous infection [16]. The reasons for the observed attenuation are still unknown. Because a mutant with *gadE* knockout showed no difference in virulence compared to the wild-type [15], the *aga* operon does not play a direct role for the diminished virulence of *S. pneumoniae* D39. Whether this attenuation is associated with the regulatory effect of RR09 on the tyrosine recombinase PsrA-catalyzed DNA inversion reactions that leads to a higher proportion of opaque colonies remains open [17,18].

However, our data suggest a potentially indirect role of TCS09 in pneumococcal virulence. The mutant deficient of HK09 showed an upregulation of *pspA* (2.6-fold) and *phtD* (2.1-fold) (Figure 2B). PspA is involved in immune defense by inhibiting complement activation and colonization due to binding and inactivation of the bactericidal apolactoferrin [53–55]. *S. pneumoniae* encodes four Pht proteins: PhtA, PhtB, PhtD, and PhtE, which are important in zinc acquisition and play a role in pneumococcal adhesion in a strain dependent manner [56,57]. The role of TCS09 and its HK and RR09 has to be reinvestigated in different experimental mouse models using pneumococcal strains with different genetic backgrounds. This is important because the regulatory mechanisms and consequences for virulence seem to be variable among pneumococcal strains [19].

Our transcriptome data indicated changes of metabolic gene expression, particularly in the *hk09*-mutant, and we measured growth defects of our mutants D39Δ*hk09*, D39Δ*cps*Δ*hk09*, and D39Δ*tcs09*. This prompted us to elucidate whether these changes are associated with phenotypic and morphologic alterations. We therefore assessed the morphology of encapsulated and nonencapsulated D39 and we further illustrated the capsular polysaccharide in CPS expressing D39 strains and mutants by electron microscopy.

Our FESEM and TEM indicated three phenotypic differences between the parental strains and the mutants. These was (i) a significantly higher amount of CPS in D39Δ*hk09* or in a subpopulation of D39Δ*tcs09*, (ii) the production of outer membrane vesicles, which are in particular visible in the nonencapsulated *hk09*- and *tcs09*-mutants, and (iii) a wrinkly and swollen surface of the nonencapsulated *hk09*- and *tcs09*-mutants (Figure 4A,B). The quantitatively higher amount of CPS in D39Δ*hk09* and D39Δ*tcs09* was confirmed by flow

cytometry (Figure 5), and we hypothesize, therefore, that the growth defect in CDM is due to the energy consumption of the CPS production. This effect is probably less pronounced in the D39Δ*tcs09* mutant because our phenotypic analysis indicated that the planktonic culture of the mutant D39Δ*tcs09* in CDM with glucose consists of a mixture of low-encapsulated and high-encapsulated pneumococci (Figures 5 and S6). The production of pneumococcal CPS under nutrient-defined conditions, as in the case of growth in CDM, causes a competition for energy against central carbon metabolism [58]. In 2011, Carvalho et al. analyzed the amount of capsule in *S. pneumoniae* D39, which showed a higher production in galactose-containing medium compared to glucose-containing medium [41]. These finding are in agreement with our data showing an even more pronounced growth defect of D39Δ*hk09* and D39Δ*tcs09* in CDM with galactose as carbon source compared to growth in CDM with glucose (Figure 1H,I). So far, we cannot explain the dramatic growth defect of nonencapsulated mutants deficient in HK09 or TCS09 (Figure 1K,L).

The variation in CPS amount has also been described when pneumococci alter their opacity [59], and the contribution of RR09 to the switch from the transparent (T) to the opaque (O) phenotype has also been described [17,18]. Furthermore, a Δ*bgaC* mutant (*bgaC*: first gene of the *aga* operon) in strain ST606 (derivative of ST556, serotype 19F) showed more T colonies than O colonies, which indicates that the transcription of the *aga* operon is involved in the stabilization of O variants [17]. Our data strongly support these previous studies because the upregulation of the *aga* operon in D39Δ*hk09* is associated with higher amounts of CPS and with exclusively O colonies. Contrary, the deficiency of RR09 or complete TCS09 resulted in a mixture of O and T variants (Figure 6).

The nonencapsulated *hk09*- and *tcs09*-mutants showed additional phenotypes: the production of membrane vesicles and a wrinkly and swollen surface (Figure 4A,B). Bacterial outer membrane vesicles (OMV) consist of various types of lipids, membrane proteins, DNA, and RNA [60,61]. In *S. pneumoniae*, these vesicles are enriched for lipoproteins, short-chain fatty acids, and pneumolysin [62]. Membrane vesicles contribute to the digestion of nutrients, quorum sensing signaling, bacterial defense mechanism by binding antimicrobial peptides, and toxin transport [63–66]. The Gram-positive pneumococci produce vesicles actively from the plasma membrane [62]. For *B. subtilis* and *P. aeruginosa*, it is known that endolysin induced peptidoglycan lysis (explosive cell lysis) is involved in OMV production of bacteria in a passive manner [67,68]. Membrane vesicle formation is further possible via cell lysis that can be triggered by autolysins. Sle1, an autolysin in *S. aureus*, modulates the membrane vesicle production by altering the cell wall permeability and strengthens this hypothesis [69].

Our phenotypic analysis by FESEM and TEM suggests that the cell membrane and cell wall of nonencapsulated *hk09*- and *tcs09*-mutants are instable and that membrane vesicle formation is a side effect of cell lysis and does not happen actively (Figure 4A). Because the D39Δ*cps*Δ*rr09* showed almost no membrane vesicles or alterations of the cell morphology, we hypothesized that this mutant is similar to the parental strain less susceptible to cell lysis compared to the *hk09*- and *tcs09*-mutants. To test this hypothesis, we induced pneumococcal autolysis Triton X-100 treatment (Figure 7). Indeed, the deficiency of HK09 and the entire TCS09 enhanced autolysis in the nonencapsulated mutants, whereas the *rr09*-mutant is even more resistant to lysis than the wild-type (Figure 7A). These data suggest a correlation between the formation of OMVs and an increased sensitivity to cell lysis. For the encapsulated D39 and isogenic mutants, the results are different. The encapsulated Δ*tcs09*-mutant showed a fast autolysis rate within 40 min, followed by stabilization to a specific survival rate. In contrast, the *rr09*-mutant was initially as stable as the wild-type but started to lyse faster after 60 min of Triton X-100 treatment (Figure 7B). Together, the data suggest a decisive role of CPS for sensitivity to cell lysis. The inhibitory effect of CPS on pneumococcal autolysis has already been shown; e.g., the nonencapsulated R6 showed more lysis in comparison to the encapsulated D39 strain. Similarly, the deletion of the *cps* locus in the D39 strain resulted in an increased lysis of this mutant. It is hypothesized that the capsule is able to block the access of the autolysins such

as LytA to its target structure peptidoglycan or slows down the translocation of LytA to the cell wall [70].

The encapsulated D39Δ*rr09* and D39Δ*tcs09* showed signs for capsule detachment in our TEM (Figure 4B), and two distinct populations (one with less capsule, one with more capsule) were identified in the flow cytometric-based quantification of CPS (Figures 5A and S6). In addition, a higher number of transparent colonies (low capsule) were observed (Figure 6) in these mutants, which showed a higher tendency for cell lysis. Thus, in *tcs09*-mutants, in which the amount of CPS is reduced or CPS is detached, cell lysis is propagated, while in the nonencapsulated mutants we showed a correlation between OMV formation and cell lysis.

A question that was still open at this point was whether the loss of CPS or the formation of OMV influences pneumococcal survival during stress. Our oxidative stress assay with hydrogen peroxide (H_2O_2) as a reactive oxygen species (ROS) indicated a lower survival rate of nonencapsulated *hk09*- and *tcs09*-mutants compared to the parental strain D39Δ*cps* or D39Δ*rr09* (Figure 8). These data are in agreement with our hypothesis that a higher proportion of OMVs correlates with a reduced integrity of the cell wall and, hence, higher sensitivity against stress conditions.

The mild impact of TCS09 on gene expression alterations suggests a role for TCS09 as a fine tuning regulatory system. There are several conceivable reasons for this observation: (i) the RR09 is modulating additional regulatory changes in the absence of the HK09 such as repression of transcription in its non-phosphorylated state, and (ii) cross talk among the different pneumococcal TCSs may provide an explanation as to why we see effects mostly only in D39Δ*hk09* and not all three *tcs09*-mutants.

5. Conclusions

Taken together, TCS09 is most likely not directly involved in the regulation of CPS genes or virulence factors. Instead, the phenotypic and morphologic changes observed are indirectly induced by changing the carbohydrate metabolism and thereby the cell wall integrity and amount of CPS. This in turn has significant consequences for metabolic fitness and resistance against stress. Therefore, it is plausible that TCS09 is most likely also essential for full virulence of pneumococci under infection conditions. However, this has to be confirmed in further studies.

Supplementary Materials: The following are available online at https://www.mdpi.com/2076-2607/9/3/468/s1: Figure S1: Genomic organization of *tcs09* gene cluster in *S. pneumoniae* D39 wild-type and isogenic *tcs09*-mutants, Figure S2: RNA integrity check with the Agilent Bioanalyzer, Figure S3: Expression profile of competence genes in D39Δ*tcs09*, Figure S4: Volcano plots of the differentially expressed genes of D39Δ*rr09*, D39Δ*hk09*, and D39Δ*tcs09* identified by RNA-seq, Figure S5: Expression profile of the 67 significantly regulated genes in D39 and *tcs09*-mutants, Figure S6: Analysis of capsule polysaccharide expression in flow cytometry. Table S1: Results of the RNA-seq analysis. Table S2: Inline barcode sequences, Table S3: Primers used for RNA preparation for RNA-sequencing. Data obtained from the RNA-seq analysis have been uploaded to the National Center for Biotechnology Information (NCBI) at the Gene Expression Omnibus (GEO) under accession number GSE165642 (link: https://www.ncbi.nlm.nih.gov/geo/query/acc.cgi?acc=GSE165642, accessed on 1 December 2020).

Author Contributions: Conceptualization, S.H. (Stephanie Hirschmann), A.G.-M., and S.H. (Sven Hammerschmidt); methodology, S.H. (Stephanie Hirschmann), A.G.-M., U.M., S.H. (Susanne Häußler), M.R., and S.H. (Sven Hammerschmidt); software, S.H. (Stephanie Hirschmann), D.D., S.H. (Susanne Häußler), and S.H. (Sven Hammerschmidt); validation, S.H. (Stephanie Hirschmann), D.D., U.M., and S.H. (Sven Hammerschmidt); formal analysis, S.H. (Stephanie Hirschmann), A.G.-M., D.D., and S.H. (Sven Hammerschmidt); investigation, S.H. (Stephanie Hirschmann), A.G.-M., J.K., G.B., and M.R.; resources, S.H. (Susanne Häußler), M.R., and S.H. (Sven Hammerschmidt); data curation, S.H. (Stephanie Hirschmann) and D.D.; writing—original draft preparation, S.H. (Stephanie Hirschmann), A.G.-M., U.M., and S.H. (Sven Hammerschmidt); writing—review and editing, all authors; visualization, S.H. (Stephanie Hirschmann), D.D., and M.R.; supervision, S.H. (Sven Hammerschmidt); project

administration, S.H. (Sven Hammerschmidt); funding acquisition, S.H. (Sven Hammerschmidt). All authors have read and agreed to the published version of the manuscript.

Funding: This research was funded by a grant from the Deutsche Forschungsgemeinschaft (DFG GRK 1870 Bacterial Respiratory Infections to S.H. (Sven Hammerschmidt)) and the Bundesministerium für Bildung und Forschung (BMBF- Zwanzig20–InfectControl 2020–project VacoME–FKZ 03ZZ0816 to S.H. (Sven Hammerschmidt)). We further acknowledge support for the Article Processing Charge from the DFG (German Research Foundation, 393148499) and the Open Access Publication Fund of the University of Greifswald.

Institutional Review Board Statement: Not applicable.

Informed Consent Statement: Not applicable.

Data Availability Statement: Data obtained from the RNA-seq analysis have been uploaded to the National Center for Biotechnology Information (NCBI) at the Gene Expression Omnibus (GEO) under accession number GSE165642 or this link: https://www.ncbi.nlm.nih.gov/geo/query/acc.cgi?acc=GSE165642, accessed on 1 December 2020.

Acknowledgments: We would like to acknowledge Jürgen Tomasch and Robert Geffers (Helmholtz Center for Infection Research, Braunschweig, Germany) for providing technical support. We appreciate the sample preparation and technical assistance of Astrid Dröge and Ina Schleicher (Helmholtz Center for Infection Research, Braunschweig, Germany) and Marc Schaffer (University Medicine Greifswald) in this study.

Conflicts of Interest: The authors declare no conflict of interest. The funders had no role in the design of the study; in the collection, analyses, or interpretation of data; in the writing of the manuscript, or in the decision to publish the results.

References

1. West, A.H.; Stock, A.M. Histidine kinases and response regulator proteins in two-component signaling systems. *Trends Biochem. Sci.* **2001**, *26*, 369–376. [CrossRef]
2. Rowland, M.A.; Deeds, E.J. Crosstalk and the evolution of specificity in two-component signaling. *Proc. Natl. Acad. Sci. USA* **2014**, *111*, 5550. [CrossRef]
3. Lange, R.; Wagner, C.; de Saizieu, A.; Flint, N.; Molnos, J.; Stieger, M.; Caspers, P.; Kamber, M.; Keck, W.; Amrein, K.E. Domain organization and molecular characterization of 13 two-component systems identified by genome sequencing of *Streptococcus pneumoniae*. *Gene* **1999**, *237*, 223–234. [CrossRef]
4. Throup, J.P.; Koretke, K.K.; Bryant, A.P.; Ingraham, K.A.; Chalker, A.F.; Ge, Y.; Marra, A.; Wallis, N.G.; Brown, J.R.; Holmes, D.J.; et al. A genomic analysis of two-component signal transduction in *Streptococcus pneumoniae*. *Mol. Microbiol.* **2000**, *35*, 566–576. [CrossRef] [PubMed]
5. Gómez-Mejia, A.; Gámez, G.; Hammerschmidt, S. *Streptococcus pneumoniae* two-component regulatory systems: The interplay of the pneumococcus with its environment. *Int. J. Med. Microbiol.* **2018**, *308*, 722–737. [CrossRef] [PubMed]
6. Reinoso-Vizcaíno, N.M.; Cian, M.B.; Cortes, P.R.; Olivero, N.B.; Hernandez-Morfa, M.; Piñas, G.E.; Badapanda, C.; Rathore, A.; Perez, D.R.; Echenique, J. The pneumococcal two-component system SirRH is linked to enhanced intracellular survival of *Streptococcus pneumoniae* in influenza-infected pulmonary cells. *PLoS Pathog.* **2020**, *16*, e1008761. [CrossRef] [PubMed]
7. Gómez-Mejia, A.; Gámez, G.; Hirschmann, S.; Kluger, V.; Rath, H.; Böhm, S.; Voss, F.; Kakar, N.; Petruschka, L.; Völker, U.; et al. Pneumococcal Metabolic Adaptation and Colonization Are Regulated by the Two-Component Regulatory System 08. *mSphere* **2018**, *3*, e00165-18. [CrossRef]
8. Grebe, T.W.; Stock, J.B. The Histidine Protein Kinase Superfamily. In *Advances in Microbial Physiology*; Poole, R.K., Ed.; Academic Press: Cambridge, MA, USA, 1999; Volume 41, pp. 139–227.
9. Gao, R.; Mack, T.R.; Stock, A.M. Bacterial response regulators: Versatile regulatory strategies from common domains. *Trends Biochem. Sci.* **2007**, *32*, 225–234. [CrossRef] [PubMed]
10. Gao, R.; Stock, A.M. Biological Insights from Structures of Two-Component Proteins. *Annu. Rev. Microbiol.* **2009**, *63*, 133–154. [CrossRef] [PubMed]
11. Nikolskaya, A.N.; Galperin, M.Y. A novel type of conserved DNA-binding domain in the transcriptional regulators of the AlgR/AgrA/LytR family. *Nucleic Acids Res.* **2002**, *30*, 2453–2459. [CrossRef]
12. Hava, D.L.; Camilli, A. Large-scale identification of serotype 4 *Streptococcus pneumoniae* virulence factors. *Mol. Microbiol.* **2002**, *45*, 1389–1406. [CrossRef] [PubMed]
13. Novak, R.; Charpentier, E.; Braun, J.S.; Park, E.; Murti, S.; Tuomanen, E.; Masure, R. Extracellular targeting of choline-binding proteins in *Streptococcus pneumoniae* by a zinc metalloprotease. *Mol. Microbiol.* **2000**, *36*, 366–376. [CrossRef]

14. Blue, C.E.; Paterson, G.K.; Kerr, A.R.; Bergé, M.; Claverys, J.P.; Mitchell, T.J. ZmpB, a Novel Virulence Factor of *Streptococcus pneumoniae* That Induces Tumor Necrosis Factor Alpha Production in the Respiratory Tract. *Infect. Immun.* **2003**, *71*, 4925. [CrossRef] [PubMed]
15. Hendriksen, W.T.; Silva, N.; Bootsma, H.J.; Blue, C.E.; Paterson, G.K.; Kerr, A.R.; de Jong, A.; Kuipers, O.P.; Hermans, P.W.M.; Mitchell, T.J. Regulation of Gene Expression in *Streptococcus pneumoniae* by Response Regulator 09 Is Strain Dependent. *J. Bacteriol.* **2007**, *189*, 1382. [CrossRef] [PubMed]
16. Blue, C.E.; Mitchell, T.J. Contribution of a Response Regulator to the Virulence of *Streptococcus pneumoniae* Is Strain Dependent. *Infect. Immun.* **2003**, *71*, 4405. [CrossRef] [PubMed]
17. Wang, J.; Li, J.-W.; Li, J.; Huang, Y.; Wang, S.; Zhang, J.-R. Regulation of pneumococcal epigenetic and colony phases by multiple two-component regulatory systems. *PLoS Pathog.* **2020**, *16*, e1008417. [CrossRef]
18. Li, J.; Wang, J.; Ruiz-Cruz, S.; Espinosa, M.; Zhang, J.-R.; Bravo, A. *In vitro* DNA Inversions Mediated by the PsrA Site-Specific Tyrosine Recombinase of *Streptococcus pneumoniae*. *Front. Mol. Biosci.* **2020**, 7. [CrossRef] [PubMed]
19. Schulz, C.; Gierok, P.; Petruschka, L.; Lalk, M.; Mäder, U.; Hammerschmidt, S. Regulation of the Arginine Deiminase System by ArgR2 Interferes with Arginine Metabolism and Fitness of *Streptococcus pneumoniae*. *mBio* **2014**, *5*, e01858-14. [CrossRef]
20. Pracht, D.; Elm, C.; Gerber, J.; Bergmann, S.; Rohde, M.; Seiler, M.; Kim, K.S.; Jenkinson, H.F.; Nau, R.; Hammerschmidt, S. PavA of *Streptococcus pneumoniae* Modulates Adherence, Invasion, and Meningeal Inflammation. *Infect. Immun.* **2005**, *73*, 2680. [CrossRef] [PubMed]
21. Rennemeier, C.; Hammerschmidt, S.; Niemann, S.; Inamura, S.; Zähringer, U.; Kehrel, B.E. Thrombospondin-1 promotes cellular adherence of Gram-positive pathogens via recognition of peptidoglycan. *FASEB J.* **2007**, *21*, 3118–3132. [CrossRef]
22. Chen, S.; Songkumarn, P.; Liu, J.; Wang, G.-L. A Versatile Zero Background T-Vector System for Gene Cloning and Functional Genomics. *Plant Physiol.* **2009**, *150*, 1111. [CrossRef]
23. Shishkin, A.A.; Giannoukos, G.; Kucukural, A.; Ciulla, D.; Busby, M.; Surka, C.; Chen, J.; Bhattacharyya, R.P.; Rudy, R.F.; Patel, M.M.; et al. Simultaneous generation of many RNA-seq libraries in a single reaction. *Nat. Methods* **2015**, *12*, 323–325. [CrossRef]
24. Bhattacharyya, R.P.; Bandyopadhyay, N.; Ma, P.; Son, S.S.; Liu, J.; He, L.L.; Wu, L.; Khafizov, R.; Boykin, R.; Cerqueira, G.C.; et al. Simultaneous detection of genotype and phenotype enables rapid and accurate antibiotic susceptibility determination. *Nat. Med.* **2019**, *25*, 1858–1864. [CrossRef] [PubMed]
25. Metsalu, T.; Vilo, J. ClustVis: A web tool for visualizing clustering of multivariate data using Principal Component Analysis and heatmap. *Nucleic Acids Res.* **2015**, *43*, W566–W570. [CrossRef] [PubMed]
26. Pfaffl, M.W. A new mathematical model for relative quantification in real-time RT–PCR. *Nucleic Acids Res.* **2001**, *29*, e45. [CrossRef]
27. Schmidt, F.; Kakar, N.; Meyer, T.C.; Depke, M.; Masouris, I.; Burchhardt, G.; Gómez-Mejia, A.; Dhople, V.; Håvarstein, L.S.; Sun, Z.; et al. In vivo proteomics identifies the competence regulon and AliB oligopeptide transporter as pathogenic factors in pneumococcal meningitis. *PLoS Pathog.* **2019**, *15*, e1007987. [CrossRef]
28. Heß, N.; Waldow, F.; Kohler, T.P.; Rohde, M.; Kreikemeyer, B.; Gómez-Mejia, A.; Hain, T.; Schwudke, D.; Vollmer, W.; Hammerschmidt, S.; et al. Lipoteichoic acid deficiency permits normal growth but impairs virulence of *Streptococcus pneumoniae*. *Nat. Commun.* **2017**, *8*, 2093. [CrossRef] [PubMed]
29. Afzal, M.; Shafeeq, S.; Ahmed, H.; Kuipers, O.P. N-acetylgalatosamine-Mediated Regulation of the aga Operon by AgaR in *Streptococcus pneumoniae*. *Front. Cell. Infect. Microbiol.* **2016**, *6*, 101. [CrossRef] [PubMed]
30. Wu, K.; Xu, H.; Zheng, Y.; Wang, L.; Zhang, X.; Yin, Y. CpsR, a GntR family regulator, transcriptionally regulates capsular polysaccharide biosynthesis and governs bacterial virulence in *Streptococcus pneumoniae*. *Sci. Rep.* **2016**, *6*, 29255. [CrossRef] [PubMed]
31. Bienert, G.P.; Schjoerring, J.K.; Jahn, T.P. Membrane transport of hydrogen peroxide. *Biochim. Biophys. Acta BBA Biomembr.* **2006**, *1758*, 994–1003. [CrossRef] [PubMed]
32. Linley, E.; Denyer, S.P.; McDonnell, G.; Simons, C.; Maillard, J.-Y. Use of hydrogen peroxide as a biocide: New consideration of its mechanisms of biocidal action. *J. Antimicrob. Chemother.* **2012**, *67*, 1589–1596. [CrossRef] [PubMed]
33. Seaver, L.C.; Imlay, J.A. Hydrogen Peroxide Fluxes and Compartmentalization inside Growing *Escherichia coli*. *J. Bacteriol.* **2001**, *183*, 7182. [CrossRef]
34. Sousa-Lopes, A.; Antunes, F.; Cyrne, L.; Marinho, H.S. Decreased cellular permeability to H_2O_2 protects *Saccharomyces cerevisiae* cells in stationary phase against oxidative stress. *FEBS Lett.* **2004**, *578*, 152–156. [CrossRef]
35. Doran, K.S.; Fulde, M.; Gratz, N.; Kim, B.J.; Nau, R.; Prasadarao, N.; Schubert-Unkmeir, A.; Tuomanen, E.I.; Valentin-Weigand, P. Host-pathogen interactions in bacterial meningitis. *Acta Neuropathol.* **2016**, *131*, 185–209. [CrossRef]
36. Subramanian, K.; Henriques-Normark, B.; Normark, S. Emerging concepts in the pathogenesis of the Streptococcus pneumoniae: From nasopharyngeal colonizer to intracellular pathogen. *Cell Microbiol.* **2019**, *21*, e13077. [CrossRef]
37. Weiser, J.N.; Ferreira, D.M.; Paton, J.C. Streptococcus pneumoniae: Transmission, colonization and invasion. *Nat. Rev. Microbiol.* **2018**, *16*, 355–367. [CrossRef] [PubMed]
38. Ogunniyi, A.D.; Giammarinaro, P.; Paton, J.C. The genes encoding virulence-associated proteins and the capsule of Streptococcus pneumoniae are upregulated and differentially expressed in vivo. *Microbiology* **2002**, *148*, 2045–2053. [CrossRef]
39. Orihuela, C.J.; Radin, J.N.; Sublett, J.E.; Gao, G.; Kaushal, D.; Tuomanen, E.I. Microarray analysis of pneumococcal gene expression during invasive disease. *Infect.Immun.* **2004**, *72*, 5582–5596. [CrossRef] [PubMed]

40. Schulz, C.; Hammerschmidt, S. Exploitation of physiology and metabolomics to identify pneumococcal vaccine candidates. *Expert Rev. Vaccines* **2013**, *12*, 1061–1075. [CrossRef]
41. Carvalho, S.M.; Kloosterman, T.G.; Kuipers, O.P.; Neves, A.R. CcpA Ensures Optimal Metabolic Fitness of *Streptococcus pneumoniae*. *PLoS ONE* **2011**, *6*, e26707. [CrossRef]
42. Hartel, T.; Eylert, E.; Schulz, C.; Petruschka, L.; Gierok, P.; Grubmuller, S.; Lalk, M.; Eisenreich, W.; Hammerschmidt, S. Characterization of central carbon metabolism of Streptococcus pneumoniae by isotopologue profiling. *J. Biol. Chem.* **2012**, *287*, 4260–4274. [CrossRef] [PubMed]
43. Leonard, A.; Gierok, P.; Methling, K.; Gomez-Mejia, A.; Hammerschmidt, S.; Lalk, M. Metabolic inventory of Streptococcus pneumoniae growing in a chemical defined environment. *Int. J. Med. Microbiol.* **2018**, *308*, 705–712. [CrossRef] [PubMed]
44. Leonard, A.; Lalk, M. Infection and metabolism—Streptococcus pneumoniae metabolism facing the host environment. *Cytokine* **2018**, *112*, 75–86. [CrossRef] [PubMed]
45. Tettelin, H.; Nelson, K.E.; Paulsen, I.T.; Eisen, J.A.; Read, T.D.; Peterson, S.; Heidelberg, J.; DeBoy, R.T.; Haft, D.H.; Dodson, R.J. Complete Genome Sequence of a Virulent Isolate of *Streptococcus pneumoniae*. *Science* **2001**, *293*, 498. [CrossRef]
46. Afzal, M.; Shafeeq, S.; Kuipers, O.P. LacR is a repressor of *lacABCD* and LacT is an activator of lacTFEG, constituting the *lac* gene cluster in *Streptococcus pneumoniae*. *Appl. Env. Microbiol.* **2014**, *80*, 5349–5358. [CrossRef] [PubMed]
47. Gaspar, P.; Al-Bayati, F.A.; Andrew, P.W.; Neves, A.R.; Yesilkaya, H. Lactate dehydrogenase is the key enzyme for pneumococcal pyruvate metabolism and pneumococcal survival in blood. *Infect. Immun.* **2014**, *82*, 5099–5109. [CrossRef] [PubMed]
48. Bidossi, A.; Mulas, L.; Decorosi, F.; Colomba, L.; Ricci, S.; Pozzi, G.; Deutscher, J.; Viti, C.; Oggioni, M.R. A Functional Genomics Approach to Establish the Complement of Carbohydrate Transporters in *Streptococcus pneumoniae*. *PLoS ONE* **2012**, *7*, e33320. [CrossRef]
49. Slager, J.; Aprianto, R.; Veening, J.-W. Deep genome annotation of the opportunistic human pathogen *Streptococcus pneumoniae* D39. *Nucleic Acids Res.* **2018**, *46*, 9971–9989. [CrossRef]
50. Andersson, B.; Dahmén, J.; Frejd, T.; Leffler, H.; Magnusson, G.; Noori, G.; Edén, C.S. Identification of an active disaccharide unit of a glycoconjugate receptor for pneumococci attaching to human pharyngeal epithelial cells. *J. Exp. Med.* **1983**, *158*, 559–570. [CrossRef]
51. Jeong, J.K.; Kwon, O.; Lee, Y.M.; Oh, D.-B.; Lee, J.M.; Kim, S.; Kim, E.-H.; Le, T.N.; Rhee, D.-K.; Kang, H.A. Characterization of the *Streptococcus pneumoniae* BgaC Protein as a Novel Surface β-Galactosidase with Specific Hydrolysis Activity for the Galβ1-3GlcNAc Moiety of Oligosaccharides. *J. Bacteriol.* **2009**, *191*, 3011–3023. [CrossRef]
52. Aprianto, R.; Slager, J.; Holsappel, S.; Veening, J.-W. High-resolution analysis of the pneumococcal transcriptome under a wide range of infection-relevant conditions. *Nucleic Acids Res.* **2018**, *46*, 9990–10006. [CrossRef] [PubMed]
53. Shaper, M.; Hollingshead, S.K.; Benjamin, W.H., Jr.; Briles, D.E. PspA protects Streptococcus pneumoniae from killing by apolactoferrin, and antibody to PspA enhances killing of pneumococci by apolactoferrin [corrected]. *Infect. Immun.* **2004**, *72*, 5031–5040. [CrossRef]
54. Tu, A.-H.T.; Fulgham, R.L.; McCrory, M.A.; Briles, D.E.; Szalai, A.J. Pneumococcal Surface Protein A Inhibits Complement Activation by *Streptococcus pneumoniae*. *Infect. Immun.* **1999**, *67*, 4720. [CrossRef] [PubMed]
55. Hammerschmidt, S.; Bethe, G.; Remane, P.H.; Chhatwal, G.S. Identification of Pneumococcal Surface Protein A as a Lactoferrin-Binding Protein of *Streptococcus pneumoniae*. *Infect. Immun.* **1999**, *67*, 1683. [CrossRef] [PubMed]
56. Kallio, A.; Sepponen, K.; Hermand, P.; Denoël, P.; Godfroid, F.; Melin, M. Role of Pht Proteins in Attachment of *Streptococcus pneumoniae* to Respiratory Epithelial Cells. *Infect. Immun.* **2014**, *82*, 1683. [CrossRef] [PubMed]
57. Plumptre, C.D.; Hughes, C.E.; Harvey, R.M.; Eijkelkamp, B.A.; McDevitt, C.A.; Paton, J.C. Overlapping Functionality of the Pht Proteins in Zinc Homeostasis of *Streptococcus pneumoniae*. *Infect. Immun.* **2014**, *82*, 4315. [CrossRef]
58. Hathaway, L.J.; Brugger, S.D.; Morand, B.; Bangert, M.; Rotzetter, J.U.; Hauser, C.; Graber, W.A.; Gore, S.; Kadioglu, A.; Mühlemann, K. Capsule Type of *Streptococcus pneumoniae* Determines Growth Phenotype. *PLoS Pathog.* **2012**, *8*, e1002574. [CrossRef] [PubMed]
59. Kim, J.O.; Weiser, J.N. Association of Intrastrain Phase Variation in Quantity of Capsular Polysaccharide and Teichoic Acid with the Virulence of *Streptococcus pneumoniae*. *J. Infect. Dis.* **1998**, *177*, 368–377. [CrossRef]
60. Dorward, D.W.; Garon, C.F.; Judd, R.C. Export and intercellular transfer of DNA via membrane blebs of *Neisseria gonorrhoeae*. *J. Bacteriol.* **1989**, *171*, 2499. [CrossRef] [PubMed]
61. Hoekstra, D.; van der Laan, J.W.; de Leij, L.; Witholt, B. Release of outer membrane fragments from normally growing *Escherichia coli*. *Biochim. Biophys. Acta BBA Biomembr.* **1976**, *455*, 889–899. [CrossRef]
62. Olaya-Abril, A.; Prados-Rosales, R.; McConnell, M.J.; Martín-Peña, R.; González-Reyes, J.A.; Jiménez-Munguía, I.; Gómez-Gascón, L.; Fernández, J.; Luque-García, J.L.; García-Lidón, C.; et al. Characterization of protective extracellular membrane-derived vesicles produced by *Streptococcus pneumoniae*. *J. Proteom.* **2014**, *106*, 46–60. [CrossRef] [PubMed]
63. Elhenawy, W.; Debelyy, M.O.; Feldman, M.F. Preferential Packing of Acidic Glycosidases and Proteases into *Bacteroides* Outer Membrane Vesicles. *mBio* **2014**, *5*, e00909-14. [CrossRef]
64. Horstman, A.L.; Kuehn, M.J. Bacterial Surface Association of Heat-labile Enterotoxin through Lipopolysaccharide after Secretion via the General Secretory Pathway. *J. Biol. Chem.* **2002**, *277*, 32538–32545. [CrossRef] [PubMed]
65. Manning, A.J.; Kuehn, M.J. Contribution of bacterial outer membrane vesicles to innate bacterial defense. *BMC Microbiol.* **2011**, *11*, 258. [CrossRef]

66. Mashburn, L.M.; Whiteley, M. Membrane vesicles traffic signals and facilitate group activities in a prokaryote. *Nature* **2005**, *437*, 422–425. [CrossRef] [PubMed]
67. Toyofuku, M.; Cárcamo-Oyarce, G.; Yamamoto, T.; Eisenstein, F.; Hsiao, C.-C.; Kurosawa, M.; Gademann, K.; Pilhofer, M.; Nomura, N.; Eberl, L. Prophage-triggered membrane vesicle formation through peptidoglycan damage in *Bacillus subtilis*. *Nat. Commun.* **2017**, *8*, 481. [CrossRef] [PubMed]
68. Turnbull, L.; Toyofuku, M.; Hynen, A.L.; Kurosawa, M.; Pessi, G.; Petty, N.K.; Osvath, S.R.; Cárcamo-Oyarce, G.; Gloag, E.S.; Shimoni, R.; et al. Explosive cell lysis as a mechanism for the biogenesis of bacterial membrane vesicles and biofilms. *Nat. Commun.* **2016**, *7*, 11220. [CrossRef] [PubMed]
69. Wang, X.; Thompson, C.D.; Weidenmaier, C.; Lee, J.C. Release of *Staphylococcus aureus* extracellular vesicles and their application as a vaccine platform. *Nat. Commun.* **2018**, *9*, 1379. [CrossRef]
70. Fernebro, J.; Andersson, I.; Sublett, J.; Morfeldt, E.; Novak, R.; Tuomanen, E.; Normark, S.; Normark, B.H. Capsular Expression in *Streptococcus pneumoniae* Negatively Affects Spontaneous and Antibiotic-Induced Lysis and Contributes to Antibiotic Tolerance. *J. Infect. Dis.* **2004**, *189*, 328–338. [CrossRef] [PubMed]

TABLES

Table S1: Results of the RNA-Seq analysis

D39 Locus_Tag	Gene Name	Gene Product	General Function	Cellular or Metabolic Process	Metabolic Pathway or Specific Function	Δ*rr09* vs D39		Δ*hk09* vs D39		Δ*tcs09* vs D39	
						log_2 fc	p-value	log_2 fc	p-value	log_2 fc	p-value
spd_0064	*cpsR*	Transcriptional regulator, GntR family	Genetic Information Processing	Transcription	Transcription Factor	-0,127671498	0,824746298	-4,125932274	3,839E-139	0,083177471	0,810165907
spd_0065	*bgoC*	Beta-galactosidase	Intermediary Metabolism	Carbohydrate Metabolism	Galactose Metabolism	0,742956769	0,010714124	4,335972261	1,5302E-112	0,003924256	0,991451848
spd_0066	*gadV*	Galactosamine-specific PTS IIB component	Environmental Information Processing	Phosphotransferase System	Galactosamine	1,776681399	4,64347E-07	5,26984439	8,90405E-85	0,04044999	0,957595737
spd_0067	*gadW*	Galactosamine-specific PTS IIC component	Environmental Information Processing	Phosphotransferase System	Galactosamine	1,285191835	9,4477E-08	4,886559485	4,5836E-155	0,082516975	0,86135137
spd_0068	*gadE*	Galactosamine-specific PTS IID component	Environmental Information Processing	Phosphotransferase System	Galactosamine	0,968496604	9,92853E-05	5,17139081	4,0283E-196	0,349067255	0,254105121
spd_0070	*agaS*	Galactosamine-6-phosphate isomerase	Intermediary Metabolism	Carbohydrate Metabolism	Galactose Metabolism	1,148924934	2,11222E-05	5,187263585	1,4499E-139	0,311170543	0,396128147
spd_0071	*galM*	Aldose 1-epimerase	Intermediary Metabolism	Carbohydrate Metabolism	Galactose Metabolism	1,131837193	0,000504403	4,981038684	3,53034E-96	0,720879303	0,031671248
spd_0094	*ptvB*	Putative membrane-associated protein	Unknown Function	Unknown Function	Unknown Function	-0,55493857	0,092129242	-1,078993791	2,37671E-07	-0,553812353	0,03118967
spd_0095	*ptvA*	Integral membrane protein (putative)	Unknown Function	Unknown Function	Unknown Function	-0,412093463	0,297132448	-1,214545745	2,52239E-09	-0,616721532	0,011025673
spd_0096	*ptvR*	Transcriptional regulator, PadR family	Genetic Information Processing	Transcription	Transcription Factor	-0,489180574	0,130040463	-1,052790487	1,18921E-07	-0,454800218	0,071531817
spd_0126	*pspA*	Surface protein PspA precursor	Cellular Processes	Pathogenesis	Colonization Factor	0,098888171	0,836628683	1,384664714	7,98437E-23	0,197515687	0,375650206
spd_0277	*celA*	6-phospho-beta-glucosidase	Intermediary Metabolism	Carbohydrate Metabolism	Glycolysis/Gluconeogenesis	-1,344255945	0,01689532	-1,781852196	2,15924E-05	-0,476820835	0,451464271
spd_0279	*celB*	Cellobiose-specific PTS IIB component	Environmental Information Processing	Phosphotransferase System	Cellobiose	-1,114956354	0,080472231	-1,690661891	0,00010292	-0,245907052	0,722990663
spd_0301	*regR*	Transcriptional regulator RegR	Genetic Information Processing	Transcription	Transcription Factor	-0,108322696	0,687690234	1,406587587	3,61677E-55	-0,162168266	0,235166036
spd_0335	*eng*	Endo-alpha-N-acetylgalactosaminidase Eng	Intermediary Metabolism	Unclassified	Unclassified	0,497159651	1,02375E-05	5,122095132	0	-0,084822794	0,610374381
spd_0373	*mip*	Macrophage infectivity potentiator protein	Unknown Function	Unknown Function	Unknown Function	-0,182693717	0,780311074	1,423930317	1,10206E-11	0,577643567	0,03033328
spd_0385	*fabF*	3-oxoacyl-(acyl-carrier-protein) synthase FabF	Intermediary Metabolism	Lipid Metabolism	Fatty Acid Biosynthesis	-0,147475578	0,75609232	-1,00932569	1,99813E-10	-0,506314206	0,009304278
spd_0386	*accB*	Biotin carboxyl carrier protein of acetyl-CoA carboxylase	Intermediary Metabolism	Lipid Metabolism	Fatty Acid Biosynthesis	-0,161475678	0,745200937	-1,018469649	1,8186E-09	-0,533571908	0,009724827
spd_0387	*fabZ*	3-hydroxyacyl-(acyl-carrier-protein) dehydratase FabZ	Intermediary Metabolism	Lipid Metabolism	Fatty Acid Biosynthesis	-0,187182263	0,656972797	-1,006645507	7,45723E-11	-0,443219487	0,022471858
spd_0388	*accC*	Biotin carboxylase of acetyl-CoA carboxylase	Intermediary Metabolism	Lipid Metabolism	Fatty Acid Biosynthesis	-0,181106183	0,687690234	-1,047010065	8,84846E-11	-0,455705224	0,024914457
spd_0404	*ilvB*	Acetolactate synthase large subunit	Intermediary Metabolism	Amino Acid Metabolism	Valine, Leucine and Isoleucine Biosynthesis	0,11134425	0,767304182	1,012153448	4,17468E-17	0,506607009	0,000347595
spd_0453		Type I restriction-modification system, specificity subunit S components 1.1-2.1	Genetic Information Processing	DNA Metabolism	Restriction and Modification	0,187931492	0,32791076	-1,044767853	1,00969E-29	-0,680736265	3,89138E-12
spd_0491		Hypothetical protein	Unknown Function	Unknown Function	Unknown Function	-0,068130827	0,956397424	1,037321087	0,000154178	0,382715387	0,323698889
spd_0524	*vncR*	Two-component system response regulator VncR	Environmental Information Processing	Signaling	Two-component system	-0,061273383	0,85399032	1,342762996	4,80116E-46	-0,322905422	0,009396004
spd_0525	*vncS*	Two-component system sensor histidine kinase VncS	Environmental Information Processing	Signaling	Two-component system	-0,242674436	0,130040463	1,401116286	4,88756E-56	-0,265904251	0,026026804
spd_0574	*rr09*	Two-component response regulator YesN	Environmental Information Processing	Signaling	Two-component system	-8,573208967	5,87654E-80	0,011478269	0,93874223	-7,789230069	2,1978E-149
spd_0575	*hk09*	Two-component sensor kinase YesM	Environmental Information Processing	Signaling	Two-component system	0,548215296	0,016777858	-7,322846497	1,9948E-202	-8,075603455	3,2655E-230
spd_0610		Hypothetical protein	Unknown Function	Unknown Function	Unknown Function	-0,077452774	0,925229986	2,891749516	4,47802E-52	0,017709402	0,964830732
spd_0611		Hypothetical protein	Unknown Function	Unknown Function	Unknown Function	-0,114482575	0,854968579	2,546068397	8,97414E-47	0,101374274	0,782008822
spd_0612		Hypothetical protein	Unknown Function	Unknown Function	Unknown Function	-0,022576548	0,983682908	2,9953438	7,05041E-80	0,300093882	0,230032374
spd_0613		Hypothetical protein	Unknown Function	Unknown Function	Unknown Function	-0,00922776	0,99188327	2,86933941	1,4136E-127	0,017055043	0,951027155
spd_0614		ABC transporter ATP-binding protein	Environmental Information Processing	ABC-Transporter	Unknown substrate	0,06312571	0,917449141	3,146104106	1,2416E-110	0,129254791	0,622938164
spd_0616	*glnQ3*	Glutamine ABC transporter ATP-binding protein GlnQ3	Environmental Information Processing	ABC-Transporter	Phosphate and Amino acids	-0,163224201	0,656972797	1,97997381	5,7774E-67	-0,01721037	0,949092973
spd_0618	*glnP3a*	Glutamine ABC transporter permease GlnP3a	Environmental Information Processing	ABC-Transporter	Phosphate and Amino acids	-0,493927415	0,378347923	1,209255039	2,79909E-06	-0,270897607	0,520628686

TABLES

Table S1: Results of the RNA-Seq analysis

D39 Locus_Tag	Gene Name	Gene Product	General Function	Cellular or Metabolic Process	Metabolic Pathway or Specific Function	Δ*rr09* vs D39		Δ*hk09* vs D39		Δ*tcs09* vs D39	
						log_2 fc	p-value	log_2 fc	p-value	log_2 fc	p-value
spd_0700	*pepN*	Lysyl aminopeptidase PepN	Intermediary Metabolism	Metabolism of other Amino Acids	Glutathione Metabolism	-0,015551311	0,976032554	1,095114243	2,07264E-44	0,016301578	0,930303847
spd_0778		Putative alpha-dextrin endo-1,6-alpha-glucosidase	Unknown Function	Unknown Function	Unknown Function	0,055566303	0,921504759	1,3127717	7,03146E-24	0,199910723	0,32754961
spd_0787	*pepX*	Xaa-Pro dipeptidyl-peptidase	Genetic Information Processing	Protein Fate	Degradation of Proteins, Peptides and Glycopeptides	-0,143618587	0,715022306	1,171768655	2,09659E-20	0,280801693	0,114975867
spd_0816		Hydrolase, HAD superfamily	Unknown Function	Unknown Function	Unknown Function	-0,072441055	0,880906076	1,440724591	8,57197E-29	0,248192572	0,195386823
spd_0889	*phtD*	Pneumococcal histidine triad protein D	Cellular Processes	Pathogenesis	Colonization Factor	-0,005381556	0,995481102	1,062116298	7,58795E-06	0,575028881	0,053352784
spd_1107	*guaC*	GMP reductase	Intermediary Metabolism	Nucleotide Metabolism	Purine Metabolism	0,042589898	0,95103527	-1,044012019	8,01555E-12	-0,761751272	5,63392E-06
spd_1300	*apbE*	Putative thiamin biosynthesis lipoprotein	Unknown Function	Unknown Function	Unknown Function	-0,061315842	0,925229986	1,911991189	5,48784E-40	0,040492929	0,900765524
spd_1301		Fumarate reductase, flavoprotein subunit precursor	Intermediary Metabolism	Unclassified	Unclassified	-0,144531079	0,837864488	1,929442842	2,16034E-24	-0,171662985	0,629573465
spd_1302		Fumarate reductase, flavoprotein subunit precursor	Intermediary Metabolism	Unclassified	Unclassified	0,084534551	0,860443084	2,60805661	3,94649E-86	0,250771606	0,2209651
spd_1379		Hypothetical protein	Unknown Function	Unknown Function	Unknown Function	-0,117842961	0,909511418	1,26595838	5,2276E-06	0,594791978	0,099854596
spd_1514		ABC transporter, ATP-binding protein	Environmental Information Processing	ABC-Transporter	Unknown substrate	0,537797566	0,289315206	1,935047079	2,38555E-14	0,307668489	0,450892579
spd_1515		Hypothetical protein	Unknown Function	Unknown Function	Unknown Function	0,53128111	0,26387573	1,915367399	2,64252E-15	0,336799607	0,371942903
spd_1516		Hypothetical protein	Unknown Function	Unknown Function	Unknown Function	0,592553508	0,127675114	1,984587656	2,06331E-18	0,356514533	0,296116731
spd_1517		Hypothetical protein	Unknown Function	Unknown Function	Unknown Function	0,442446737	0,4112312	2,084020377	4,48866E-18	0,342482907	0,362121162
spd_1588		Hypothetical protein	Unknown Function	Unknown Function	Unknown Function	-0,126358517	0,818476306	2,502910431	6,41612E-56	-0,018527004	0,958799786
spd_1589		Small integral membrane protein	Unknown Function	Unknown Function	Unknown Function	-0,13086681	0,854968579	2,829206432	1,15563E-41	0,106336868	0,806675766
spd_1590	*gls24*	General stress protein, Gls24 family	Unknown Function	Unknown Function	Unknown Function	-0,032543341	0,976032554	2,837882419	1,85332E-68	-0,054445493	0,876533806
spd_1591		Hypothetical protein	Unknown Function	Unknown Function	Unknown Function	-0,020475906	0,987441001	3,215754522	3,05977E-57	0,01524951	0,973575161
spd_1592		Acetyltransferase	Unknown Function	Unknown Function	Unknown Function	-0,364309806	0,527106285	1,588526803	3,51189E-13	0,068608657	0,879542673
spd_1593	*cclA*	Type IV prepilin peptidase	Genetic Information Processing	Protein Fate	Secretion	0,307928985	0,912152821	1,731324177	0,036843693	3,091555876	0,000180781
spd_1609		ABC transporter, substrate-binding protein	Environmental Information Processing	ABC-Transporter	Mineral and organic iron	-0,036973133	0,983842077	-1,314356731	0,000204787	0,586144255	0,162720013
spd_1727		Hypothetical protein	Unknown Function	Unknown Function	Unknown Function	-0,046783412	0,912152821	1,003393751	6,65445E-21	0,002068197	0,991451848
spd_1728		Hypothetical protein	Unknown Function	Unknown Function	Unknown Function	0,062117629	0,832001038	1,034691811	1,29037E-35	-0,126587711	0,335589169
spd_1729		Hypothetical protein	Unknown Function	Unknown Function	Unknown Function	0,087664495	0,681078737	1,423115185	2,66675E-89	-0,026897611	0,863779194
spd_1748	*pneA2*	Class II two-component lantibiotic peptide PneA2	Cellular Processes	Pathogenesis	Toxin production and resistance	0,236163726	0,745200937	1,113268418	5,85436E-06	0,555445123	0,077449215
spd_1792		Hypothetical protein	Unknown Function	Unknown Function	Unknown Function	-0,203479477	0,80463403	1,274696239	6,25856E-07	0,165770617	0,71483922
spd_1801		ABC transporter, ATP-binding protein	Environmental Information Processing	ABC-Transporter	Unknown substrate	-0,220531226	0,716889606	-1,412785031	2,66838E-10	-0,441464086	0,129608775
spd_1802		Hypothetical protein	Unknown Function	Unknown Function	Unknown Function	0,129200974	0,909511418	-1,784947383	2,19081E-07	-0,69686474	0,083397542
spd_1865	*adh*	Putative Zn-dependent alcohol dehydrogenase	Intermediary Metabolism	Carbohydrate Metabolism	Propanoate Metabolism	-0,014012498	0,99188327	1,179252237	1,56699E-09	0,217806438	0,48554653
spd_1866	*nagA*	N-acetylglucosamine-6-phosphate deacetylase	Intermediary Metabolism	Carbohydrate Metabolism	Aminosugar and Nucleotidesugar Metabolism	-0,106864217	0,696638548	1,734802808	5,16212E-76	0,083906946	0,622938164
spd_1916		Transcriptional regulator	Genetic Information Processing	Transcription	Transcription Factor	0,225963343	0,760405734	-1,019344838	0,000326782	-0,334083158	0,374237822
spd_1931		Hypothetical protein	Unknown Function	Unknown Function	Unknown Function	0,095349212	0,865942581	1,369829469	1,24604E-17	0,493244084	0,016120785
spd_1974		Glycosyl hydrolase family 29 alpha-L-fucosidase	Intermediary Metabolism	Glycan Biosynthesis and Metabolism	Other Glycan Degradation	0,071462003	0,912152821	1,415567952	3,81555E-18	-0,147091475	0,610150013
spd_1985	*adh2*	Lactaldehyde dehydrogenase involved in fucose or rhamnose utilization	Intermediary Metabolism	Unclassified	Unclassified	0,20247719	0,838878681	1,003343178	0,001470637	0,113092472	0,854904956
spd_1996	*fucR*	L-fucose operon activator	Genetic Information Processing	Transcription	Transcription Factor	-0,005636869	0,995481102	1,135340843	1,57795E-07	0,288518222	0,379211409

TABLES

Table S1: Results of the RNA-Seq analysis

D39 Locus_Tag	Gene Name	Gene Product	General Function	Cellular or Metabolic Process	Metabolic Pathway or Specific Function	Δ*rr09* vs D39		Δ*hk09* vs D39		Δ*tcs09* vs D39		D39:Δ*tcs09*				D39			
						log_2 fc	p-value	log_2 fc	p-value	log_2 fc	p-value	FPKM R1	FPKM R2	FPKM R3	FPKM R4	FPKM R1	FPKM R2	FPKM R3	FPKM R4
genes excluded in D39Δ*tcs09*																			
spd_0014	*comX1*	Competence-specific sigma factor ComX	Genetic Information Processing	Transcription	Sigma Factor	0,366657302	0,940973056	-0,053881991	0,969812705	6,014564798	7,86492E-07	2991,458706	28,49573337	24,86612025	3574,072678	19,84100274	23,13409555	29,00011016	30,40505674
spd_0023	*comW*	Competence positive regulator ComW	Genetic Information Processing	Transcription	Transcription Factor	-0,200105324	0,963248106	-0,453330769	0,705737104	3,583539961	0,000161341	1872,682591	70,35983549	83,37721823	1900,973731	68,93611183	92,61798393	84,29380194	81,79138069
spd_0024	*purA*	Adenylosuccinate synthetase	Intermediary Metabolism	Nucleotide Metabolism	Purine Metabolism	-0,05770051	0,985763592	0,698729487	0,280850616	1,478809991	0,020752333	2120,50783	399,670927	355,7660816	2126,782227	474,7833369	426,3206285	420,2506392	473,5892532
spd_0049	*comA*	Competence-stimulating peptide ABC transporter ATP-binding protein ComA	Environmental Information Processing	ABC-Transporter	Competence	-0,036947758	0,993530562	-0,56433688	0,670080286	4,281459262	3,62321E-05	1415,507616	34,84575752	34,31816788	1538,546084	35,13428659	38,75628422	41,4532439	40,11809275
spd_0050	*comB*	Competence-stimulating peptide ABC transporter permease protein ComB	Environmental Information Processing	ABC-Transporter	Competence	-0,226863084	0,963248106	-0,465498101	0,734286706	4,532378004	1,95404E-05	2151,536733	47,23959354	42,27472619	2325,384771	57,25546506	44,8728012	39,80210859	55,40477005
spd_0051	*purC*	Phosphoribosylaminoimidazole-succinocarboxamide synthase	Intermediary Metabolism	Nucleotide Metabolism	Purine Metabolism	0,28134018	0,879911426	-0,593422826	0,409220573	1,610692998	0,011865913	32,58906618	5,24321494	4,012012679	24,40637077	3,85482339	6,21315709	5,577637768	6,145021993
spd_0052	*purL*	Phosphoribosylformylglycinamidine synthase, synthetase and glutamine amidotransferase subunits	Intermediary Metabolism	Nucleotide Metabolism	Purine Metabolism	0,076190788	0,967416002	-0,173766013	0,715062885	1,01662509	0,012021792	21,15534187	7,318952452	5,895268228	17,86652678	5,0891921	6,678925675	6,291063755	7,808061862
spd_0132	*cibB*	Two-peptide bacteriocin peptide CibB	Unknown Function	Unknown Function	Unknown Function	0,184269162	0,982188005	-0,116379553	0,955190685	5,828746264	7,15526E-05	827,7971356	2,79369935	1,966672882	763,5455895	4,44616308	6,480138808	10,84226409	6,275553506
spd_0133	*cibA*	Two-peptide bacteriocin peptide CibA	Unknown Function	Unknown Function	Unknown Function	0,083047657	0,99188327	0,368830866	0,843753672	6,368225382	2,44043E-06	1831,044398	6,434520439	9,167233272	1804,853347	10,05765116	6,396524114	9,694170203	18,06752098
spd_0391	*bnlC*	Biofilm-regulating peptide	Unknown Function	Unknown Function	Unknown Function	-0,28995228	0,925229986	-0,483058675	0,656146306	2,730375958	0,002723895	3673,138975	223,3697809	231,3378279	3442,126432	168,6942399	349,1436079	329,2140201	293,7262697
spd_0553		Hypothetical protein	Unknown Function	Unknown Function	Unknown Function	-0,022816409	0,99188327	-0,730949643	0,065780938	-1,00046668	0,018316739	11,17112054	25,66971023	15,74963655	5,470787149	22,25378112	25,12794321	30,79701674	37,55996569
spd_0817		CAAX amino terminal protease family protein	Genetic Information Processing	Protein Fate	Degradation of Proteins, Peptides and Glycopeptides	-0,380603082	0,774546048	0,252559771	0,686700647	1,107406041	0,048477927	306,4317886	69,331137	87,46426451	251,9630911	65,04002175	118,7687941	81,9988311	66,29674025
spd_0843	*comEA*	Late competence DNA receptor ComEA	Cellular Processes	Competence	DNA Transformation	0,0832944	0,988900948	-1,266577577	0,349334994	4,839440641	2,04992E-05	351,6431235	6,040570208	7,087272782	409,5669558	6,792180005	7,005716887	7,201383579	6,047088655
spd_0844	*comEC*	Late competence DNA transporter ComEC	Cellular Processes	Competence	DNA Transformation	0,266029556	0,9512	-0,614856349	0,648337094	4,18990192	9,11396E-05	241,3591772	5,187978231	5,952673877	262,3818939	5,615736099	8,981108043	7,91729499	5,698404207
spd_0846		ABC-2 type transport system permease protein	Environmental Information Processing	ABC-Transporter	Unknown substrate	-0,140656088	0,948746367	-0,108209081	0,886690132	1,638740451	0,005206868	307,261356	68,63566236	64,06661533	328,4989745	78,70216462	53,0960206	64,07009951	50,93232854
spd_0994	*ribF*	Bifunctional FMN adenylyltransferase/riboflavin kinase RibF	Intermediary Metabolism	Metabolism of Cofactors and Vitamins	Roboflavin Metabolism	-0,069816495	0,97961836	0,266059023	0,685561734	1,265253519	0,027111973	332,087038	73,56741622	74,84282912	328,1609463	98,46398654	82,18976055	72,59602909	83,25567651
spd_1122	*dprA*	DNA protecting protein DprA	Genetic Information Processing	DNA Metabolism	Replicaion and Repair	0,070869492	0,987441001	-0,46414232	0,618035028	2,128850245	0,009304278	179,9307983	14,70097905	16,4213711	112,6835906	15,22378807	18,56800198	19,79391982	20,46983548
spd_1380		Cell shape-determining protein	Unknown Function	Unknown Function	Unknown Function	0,108065272	0,953479451	0,36507662	0,495003072	1,338154845	0,005056703	474,8511512	132,4623095	135,4934107	498,9084251	127,1230734	117,5341267	116,0953415	130,4277068
spd_1381	*def2*	Peptide deformylase	Genetic Information Processing	Protein Synthesis	Other	0,389971881	0,784134276	0,319833538	0,612739813	1,475440056	0,00797202	291,2634274	77,37527602	62,23012367	293,4831632	62,48157277	63,6851014	62,99936945	71,48634161
spd_1527	*qsrB*	ABC transporter membrane-spanning permease - Na+ export	Environmental Information Processing	ABC-Transporter	Metallic cation	-0,004861011	0,995481102	0,159155799	0,784244363	1,237744162	0,010388735	2228,879187	541,1339767	549,8129042	2280,686127	516,220375	677,7463777	630,9101686	550,0114737
spd_1528	*qsrA*	ABC transporter ATP-binding protein - Na+ export	Environmental Information Processing	ABC-Transporter	Metallic cation	-0,0971462	0,963248106	0,085487191	0,891970154	1,139250926	0,02468565	2331,962427	522,1986575	582,0559782	2195,669373	537,5903524	800,3776009	686,3940947	532,5986448
spd_1596	*trpA*	Tryptophan synthase alpha chain	Intermediary Metabolism	Amino Acid Metabolism	Phenylalanin, Tyrosine and Tryptophan Metabolism	0,072486862	0,962897932	0,326545213	0,405664116	1,202540191	0,000400777	325,8620649	111,8925129	144,8352068	361,3750171	140,6270741	101,5705464	89,48280535	78,59222143
spd_1711	*ssbB*	Single-stranded DNA-binding protein SsbB	Genetic Information Processing	DNA Metabolism	Replicaion and Repair	0,01211505	0,995481102	-0,343929083	0,839967845	5,907165019	1,94431E-06	5715,430925	40,58483238	32,42030448	5392,095029	42,08697552	41,8116229	53,18280526	49,22030716

TABLES

Table S1: Results of the RNA-Seq analysis

D39 Locus_Tag	Gene Name	Gene Product	General Function	Cellular or Metabolic Process	Metabolic Pathway or Specific Function	Δ*rr09* vs D39		Δ*hk09* vs D39		Δ*tcs09* vs D39		D39Δ*tcs09*				D39			
						log_2 fc	p-value	log_2 fc	p-value	log_2 fc	p-value	FPKM R1	FPKM R2	FPKM R3	FPKM R4	FPKM R1	FPKM R2	FPKM R3	FPKM R4
genes excluded in D39Δ*tcs09*																			
spd_1740	*cinA*	Bifunctional ADP-ribose pyrophosphatase/nicotinamide-nucleotide amidase	Intermediary Metabolism	Metabolism of Cofactors and Vitamins	Nicotinate and Nicotinamide Metabolism	-0,014675968	0,995481102	0,076524376	0,936573673	2,23795369	0,001861705	2134,30454	263,4665181	279,1173499	2481,356492	291,0194129	262,260033	280,5802885	259,6326789
spd_1744	*comM*	Immunity factor ComM	Cellular Processes	Competence	Unclassified	0,604348137	0,853030402	-0,048088931	0,969812705	4,759299885	1,01127E-05	391,8881723	8,810275052	8,398738298	459,3852488	6,29873103	9,260024442	8,013847367	8,503829751
spd_1818	*comX2*	Competence-specific sigma factor ComX	Genetic Information Processing	Transcription	Sigma Factor	0,318290362	0,948746367	-0,157659515	0,925935001	5,971808547	7,66492E-07	3070,385351	26,18045504	26,5377922	3624,799362	23,38403895	26,43896634	25,69439812	32,00532288
spd_1827		Malonate permease	Environmental Information Processing	Other	Unknown substrate	-0,109981286	0,946504168	0,316341985	0,501921694	1,148786776	0,006346189	318,5518509	117,1781073	118,4324109	392,5952468	92,49189249	106,8600098	104,0883242	123,626968
spd_1828		Hypothetical protein	Unknown Function	Unknown Function	Unknown Function	-0,382872843	0,909511418	-0,048589499	0,968703644	3,933955918	9,11396E-05	11735,48226	448,9173996	363,6529441	14948,9021	467,462746	344,2150041	418,6927025	568,7099681
spd_1857	*comGG*	Late competence protein ComGG	Cellular Processes	Competence	Unclassified	-0,058473563	0,993026962	-0,838183057	0,582349841	5,873154726	1,51602E-06	1616,3039	16,72575654	14,29400653	1906,851996	12,11821079	11,97416954	14,9824103	21,56880455
spd_1858	*comGF*	Late competence protein ComGF	Cellular Processes	Competence	Secretion	0,172382729	0,981012573	0,142831912	0,93714392	5,936916596	3,25595E-06	845,988303	6,846377498	5,210406077	939,1234772	4,417291891	5,794253986	7,493467668	11,63829923
spd_1859	*comGE*	Late competence protein ComGE	Cellular Processes	Competence	Unclassified	-1,12379882	0,748639303	-1,73912661	0,247274038	5,825912942	5,63877E-06	1054,590014	8,18842913	6,532970838	1255,451327	9,773892977	6,837663708	8,566526496	15,8187228
spd_1860	*comGD*	Late competence protein ComGD	Cellular Processes	Competence	Secretion	-0,687919956	0,858575803	-0,975679032	0,550435944	5,688209366	1,36311E-05	1088,564058	4,070819053	8,929427805	1203,476752	11,97150121	8,826673545	10,1541917	13,71656695
spd_1861	*comGC*	Late competence protein ComGC	Cellular Processes	Competence	Secretion	-0,113472618	0,987441001	-0,643142844	0,719049178	5,572828696	5,27062E-05	642,6419796	4,705717438	1,53364399	726,1286094	5,720865798	3,941589018	5,734679768	13,50683351
spd_1862	*comGB*	Late competence protein ComGB	Cellular Processes	Competence	Secretion	0,0239982	0,995481102	-0,500009453	0,75317193	5,917910757	7,66492E-07	1190,300567	11,9362659	10,65136109	1392,529684	8,110312963	8,481526812	12,05623055	14,44488024
spd_1863	*comGA*	Late competence protein ComGA	Cellular Processes	Competence	Secretion	-0,241272344	0,976032554	-0,336812582	0,848741591	6,002096887	2,71813E-06	1411,500956	9,256575809	9,369880991	1714,216839	9,207380709	8,314802312	11,86764021	19,67206152
spd_2028	*cbpD*	Choline-binding protein D	Cellular Processes	Competence	Unclassified	-0,007249996	0,995481102	-0,772630859	0,304048554	1,812028335	0,011806807	265,9944787	37,44428216	42,14549325	323,9636243	41,41170156	54,8358294	44,28141496	50,18206527
spd_2034	*comFC*	Phosphoribosyltransferase domain protein, ComF operon protein C	Cellular Processes	Competence	Secretion	0,286142778	0,961198537	-0,164634301	0,926975624	4,402251241	0,00088121	82,69592842	1,93409955	1,664107823	92,59439095	0,769528225	1,944041643	4,133839819	1,593025121
spd_2035	*comFA*	DNA transporter ATPase, ComF operon protein A	Environmental Information Processing	Other	Other	0,358152695	0,925229986	0,412114785	0,765513741	4,010661035	0,000140282	37,204083	1,316200156	1,775910154	61,35093093	0,981903798	1,755474093	1,943311717	1,626136497
spd_2063	*comE*	Two-component system response regulator ComE	Environmental Information Processing	Signaling	Two-component system	-0,279711304	0,953822916	-0,240082511	0,88309139	5,045029539	9,32693E-06	3593,015366	44,2762391	47,55273992	3834,192597	54,31714468	60,04068053	47,60416902	65,79580321
spd_2064	*comD*	Two-component system sensor histidine kinase ComD	Environmental Information Processing	Signaling	Two-component system	-0,154552315	0,979147972	-0,14579125	0,92556218	5,034561163	5,37582E-06	3656,760332	53,83243748	56,80658978	3807,960607	48,4802782	53,38637434	53,52234712	75,74110347
spd_2065	*comC1*	Competence-stimulating peptide precursor ComC	Environmental Information Processing	Signaling	Two-component system	0,138509554	0,983183693	0,097559572	0,954954271	5,384522927	5,09774E-06	5476,479709	61,0622858	63,68274094	5622,592997	66,13667581	66,88428984	50,37275488	85,34752768
Enolase																			
spd_1012	*eno*	Enolase	Intermediary Metabolism	Carbohydrate Metabolism	Glycolysis/Gluconeogenesis	0,074882762	0,90656423	0,569483667	0,001621332	0,327866171	0,158555559								
up- and downstream genes of *tcs09*																			
spd_0573	*msrAB2*	Peptide methionine sulfoxide reductase MsrAB2	Cellular Processes	Adaptations to atypical conditions	Oxidoreductase	-0,192747132	0,53737984	-0,212989833	0,172193061	-0,108008448	0,604578798	2228,879187	541,1339767	549,8129042	2280,686127	516,220375	677,7463777	630,9101686	550,0114737
spd_0576		Unknown Function	Unknown Function	Unknown Function	Unknown Function	0,01115563	0,981012573	0,095949445	0,340519515	0,129014663	0,243172011	2331,962427	522,1986575	582,0559782	2195,669373	537,5903524	800,3776009	686,3940947	532,5986448
spd_0577	*zmpB*	Zinc metalloprotease ZmpB precursor	Intermediary Metabolism	Glycan Biosynthesis and Metabolism	Other Glycan Degradation	-0,050130516	0,774546048	0,187843323	0,002350529	0,096033401	0,241837261	325,8620649	111,8925129	144,8352068	361,3750171	140,6270741	101,5705464	89,48280535	78,59222143

Table S2. Inline barcode sequences.

BC ID	Barcode sequence 5′-3′	Oligonucleotide sequence
L01	CCAAGTCG	ACCAAGTCGAGATCGGAAGAGCGTCGTGTA
L02	GCAGCCAC	AGCAGCCACAGATCGGAAGAGCGTCGTGTA
L03	GTAACTGC	AGTAACTGCAGATCGGAAGAGCGTCGTGTA
L04	TCATCGTG	ATCATCGTGAGATCGGAAGAGCGTCGTGTA
L05	TTACCACG	ATTACCACGAGATCGGAAGAGCGTCGTGTA
L06	AGAATTAT	AAGAATTATAGATCGGAAGAGCGTCGTGTA
L07	GGCCCAAG	AGGCCCAAGAGATCGGAAGAGCGTCGTGTA
L08	TACAACAT	ATACAACATAGATCGGAAGAGCGTCGTGTA
L09	TGAACCAG	ATGAACCAGAGATCGGAAGAGCGTCGTGTA
L10	ATATGGAC	AATATGGACAGATCGGAAGAGCGTCGTGTA
L11	CAACTCGC	ACAACTCGCAGATCGGAAGAGCGTCGTGTA
L12	CGGAGGGC	ACGGAGGGCAGATCGGAAGAGCGTCGTGTA
L13	ACATTATT	AACATTATTAGATCGGAAGAGCGTCGTGTA
L14	ATCACTTG	AATCACTTGAGATCGGAAGAGCGTCGTGTA
L15	CCCGTCTT	ACCCGTCTTAGATCGGAAGAGCGTCGTGTA
L16	CTCGGTAC	ACTCGGTACAGATCGGAAGAGCGTCGTGTA
L17	GTCTGGCG	AGTCTGGCGAGATCGGAAGAGCGTCGTGTA
L18	TCCCGCGG	ATCCCGCGGAGATCGGAAGAGCGTCGTGTA
L19	CGGCACTT	ACGGCACTTAGATCGGAAGAGCGTCGTGTA
L20	GAGATTGT	AGAGATTGTAGATCGGAAGAGCGTCGTGTA
L21	TACAGATG	ATACAGATGAGATCGGAAGAGCGTCGTGTA
L22	TGGGAGAC	ATGGGAGACAGATCGGAAGAGCGTCGTGTA
L23	CCCTACAG	ACCCTACAGAGATCGGAAGAGCGTCGTGTA
L24	CTCTAACT	ACTCTAACTAGATCGGAAGAGCGTCGTGTA
L25	AAGTGTTG	AAAGTGTTGAGATCGGAAGAGCGTCGTGTA
L26	GAGCCATC	AGAGCCATCAGATCGGAAGAGCGTCGTGTA
L27	GGTCCTCT	AGGTCCTCTAGATCGGAAGAGCGTCGTGTA
L28	TACCGGCC	ATACCGGCCAGATCGGAAGAGCGTCGTGTA
L29	CCCTCGGC	ACCCTCGGCAGATCGGAAGAGCGTCGTGTA
L30	CTGGATCG	ACTGGATCGAGATCGGAAGAGCGTCGTGTA
L31	TTTCTAAC	ATTTCTAACAGATCGGAAGAGCGTCGTGTA
L32	CCGGTACC	ACCGGTACCAGATCGGAAGAGCGTCGTGTA

Table S3. Primers used for RNA preparation for RNA-sequencing.

Index code	Barcode sequence 5′-3′	Primer sequence 5′→3′
AR2		TACACGACGCTCTTCCGAT
3Tr3		iCiGiCCAGACGTGTGCTCTTCCGATCTrGrGrG
P5		AATGATACGGCGACCACCGAGATCTACACTCTTTC CCTACACGACGCTCTTCCGATCT
X01	AAGTAGAG	CAAGCAGAAGACGGCATACGAGATAAGTAGAGGT GACTGGAGTTCAGACGTGTGCTCTTCCGATCT

iC = iso-dC; iG = iso-dG; rG = ribonucleotide G

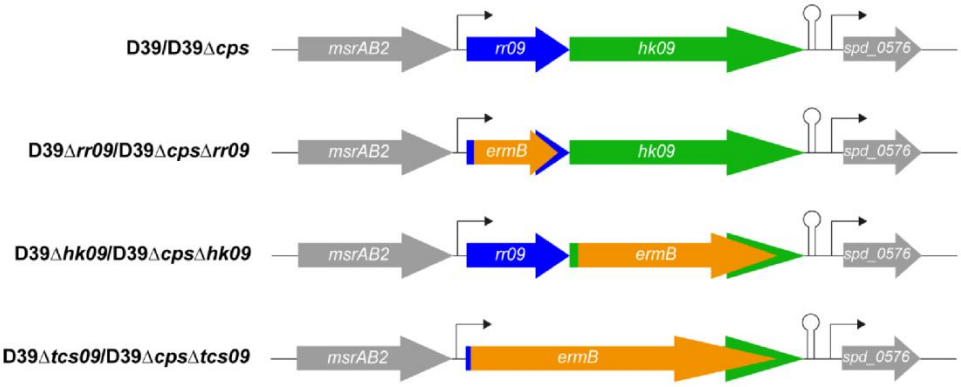

Figure S1: Genomic organization of the *tcs09* gene cluster in *S. pneumoniae* D39 wild-type and isogenic *tcs09*-mutants. The *rr09* gene is shown in blue and the *hk09* gene in green within its operon organization, the genes upstream and downstream of *rr09* and *hk09* are shown in grey and the inserted *ermB*- cassette for *tcs09* deletions is indicated by orange. The large and filled arrows represent their relative gene size and orientation in the genome. Transcriptional start sites are indicated with a thin arrow and terminators with lollypops.

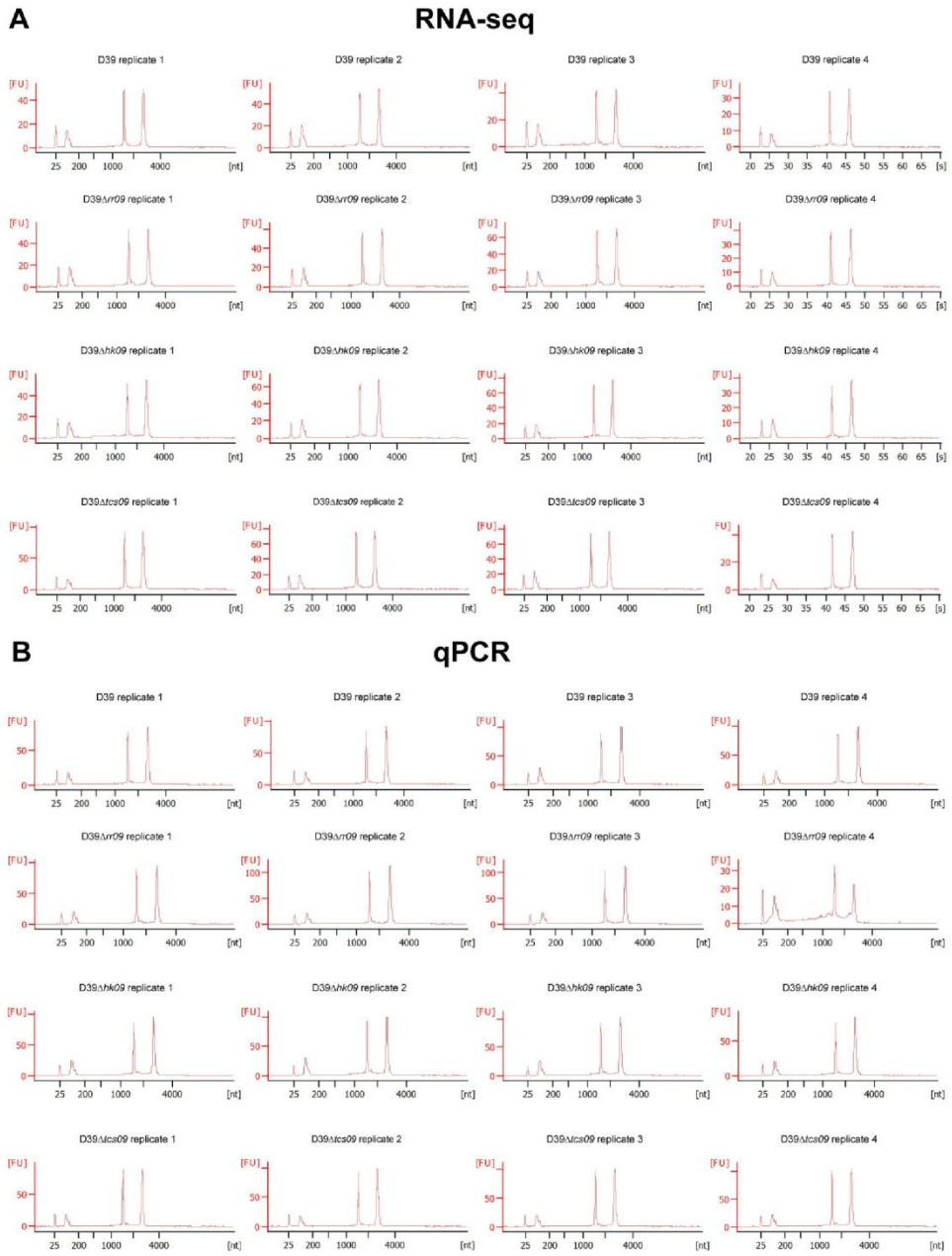

Figure S2. RNA integrity check with the Agilent Bioanalyzer. Shown are the electrophoretic representations of the individual RNA samples used for (**A**) RNA-seq and (**B**) qPCR. The curves consist of added marker and the individual ribosomal RNAs, which are used to calculate the RNA quality.

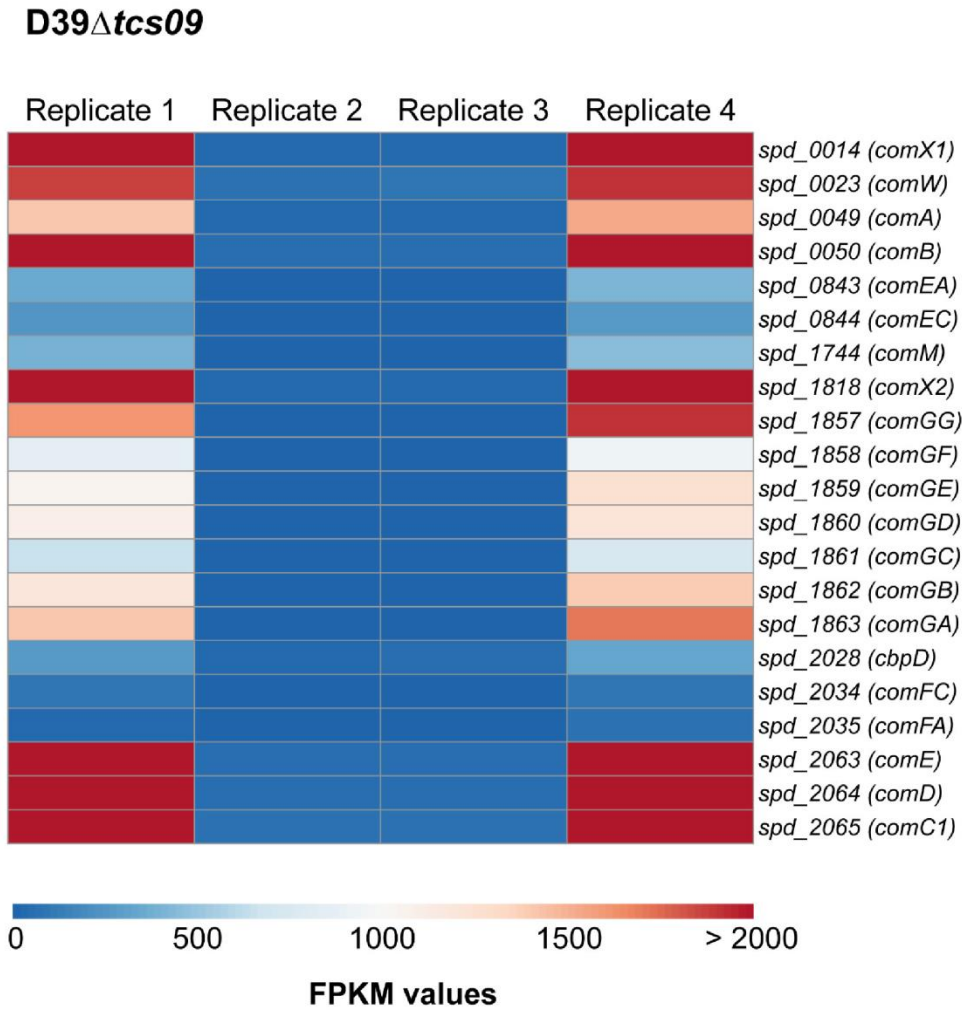

Figure S3. Expression profile of competence genes in D39Δ*tcs09*. Heat map showing FPKM values of competence genes in individual replicates of D39Δ*tcs09*. Red boxes show high values in the replicates, blue boxes low values.

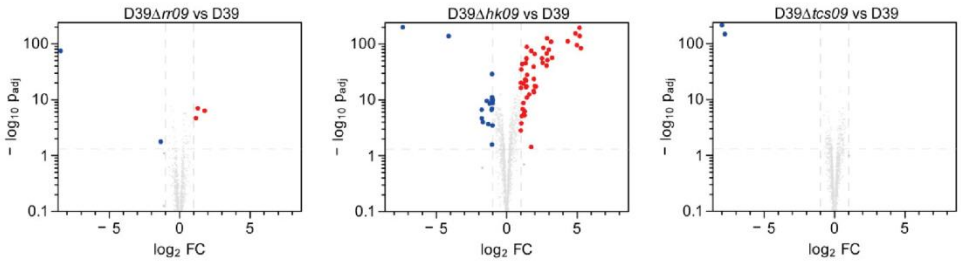

Figure S4. Volcano plots of the differentially expressed genes of D39Δ*rr09*, D39Δ*hk09* and D39Δ*tcs09* identified by RNA-seq. Histograms represent the two-dimensional distribution of identified genes by fold change and p-value. Genes with a $-\log_{10} p_{adj}$-value ≥ 1.3 and a $\log_2$ fold change ≥ 1 or ≤ -1 were set significant. Significantly downregulated genes are shown in blue and significantly upregulated genes in red.

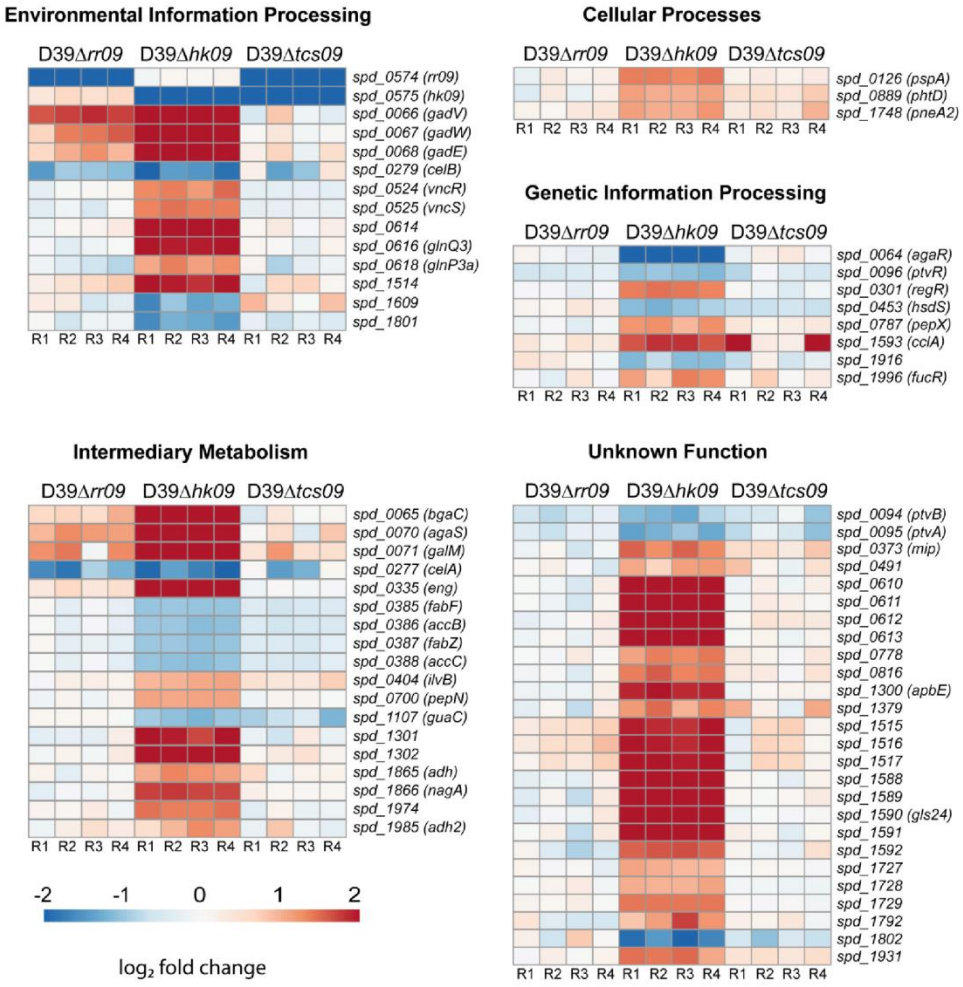

Figure S5. Expression profiles of 67 significantly regulated genes in D39 and *tcs09*-mutants. Heat maps showing the $\log_2$ fold changes in individual replicates of D39Δ*rr09*, D39Δ*hk09* and D39Δ*tcs09*. Red boxes show upregulation, whereas blue boxes show downregulation in the corresponding replicate.

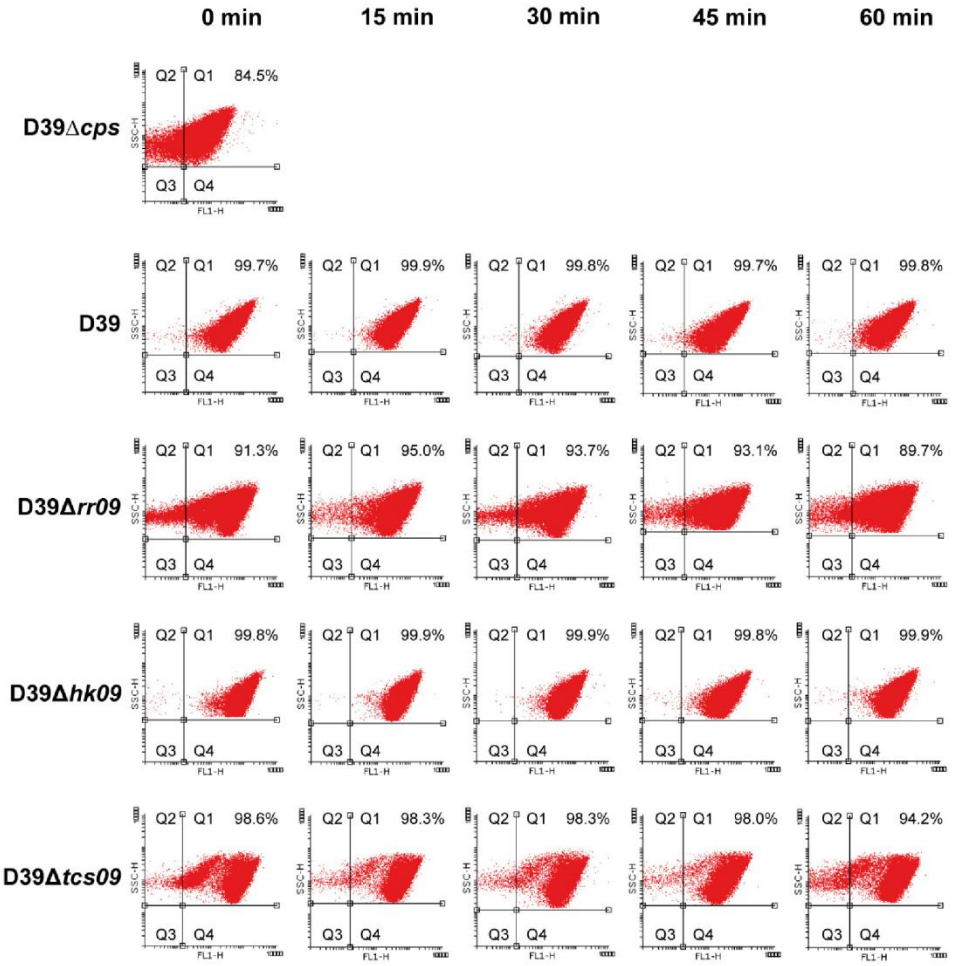

Figure S6. Analysis of capsule polysaccharide expression in flow cytometry. 2 x 10^8 bacteria of the parental strains D39 and their isogenic Δ*rr09*-, Δ*hk09*- and Δ*tcs09*-mutants were incubated up to 60 min in PBS and afterwards capsule expression was analyzed with anti-serotype 2 and secondary Alexa conjugated antibody as described. As a control, 2 x 10^8 bacteria of the nonencapsulated D39Δ*cps* was used in the analysis. Shown are the scatter plots of one representative measurement per time point. The percentages indicate the proportion of fluorescent cells within the selection of all cells in Q1. Q1-4: quadrant 1-4, SSC-H: side scatter height

4.2. Publication 2

The two-component system 09 of *Streptococcus pneumoniae* is important for metabolic fitness and resistance during dissemination in the host

Stephanie Hirschmann, Alejandro Gómez-Mejia, Thomas P. Kohler, Franziska Voß, Manfred Rohde, Max Brendel and Sven Hammerschmidt

Submitted to the journal Microorganisms, May 2021
Manuscript ID: microorganisms-1253919

PUBLICATION 2

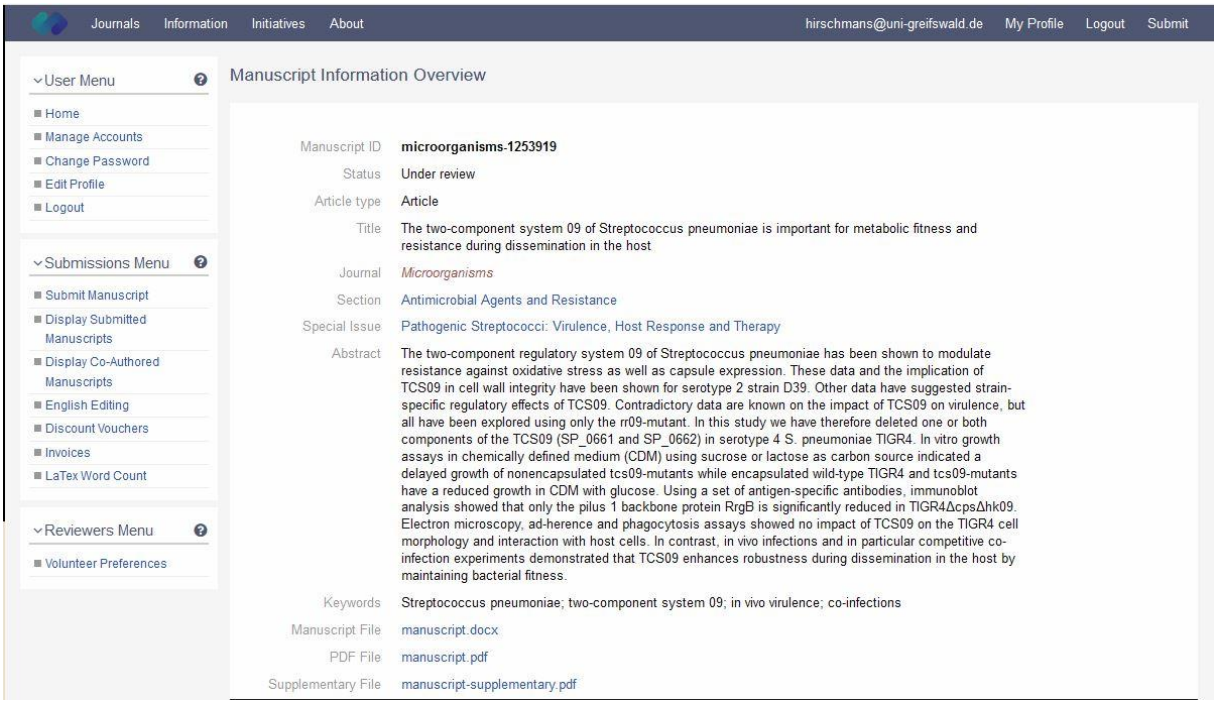

Journals Information Initiatives About hirschmans@uni-greifswald.de My Profile Logout Submit

User Menu
- Home
- Manage Accounts
- Change Password
- Edit Profile
- Logout

Submissions Menu
- Submit Manuscript
- Display Submitted Manuscripts
- Display Co-Authored Manuscripts
- English Editing
- Discount Vouchers
- Invoices
- LaTex Word Count

Reviewers Menu
- Volunteer Preferences

Manuscript Information Overview

Manuscript ID	**microorganisms-1253919**
Status	Under review
Article type	Article
Title	The two-component system 09 of Streptococcus pneumoniae is important for metabolic fitness and resistance during dissemination in the host
Journal	*Microorganisms*
Section	Antimicrobial Agents and Resistance
Special Issue	Pathogenic Streptococci: Virulence, Host Response and Therapy
Abstract	The two-component regulatory system 09 of Streptococcus pneumoniae has been shown to modulate resistance against oxidative stress as well as capsule expression. These data and the implication of TCS09 in cell wall integrity have been shown for serotype 2 strain D39. Other data have suggested strain-specific regulatory effects of TCS09. Contradictory data are known on the impact of TCS09 on virulence, but all have been explored using only the rr09-mutant. In this study we have therefore deleted one or both components of the TCS09 (SP_0661 and SP_0662) in serotype 4 S. pneumoniae TIGR4. In vitro growth assays in chemically defined medium (CDM) using sucrose or lactose as carbon source indicated a delayed growth of nonencapsulated tcs09-mutants while encapsulated wild-type TIGR4 and tcs09-mutants have a reduced growth in CDM with glucose. Using a set of antigen-specific antibodies, immunoblot analysis showed that only the pilus 1 backbone protein RrgB is significantly reduced in TIGR4ΔcpsΔhk09. Electron microscopy, ad-herence and phagocytosis assays showed no impact of TCS09 on the TIGR4 cell morphology and interaction with host cells. In contrast, in vivo infections and in particular competitive co-infection experiments demonstrated that TCS09 enhances robustness during dissemination in the host by maintaining bacterial fitness.
Keywords	Streptococcus pneumoniae; two-component system 09; in vivo virulence; co-infections
Manuscript File	manuscript.docx
PDF File	manuscript.pdf
Supplementary File	manuscript-supplementary.pdf

microorganisms

MDPI

Article

The two-component system 09 of *Streptococcus pneumoniae* is important for metabolic fitness and resistance during dissemination in the host

Stephanie Hirschmann [1], Alejandro Gómez-Mejia [1], Thomas P. Kohler [1], Franziska Voß [1], Manfred Rohde [2], Max Brendel [1], and Sven Hammerschmidt [1,*]

[1] Department of Molecular Genetics and Infection Biology, Interfaculty Institute for Genetics and Functional Genomics, Center for Functional Genomics of Microbes, University of Greifswald, Germany. hirschmans@uni-greifswald.de (S.HI.); alejandro.gomezmejia@usz.ch (A.GM.); thomas.kohler@uni-greifswald.de (T.K.); franziska.voss@uni-greifswald.de (F.V.); max.brendel@uni-greifswald.de (M.B.); sven.hammerschmidt@uni-greifswald.de (S.HA.)

[2] Central Facility for Microscopy, Helmholtz Centre for Infection Research, Braunschweig, Germany. Manfred.rohde@helmholtz-hzi.de (M.R.)

* Correspondence: sven.hammerschmidt@uni-greifswald.de

Abstract: The two-component regulatory system 09 of *Streptococcus pneumoniae* has been shown to modulate resistance against oxidative stress as well as capsule expression. These data and the implication of TCS09 in cell wall integrity have been shown for serotype 2 strain D39. Other data have suggested strain-specific regulatory effects of TCS09. Contradictory data are known on the impact of TCS09 on virulence, but all have been explored using only the *rr09*-mutant. In this study we have therefore deleted one or both components of the TCS09 (SP_0661 and SP_0662) in serotype 4 *S. pneumoniae* TIGR4. *In vitro* growth assays in chemically defined medium (CDM) using sucrose or lactose as carbon source indicated a delayed growth of nonencapsulated *tcs09*-mutants while encapsulated wild-type TIGR4 and *tcs09*-mutants have a reduced growth in CDM with glucose. Using a set of antigen-specific antibodies, immunoblot analysis showed that only the pilus 1 backbone protein RrgB is significantly reduced in TIGR4Δ*cps*Δ*hk09*. Electron microscopy, adherence and phagocytosis assays showed no impact of TCS09 on the TIGR4 cell morphology and interaction with host cells. In contrast, *in vivo* infections and in particular competitive co-infection experiments demonstrated that TCS09 enhances robustness during dissemination in the host by maintaining bacterial fitness.

Keywords: *Streptococcus pneumoniae*; two-component system 09; *in vivo* virulence

Citation: Hirschmann, S.; Gómez-Mejia, A.; Kohler, T.P.; Voß, F.; Brendel, M.; Rohde, M.; Hammerschmidt, S. The two-component system 09 of *Streptococcus pneumoniae* is important for metabolic fitness and resistance during dissemination in the host. *Microorganisms* **2021**, *9*, x. https://doi.org/10.3390/xxxxx

Academic Editor: Firstname Lastname

Received: date
Accepted: date
Published: date

Publisher's Note: MDPI stays neutral with regard to jurisdictional claims in published maps and institutional affiliations.

1. Introduction

As a pathobiont of the respiratory tract, *Streptococcus pneumoniae* (the pneumococcus) colonizes asymptomatically up to 60% of the human population [1]. In addition to be a natural commensal of the upper respiratory tract, the pneumococcus causes various diseases ranging from local infections with harmless clinical outcome to harmful severe invasive diseases. These include otitis media, pneumonia, meningitis and sepsis [2-4]. Worldwide, pneumococcal infections cause several million deaths every year, including 294,000 children under the age of five in 2015 [5]. Typically, pneumococci are transmitted via aerosols and acquired via the nasopharynx [6,7]. After overcoming the mucosal barrier, evading antimicrobial compounds, and antibodies, they have a high potential to attach to epithelial cells of the respiratory mucosa [2]. From this host compartment the bacteria gain access to the bloodstream and depending on the route, overcome the blood-brain-barrier [8-10].

There is a high demand on the one hand to produce virulence determinants such as the capsular polysaccharide (CPS), the toxin pneumolysin or adhesive molecules to escape the immune system and to facilitate colonization, the interaction with host molecules or cellular structures [3,11,12]. On the other hand pneumococcal fitness has been shown to be crucial for colonization but also invasive disease [13,14]. The adaptation of pneumococcal metabolism to the conditions of the conquered host compartments is pivotal to maintain fitness and survival for a successful colonization and invasion [13-15]. However, the expression of virulence factors and genes that contribute to bacterial fitness correlate with the stage of infection and is, in many cases, triggered by the response to environmental factors [3,12,16]. When this signaling is mediated by two-component regulatory systems (TCS) the external stimulus is sensed by a membrane-bound receptor, typically a histidine kinase, which autophosphorylates and transmits the signal to the intracellular regulatory protein [17-19].

Similar to other human pathogenic bacteria, pneumococcal TCSs are directly associated with adaptation to host compartments or the virulence properties of *S. pneumoniae* [13,17,20-22]. Pneumococci express 13 TCSs and one orphan response regulator. Their role in pneumococcal physiology, fitness and virulence has been extensively discussed recently [13,17,23]. For TCS09, the impact on virulence has already been demonstrated by several studies [11,24-26]. The deletion of the RR09 attenuated virulence of serotype 2 strain *S. pneumoniae* D39 in a mouse pneumonia and bacteremia model, whereas virulence of the *rr09*-mutant of pneumococcal serotype 3 strain 0100993 was unaffected [24]. For TIGR4, the strain which is used in this study, RR09 has been shown to contribute to the development of pneumonia but not bacteremia [11]. Thus, TCS09 has a strain- and serotype-specific impact on pneumococcal metabolic processes and virulence. However, the environmental stimulus, the target genes and the reasons for the strain-specific effects have not yet been explored.

In a previous study, we deciphered the role of TCS09 for *S. pneumoniae* D39 metabolic fitness, autolysis and oxidative stress. Using transcriptomics, we indicated differential gene expression of genes involved in carbohydrate metabolism and illustrated an altered CPS amount as well as phenotype in *tcs09*-mutants [23]. Because of these changes, we hypothesized that the TCS09 contributes at least indirectly to pneumococcal colonization and virulence. So far, the individual role of all TCS09 components (RR09, HK09 and both) on the phenotype and virulence in TIGR4 has not been investigated. In this study, we report the impact of RR09, HK09 and the complete TCS09 on the pathophysiology and virulence of *S. pneumoniae* TIGR4 by growth experiments, *in vitro* adherence and phagocytosis assays, and finally, by *in vivo* mouse infection assays. Our data suggest that TCS09 is crucial for full fitness and colonization under *in vivo* conditions.

2. Materials and Methods

2.1. Bacterial strains and culture conditions

Encapsulated and nonencapsulated (Δ*cps*) *Streptococcus pneumoniae* serotype 4 (TIGR4) parental strains and isogenic *tcs09*-mutants (Table 1) were used in this study. Pneumococci grown on blood agar plates (Oxoid) with appropriate antibiotics were inoculated in chemically-defined medium (CDM) $RPMI_{modi}$ (RPMI1640: GE Healthcare; $RPMI_{modi}$: [14]) supplemented with 1% w/v carbon source (glucose, sucrose or lactose) or Todd-Hewitt-Broth (Roth) supplemented with 0.5% yeast extract. The bacteria were cultivated at 37°C without agitation up to the early logarithmic (OD_{600nm} 0.35) or middle logarithmic phase (OD_{600nm} 0.6). For growth analysis, the data were plotted linearly against time. The doubling time of the strains was calculated as follow.

$$\mu\ [min^{-1}] = \frac{((\ln X\ (t_2) - \ln X\ (t_1))}{(t_2 - t_1)}$$

$$g\ [min] = \frac{ln2}{\mu}$$

μ = growth rate
X (t_1) = cell density at time t_1
X (t_2) = cell density at time t_2
g = doubling time

Table 1. *S. pneumoniae* wild-type strains and mutants used in this study.

Strain	Capsule Type	Resistance	Knockout genes	Reference
TIGR4	4	-	-	[27]
TIGR4Δ*rr09*	4	erythromycin	*sp_0661*	This study
TIGR4Δ*hk09*	4	erythromycin	*sp_0662*	This study
TIGR4Δ*tcs09*	4	erythromycin	*sp_0661*, *sp_0662*	This study
TIGR4*lux*	4	kanamycin	-	[14]
TIGR4*lux*Δ*rr09*	4	kanamycin, erythro-mycin	*sp_0661*	This study
TIGR4*lux*Δ*hk09*	4	kanamycin, erythro-mycin	*sp_0662*	This study
TIGR4*lux*Δ*tcs09*	4	kanamycin, erythro-mycin	*sp_0661*, *sp_0662*	This study
TIGR4Δ*cps*	4	kanamycin	*sp_0343 – sp_0360*	[14]
TIGR4Δ*cps*Δ*rr09*	4	kanamycin, erythro-mycin	*sp_0343 – sp_0360*, *sp_0661*	This study
TIGR4Δ*cps*Δ*hk09*	4	kanamycin, erythro-mycin	*sp_0343 – sp_0360*, *sp_0662*	This study
TIGR4Δ*cps*Δ*tcs09*	4	kanamycin, erythro-mycin	*sp_0343 – sp_0360 sp_0661*, *sp_0662*,	This study

2.2. Generation of pneumococcal mutants

Pneumococcal single mutants (RR09 or HK09) or double mutants (RR09 and HK09), were generated by insertion-deletion mutagenesis in *S. pneumoniae* TIGR4, TIGR4Δ*cps* and TIGR4*lux* using the protocol and plasmid constructs described in a previous study [23].

2.3. Immunoblot analysis of whole bacterial lysates using the LI-COR technology

Nonencapsulated *S. pneumoniae* TIGR4Δ*cps* and isogenic *tcs09*-mutants were cultured to an OD_{600nm} of 0.6 in glucose supplemented CDM in triplicates. Subsequently, the cultures were centrifuged for 6 min at 3200 x g at room temperature (RT) and the bacterial pellet was resuspended in PBS (pH 7.4). A concentration of 2 x 10^8 bacteria was loaded onto a 12% SDS-PAGE and then blotted onto a nitrocellulose membrane by semidry blotting. The membrane was blocked for 2 h at RT using 5% skim milk (Roth) in TBS, pH 7.4. Incubation with mouse polyclonal antibodies (1:500 in 5% skim milk + TBS/0.01% Tween) against selected proteins was performed overnight at 4°C. Membranes were then washed with TBS/0.01% Tween and detection of various pneumococcal proteins was performed using a

secondary fluorescent labeled IRDye® 800CW (goat-anti-mouse IgG; 1:15,000 in 5% skim milk in TBS/0.01% Tween). A rabbit polyclonal anti-enolase antibody (1:12,500 in 5% skim milk + TBS/0.01% Tween) was used as a loading control and detected using fluorescent labeled IRDye® 680RD goat-anti-rabbit IgG. The primary antibodies were detected by incubation with the appropriate antibodies for 60 min in the dark at RT. Membranes were washed with TBS/0.01% Tween and finally twice with TBS. Scanning of the membranes was performed using an Odyssey®CLx (LI-COR) scanner.

2.4. Field emission scanning electron microscopy (FESEM) and Transmission electron microscopy (TEM)

FESEM and TEM were performed to study the cell morphology and capsule of pneumococcal wild-types TIGR4, TIGR4Δ*cps* and their respective isogenic *tcs09*-mutants. Bacteria were cultivated in CDM with glucose until OD_{600nm} 0.3 (encapsulated strains) or 0.6 (nonencapsulated strains) at 37°C. Samples were prepared for FESEM and TEM as described [23]. In brief, encapsulated strains were fixed first with 2.5% glutardialdehyde, 2% paraformaldehyde, 0.075% ruthenium red and 75 mM L-lysine acetate salt and stained with 1% osmium solution containing ruthenium red. In contrast, nonencapsulated pneumococci were fixed with 2% glutardialdehyde and 5% paraformaldehyde. For FESEM samples were placed on coverslips, fixed with 1% glutaraldehyde and dehydrated in a graded series of acetone (10% - 100%). Samples were then subjected to critical-point-drying with liquid CO_2 and covered with a gold-palladium film by sputter coating. Processed samples were examined in a field emission scanning electron microscope (Zeiss Merlin) using the HESE2 Everhart Thornley SE detector and the in-lens SE detector in a 75:25 ratio with an acceleration voltage of 5 kV. For TEM, bacteria were fixed as described above, mixed with an equal volume of 2% water agar solidified, cut and dehydrated in a graded series of ethanol (10% - 50%) followed by incubation in 70% ethanol with 2% uranylacetate. Samples were then dehydrated and infiltrated with aromatic acrylic resin LRWhite. Ultrathin sections were cut, counterstained with 4% aqueous uranyl acetate, and examined in a Zeiss TEM 910 transmission electron microscope at an acceleration voltage of 80 kV.

2.5. Infection of epithelial cells for pneumococcal adherence analysis by immunofluorescence microscopy

Epithelial A549 cells (ATCC CCL-185) were seeded at 5 x 10^4 cells per well in 24-well tissue culture plates (Greiner Bio One, Germany) on 12 mm diameter glass coverslips and cultured for 2 days at 37°C and 5% CO_2 in DMEM High Glucose (HyClone™, Germany) supplemented with 10% (v/v) heat-inactivated fetal bovine serum (FBS) (Gibco, Germany), 4 mM glutamine, 1 mM sodium pyruvate. The cells were washed three times with DMEM containing 1% heat-inactivated FBS (infection medium). Cells were infected with TIGR4Δ*cps* and isogenic *tcs09*-mutants using a multiplicity of infection (MOI) of 25 pneumococci per cell. Pneumococci were grown in THY medium on the day of infection to OD_{600nm} 0.35 and adjusted to an MOI 25 in infection medium. Infections were performed at 37°C and 5% CO_2 for 3 h. After 3 h non-adherent bacteria were removed by washing three times with PBS. Cells were fixed with 1% paraformaldehyde overnight at 4°C and subsequently used for immunofluorescence staining. For double-immunofluorescence (DIF) staining, the coverslips were carefully removed from the wells and washed three times with PBS. To avoid nonspecific binding of the pneumococcal antibody, cells were blocked with 10% FBS in PBS (3 h, RT). Visualization of extracellular adherent pneumococci was performed with pneumococcal-specific polyclonal antibodies (1:500, in PBS/10%FBS) for 30 min at RT. After washing the coverslips three times with PBS, bacteria were stained with Alexa 568-coupled goat anti-rabbit IgG (abcam, Germany) (30 min, 1:500, in PBS/10% FBS). Coverslips were then washed again three times with PBS. Visualization of the actin cytoskeleton was conducted after permeabilization of the cells with 0.1% Triton X-100 (10 min) and incubation with Phalloidin-iFlour®-488 conjugate (abcam, Germany) (1:2000, in

PBS/10% FCS) for 30 min at RT. After the coverslips were repeatedly washed three times in PBS, they were fixed on a slide using Mowiol. Image acquisition was performed with a fluorescence microscope (Zeiss Axiovert) and VisiView® software (Visitron Systems GmbH).

2.6. Quantification of phagocytosed pneumococci by the antibiotic protection assay

In a 24-well cell culture plate, 5 x 10^4 J774 cells (ATCC TIB-67) per well were seeded for triplicates, cultured in RPMI1640 with L-glutamine supplemented with 1 mM sodium pyruvate and 10% (v/v) heat-inactivated FBS for 48 h at 37°C with 5% CO_2. On the day of infection, J774 cells were washed three times with infection medium (RPMI1640 + 1% FBS). Cultivation of TIGR4Δ*cps* and isogenic *tcs09*-mutants was performed in THY to an OD_{600nm} of 0.35. The infection dose was set to a MOI of 50. Subsequently, the cell culture plate was centrifuged at 9 x g for 2 min to allow contact of the bacteria with the phagocytes and incubated at 37°C and 5% CO_2 for 30 min. After infection, the cells were washed three times with infection medium. To kill extracellular pneumococci, J774 cells were incubated in infection medium supplemented with gentamicin (100 µg/ml) and penicillin G (300(U/ml) for 1 h at 37°C and 5% CO_2. Cells were washed again three times with infection medium and subsequently or 1 – 3 h later, J774 cells were lysed by adding 1% saponin (in infection medium) at 37°C and 5% CO_2 for 10 min, resulting in the release of intracellular pneumococci. The number of recovered bacteria was determined by plating the lysate on blood agar plates and after overnight incubation at 37°C and 5% CO_2, colony forming units (CFU) were enumerated by counting. Experiments were performed at least three times in triplicates.

2.7. Quantification of phagocyte-associated and intracellular pneumococci by immunofluorescence microscopy

J774 cells were seeded (5 x 10^4 cells/well) in a 24-well cell culture plate on 12 mm sterile glass coverslips. Cultivation and preparation of the cells for infections was performed as described above. After 30 min infection with pneumococci, each well was carefully washed with infection medium. J774 cells and pneumococci were then fixed with 1% paraformaldehyde in PBS overnight at 4°C. The coverslips were removed and washed three times with PBS followed by blocking with 10% FBS in PBS (3 h, RT). Subsequently, the cells were washed three times with PBS, followed by an incubation with the pneumococcal-specific antibody (1:500 in PBS/10%FBS) for 30 min at RT. Another wash step (3 x in PBS) was followed by staining with the secondary Alexa 488-coupled goat anti-rabbit IgG (abcam) (30 min, 1:500 in PBS/10% FBS). The visualization of the internalized bacteria was done after Triton X-100 conveyed permeabilization of the cells (0.1%) and after renewed incubation with the rabbit anti-pneumococci IgG (30 min, 1:500) and the Alexa 568-coupled goat anti-rabbit IgG (30 min, 1:500). After incubation was complete, the coverslips were washed again three times in PBS and finally fixed on a slide using Mowiol. Image acquisition was performed with a fluorescence microscope (Zeiss Axiovert) and VisiView® software (Visitron Systems GmbH).

2.8. Acute pneumonia infection model

For acute pneumonia, 8 - 10 week old female CD-1 mice (Charles River) (n = 10) were intranasally infected with the bioluminescent wild-type strain TIGR4*lux* or isogenic *tcs09*-mutants [14]. Bacteria were cultured in THY supplemented with 10% heat-inactivated FBS to an OD_{600nm} 0.35. After centrifugation at 3200 x g for 10 min, an infection dose of 1 x 10^8 CFU in 10 µl was prepared. Prior to intranasal infections, mice were anesthetized by an intraperitoneal injection of a mixture of ketamine (Ketanest S) and xylazine (Rompun®) according to their average weight. 90 U/10 µl of hyaluronidase was added per infection dose. The final infection dose (20 µl) was added dropwise to the nostrils of the mice for intranasal infection. The infected mouse was further held up for a brief moment, preventing

the inoculum from receding. Animals were observed daily for weight. Real-time visualization and documentation of the spread of bioluminescent pneumococci was performed using IVIS® Spectrum Imaging System (Caliper Life Sciences). The first measurement was taken approximately 24 h after infection followed by 8 h intervals. During the measurements, the animals were anesthetized with isoflurane and bioluminescence was measured for 1 min with medium "binning" factor. The emitted photons were recorded and quantified using LivingImage® 4.1 software (Caliper Life Sciences).

2.9. Systemic infection model

To investigate the systemic course of infection, 8 – 10 week old female CD-1 mice (Charles River) (n = 8) were infected intraperitoneally with 1 x 10^4 CFU wild-type bioluminescent strain TIGR4*lux* or isogenic *tcs09*-mutants in 200 µl PBS. Post infection, the weight and severity of disease of infected mice was monitored at 8 h intervals starting 24 h post-infection. Animals were observed daily for clinical score monitoring.

2.10. Co-infection model

Pneumococci were cultured in THY supplemented with 10% heat-inactivated FBS to an OD_{600nm} 0.35. In a competition infection experiment, 8 - 10 week old female CD-1 mice (Charles River) (n = 10) were intranasally infected with 1 x 10^7 CFU of bioluminescent wild-type TIGR4*lux* and 1 x 10^7 CFU of one of the *tcs09*-mutant strains in a 1:1 ratio. The CFU was determined in the nasopharynx, bronchi, blood, lung tissue and brain after intranasal infection 24 h and 48 h post-infection. Briefly, mice were sacrificed, blood taken from the heart and the trachea was dissected for nasal and bronchoalveolar lavage. 1 ml of sterile PBS was passed through the nasopharynx or inserted into the lungs with the inserted trachea cannula and collected after passage. Afterwards, lung tissue and brain was removed and homogenized in 1 ml PBS. The output of mutant versus wild-type bacteria was determined on selective blood agar plates containing kanamycin and/or erythromycin. The competitive index (CI) was calculated. A value of 1 indicates identical output CFU of wild-type and mutant bacteria, while CI values < 1 indicate a higher output of wild-type bacteria and values > 1 a higher output of mutant bacteria.

2.11. Statistical analysis

Unless stated otherwise, all the data collected in this study are presented as mean of at least three independent experiments with the standard deviation ±SD. The results were statistically evaluated using a two-way Anova or the unpaired two-tailed student's t-test (GraphPad Prism 5.01). A p-value < 0.05 was considered as statistically significant. All Kaplan-Meier survival curves were compared using the Log-rank-test.

3. Results

3.1. Growth analysis of encapsulated and nonencapsulated wild-type TIGR4 and tcs09-mutants under nutrient-defined conditions

To assess how the TCS09 affects *S. pneumoniae* fitness when various carbon sources are provided, we cultured encapsulated and nonencapsulated wild-type strains TIGR4, TIGR4Δ*cps* and isogenic *tcs09*-mutants in chemically defined medium $RPMI_{modi}$ in the presence of different carbon sources. In glucose-supplemented CDM, the encapsulated TIGR4 strains showed only a moderate growth and reached the stationary phase already after 4 h. Growth of the mutants TIGR4Δ*rr09* (g = 121 min), TIGR4Δ*hk09* (g = 457 min) and TIGR4Δ*tcs09* (g = 133 min) was significantly slower than growth of the wild-type TIGR4 (g = 106 min) (Figure 1A-C). In contrast, growth kinetics of nonencapsulated wild-type TIGR4Δ*cps* and isogenic *tcs09*-mutant strains showed growth curves with a short lag phase of 1 h and an exponential phase of 6 h, followed by a stationary phase after ap-

proximately 7 h (Figure 1D-F). The three nonencapsulated *tcs09*-mutants had a slight delay in growth compared to the wild-type, with an average doubling time of 99 min versus 81 min, respectively. For TIGR4, TIGR4Δ*cps* and their isogenic *tcs09*-mutants we did not observe bacterial cell lysis immediately after reaching the stationary phase. When we used disaccharides such as sucrose and lactose as carbon sources, the three nonencapsulated *tcs09*-mutants showed an extended lag phase compared to the parental TIGR4Δ*cps* (Figure 1G-L). Growth of TIGR4Δ*cps*Δ*rr09* (g = 70 - 98 min), TIGR4Δ*cps*Δ*hk09* (g = 76 – 101 min) and TIGR4Δ*cps*Δ*tcs09* (g = 70 - 96 min) was slightly slower than growth of wild-type TIGR4Δ*cps* (g = 57 – 75 min). A stationary phase was not observed, instead, the nonencapsulated parental strain TIGR4Δ*cps* and isogenic *tcs09*-mutants started to lyse immediately after reaching their maximum optical density, which was measured after 6 h and 8 h (sucrose) or 9 h (lactose). Importantly, the maximum cell density was twice as high compared to the cultures in which glucose was used as a carbon source (Figure 1G-L).

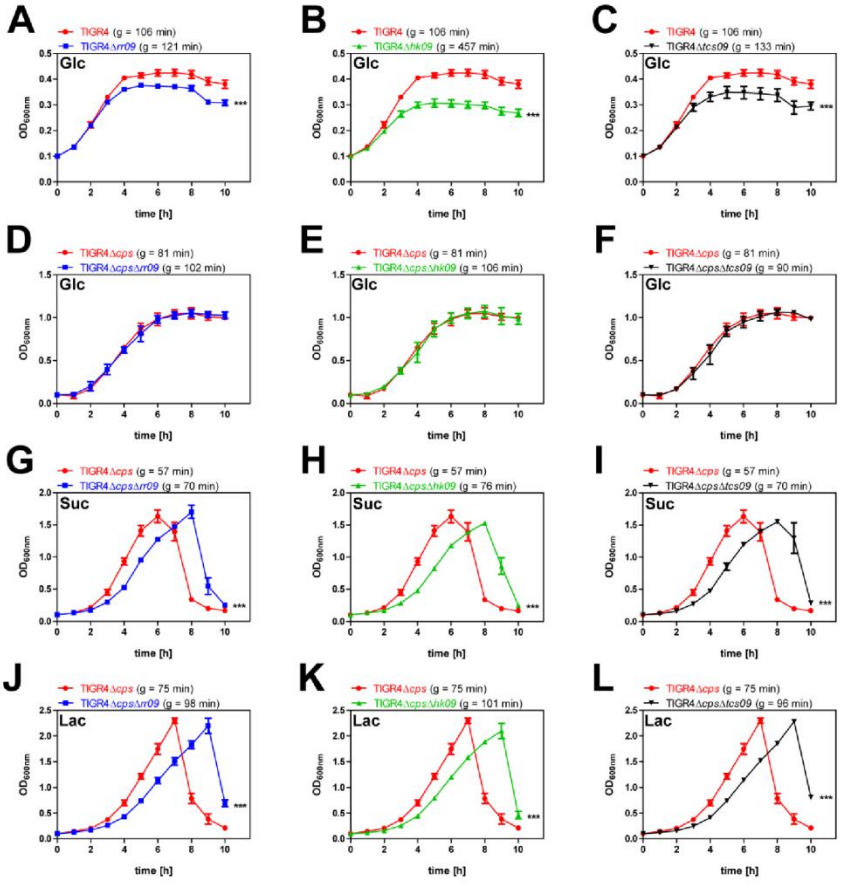

Figure 1. Growth analyses of *S. pneumoniae* TIGR4, TIGR4Δ*cps* and isogenic *tcs09*-mutants in CDM. Growth of encapsulated (**A-C**) and nonencapsulated (**D-L**) *tcs09*-mutants compared to the corresponding parental wild-type strains TIGR4 or TIGR4Δ*cps* were analyzed under nutrient-defined conditions with glucose (Glc) (**A-F**), sucrose (Suc) (**G-I**) and lactose (Lac) (**J-L**) as sole carbon source at 37°C under microaerophilic conditions without agitation. Results are presented as the mean ±SD of three independent experiments. The mean value of the doubling time (g) from three biological replicates of the respective strain is given in brackets. A two-way Anova proved a significance with a p-value *** < 0.001 relative to the parental pneumococcal strain.

3.2. Expression of important virulence factors in TIGR4Δcps wild-type and isogenic tcs09-mutants

A strain-dependent effect on gene regulation of phosphotransferase systems (PTS) and enzymes of carbohydrate metabolism were indicated for *rr09*-mutants, when D39 and TIGR4 were compared [25]. RR09 is associated with pili regulation, whereas no other important virulence factors have yet been found to be differentially regulated by RR09 [25]. In a *hk09*-mutant of D39, *pspA* and *phtD* encoding important adhesins as well as the *aga* operon involved in galactose utilization were shown to be upregulated [23], highlighting the importance of screening *rr09*- *hk09*- and *tcs09*-mutants for differential gene and protein expression. Hence, we have investigated the expression of important proteins for pneumococcal fitness and virulence by immunoblot analysis. We have chosen representative candidates of lipoproteins, choline-binding proteins, sortase-anchored proteins and intracellular proteins for a quantitative analysis. For this purpose, we cultured nonencapsulated *tcs09*-mutants and the parental strain TIGR4Δ*cps* in glucose-supplemented CDM to an OD_{600nm} of 0.6 and applied 2 x 10^8 cells for protein expression. Only RrgB, the backbone protein of type 1 pilus, showed a lower expression in the *hk09*-mutant (Figure 2). Apart from this, none of the other proteins showed a differential protein expression.

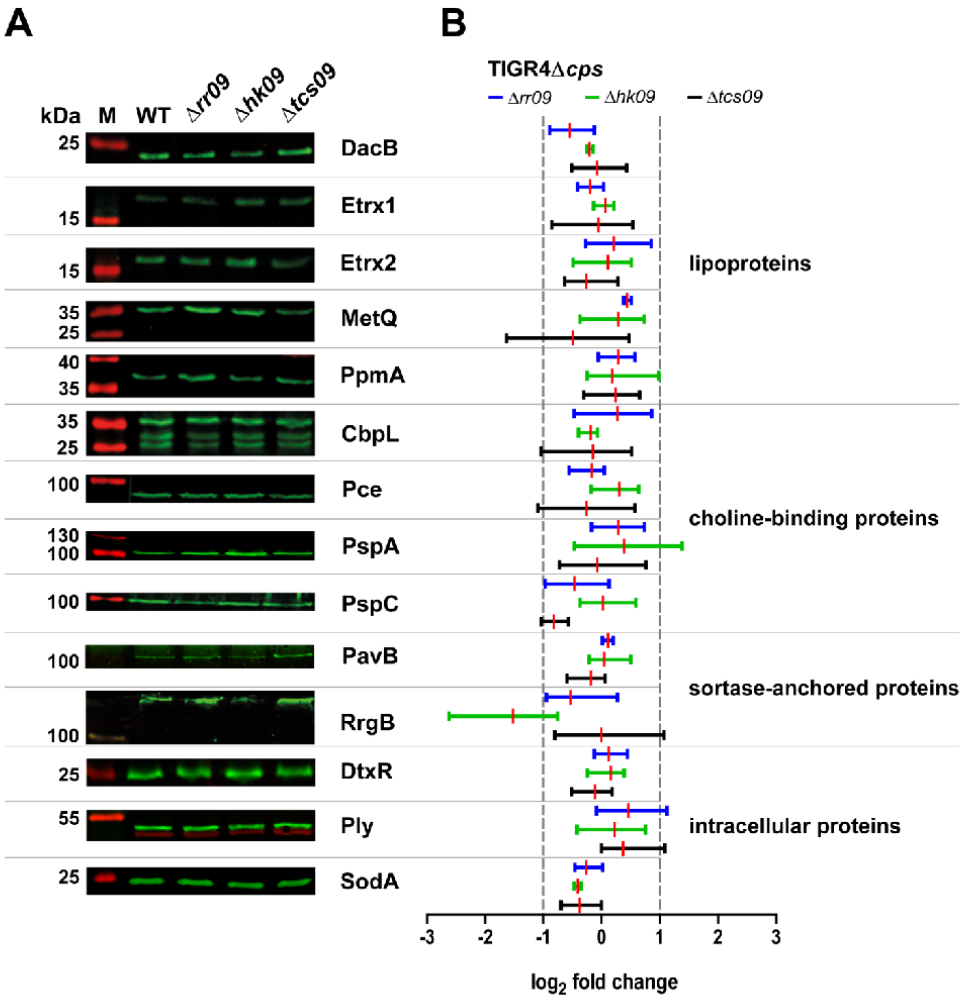

Figure 2. Immunoblot analysis of pneumococcal virulence factors. Pneumococcal strains were cultured to mid-exponential growth phase and total cell lysates of 2 x 10^8 bacteria were separated in a SDS-PAGE and plotted on nitrocellulose. Expression of indicated pneumococcal proteins was analyzed by immunoblot analysis using antigen-specific polyclonal mouse IgG and a secondary fluorescently labelled IRDye® 800CW goat anti-mouse IgG antibody. A specific rabbit polyclonal anti-enolase IgG and a secondary fluorescent-labelled IRDye® 680RD goat anti-rabbit IgG antibody served as normalization control. Shown are representative immunoblot images (**A**) and the differential expression pattern as $\log_2$ fold changes of representative candidates of lipoproteins, choline-binding proteins, sortase-anchored proteins and intracellular proteins (**B**).

3.3. Analysis of pneumococcal morphology and capsule content

As mentioned, we have observed changes in the cell morphology of pneumococcal D39 mutant lacking components of the TCS09 [23]. We therefore investigated as part of phenotypic characterization the influence of TCS09-deficiency on TIGR4 cell morphology, cell division and capsule amount. Encapsulated and nonencapsulated TIGR4 and

TIGR4Δ*cps*, as well as the isogenic *tcs09*-mutants were cultured in CDM with glucose as carbon source. We applied field emission scanning electron microscopy (FESEM) and transmission electron microscopy (TEM) to illustrate potential alterations. FESEM and TEM images of the isogenic *tcs09*-mutants and the wild-type strains TIGR4 and TIGR4Δ*cps* showed no morphological differences in cell shape or changes in cell division (Figure 3). In addition to cell shape, size and arrangement of septa, we further examined *tcs09*-mutants for alterations in capsule structures or capsule amount. To visualize the effect of TCS09-deficiency on the capsule amount, we used the lysine-ruthenium red (LRR) treatment to preserve the CPS. In contrast to *tcs09*-mutants of *S. pneumoniae* D39 from our previous study, all TIGR4 *tcs09*-mutants showed capsule structures that were similar to the parental TIGR4 strain (Figure 3B). Although the cytoplasm of all *tcs09*-mutants of nonencapsulated strains exhibit more distinct small white areas suggesting alterations in cell morphology, we could not detect vesicle formation in TIGR4-mutants (Figure 3) that were recently indicated for *tcs09*-mutants of strain D39 [23]. In conclusion, the TCS09 of TIGR4 has little, if any, effect on pneumococcal cell morphology and capsule layer, suggesting the effects of TCS09 on cellular processes being strain-specific.

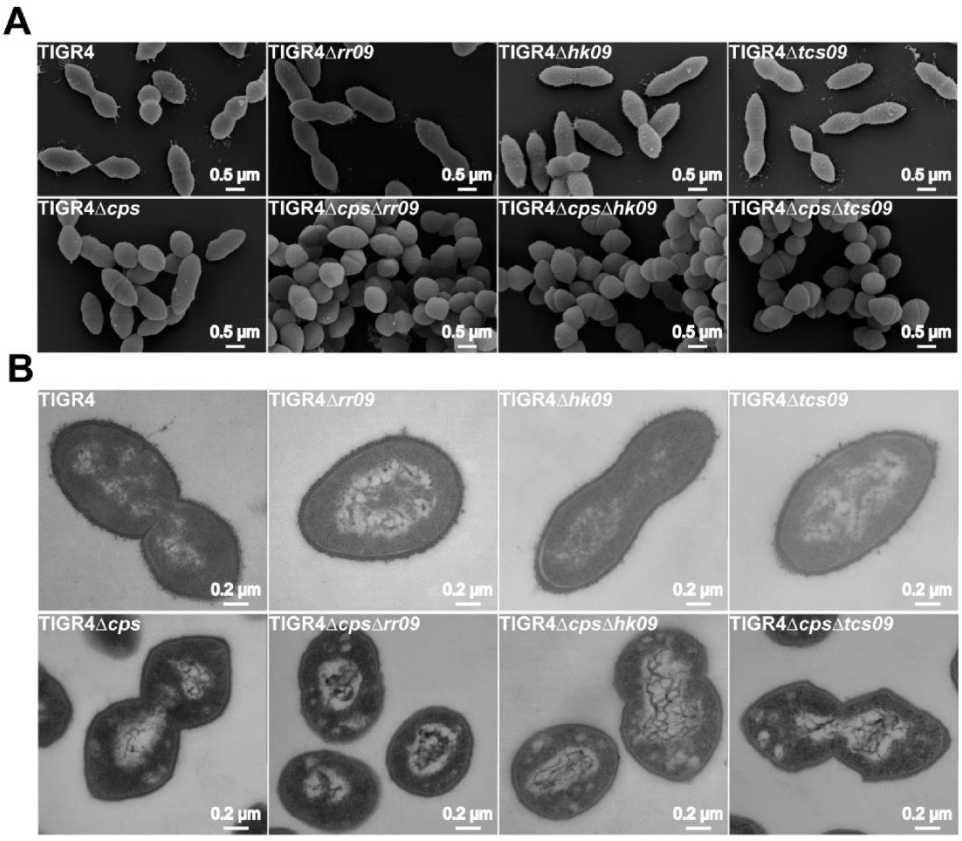

Figure 3. Illustration of the pneumococcal cell morphology in TCS09-deficient mutants using FESEM and TEM. Parental strains TIGR4, TIGR4Δ*cps* and isogenic *tcs09*-mutants were cultured in glucose-supplemented CDM. Pneumococci were subsequently fixed with paraformaldehyde and glutardialdehyde. The capsule of encapsulated pneumococci was pre-

served with a lysine-ruthenium-red solution. White bars in FESEM images (**A**) correspond to 500 nm and in TEM images (**B**) to 200 nm.

3.4. Role of the TCS09 on pneumococcal adherence

To investigate the effect of loss of function of TCS09 on pneumococcal adherence, we infected human lung epithelial cells (A549) with the nonencapsulated *S. pneumoniae* strain TIGR4Δ*cps* and isogenic *tcs09*-mutants for 3 h. We quantified the number of adherent pneumococci of the different strains by counting host cell attached bacteria after immunofluorescence staining. The *tcs09*-mutants did not show significant changes in their capacity to interact with A549 epithelial cells 3 h post-infection compared to the parental strain TIGR4Δ*cps* (Figure 4). The adherence data suggest that under this selected condition the TCS09 does not significantly affect the interaction of pneumococci with epithelial cells.

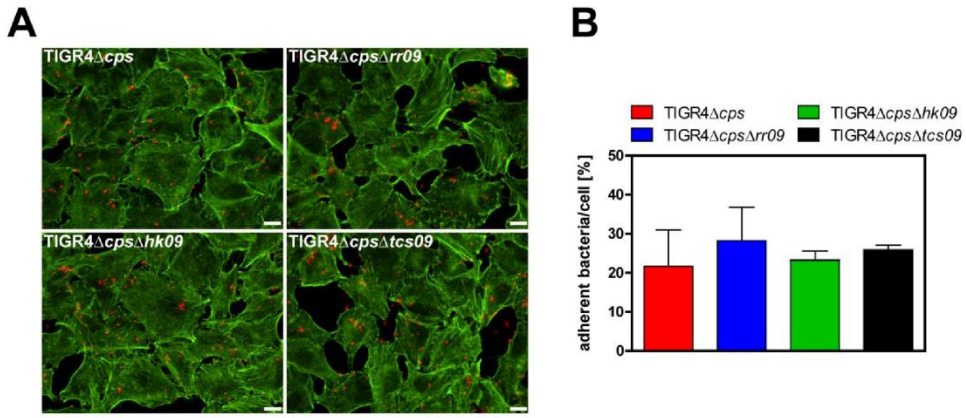

Figure 4. Adherence of *S. pneumoniae* TIGR4Δ*cps* and isogenic *tcs09*-mutants to A549 epithelial cells. Approximately 2 x 10^5 A549 lung epithelial cells were infected with a MOI 25 of TIGR4Δ*cps* or isogenic *tcs09*-mutants for 3 h. Host cell bound pneumococci were labelled using polyclonal anti-pneumococcal antibodies and secondary antibody Alexa Fluor 568. After cell permeabilization the actin cytoskeleton was stained using Phalloidin-iFlour®-488 conjugate. (**A**) Representative fluorescence images of adherent pneumococci on human lung epithelial cells A549 with a magnification of 630x. White bar represents 10 μm. (**B**) Adherent pneumococci of at least 50 cells/coverslip were counted via immunofluorescence microscopy. The results of three independent experiments are given as normalized percentage by relating the counted bacteria to the MOI set to 100%. Statistical analysis was performed with an unpaired t-test and revealed no significance.

3.5. Impact of the pneumococcal TCS09 on uptake by phagocytes

A critical step in pneumococcal invasive disease is the protection against phagocytosis by innate immune cells. To decipher whether the TCS09 of *S. pneumoniae* TIGR4 affects uptake by phagocytes and intracellular killing, we investigated uptake of TIGR4Δ*cps* and isogenic *tcs09*-mutants in *in vitro* infection experiments using murine J774 macrophages. Double-immunofluorescence staining was performed to visualize extracellular and intracellular pneumococci and to quantify associated and intracellular bacteria (Figure 5A). Thirty minutes post-infection uptake of the *tcs09*-mutants by phagocytes was similar compared to wild-type TIGR4Δ*cps* (Figure 5B). In accordance with these data the antibiotic protection assay, which is used to quantify intracellular survivors confirmed the results of the immunofluorescence microscopy (Figure 5C). Both approaches showed that uptake and intracellular survival of pneumococci is not altered in

the absence of a functional TCS09. We therefore tested, whether the intracellular survival of *tcs09*-mutants is affected over time compared to the parental strain TIGR4Δ*cps*. In kinetic experiments, intracellular pneumococci were isolated over 3 h. Intracellular bacterial survivors were recovered from macrophages after incubation for 1, 2 or 3 h post-killing of extracellular pneumococci by antibiotic treatment. In general, pneumococci are killed intracellularly in macrophages. This has been described earlier and is independent of the pneumococcal strain [28,29]. Interestingly, 1 h post incubation, killing of TIGR4Δ*cps*Δ*rr09* and TIGR4Δ*cps*Δ*hk09* was significantly delayed compared to the wild-type strain (Figure 5D). At this time point the survival rate of these two mutants and TIGR4Δ*cps*Δ*tcs09* was significantly higher compared to TIGR4Δ*cps*. However, 1 h later and 2 h post incubation, the killing rate of the RR09- and HK09-deficient mutants reached the levels of the parental strain. Finally, 3 h post incubation, only the double mutant TIGR4Δ*cps*Δ*tcs09* was significantly better killed than the other mutants or parental TIGR4Δ*cps* strain. Although the intracellular fate of *tcs09*-mutants is moderately changed, the overall effect of the TCS09 on TIGR4 uptake by professional phagocytes and intracellular survival seems to be of minor importance.

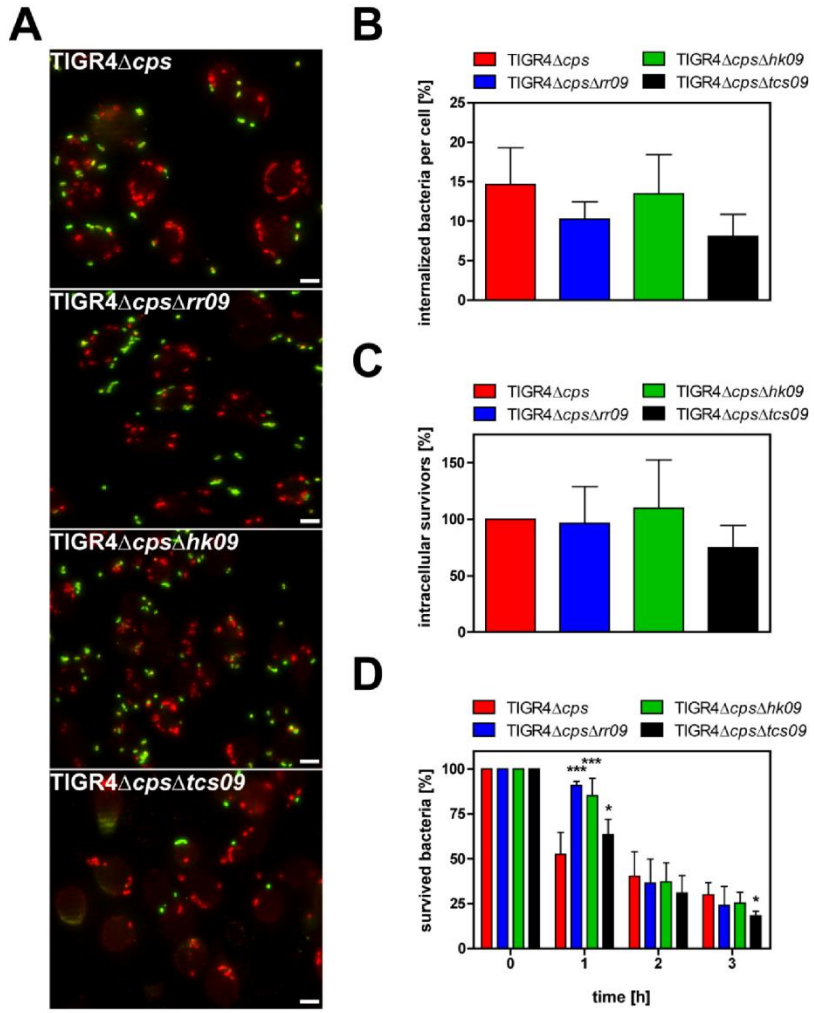

Figure 5. Uptake of *S. pneumoniae* TIGR4Δ*cps* and isogenic *tcs09*-mutants by murine macrophages. Approximately 2 x 10^5 J774 cells were infected for 30 min with TIGR4Δ*cps* or isogenic *tcs09*-mutants with a MOI 50. Experiments were performed at least three times in triplicates. (**A**) Representative immunofluorescence images of pneumococcal uptake after 30 min of infection by double-immunofluorescence staining. Extracellular bacteria were labeled with primary polyclonal anti-pneumococcal antibody followed by secondary Alexa Fluor 488 coupled antibody (green) and intracellular bacteria with primary antibody and secondary Alexa Fluor 568 coupled antibody (red). Visualization was performed using a fluorescence microscope at 630x magnification. White bar represents 10 μm. (**B**) Intracellular pneumococci per cell in percentage of the inoculum. At least 50 cells were counted per coverslip to quantify the number of intracellular bacteria. (**C**) Intracellular pneumococcal survivors post-incubation of macrophages and killing of extracellular bacteria by antibiotics. Intracellular pneumococci were recovered by permeabilization of J774 cells and CFUs were determined by plating the cell lysates on blood agar. CFUs of wild-type TIGR4Δ*cps* were set to 100%. Data were normalized against the MOI. (**D**) Intracellular survival in macrophages over a time period of 3 h. After killing extracellular bacteria with antibiotics, infected macrophages were further incubated in infection medium in the absence of antibiotics. Numbers of intracellular pneumococci were determined by lysing J774 cells at different time points and plating the lysates on blood agar plates. Data were normalized against the number of bacteria isolated directly after antibiotic treatment (time point 0). A two-way Anova revealed a significance with p-value * < 0.05 and *** < 0.001 relative to the parental pneumococcal strain at the indicated time points.

3.6. Influence of TCS09 on lung infections caused by S. pneumoniae TIGR4

We further employed the acute pneumonia mouse infection model to investigate the role of TCS09 on the pathophysiology of TIGR4 under *in vivo* conditions. We visualized the progression of pneumococcal disease by *in vivo* bioimaging of mice intranasally infected with bioluminescent TIGR4*lux* or its isogenic *tcs09*-mutants. In addition, we monitored the severity of disease and mouse survival rates, which are illustrated in a Kaplan-Meier diagram (Figure 6). Mice infected individually with wild-type TIGR4*lux*, or the mutants TIGR4*lux*Δ*rr09*, TIGR4*lux*Δ*hk09* or TIGR4*lux*Δ*tcs09* survived for at least 32 h (Figure 6B). Dissemination of pneumococci from the nasopharynx into the lungs and blood occurred independently from the genetic background of the strain as indicated by the bioluminescence (Figure 6A). First signs of pneumococci in the lungs could be detected already 24 h post-infection and disease progression was similar for all strains. After 88 h, 80% of mice infected with TIGR4*lux*Δ*hk09* died, whereas this was the case after 112 h or 144 h for mice infected with the wild-type TIGR4*lux* and TIGR4*lux*Δ*tcs09*, or TIGR4*lux*Δ*rr09*, respectively. These results suggest that the virulence potential of TIGR4 is not modulated by the TCS09 *in vivo*.

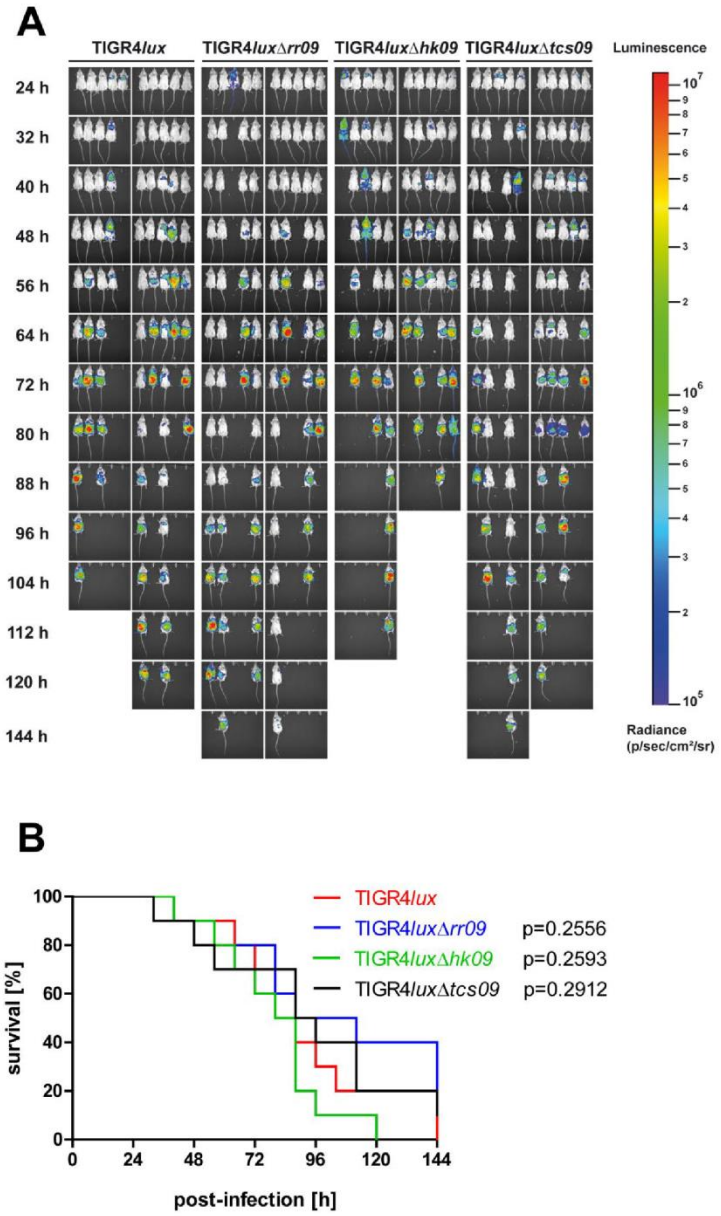

Figure 6. Survival of TIGR4 TCS09 deletion mutants in the acute pneumonia mouse infection model. CD-1 mice (n = 10) were intranasally infected with a CFU of 1 x 10^8 bacteria of TIGR4*lux*, TIGR4*luxΔrr09*, TIGR4*luxΔhk09* or TIGR4*luxΔtcs09* per mouse. (**A**) Spread of bioluminescent pneumococci was visualized at specific time points of infection by measurement of luminescence intensity (photons/second) using the IVIS® Spectrum system. (**B**) Survival rates of infected mice were illustrated in a Kaplan-Meier diagram. Statistical analysis was performed with a log rank test and revealed no significance.

3.7. Impact of TCS09 on virulence in the systemic mouse infection model

To analyze the effect of TCS09 deficiency on pneumococcal induced sepsis, we infected CD-1 mice intraperitoneally with pneumococcal strains TIGR4*lux*, TIGR4*luxΔrr09*, TIGR4*luxΔhk09* or TIGR4*luxΔtcs09*. The survival rate of infected mice was monitored. The results are represented in a Kaplan-Meier diagram (Figure 7A). All mice, independently of the mutant, showed no clinical sign of disease and survived for at least 40 h. After 48-64 h, monitoring of infected mice indicated severe signs of disease. The exceptions were each one mouse infected with the *hk09*- or *tcs09*–mutant surviving for 120 h (Figure 7). Similar to the acute pneumonia infection model the systemic mouse infection model revealed no statistical differences in the survival rates between mice infected with the wild-type strain and one of the *tcs09*-mutants. Thus, TCS09 deficiency has no effect on pneumococcal-induced sepsis.

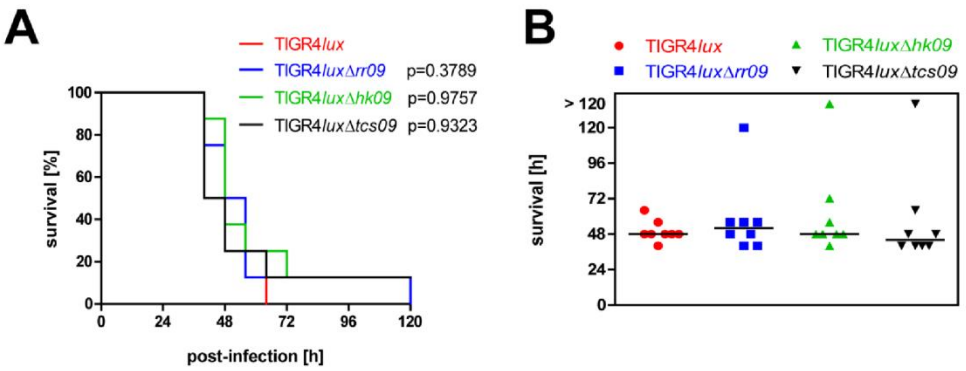

Figure 7. Survival of mice in a systemic mouse infection model. CD-1 mice (n = 8) were intraperitoneally infected with a CFU of 1 x 10^4 of *S. pneumoniae* strains TIGR4*lux*, TIGR4*luxΔrr09*, TIGR4*luxΔhk09* and TIGR4*luxΔtcs09*. (**A**) Kaplan-Meier diagram of surviving mice after intraperitoneal infection. Statistical analysis was performed with a log rank test and revealed no significance. (**B**) Scatter plot showing individual and median survival times per infected mouse group.

3.8. Importance of TCS09 for the bacterial load in the respiratory tract after co-infection

The results so far suggested that TCS09 of TIGR4 does not dramatically affect virulence during pneumonia and invasive pneumococcal disease. However, the impact on pneumococcal fitness in the respiratory tract and dissemination has not been addressed in a competitive manner. We have therefore analyzed the role of TCS09 on pneumococcal fitness using the competitive colonization and infection model. Mice were intranasally co-infected with equal CFUs of *S. pneumoniae* TIGR4*lux* and TIGR4*luxΔrr09* or TIGR4*luxΔhk09* or TIGR4*luxΔtcs09*. We then determined the bacterial load 24 h and 48 h post-infection by recovering the bacteria from the nasopharynx, respiratory airways, blood, lung and brain. Finally, competitive indexes (CIs) were calculated using the determined CFU of the *tcs09*-mutants and wild-type TIGR4*lux*. At 24 h and 48 h post-co-infection the bacterial loads in the nasopharynx (NP) showed no significant differences between wild-type TIGR4*lux* and *tcs09*-mutants (Figure 8). The *rr09*-mutant was out-competed by the wild-type TIGR4*lux* in the blood 24 h post-infection (CI: 0.47) and remained low 48 h (CI: 0.57) post-infection (Figure 8A). After 48 h, TIGR4*luxΔrr09* was also present with a significantly lower number of bacteria in the brain compared to the wild-type TIGR4*lux* (CI: 0.48) (Figure 8A). The co-infection and competitive infections further showed that the TIGR4*luxΔhk09* was out-competed by the wild-type bacteria in the pulmonary bronchi (CI: 0.38) and lung tissue (CI: 0.35) 48 h post-infection (Figure 8B). Interestingly, the observed effect was more pronounced with TIGR4*lux*/TIGR4*luxΔtcs09*.

Here, the double mutant TIGR4*lux*Δ*tcs09* was already out-competed by the wild-type TIGR4*lux* in the lung tissue (CI: 0.48) after 24 h (Figure 8C). After 48 h, this mutant was additionally out-competed by the wild-type bacteria in the blood (CI: 0.45) and brain (CI: 0.41) (Figure 8C). These results suggest that the regulatory function of TCS09 under *in vivo* conditions is required to maintain physiological fitness and robustness, which in turn allows a higher efficiency to initiate invasive infections (Figure 8).

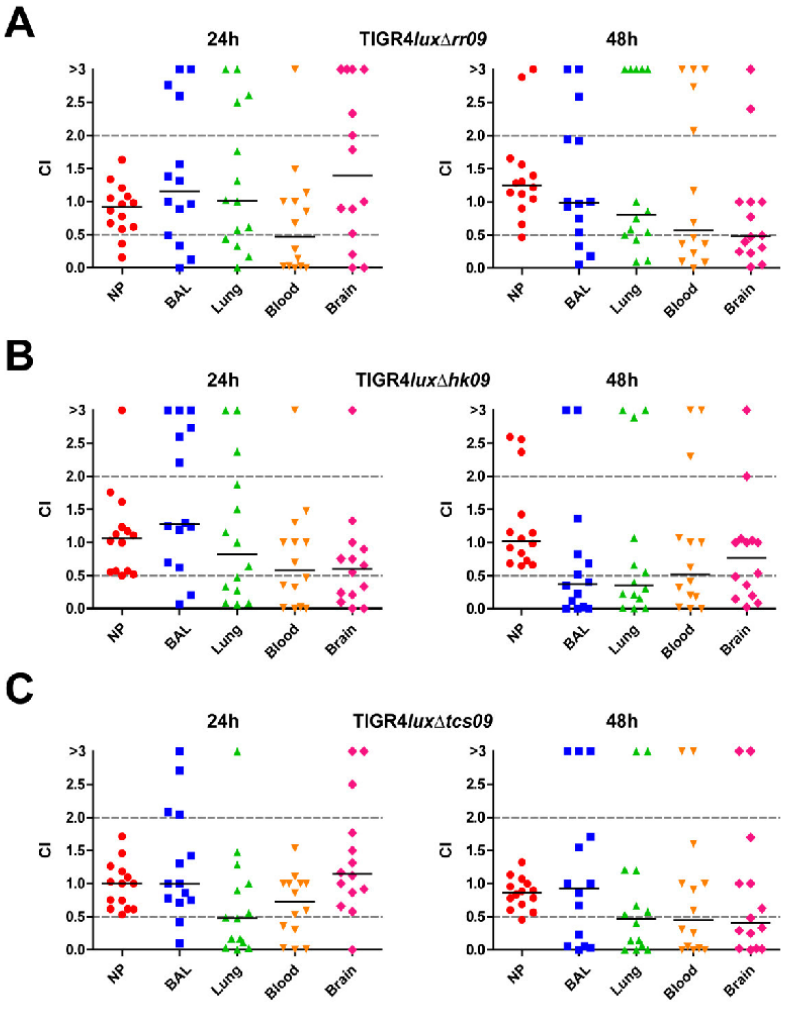

Figure 8. Intranasal co-infection of mice with bioluminescent TIGR4*lux* and isogenic *tcs09*-mutants. Three groups of CD-1 mice (n = 14) were infected with 1 x 10^7 CFU of wild-type TIGR4*lux* together with 1 x 10^7 CFU of one of the isogenic *tcs09*-mutants. At indicated time points (24 h or 48 h), mice were sacrificed and bacterial loads were counted in the nasopharynx (NP), bronchi (BAL: bronchoalveolar lavage), lung tissue, blood and brain after plating the recovered bacteria on blood agar plates. Shown are the CI values with median of the intranasal co-infection with (**A**) TIGR4*lux* and TIGR4*lux*Δ*rr09*, (**B**) TIGR4*lux* and TIGR4*lux*Δ*hk09* and (**C**) TIGR4*lux* and TIGR4*lux*Δ*tcs09*. CI values < 1 indicate a higher growth of wild-type bacteria than the respective mutant.

4. Discussion

In this study, we have explored the role of *S. pneumoniae* TIGR4 TCS09, which is also referred to as ZmpRS [11] on bacterial fitness and virulence by applying relevant culture experiments and mouse infection models. The *in vivo* infection models included the acute pneumonia, sepsis and a co-infection model. To monitor disease progression, we imaged the dissemination and localization of bacteria in mice using real-time bioluminescent parental TIGR4*lux* and *tcs09*-mutants.

Initial results of growth experiments indicated a lower fitness of *tcs09*-mutants depending on the state of encapsulation and carbon source provided in CDM. Using glucose, the main carbon source in the blood [30], only the encapsulated wild-type TIGR4 and isogenic *tcs09*-mutants showed a substantial growth defect in CDM, which was even more pronounced in the mutant strains (Figure 1A-C). The reason for the reduced fitness has to be explored further, but we hypothesize that required nutrients for high energy demanding capsule production are limited for the mutants when cultured in CDM. As shown by *in vitro* proteome analysis, limited iron availability in CDM leads to a decreased amount of uridine diphosphate-*N*-acetyl-D-mannosamine, which is an important precursor for capsule biosynthesis [31]. In our previous TCS09 study with serotype 2 strain D39 we monitored an indirect influence of TCS09 on capsule expression, which reduced the growth rate in glucose-supplemented CDM [23]. Hence, the similar observation for TIGR4 with increased doubling time strengthens the hypothesis that TCS09 contributes to capsule modulation in pneumococci.

However, the level of glucose is limited in the nasopharynx, therefore pneumococci use di- and monosaccharides cleaved from glycoproteins including e.g. lactose, fructose, sucrose, mannose, sialic acid and galactose, as their main energy source [32-34]. Uptake of lactose occurs via the lactose-specific PTS IIABC (SP_0476, SP_0478, SP_1185, and SP_1186) transporter systems and the resulting lactose-6-phosphate is converted in several metabolic steps in glyceraldehyde-3-phosphate and dihydroxyacetone, both intermediates of the glycolysis [32,35-38]. Sucrose is a disaccharide of glucose and fructose that is taken up by the sucrose-specific PTS IIBCA components (SP_1722), phosphorylated to sucrose-6-phosphate, and enters glycolysis as glucose-6-phosphate [39]. Growth analyses with lactose and sucrose revealed that *S. pneumoniae* can utilize sucrose and lactose equally, whereas the *tcs09*-mutants showed an extended lag phase (Figure 1G-L). In a previous study, we demonstrated a link between TCS09 and carbohydrate metabolism in D39. We indicated downregulation of the regulator AgaR in mutants deficient for the TCS09 system, which in turn leads to an upregulation of the *aga* operon involved in galactose and galactosamine metabolism [23]. For both encapsulated as well as nonencapsulated strains, no growth defects were observed in complex medium THY suggesting that e.g., oligopeptides or other components compensate for the regulatory deficits induced by the *tcs09*-mutation (Figure S1).

Similar to D39 [23], we also investigated the TIGR4 cell morphology of *tcs09*-mutants. However, in contrast to D39, our FESEM and TEM did not show dramatic alterations of the cell morphology and altered septum formation of generated *tcs09*-mutants in TIGR4 and TIGR4Δ*cps* as we have visualized for D39 mutants (Figure 3). LRR staining of pneumococci enabling illustration of CPS also showed no visible alterations in the CPS amount of *tcs09*-mutants. Thus, the regulatory impact of TCS09 on pneumococcal cell morphology and capsule amount is a strain-specific effect and current data suggest that TCS09 has only a minor influence on the TIGR4 morphology under *in vitro* conditions when compared to D39 pneumococci [23].

Successful colonization of the host is an important step to disseminate in submucosa tissues during invasive infections. For adhesion to and invasion into host cells, pneumococci produce enzymes unmasking receptors and adhesins such as PspC, Pilus-1 and PavB that facilitate the interaction with host cell receptors [16,40,41]. In the *hk09*-mutant the expression of the pilus backbone RrgB protein is reduced, confirming previous results [42] and suggesting an influence on adherence or colonization. However, our *in vitro* cell

culture based infection experiments revealed no significant difference between the parental TIGR4Δ*cps* and *tcs09*-mutants (Figure 4). Thus, the amount of type 1 pilus on *tcs09*-mutants seems to be sufficient for pneumococcal adherence. It has to be mentioned that the receptor for the type 1 pilus and its adhesion RrgA is still unknown [43].

Pneumococci have to evade the host immune system for successful colonization and invasion. Macrophages are evolutionarily ancient members of the innate immune system and serve to eliminate microorganisms by phagocytosis. Capsule production directly prevents phagocytosis and the capsule is therefore the *sine qua non* virulence factor. Several TCSs have already been shown to regulate proteins contributing to immune evasion: i) TCS09 influences capsule production in D39 [23]; TCS02 regulates PspA [44] and iii) TCS06 controls PspC expression [45]. Thus, phagocytosis assays were performed to determine the impact of TCS09 on the immune evasion potential of TIGR4 pneumococci. Proteins contributing to immune evasion like CbpL, Ply and PspC [46-49] were not differentially produced in *tcs09*-mutants as shown by immunoblot analysis (Figure 2). However, a multitude of proteins are involved in immune evasion and resistance against phagocytosis including e.g., ClpP, ZmpC and EndA [50-52]. Immunofluorescence microscopy demonstrated that uptake of the pneumococcal *tcs09*-mutant strains by macrophages was similar to the wild-type (Figure 5A and B). In addition, the number of recovered wild-typeTIGR4Δ*cps* and *tcs09*-mutants was also unchanged (Figure 5C). In a following approach, we have further tested whether the loss of function of the TCS09 impairs intracellular survival of pneumococci in macrophages. Intracellular pneumococci are confronted with a harsh environment and especially reactive oxygen species (ROS) and acidic conditions. Our earlier studies with D39 indicated a higher sensitivity of *tcs09*-mutants against hydrogen peroxide [23]. In this study a significant lower number of viable pneumococci deficient in the complete TCS09 was recovered 3 h after *S. pneumoniae* TIGR4 phagocytosis (Figure 5D). This effect was significant but not dramatic, suggesting only a minor influence of TCS09 on the intracellular fate of TIGR4. Other proteins that likely contribute to the survival in the macrophages after phagocytosis include i) the arginine-deaminase-system (*arc*-operon), which produces ammonium and contributes to tolerate the low pH in phagolysosomes [14,53,54] and ii) other proteins like Etrx1, Etrx2 and SodA, whose expression is unchanged in *tcs09*-mutants, and NADH oxidase, PsaBCA, and HtrA as well. The latter proteins are involved in defense against oxidative stress [29,55-57]. However, all published data and this study showed no differential gene or protein expression for these virulence candidates, which is in accordance with the intracellular behavior of our *tcs09*-mutants.

We further conducted *in vivo* infection experiments because all *in vitro* studies can only partially mirror the complex *in vivo* conditions, such as nutrient availability, oxygen level, temperature, and attack by the host immune system. In the mouse infection models of acute pneumonia and septicemia all *tcs09*-mutants were as virulent as the parental strain TIGR4*lux* (Figure 6B and Figure 7). In contrast to our results are virulence studies, in which the deficiency of RR09 in TIGR4 attenuated the mutant. The route of infection was identical, whereas different outbred mice were used [11,25]. Based on these conflicting data we extended our *in vivo* experiments to investigate the impact of TCS09 on virulence in a competitive mouse infection model.

Here, the infection doses of the parental and mutant strain co-infected in a mouse are identical. This model is used to show the higher bacterial fitness by superiority over the other strain in a defined host compartment. Lower bacterial loads of *tcs09*-mutants were detected mainly in the bronchoalveolar lavage, lungs, blood and brain (Figure 8), while the CFU of *tcs09*-mutants and wild-type in nasopharynx was similar as indicated by median CI values between 0.86 and 1.25. The mouse co-infection experiments clearly indicate that the TCS09 is crucial for full virulence of pneumococci, a finding which is probably independent of the genetic background of *S. pneumoniae*. However, the degree of attenuation is probably a strain-specific matter, which explains the different results in the TCS09 studies published so far. This in turn is most likely linked to the strain-specific

regulation of fitness and virulence factors. Because the environmental signal sensed by HK09 is still unknown, one can only speculate under what conditions TCS09 is switched on and required for pneumococci during colonization or under infection-relevant conditions.

Moreover, we cannot exclude cross talk between individual pneumococcal TCSs or compensation mechanisms, making it yet impossible to accurately define the role of TCS09 during pneumococcal pathogenesis. It will be interesting to analyze the *in vivo* transcriptome and proteome of RR09-, HK09- and TCS09-deficient pneumococci recovered from different host compartments to identify the genes targeted by the RR09 of TCS09.

5. Conclusions

In conclusion, these data confirm that TCS09 of TIGR4 and other pneumococcal strains is most likely not directly involved in regulation of factors essential for pneumococcal virulence. Instead, TCS09 seems to be crucial to maintain metabolic fitness and resistance under *in vivo* conditions, thereby facilitating dissemination and survival in different host compartments. The orchestrated activities of regulators enable pneumococci to survive and spread within the host. However, the specific impact of TCS09 on these processes and the environmental signal that triggers TCS09 needs to be elucidated in future studies.

Ethics statement: All animal experiments were conducted in strict accordance with the recommendations in the Guide for the Care and Use of Laboratory Animals (National Research Council, USA), the guidelines of the ethics committee at The University of Greifswald and the German regulations of the Society for Laboratory Animal Science (GVSOLAS) and the European Health Law of the Federation of Laboratory Animal Science Associations (FELASA). All experiments were approved by the Landesamt für Landwirtschaft, Lebensmittelsicherheit und Fischerei Mecklenburg–Vorpommern (LALLFV M-V, Rostock, Germany) and the LALLFV M-V ethical board (LALLF M-V permit no. 7221.3-1-056/16-4). All efforts were made to minimize suffering, ensure the highest ethical standard and adhere to the 3R principle (reduction, refinement and replacement).

Supplementary Materials: The following are available online at www.mdpi.com/xxx/s1, Figure S1: Growth behavior of RR09-, HK09- and TCS09-deficient pneumococci and its parental strains TIGR4, TIGR4*lux* or TIGR4Δ*cps* in THY-medium, Figure S2: Impact of TCS09 on pneumococcal virulence factor expression, Table S1: Calculation of the Competitive Index – nasopharyngeal cavity, Table S2: Calculation of the Competitive Index – bronchoalveolar lavage, Table S3: Calculation of the Competitive Index – lungs, Table S4: Calculation of the Competitive Index – blood, Table S5: Calculation of the Competitive Index – brain.

Author Contributions: Conceptualization, S.HI., A.GM., and S.HA.; methodology, S.HI., A.GM., M.R., and S.HA.; investigation, S.HI., A.GM., T.K., F.V., M.R., and M.B.; resources, S.HI., M.R. and S.HA.; writing—original draft preparation, S.HI., A.GM., T.K., F.V., and S.HA.; writing—review and editing, all authors; visualization, S.HI., A.GM., and M.R.; supervision, S.HA.; project administration, S.HA.; funding acquisition, S.HA. All authors have read and agreed to the published version of the manuscript.

Funding: This research was funded by a grant from the Deutsche Forschungsgemeinschaft (DFG GRK 1870 Bacterial Respiratory Infections to S.HA.) and the Bundesministerium für Bildung und Forschung (BMBF- Zwanzig20 – InfectControl 2020: project VacoME (FKZ 03ZZ0816) and project PathoWIKI (FKZ 03ZZ0839B)).

Acknowledgments: We appreciate the sample preparation and technical assistance of Ina Schleicher (Helmholtz Center for Infection Research, Braunschweig, Germany) in this study.

Conflicts of Interest: The authors declare no conflict of interest. The funders had no role in the design of the study; in the collection, analyses, or interpretation of data; in the writing of the manuscript, or in the decision to publish the results.

References

1. Austrian, R. Some aspects of the pneumococcal carrier state. *J Antimicrob Chemother* **1986**, *18 Suppl A*, 35-45, doi:10.1093/jac/18.supplement_a.35.
2. Bogaert, D.; De Groot, R.; Hermans, P.W. *Streptococcus pneumoniae* colonisation: the key to pneumococcal disease. *Lancet Infect Dis* **2004**, *4*, 144-154, doi:10.1016/s1473-3099(04)00938-7.
3. Kadioglu, A.; Weiser, J.N.; Paton, J.C.; Andrew, P.W. The role of *Streptococcus pneumoniae* virulence factors in host respiratory colonization and disease. *Nat Rev Microbiol* **2008**, *6*, 288-301, doi:10.1038/nrmicro1871.
4. Tuomanen, E.I.; Austrian, R.; Masure, H.R. Pathogenesis of pneumococcal infection. *N Engl J Med* **1995**, *332*, 1280-1284, doi:10.1056/nejm199505113321907.
5. Wahl, B.; O'Brien, K.L.; Greenbaum, A.; Majumder, A.; Liu, L.; Chu, Y.; Lukšić, I.; Nair, H.; McAllister, D.A.; Campbell, H., et al. Burden of *Streptococcus pneumoniae* and *Haemophilus influenzae* type b disease in children in the era of conjugate vaccines: global, regional, and national estimates for 2000-15. *The Lancet. Global health* **2018**, *6*, e744-e757, doi:10.1016/S2214-109X(18)30247-X.
6. Cooper, V.S.; Honsa, E.; Rowe, H.; Deitrick, C.; Iverson, A.R.; Whittall, J.J.; Neville, S.L.; McDevitt, C.A.; Kietzman, C.; Rosch, J.W. Experimental Evolution *In Vivo* To Identify Selective Pressures during Pneumococcal Colonization. *mSystems* **2020**, *5*, e00352-00320, doi:10.1128/mSystems.00352-20.
7. Rowe, H.M.; Karlsson, E.; Echlin, H.; Chang, T.-C.; Wang, L.; van Opijnen, T.; Pounds, S.B.; Schultz-Cherry, S.; Rosch, J.W. Bacterial Factors Required for Transmission of *Streptococcus pneumoniae* in Mammalian Hosts. *Cell Host & Microbe* **2019**, *25*, 884-891.e886, doi:https://doi.org/10.1016/j.chom.2019.04.012.
8. Bermpohl, D.; Halle, A.; Freyer, D.; Dagand, E.; Braun, J.S.; Bechmann, I.; Schröder, N.W.; Weber, J.R. Bacterial programmed cell death of cerebral endothelial cells involves dual death pathways. *J Clin Invest* **2005**, *115*, 1607-1615, doi:10.1172/jci23223.
9. Iovino, F.; Seinen, J.; Henriques-Normark, B.; van Dijl, J.M. How Does *Streptococcus pneumoniae* Invade the Brain? *Trends in Microbiology* **2016**, *24*, 307-315, doi:https://doi.org/10.1016/j.tim.2015.12.012.
10. Weber, J.R.; Tuomanen, E.I. Cellular damage in bacterial meningitis: an interplay of bacterial and host driven toxicity. *J Neuroimmunol* **2007**, *184*, 45-52, doi:10.1016/j.jneuroim.2006.11.016.
11. Hava, D.L.; Camilli, A. Large-scale identification of serotype 4 *Streptococcus pneumoniae* virulence factors. *Molecular microbiology* **2002**, *45*, 1389-1406, doi:https://doi.org/10.1046/j.1365-2958.2002.03106.x.
12. Kohler, S.; Voß, F.; Gómez Mejia, A.; Brown, J.S.; Hammerschmidt, S. Pneumococcal lipoproteins involved in bacterial fitness, virulence, and immune evasion. *FEBS Lett* **2016**, *590*, 3820-3839, doi:10.1002/1873-3468.12352.
13. Gómez-Mejia, A.; Gámez, G.; Hirschmann, S.; Kluger, V.; Rath, H.; Böhm, S.; Voss, F.; Kakar, N.; Petruschka, L.; Völker, U., et al. Pneumococcal Metabolic Adaptation and Colonization Are Regulated by the Two-Component Regulatory System 08. *mSphere* **2018**, *3*, e00165-00118, doi:10.1128/mSphere.00165-18.
14. Schulz, C.; Gierok, P.; Petruschka, L.; Lalk, M.; Mäder, U.; Hammerschmidt, S. Regulation of the Arginine Deiminase System by ArgR2 Interferes with Arginine Metabolism and Fitness of *Streptococcus pneumoniae*. *mBio* **2014**, *5*, e01858-01814, doi:10.1128/mBio.01858-14.
15. Schmidt, F.; Kakar, N.; Meyer, T.C.; Depke, M.; Masouris, I.; Burchhardt, G.; Gómez-Mejia, A.; Dhople, V.; Håvarstein, L.S.; Sun, Z., et al. *In vivo* proteomics identifies the competence regulon and AliB oligopeptide transporter as pathogenic factors in pneumococcal meningitis. *PLOS Pathogens* **2019**, *15*, e1007987, doi:10.1371/journal.ppat.1007987.
16. Bergmann, S.; Hammerschmidt, S. Versatility of pneumococcal surface proteins. *Microbiology (Reading)* **2006**, *152*, 295-303, doi:10.1099/mic.0.28610-0.
17. Gómez-Mejia, A.; Gámez, G.; Hammerschmidt, S. *Streptococcus pneumoniae* two-component regulatory systems: The interplay of the pneumococcus with its environment. *Int J Med Microbiol* **2018**, *308*, 722-737, doi:10.1016/j.ijmm.2017.11.012.

18. Laub, M.T.; Goulian, M. Specificity in two-component signal transduction pathways. *Annu Rev Genet* **2007**, *41*, 121-145, doi:10.1146/annurev.genet.41.042007.170548.
19. Stock, A.M.; Robinson, V.L.; Goudreau, P.N. Two-component signal transduction. *Annu Rev Biochem* **2000**, *69*, 183-215, doi:10.1146/annurev.biochem.69.1.183.
20. Glanville, D.G.; Han, L.; Maule, A.F.; Woodacre, A.; Thanki, D.; Abdullah, I.T.; Morrissey, J.A.; Clarke, T.B.; Yesilkaya, H.; Silvaggi, N.R., et al. RitR is an archetype for a novel family of redox sensors in the streptococci that has evolved from two-component response regulators and is required for pneumococcal colonization. *PLOS Pathogens* **2018**, *14*, e1007052, doi:10.1371/journal.ppat.1007052.
21. Paterson, G.K.; Blue, C.E.; Mitchell, T.J. Role of two-component systems in the virulence of *Streptococcus pneumoniae*. *J Med Microbiol* **2006**, *55*, 355-363, doi:10.1099/jmm.0.46423-0.
22. Reinoso-Vizcaíno, N.M.; Cian, M.B.; Cortes, P.R.; Olivero, N.B.; Hernandez-Morfa, M.; Piñas, G.E.; Badapanda, C.; Rathore, A.; Perez, D.R.; Echenique, J. The pneumococcal two-component system SirRH is linked to enhanced intracellular survival of *Streptococcus pneumoniae* in influenza-infected pulmonary cells. *PLOS Pathogens* **2020**, *16*, e1008761, doi:10.1371/journal.ppat.1008761.
23. Hirschmann, S.; Gómez-Mejia, A.; Mäder, U.; Karsunke, J.; Driesch, D.; Rohde, M.; Häussler, S.; Burchhardt, G.; Hammerschmidt, S. The Two-Component System 09 Regulates Pneumococcal Carbohydrate Metabolism and Capsule Expression. *Microorganisms* **2021**, *9*, 468, doi:10.3390/microorganisms9030468.
24. Blue, C.E.; Mitchell, T.J. Contribution of a response regulator to the virulence of *Streptococcus pneumoniae* is strain dependent. *Infection and immunity* **2003**, *71*, 4405-4413, doi:10.1128/iai.71.8.4405-4413.2003.
25. Hendriksen, W.T.; Silva, N.; Bootsma, H.J.; Blue, C.E.; Paterson, G.K.; Kerr, A.R.; de Jong, A.; Kuipers, O.P.; Hermans, P.W.; Mitchell, T.J. Regulation of gene expression in *Streptococcus pneumoniae* by response regulator 09 is strain dependent. *J Bacteriol* **2007**, *189*, 1382-1389, doi:10.1128/jb.01144-06.
26. Throup, J.P.; Koretke, K.K.; Bryant, A.P.; Ingraham, K.A.; Chalker, A.F.; Ge, Y.; Marra, A.; Wallis, N.G.; Brown, J.R.; Holmes, D.J., et al. A genomic analysis of two-component signal transduction in *Streptococcus pneumoniae*. *Molecular microbiology* **2000**, *35*, 566-576, doi:https://doi.org/10.1046/j.1365-2958.2000.01725.x.
27. Tettelin, H.; Nelson, K.E.; Paulsen, I.T.; Eisen, J.A.; Read, T.D.; Peterson, S.; Heidelberg, J.; DeBoy, R.T.; Haft, D.H.; Dodson, R.J., et al. Complete Genome Sequence of a Virulent Isolate of *Streptococcus pneumoniae*. *Science* **2001**, *293*, 498, doi:10.1126/science.1061217.
28. Abdullah, M.R.; Gutiérrez-Fernández, J.; Pribyl, T.; Gisch, N.; Saleh, M.; Rohde, M.; Petruschka, L.; Burchhardt, G.; Schwudke, D.; Hermoso, J.A., et al. Structure of the pneumococcal l,d-carboxypeptidase DacB and pathophysiological effects of disabled cell wall hydrolases DacA and DacB. *Molecular microbiology* **2014**, *93*, 1183-1206, doi:10.1111/mmi.12729.
29. Saleh, M.; Bartual, S.G.; Abdullah, M.R.; Jensch, I.; Asmat, T.M.; Petruschka, L.; Pribyl, T.; Gellert, M.; Lillig, C.H.; Antelmann, H., et al. Molecular architecture of *Streptococcus pneumoniae* surface thioredoxin-fold lipoproteins crucial for extracellular oxidative stress resistance and maintenance of virulence. *EMBO Molecular Medicine* **2013**, *5*, 1852-1870, doi:https://doi.org/10.1002/emmm.201202435.
30. Krebs, H.A. Chemical Composition of Blood Plasma and Serum. *Annual Review of Biochemistry* **1950**, *19*, 409-430, doi:10.1146/annurev.bi.19.070150.002205.
31. Nanduri, B.; Shah, P.; Ramkumar, M.; Allen, E.B.; Swiatlo, E.; Burgess, S.C.; Lawrence, M.L. Quantitative analysis of *Streptococcus pneumoniae* TIGR4 response to in vitro iron restriction by 2-D LC ESI MS/MS. *Proteomics* **2008**, *8*, 2104-2114, doi:10.1002/pmic.200701048.

32. Bidossi, A.; Mulas, L.; Decorosi, F.; Colomba, L.; Ricci, S.; Pozzi, G.; Deutscher, J.; Viti, C.; Oggioni, M.R. A Functional Genomics Approach to Establish the Complement of Carbohydrate Transporters in *Streptococcus pneumoniae*. *PLOS ONE* **2012**, *7*, e33320, doi:10.1371/journal.pone.0033320.
33. Buckwalter, C.M.; King, S.J. Pneumococcal carbohydrate transport: food for thought. *Trends Microbiol* **2012**, *20*, 517-522, doi:10.1016/j.tim.2012.08.008.
34. Trappetti, C.; Kadioglu, A.; Carter, M.; Hayre, J.; Iannelli, F.; Pozzi, G.; Andrew, P.W.; Oggioni, M.R. Sialic Acid: A Preventable Signal for Pneumococcal Biofilm Formation, Colonization, and Invasion of the Host. *The Journal of Infectious Diseases* **2009**, *199*, 1497-1505, doi:10.1086/598483.
35. Abranches, J.; Chen, Y.-Y.M.; Burne, R.A. Galactose metabolism by *Streptococcus mutans*. *Applied and environmental microbiology* **2004**, *70*, 6047-6052, doi:10.1128/AEM.70.10.6047-6052.2004.
36. Afzal, M.; Shafeeq, S.; Kuipers, O.P. LacR is a repressor of *lacABCD* and LacT is an activator of *lacTFEG*, constituting the *lac* gene cluster in *Streptococcus pneumoniae*. *Applied and environmental microbiology* **2014**, *80*, 5349-5358, doi:10.1128/AEM.01370-14.
37. Carvalho, S.M.; Kloosterman, T.G.; Kuipers, O.P.; Neves, A.R. CcpA Ensures Optimal Metabolic Fitness of *Streptococcus pneumoniae*. *PLOS ONE* **2011**, *6*, e26707, doi:10.1371/journal.pone.0026707.
38. Iskandar, C.F.; Cailliez-Grimal, C.; Borges, F.; Revol-Junelles, A.-M. Review of lactose and galactose metabolism in Lactic Acid Bacteria dedicated to expert genomic annotation. *Trends in Food Science & Technology* **2019**, *88*, 121-132, doi:https://doi.org/10.1016/j.tifs.2019.03.020.
39. Iyer, R.; Camilli, A. Sucrose metabolism contributes to *in vivo* fitness of *Streptococcus pneumoniae*. *Molecular microbiology* **2007**, *66*, 1-13, doi:10.1111/j.1365-2958.2007.05878.x.
40. Jensch, I.; Gámez, G.; Rothe, M.; Ebert, S.; Fulde, M.; Somplatzki, D.; Bergmann, S.; Petruschka, L.; Rohde, M.; Nau, R., et al. PavB is a surface-exposed adhesin of *Streptococcus pneumoniae* contributing to nasopharyngeal colonization and airways infections. *Molecular microbiology* **2010**, *77*, 22-43, doi:https://doi.org/10.1111/j.1365-2958.2010.07189.x.
41. Voß, S.; Gámez, G.; Hammerschmidt, S. Impact of pneumococcal microbial surface components recognizing adhesive matrix molecules on colonization. *Molecular Oral Microbiology* **2012**, *27*, 246-256, doi:https://doi.org/10.1111/j.2041-1014.2012.00654.x.
42. Kreikemeyer, B.; Gámez, G.; Margarit, I.; Giard, J.C.; Hammerschmidt, S.; Hartke, A.; Podbielski, A. Genomic organization, structure, regulation and pathogenic role of pilus constituents in major pathogenic *Streptococci* and *Enterococci*. *Int J Med Microbiol* **2011**, *301*, 240-251, doi:10.1016/j.ijmm.2010.09.003.
43. Hilleringmann, M.; Giusti, F.; Baudner, B.C.; Masignani, V.; Covacci, A.; Rappuoli, R.; Barocchi, M.A.; Ferlenghi, I. Pneumococcal pili are composed of protofilaments exposing adhesive clusters of Rrg A. *PLoS Pathog* **2008**, *4*, e1000026, doi:10.1371/journal.ppat.1000026.
44. Ng, W.-L.; Tsui, H.-C.T.; Winkler, M.E. Regulation of the *pspA* Virulence Factor and Essential *pcsB* Murein Biosynthetic Genes by the Phosphorylated VicR (YycF) Response Regulator in *Streptococcus pneumoniae*. *Journal of Bacteriology* **2005**, *187*, 7444, doi:10.1128/JB.187.21.7444-7459.2005.
45. Standish, A.J.; Stroeher, U.H.; Paton, J.C. The two-component signal transduction system RR06/HK06 regulates expression of *cbpA* in *Streptococcus pneumoniae*. *Proceedings of the National Academy of Sciences of the United States of America* **2005**, *102*, 7701, doi:10.1073/pnas.0409377102.
46. Gutiérrez-Fernández, J.; Saleh, M.; Alcorlo, M.; Gómez-Mejía, A.; Pantoja-Uceda, D.; Treviño, M.A.; Voß, F.; Abdullah, M.R.; Galán-Bartual, S.; Seinen, J., et al. Modular Architecture and Unique Teichoic Acid Recognition Features of Choline-Binding Protein L (CbpL) Contributing to Pneumococcal Pathogenesis. *Scientific Reports* **2016**, *6*, 38094, doi:10.1038/srep38094.
47. Bewley, M.A.; Naughton, M.; Preston, J.; Mitchell, A.; Holmes, A.; Marriott, H.M.; Read, R.C.; Mitchell, T.J.; Whyte, M.K.B.; Dockrell, D.H. Pneumolysin Activates Macrophage Lysosomal Membrane Permeabilization and Executes Apoptosis by Distinct Mechanisms without Membrane Pore Formation. *mBio* **2014**, *5*, e01710-01714, doi:10.1128/mBio.01710-14.

48. Hammerschmidt, S.; Talay, S.R.; Brandtzaeg, P.; Chhatwal, G.S. SpsA, a novel pneumococcal surface protein with specific binding to secretory Immunoglobulin A and secretory component. *Molecular microbiology* **1997**, *25*, 1113-1124, doi:https://doi.org/10.1046/j.1365-2958.1997.5391899.x.
49. Dave, S.; Brooks-Walter, A.; Pangburn, M.K.; McDaniel, L.S. PspC, a Pneumococcal Surface Protein, Binds Human Factor H. *Infection and Immunity* **2001**, *69*, 3435, doi:10.1128/IAI.69.5.3435-3437.2001.
50. Cao, J.; Gong, Y.; Dong, S.; Zhang, L.; Lai, X.; Zhang, X.; Yin, Y. Pneumococcal ClpP modulates the maturation and activation of human dendritic cells: implications for pneumococcal infections. *Journal of Leukocyte Biology* **2013**, *93*, 737-749, doi:https://doi.org/10.1189/jlb.0812428.
51. Surewaard, B.G.J.; Trzciński, K.; Jacobino, S.R.; Hansen, I.S.; Vughs, M.M.; Sanders, E.A.M.; van der Ende, A.; van Strijp, J.A.G.; de Haas, C.J.C. Pneumococcal immune evasion: ZmpC inhibits neutrophil influx. *Cellular Microbiology* **2013**, *15*, 1753-1765, doi:https://doi.org/10.1111/cmi.12147.
52. Beiter, K.; Wartha, F.; Albiger, B.; Normark, S.; Zychlinsky, A.; Henriques-Normark, B. An endonuclease allows *Streptococcus pneumoniae* to escape from neutrophil extracellular traps. *Curr Biol* **2006**, *16*, 401-407, doi:10.1016/j.cub.2006.01.056.
53. Ohkuma, S.; Poole, B. Fluorescence probe measurement of the intralysosomal pH in living cells and the perturbation of pH by various agents. *Proceedings of the National Academy of Sciences of the United States of America* **1978**, *75*, 3327-3331, doi:10.1073/pnas.75.7.3327.
54. Casiano-Colón, A.; Marquis, R.E. Role of the arginine deiminase system in protecting oral bacteria and an enzymatic basis for acid tolerance. *Applied and environmental microbiology* **1988**, *54*, 1318-1324, doi:10.1128/AEM.54.6.1318-1324.1988.
55. Gennaris, A.; Collet, J.-F. The 'captain of the men of death', *Streptococcus pneumoniae*, fights oxidative stress outside the 'city wall'. *EMBO Molecular Medicine* **2013**, *5*, 1798-1800, doi:https://doi.org/10.1002/emmm.201303482.
56. Tseng, H.-J.; McEwan, A.G.; Paton, J.C.; Jennings, M.P. Virulence of *Streptococcus pneumoniae*: PsaA Mutants Are Hypersensitive to Oxidative Stress. *Infection and Immunity* **2002**, *70*, 1635, doi:10.1128/IAI.70.3.1635-1639.2002.
57. Ibrahim, Y.M.; Kerr, A.R.; McCluskey, J.; Mitchell, T.J. Role of HtrA in the virulence and competence of *Streptococcus pneumoniae*. *Infection and immunity* **2004**, *72*, 3584-3591, doi:10.1128/IAI.72.6.3584-3591.2004.

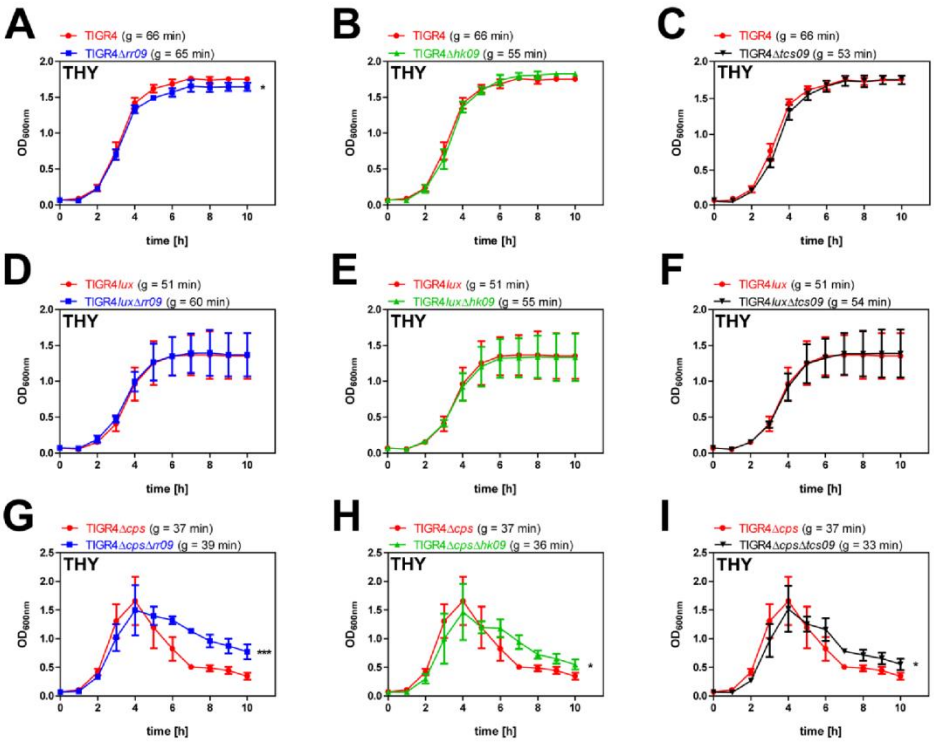

Figure S1: Growth behavior of RR09-, HK09- and TCS09-deficient pneumococci and its parental strains TIGR4, TIGR4*lux* or TIGR4Δ*cps* in THY-medium. Isogenic *tcs09*-mutants and parental strains TIGR4 (**A-C**), TIGR4*lux* (**D-F**) or TIGR4Δ*cps* (**G-I**) were cultivated in THY-medium at 37°C under microaerophilic conditions without agitation. Results are presented as the mean ±SD for three independent experiments. The mean value of the doubling time (g) from three biological replicates of the respective strain is provided. A two-way Anova proved a significance with p-value * < 0.05 and *** < 0.001 relative to the parental pneumococcal strain.

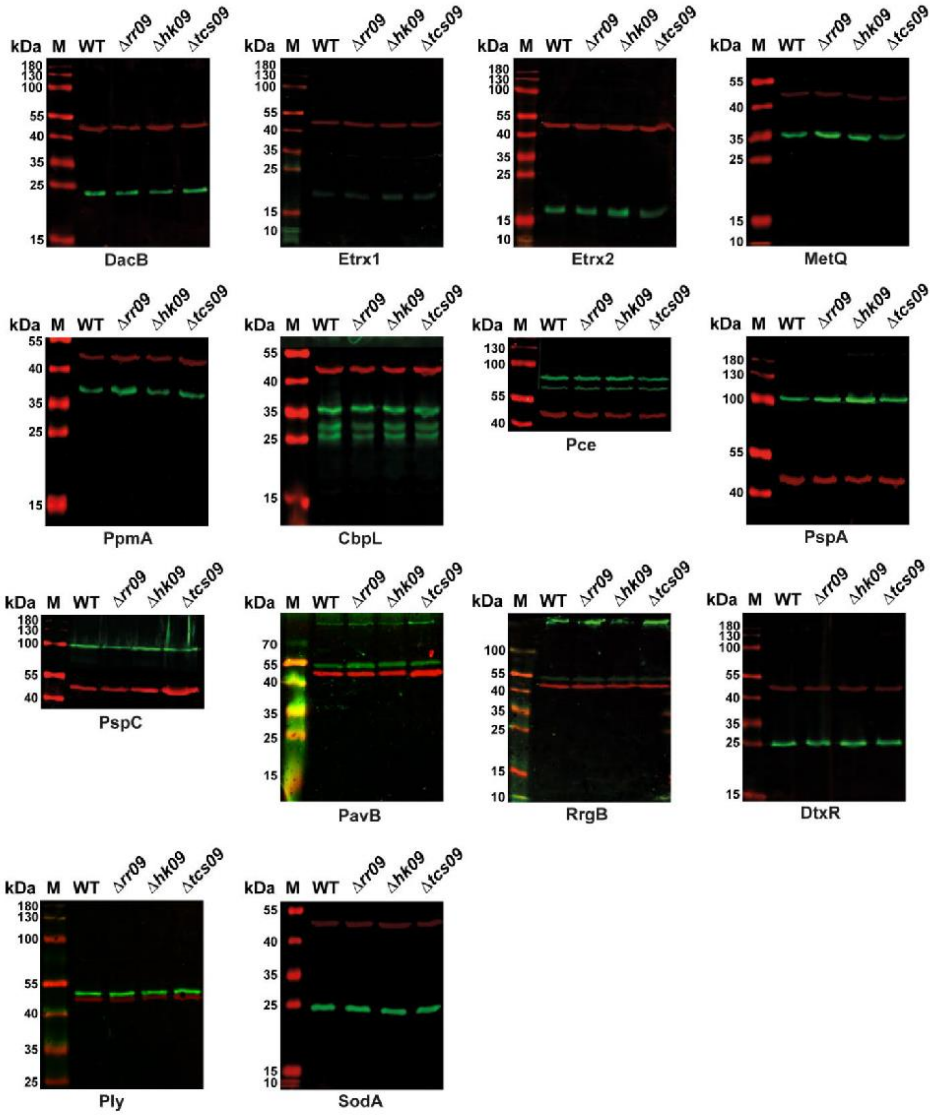

Figure S2: Impact of TCS09 on pneumococcal virulence factor expression. The pneumococcal *rr09*- *hk09*- and *tcs09*-mutants of TIGR4Δ*cps* were analyzed for lipoprotein, choline-binding protein, sortase-anchored protein and intracellular protein expression, respectively. Protein expression of selected candidates was detected with polyclonal protein-specific antibodies (1:500) generated in mice followed by IRDye® 800CW fluorescence-coupled secondary antibody (1:15000; green). Detection of Enolase (47 kDa) as loading control was performed with rabbit anti-Eno antibody (1:12,500) and IRDye® 680RD fluorescence coupled secondary antibody (1:15000; red). Scanning of the immunoblots was conducted with Odyssey® CLx Scanner.

CI values

The following tables provide a list of all calculated competitive index (CI) values for Figure 8. CI values were calculated using the following formula:

$$CI = \frac{Mutant\ x\ (CFU\ x\ 10^6)}{Wild-type\ x\ (CFU\ x\ 10^6)}$$

Table S1. Calculation of the Competitive Index – nasopharyngeal cavity

TIGR4*lux* vs TIGR4*luxΔrr09*		**TIGR4*lux* vs TIGR4*luxΔhk09***		**TIGR4*lux* vs TIGR4*luxΔtcs09***	
24 h	**48 h**	**24 h**	**48 h**	**24 h**	**48 h**
0.673075	0.901638	4.846191	1.159096	1.459463	1.071431
0.584699	1.140347	0.553030	1.148144	1.264147	0.897107
1.337075	1.119656	1.127265	0.987343	1.000000	0.999994
0.617355	0.662339	1.000000	1.060600	0.746031	0.884615
1.051277	3.40916	1.023807	0.923079	1.027775	0.600719
0.156862	1.219297	1.172406	0.729732	1.184217	0.781816
1.634408	1.046875	1.108698	0.842105	1.096154	0.835165
1.205869	1.563636	0.518987	2.560006	0.617021	1.322566
0.982858	1.303027	1.759995	1.426664	1.000000	0.777778
0.363636	0.464843	1.234567	2.595236	0.610386	0.686567
0.962025	1.283779	0.501155	0.687495	1.714286	0.452784
0.865671	1.395605	1.617016	2.369226	0.530249	1.133333
1.077918	2.882330	0.567568	0.651027	0.753558	0.956898
0.776316	1.655175	0.569890	0.662870	0.617250	0.563981
Median:					
0.9138	**1.252**	**1.066**	**1.024**	**1.000**	**0.8599**

Table S2. Calculation of the Competitive Index – bronchoalveolar lavage

TIGR4*lux* vs TIGR4*luxΔrr09*		**TIGR4*lux* vs TIGR4*luxΔhk09***		**TIGR4*lux* vs TIGR4*luxΔtcs09***	
24 h	**48 h**	**24 h**	**48 h**	**24 h**	**48 h**
0.000000	1.000000	0.696968	0.522248	2.708325	0.002445
1.312501	0.928570	2.599928	0.824072	0.858973	1.000000
0.491329	5.000000	3.421041	0.000000	0.750002	0.666600
1.000000	1.000000	2.735302	0.000000	0.096345	1.705882
1.384626	1.940300	0.067285	0.226415	3.499978	0.034479
0.124694	0.333330	1.238086	0.400000	0.708325	> 3
0.333300	0.052627	0.620553	0.025638	1.417584	0.857144
2.596159	0.750002	3.571429	0.116667	0.999963	0.052627
5.50000	0.181818	2.208331	0.000000	0.776311	0.230900
1.565891	0.538461	3.360013	0.354166	1.303027	0.052627
0.888413	> 3	1.190476	1.365854	0.416663	1.000000
2.760873	0.968744	1.249995	3.199979	0.999850	1.545451
3.321440	2.586225	0.200000	0.683330	2.043461	> 3
0.960782	1.924241	1.296294	> 3	2.083325	16.665000
Median:					
1.156	**0.8393**	**1.273**	**0.3771**	**0.9999**	**0.9286**

Table S3. Calculation of the Competitive Index – lungs

TIGR4*lux* vs TIGR4*luxΔrr09*		**TIGR4*lux* vs TIGR4*luxΔhk09***		**TIGR4*lux* vs TIGR4*luxΔtcs09***	
24 h	**48 h**	**24 h**	**48 h**	**24 h**	**48 h**
2.500009	0.499998	3.000000	1.072916	1.285716	0.000495
0.004785	> 3	0.474967	0.662497	0.892563	0.064195
1.021281	1.000000	> 3	0.230769	0.485980	0.575758
1.000000	17.499025	0.643192	0.399999	0.023809	0.000266
0.442307	0.541095	0.077821	13.750318	0.165311	0.002132
36.00400	0.096000	0.330509	0.008215	0.166664	4.750000
1.314811	0.856287	1.875012	0.015269	0.555553	4.583331
1.764727	0.584268	1.000000	0.006589	0.032258	0.139286
0.328225	0.754386	2.376630	0.307692	1.475412	0.403588
0.617312	0.428572	1.500000	0.216931	0.000000	0.666667
0.169687	4.933320	0.063830	0.160950	4.998800	1.200001
2.607841	0.111111	0.274298	8.833300	0.111100	1.210521
0.573499	5.555533	1.156629	0.554349	0.470588	0.533330
> 3	3.073186	0.084416	2.894747	1.000000	0.142856
Median:					
1.011	**0.8053**	**0.8216**	**0.3538**	**0.4783**	**0.4685**

Table S4. Calculation of the Competitive Index – blood

TIGR4*lux* vs TIGR4*luxΔrr09*		**TIGR4*lux* vs TIGR4*luxΔhk09***		**TIGR4*lux* vs TIGR4*luxΔtcs09***	
24 h	**48 h**	**24 h**	**48 h**	**24 h**	**48 h**
0.026313	0.366012	1.000000	> 3	0.302325	0.000337
1.000000	0.224189	0.697337	0.625000	0.352941	0.024911
0.999999	0.000000	1.000000	1.000000	1.103438	0.307692
0.000000	2.070800	5.000000	1.000000	0.008621	0.000230
0.029411	0.367431	0.022280	1.068966	0.593176	0.001473
1.133320	> 3	0.467479	0.000000	0.002865	4.222200
1.489797	1.166665	0.000000	0.018348	0.857144	7.764797
0.000000	0.083798	1.000000	0.000000	1.000000	0.047847
0.851850	0.687152	0.321284	0.317391	1.533332	0.251967
0.024622	0.459459	1.475412	0.204663	0.025638	0.905108
0.138421	3.199979	0.000000	0.178451	1.000000	1.000000
0.272729	0.095994	0.354838	2.296289	1.000000	1.599993
0.671643	2.739837	1.298848	0.409091	0.529412	0.594061
> 3	> 3	0.012346	12.916650	1.000000	1.000000
Median:					
0.4722	**0.5733**	**0.5824**	**0.5170**	**0.7252**	**0.4509**

Table S5. Calculation of the Competitive Index – brain

TIGR4*lux* vs TIGR4*luxΔrr09*		**TIGR4*lux* vs TIGR4*luxΔhk09***		**TIGR4*lux* vs TIGR4*luxΔtcs09***	
24 h	**48 h**	**24 h**	**48 h**	**24 h**	**48 h**
1.000000	0.312500	11.333300	0.536424	1.312508	0.002278
2.000300	0.018518	0.754098	0.486488	6.000000	0.624997
> 3	1.000000	1.000000	1.000000	1.120000	0.333330
0.000000	0.490566	0.548377	0.199998	1.769188	0.250000
0.519998	0.225071	0.333333	1.033330	1.500000	0.012657
2.3333	2.400002	0.099990	> 3	1.000000	0.020406
1.785754	1.000000	0.000000	1.000000	0.863636	3.789494
3.190471	0.249998	0.238086	1.000000	0.000000	0.020406
4.000043	0.7743889	0.902434	0.087500	0.575755	0.480767
0.000000	1.000000	0.209801	0.152174	1.166667	> 3
0.200012	0.473684	0.656254	0.025532	2.499775	1.000000
0.888866	0.052631	0.750003	1.999985	0.655167	1.699995
7.666650	> 3	1.327578	0.358488	0.916650	0.290779
0.900000	0.398601	0.000000	1.062497	5.000000	1.000000
Median:					
1.393	**0.4821**	**0.6023**	**0.7682**	**1.143**	**0.4070**

4.3. Publication 3

Pneumococcal Metabolic Adaptation and Colonization Are Regulated by the Two-Component Regulatory System 08

Alejandro Gómez-Mejia, Gustavo Gámez, **Stephanie Hirschmann**, Viktor Kluger, Hermann Rath, Sebastian Böhm, Franziska Voss, Niamatullah Kakar, Lothar Petruschka, Uwe Völker, Reinhold Brückner, Ulrike Mäder and Sven Hammerschmidt

Published in the journal mSphere, 2018 May 16;3(3):e00165-18.
doi: 10.1128/mSphere.00165-18

AMERICAN SOCIETY FOR MICROBIOLOGY | mSphere®

RESEARCH ARTICLE
Host-Microbe Biology

Pneumococcal Metabolic Adaptation and Colonization Are Regulated by the Two-Component Regulatory System 08

Alejandro Gómez-Mejia,[a] Gustavo Gámez,[b,c] Stephanie Hirschmann,[a] Viktor Kluger,[a] Hermann Rath,[d] Sebastian Böhm,[a] Franziska Voss,[a] Niamatullah Kakar,[a] Lothar Petruschka,[a] Uwe Völker,[d] Reinhold Brückner,[e] Ulrike Mäder,[d] Sven Hammerschmidt[a]

[a]Department of Molecular Genetics and Infection Biology, Interfaculty Institute for Genetics and Functional Genomics, Center for Functional Genomics of Microbes, University of Greifswald, Greifswald, Germany
[b]Genetics, Regeneration and Cancer (GRC) Research Group, University Research Center (SIU), Universidad de Antioquia (UdeA), Medellin, Colombia
[c]Basic and Applied Microbiology (MICROBA) Research Group, School of Microbiology, Universidad de Antioquia (UdeA), Medellin, Colombia
[d]Department of Functional Genomics, Interfaculty Institute for Genetics and Functional Genomics, Center for Functional Genomics of Microbes, University Medicine Greifswald, Greifswald, Germany
[e]Department of Microbiology, University of Kaiserslautern, Kaiserslautern, Germany

ABSTRACT *Streptococcus pneumoniae* two-component regulatory systems (TCS) enable adaptation and ensure its maintenance in host environments. This study deciphers the impact of TCS08 on pneumococcal gene expression and its role in metabolic and pathophysiological processes. Transcriptome analysis and real-time PCR demonstrated a regulatory effect of TCS08 on genes involved mainly in environmental information processing, intermediary metabolism, and colonization by *S. pneumoniae* D39 and TIGR4. Striking examples are genes for fatty acid biosynthesis, genes of the arginine deiminase system, and the *psa* operon encoding the manganese ABC transport system. *In silico* analysis confirmed that TCS08 is homologous to *Staphylococcus aureus* SaeRS, and a SaeR-like binding motif is displayed in the promoter region of *pavB*, the upstream gene of the *tcs08* operon encoding a surface-exposed adhesin. Indeed, PavB is regulated by TCS08 as confirmed by immunoblotting and surface abundance assays. Similarly, pilus-1 of TIGR4 is regulated by TCS08. Finally, *in vivo* infections using the acute pneumonia and sepsis models showed a strain-dependent effect. Loss of function of HK08 or TCS08 attenuated D39 virulence in lung infections. The RR08 deficiency attenuated TIGR4 in pneumonia, while there was no effect on sepsis. In contrast, lack of HK08 procured a highly virulent TIGR4 phenotype in both pneumonia and sepsis infections. Taken together, these data indicate the importance of TCS08 in pneumococcal fitness to adapt to the milieu of the respiratory tract during colonization.

IMPORTANCE *Streptococcus pneumoniae* interplays with its environment by using 13 two-component regulatory systems and one orphan response regulator. These systems are involved in the sensing of environmental signals, thereby modulating pneumococcal pathophysiology. This study aimed to understand the functional role of genes subject to control by the TCS08. The identified genes play a role in transport of compounds such as sugars or amino acids. In addition, the intermediary metabolism and colonization factors are modulated by TCS08. Thus, TCS08 regulates genes involved in maintaining pneumococcal physiology, transport capacity, and adhesive factors to enable optimal colonization, which represents a prerequisite for invasive pneumococcal disease.

KEYWORDS *Streptococcus pneumoniae*, colonization, gene regulation, physiology, two-component regulatory systems

Received 10 April 2018 **Accepted** 30 April 2018 **Published** 16 May 2018

Citation Gómez-Mejia A, Gámez G, Hirschmann S, Kluger V, Rath H, Böhm S, Voss F, Kakar N, Petruschka L, Völker U, Brückner R, Mäder U, Hammerschmidt S. 2018. Pneumococcal metabolic adaptation and colonization are regulated by the two-component regulatory system 08. mSphere 3:e00165-18. https://doi.org/10.1128/mSphere.00165-18.

Editor Paul D. Fey, University of Nebraska Medical Center

Address correspondence to Sven Hammerschmidt, sven.hammerschmidt@uni-greifswald.de.

Regulatory systems are inherent features of living organisms, ensuring a rapid response and adaptation to diverse environmental conditions and acting as on/off switches for gene expression (1). Regulation in bacteria is predominantly conducted by two-component regulatory systems (TCS), quorum sensing proteins, and stand-alone regulators (2–4). TCS are the most common and widespread sensing mechanisms in prokaryotes, functioning by activation of effectors through the autophosphorylation of a conserved histidine kinase (HK) and the phosphor transfer to its cognate partner protein, also referred to as a response regulator (RR). These systems are able to sense environmental conditions and coordinate the appropriate response to ensure survival, fitness, and pathogenicity (4–9).

In silico and functional analysis of the pneumococcal genome identified 13 cognate HK-RR pairs and an additional orphan unpaired RR in different pneumococcal strains (10, 11). TCS in pneumococci have been associated with fitness and regulation of virulence factors, and 11 TCS are reported to contribute to pneumococcal pathogenicity (11, 12). ComDE and CiaRH, both involved in the control of competence and cell survival under stress conditions, have been studied most extensively (13–18). WalRK is another well-characterized TCS in pneumococci, featuring the only PAS (Per-Arnt-Sim) domain in *Streptococcus pneumoniae* and involved in maintenance of cell wall integrity by regulating the proteins PcsB and FabT (19–21). Furthermore, this system is the only TCS which has been shown to be essential for pneumococcal viability. However, it was proven later that this effect on viability was due to the regulation of the peptidoglycan hydrolase PcsB, whose loss of function leads to an unstable membrane and impaired cell viability (22, 23). Pneumococcal TCS08 (in TIGR4, genes *sp_0083* to *sp_0084* encode RR08 and HK08) is highly homologous to the SaeRS system of *Staphylococcus aureus* (24), where it has been associated with the regulation of genes encoding α-hemolysin (*hla*), coagulase (*coa*), fibronectin (Fn) binding proteins, and 20 other virulence factors (25–27). Interestingly, the SaeRS system of *S. aureus* has been shown to respond to subinhibitory concentrations of α-defensins and high concentrations of H_2O_2, suggesting a sensing mechanism responsive to host immune system molecules and membrane alterations (26, 27). In pneumococci, a previous study on TCS08 has revealed its importance for pneumococcal virulence (11). Moreover, two reports have shown a regulatory effect of the pneumococcal TCS08 on the *rlrA* pathogenicity islet (pilus-1 [PI-1]) and the cellobiose phosphotransfer system (PTS) (24, 28). Hence, the initial information available about this system suggests its involvement in pneumococcal adaptation, fitness, and virulence. Nevertheless, its target genes and its precise role in pneumococcal pathogenicity are yet to be defined.

RESULTS

Influence of TCS08 on pneumococcal growth behavior in CDM. To investigate the effect of loss of function of TCS08 components on pneumococcal fitness, nonencapsulated *S. pneumoniae* D39 and TIGR4 parental strains and their isogenic mutants were cultured in a chemically defined medium (CDM). All strains presented similar growth patterns and reached similar cell densities in the stationary phase, with the exception of the TIGR4 Δ*cps* Δ*rr08* mutant (Fig. 1). A steeper logarithmic phase was detected in the *rr08* mutant in TIGR4 (Fig. 1A and E). Additionally, the calculated growth rates of the different mutants in both D39 and TIGR4 strains suggested a significant reduction in the generation time of the *rr08* mutant in TIGR4 (Fig. 1A). The observed behavior among the TCS08 mutants in the CDM used in this study may point to strain-dependent specific effects.

Impact of TCS08 on TIGR4 gene expression. The initial screening for the effects of TCS08 inactivation on gene expression was conducted by microarrays using RNA samples extracted from TIGR4Δ*cps* and its isogenic *rr08*, *hk08*, and *tcs08* mutants grown in CDM. Genes presenting significant changes in gene expression higher than 2-fold with known functions or with functional domains were considered for further analysis. This led to the selection of 159 protein-encoding genes showing significant differences in expression compared to the wild type (WT) in at least one of the mutants deficient

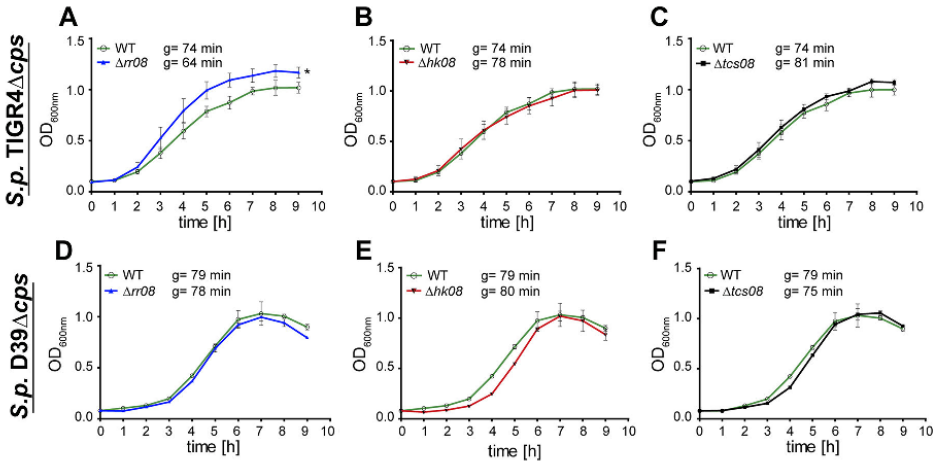

FIG 1 Growth behavior of pneumococcal *tcs08* mutants. Growth in CDM of *S. pneumoniae* TIGR4 Δ*cps* and D39 Δ*cps* parental strains versus Δ*rr08* (A and D), Δ*hk08* (B and E), and Δ*tcs08* (C and F) mutants, respectively. The symbol "g" indicates generation time. An unpaired two-tailed *t* test was used with the generation times for statistics, and the error bars indicate the standard deviation for $n = 3$. The asterisk indicates statistical significance among the generation times of the different strains ($P < 0.05$).

in RR08, HK08, or both (TCS08). Loss of HK08 triggered the strongest changes in expression compared to the wild type and influenced 114 genes. Differences in expression profiles of the 159 genes found in the microarray were classified by their annotated biochemical functions in 5 different categories (Fig. 2; see also Table S1 in the supplemental material). (i) The largest number of genes influenced in their expression by TCS08 was observed for genes belonging to environmental information processing (EIP). Genes belonging to this functional class are mostly involved in membrane transport by ABC transporters and phosphotransferase systems and represented 88 genes affected by mutations in TCS08. The strongest changes in gene expression within the EIP category were detected for the ABC transporters *aliB* (oligopeptide substrate-binding protein) and *sp_1434*, both in the *hk08* mutant. (ii) The second most predominant category, with 41 genes, was the intermediary metabolism (IM). Here, significant changes in the expression of genes involved in fatty acid (*fab* operon), carbon (cellobiose, mannitol, and maltose PTS), and amino acid (*arc* operon) metabolism were seen. Indeed, the absence of RR08 led to a significant reduction in the expression of the *arc* operon, involved in arginine uptake and utilization. In contrast, the expression of the *arc* genes in the strain lacking HK08 was upregulated. These changes observed in the expression of the *arc* operon were the most prominent within the IM category. (iii) Genes reported to play a role as colonization factors (CF) accounted for 13 of the 159 genes displaying expression changes in the microarray analysis. The genes found in this group encode surface-exposed proteins involved in peptidoglycan synthesis and adhesion. Among them, the gene *sp_2136*, encoding the choline-binding protein PcpA, showed the strongest upregulation in the whole-microarray analysis. The genes encoding PavB, MucBP, PepO, PrtA, and NanA displayed changes in their expression in the different *tcs08* mutants as well. These important proteins are involved in pneumococcal colonization and highlight the role of TCS08 for pneumococcal adhesion and colonization. Additionally, the lack of both components of TCS08 resulted in changes in the expression of the *rrgABC-srtC* operon, confirming the regulation of the region of diversity 4 (RD4) (identified as *rlrA* or PI-1 pathogenicity islet) by TCS08. It is noteworthy that most of these genes encode surface-displayed proteins often covalently anchored in the peptidoglycan via a transpeptidase. (iv) The fourth category encompasses genes playing a role in genetic information processing (GIP), of which 9 genes were detected

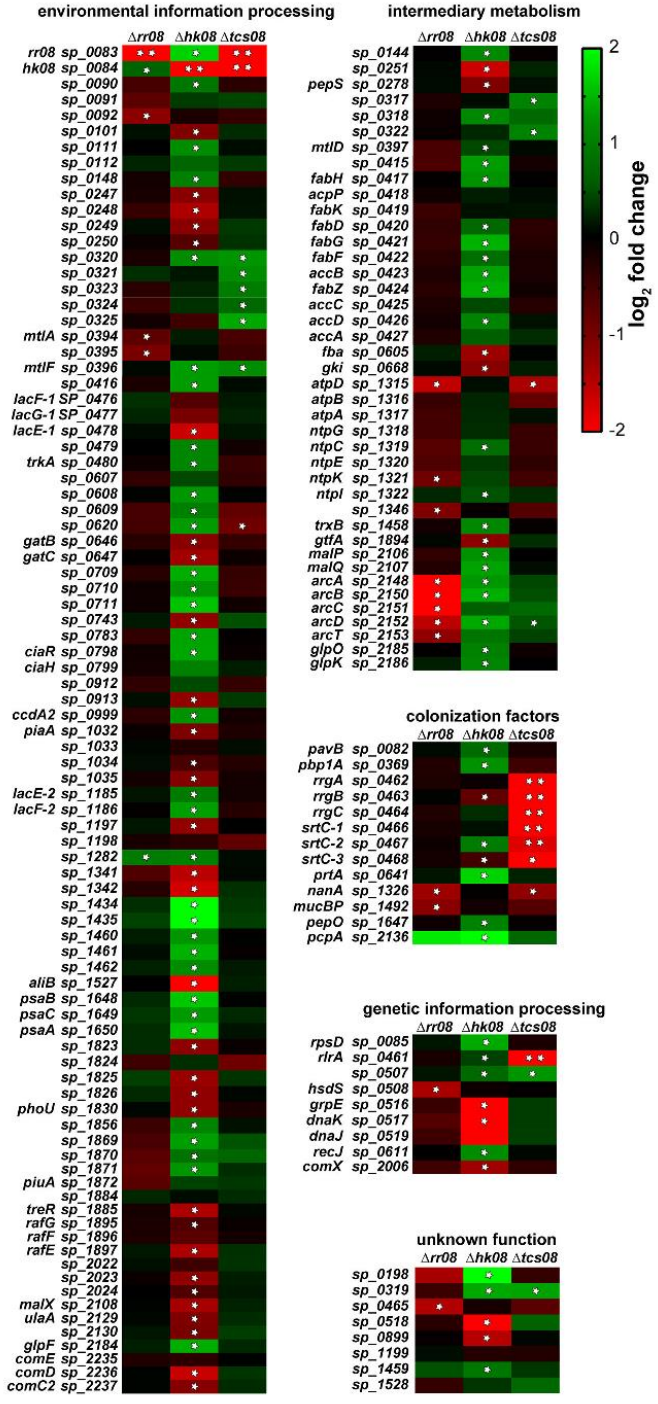
environmental information processing
Δrr08 Δhk08 Δtcs08
rr08 sp_0083
hk08 sp_0084
sp_0090
sp_0091
sp_0092
sp_0101
sp_0111
sp_0112
sp_0148
sp_0247
sp_0248
sp_0249
sp_0250
sp_0320
sp_0321
sp_0323
sp_0324
sp_0325
mtlA sp_0394
sp_0395
mtlF sp_0396
sp_0416
lacF-1 SP_0476
lacG-1 SP_0477
lacE-1 sp_0478
sp_0479
trkA sp_0480
sp_0607
sp_0608
sp_0609
sp_0620
gatB sp_0646
gatC sp_0647
sp_0709
sp_0710
sp_0711
sp_0743
sp_0783
ciaR sp_0798
ciaH sp_0799
sp_0912
sp_0913
ccdA2 sp_0999
piaA sp_1032
sp_1033
sp_1034
sp_1035
lacE-2 sp_1185
lacF-2 sp_1186
sp_1197
sp_1198
sp_1282
sp_1341
sp_1342
sp_1434
sp_1435
sp_1460
sp_1461
sp_1462
aliB sp_1527
psaB sp_1648
psaC sp_1649
psaA sp_1650
sp_1823
sp_1824
sp_1825
sp_1826
phoU sp_1830
sp_1856
sp_1869
sp_1870
sp_1871
piuA sp_1872
sp_1884
treR sp_1885
rafG sp_1895
rafF sp_1896
rafE sp_1897
sp_2022
sp_2023
sp_2024
malX sp_2108
ulaA sp_2129
sp_2130
glpF sp_2184
comE sp_2235
comD sp_2236
comC2 sp_2237
intermediary metabolism
Δrr08 Δhk08 Δtcs08
sp_0144
sp_0251
pepS sp_0278
sp_0317
sp_0318
sp_0322
mtlD sp_0397
sp_0415
fabH sp_0417
acpP sp_0418
fabK sp_0419
fabD sp_0420
fabG sp_0421
fabF sp_0422
accB sp_0423
fabZ sp_0424
accC sp_0425
accD sp_0426
accA sp_0427
fba sp_0605
gki sp_0668
atpD sp_1315
atpB sp_1316
atpA sp_1317
ntpG sp_1318
ntpC sp_1319
ntpE sp_1320
ntpK sp_1321
ntpI sp_1322
sp_1346
trxB sp_1458
gtfA sp_1894
malP sp_2106
malQ sp_2107
arcA sp_2148
arcB sp_2150
arcC sp_2151
arcD sp_2152
arcT sp_2153
glpO sp_2185
glpK sp_2186
2
1
0
-1
-2
log2 fold change
colonization factors
Δrr08 Δhk08 Δtcs08
pavB sp_0082
pbp1A sp_0369
rrgA sp_0462
rrgB sp_0463
rrgC sp_0464
srtC-1 sp_0466
srtC-2 sp_0467
srtC-3 sp_0468
prtA sp_0641
nanA sp_1326
mucBP sp_1492
pepO sp_1647
pcpA sp_2136
genetic information processing
Δrr08 Δhk08 Δtcs08
rpsD sp_0085
rlrA sp_0461
sp_0507
hsdS sp_0508
grpE sp_0516
dnaK sp_0517
dnaJ sp_0519
recJ sp_0611
comX sp_2006
unknown function
Δrr08 Δhk08 Δtcs08
sp_0198
sp_0319
sp_0465
sp_0518
sp_0899
sp_1199
sp_1459
sp_1528

as significantly influenced by TCS08. Genes like *rlrA*, *dnaK*, and *grpE* are mostly involved in DNA and protein processing. Remarkably, in the absence of both components of TCS08 a significant downregulation is seen for the positive regulator *rlrA*, involved in the expression of PI-1. (v) The last category involves genes with an unknown function (UF). Here, 8 genes out of the 159 identified genes presented changes in their expression in the microarray, including hypothetical lipoproteins like SP_0198 and SP_0899 (29). These proteins contain conserved lipobox motifs and are therefore also thought to be surface exposed and might be involved in unknown fitness-related processes.

TCS08 is involved in the regulation of metabolic functions of *S. pneumoniae*. Results obtained by the microarray screening suggested a regulatory effect of TCS08 in the expression of genes involved in the uptake and transport of essential nutrients for *S. pneumoniae* TIGR4, such as arginine and manganese (Fig. 2; Table S1). These metabolites/ions are transported into the cell via specific ABC transporter systems. Of particular interest is the arginine deiminase system (ADS), which is essential for arginine uptake and utilization in pneumococci. All genes of the *arcABCDT* operon displayed important changes in their expression in the absence of the RR or HK08. Interestingly, these changes were not consistent in the two mutants, as the Δ*rr08* strain displayed a significant downregulation of this operon while the *hk08* mutant showed an upregulation (Fig. 2; Table S1). Additionally, no significant effects were observed for the *arc* operon in the Δ*tcs08* mutant. Analysis by real-time PCR (qPCR) partially confirmed the initial findings on the expression of the *arc* operon and demonstrated a strain-dependent effect for these genes. Indeed, the expression of the arginine deiminase gene *arcA* was only significantly increased in the Δ*rr08* and Δ*hk08* mutants in TIGR4 (Fig. 3A), whereas no differences were found in D39 (Fig. 3B). Furthermore, the arginine-ornithine antiporter *arcD* (30, 31) presented a similar expression as *arcA* in TIGR4 and D39 TCS08 mutants; however, the changes were not significant (Fig. 3). An additional key player in the pneumococcal fitness is the *psa* operon. This operon plays a role in the uptake of manganese and in the response to oxidative stress in the pneumococci. The analysis by microarray showed a significant increase of 2-fold in the expression of the *psa* operon for the *hk08* mutant in the TIGR4 strain (Fig. 2; Table S1). Conversely, no statistically important effects were observed in the *psa* operon in the *rr08* and *tcs08* mutants in the same strain (Fig. 2; Table S1). Validation of the microarray data by qPCR discovered a significant increase in the expression of *psaA* in the *rr08* mutant of D39. Surprisingly, the microarray data for the *psa* operon could not be confirmed by qPCR in TIGR4 (Fig. 3A).

Immunoblot analyses of pneumococci cultured in CDM were carried out to elucidate the effect of TCS08 components on the protein levels of selected candidates from D39 and TIGR4 based on gene expression data (Fig. 4). For the ADS, the arginine deiminase ArcA was selected as a representative protein. Analysis of protein abundance of ArcA in D39 revealed a significant increase in the Δ*hk08* mutant (Fig. 4B). In contrast, the loss of HK08 in TIGR4 resulted in a 2-fold-lower abundance of ArcA (Fig. 4A). The remaining *rr08* and *tcs08* mutants in both strains showed nonsignificant effects in the protein levels of ArcA. Interestingly, the results obtained for the ArcA protein in the absence of HK08 in both strains did not reflect the transcriptome (2-fold upregulation) or qPCR results. In the case of PsaA, the immunoblot analysis confirmed a significantly higher expression of 1.5-fold in the TIGR4 *hk08* mutant (Fig. 4A), correlating with the microarray data (Fig. 2).

In a complementary approach, the surface abundance of PsaA was examined by a flow cytometric approach (Fig. 5). For D39, a nonsignificant increase in the surface

FIG 2 Gene expression heat map for TIGR4 wild type and isogenic *tcs08* mutants. Output of results for the microarray study using *S. pneumoniae* TIGR4 Δ*cps* and its corresponding *tcs08* mutants. The heat map indicates alterations in gene expression, where upregulation is indicated by green and downregulation is indicated by red. Single white stars indicate *P* values of <0.05, and double white stars indicate *q* values of <0.05, where *q* indicates the false discovery rate statistic result.

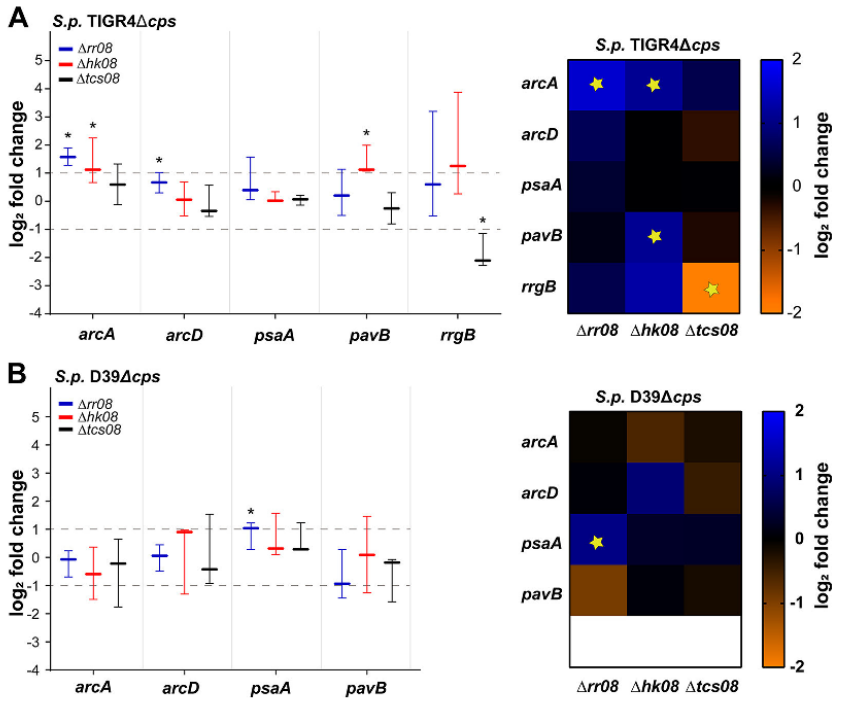

FIG 3 Impact of pneumococcal TCS08 on gene expression by real-time PCR. Differential gene expression in *tcs08* mutants (Δ*rr08*, Δ*hk08*, and Δ*tcs08*) analyzed by qPCR after pneumococcal cultivation in CDM. *S. pneumoniae* TIGR4 Δ*cps* (A) and D39 Δ*cps* (B). Specific primers for the ribosomal protein S16 (*sp_0775*) were used as normalization control. Data indicate the $\Delta\Delta C_T$ of the fold change in the graph bar and heat map for the different *tcs08* mutants from three independent experiments. D39 Δ*cps* or TIGR4 Δ*cps* wild type was normalized to 0 and used for statistical analysis with the unpaired Student *t* test. Asterisks and yellow stars indicate *P* values of <0.05 in both the graph and the heat map for $n = 3$, respectively. Data are presented as boxes and whiskers with the median and 95% confidence intervals.

abundance of PsaA was measured in mutants lacking both TCS08 components. The modest effect of TCS08 on PsaA observed for surface abundance correlates with the immunoblot analysis (Fig. 4 and 5). Similarly, the increased surface abundance of PsaA in TIGR4 mutants lacking HK08 (Fig. 5) correlated with the immunoblot and microarray analysis.

TCS08 regulates pneumococcal colonization factors. The adhesins PavB and PI-1 were shown to be regulated in the TIGR4 strain by our initial microarray analysis (Fig. 2; Table S1) and confirmed by qPCR. Interestingly, *pavB* is a gene upstream of the 5′ region of the *tcs08* operon presenting properties of a sortase-anchored adhesin. PavB has been shown to interact with various extracellular matrix (ECM) proteins and probably also directly with a cellular receptor (32, 33), thereby linking pneumococci with host cells. Similarly, PI-1 is composed of the proteins RrgA, RrgB, and RrgC, with RrgB functioning as the backbone (34). The genes of *pilus-1* are part of the RD4 or *rlrA* pathogenicity island and belong to the accessory genome of some pneumococcal strains and clinical isolates, including TIGR4 (35, 36). Both PI-1 and *pavB* genes presented significant changes in gene expression with an upregulation in mutants lacking HK08 by at least 2-fold (Fig. 3). Moreover, the absence of both components of TCS08 leads to a significantly reduced expression of *pilus-1* in TIGR4, while no significant effect was seen for *pavB* in either the *rr08* or *tcs08* mutant in either the D39 or TIGR4 strain at the gene expression level.

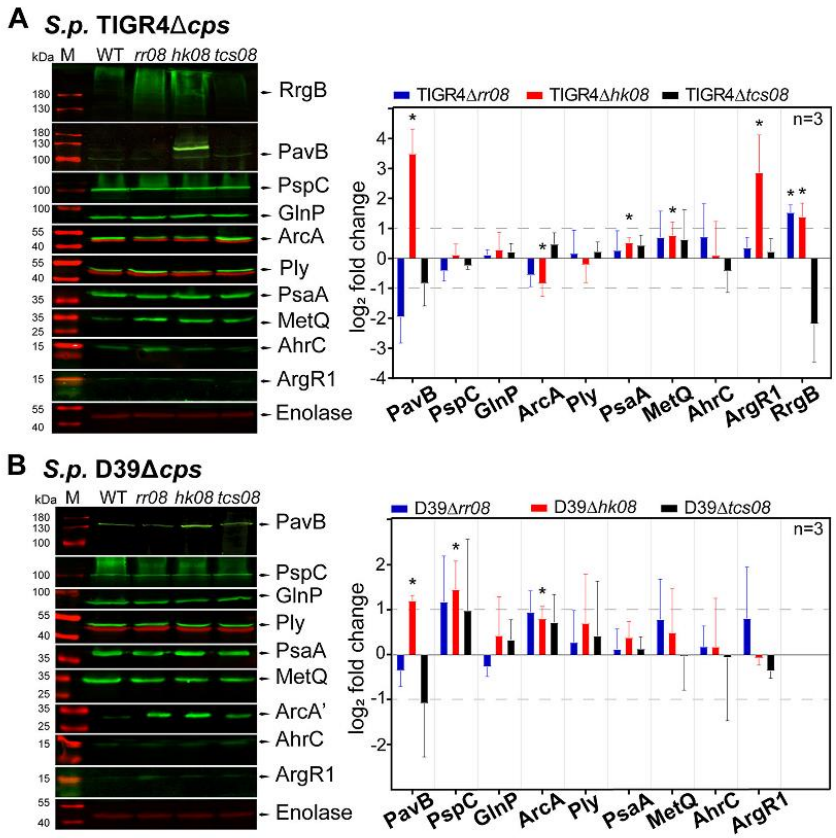

FIG 4 Protein expression levels in pneumococcal *tcs08*-deficient strains. Quantification of different proteins in pneumococci by immunoblotting in *S. pneumoniae* TIGR4 Δ*cps* (A) and D39 Δ*cps* (B) and their corresponding isogenic *tcs08* mutants. The unpaired Student *t* test was applied, and the enolase of D39 Δ*cps* or TIGR4 Δ*cps* was used as reference. *, *P* values < 0.05; *n* = number of biological replicates. The horizontal segmented lines indicate the 2-fold change, and the error bars indicate the standard deviation. M, molecular mass markers.

On the protein level, quantifications were performed by immunoblotting (Fig. 4) and the levels of surface abundance were evaluated by flow cytometry (Fig. 5). For PI-1, the backbone protein RrgB was used as a representative. Immunoblot analysis and flow cytometry indicated higher protein levels and surface abundance, respectively, in mutants lacking HK08 and RR08. These results are in line with gene expression analyses. Importantly, the lower protein levels of RrgB in the absence of both TCS08 components correlated with the downregulation measured by qPCR and transcriptomics (Fig. 4A and 5A). For PavB, immunoblot assays revealed a high impact on PavB amounts in the different mutants with a 2-fold increase in the absence of HK08 in D39 and even 10-fold in TIGR4. In contrast, the lack of either RR08 or both components of TCS08 procured a 2-fold decrease of PavB in both D39 and TIGR4 (Fig. 4). Similarly, the surface abundance of PavB was higher in the *hk08* mutant and lower in the *rr08* and *tcs08* mutants as indicated by flow cytometry (Fig. 5). Importantly, these data fit with the gene expression analysis of the mutants by microarrays.

Furthermore, an *in silico* comparison of a 300-bp upstream region of the pneumococcal gene *pavB* and the staphylococcal *saeP* and *fnbA* genes revealed the presence of a SaeR-like binding motif for *pavB* (Fig. 6). The SaeR-like binding motif is 76 bp

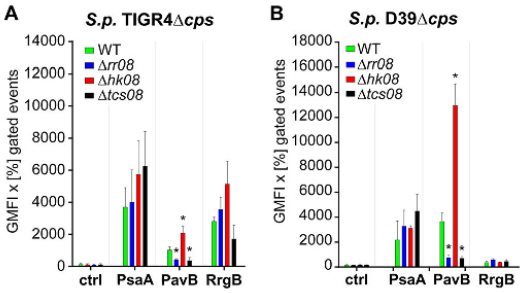

FIG 5 Impact of HK08 and RR08 on the abundance of pneumococcal surface proteins. The surface expression and abundance of surface proteins were analyzed by flow cytometry in *S. pneumoniae* TIGR4 Δ*cps* (A) and D39 Δ*cps* (B) strains and their corresponding isogenic *tcs08* mutants, all cultured in CDM. The unpaired Student *t* test was applied for the statistics, and D39 Δ*cps* or TIGR4 Δ*cps* was used as a reference accordingly. *, *P* value < 0.05 for $n = 3$. Error bars indicate the standard deviation.

upstream of the starting ATG of *pavB* and within its putative promoter region. In conclusion, TCS08 interferes with the regulation of adhesins and may therefore also have an impact on colonization.

TCS08 modulation of lung infections and sepsis is strain dependent. To assess the impact of TCS08 or its individual components on pneumococcal colonization, lung infection, or sepsis, CD-1 mice were intranasally or intraperitoneally infected with bioluminescent wild-type strains (D39 or TIGR4) and corresponding isogenic mutants. In D39, intranasal infections with mutants lacking either HK08 or both components of TCS08 increased the survival time of mice; thus, the mutants were attenuated and represent a less virulent phenotype (Fig. 7B and F). The *rr08* mutant of D39 showed no differences in developing lung infections (Fig. 7B and F). In the sepsis model, no differences between the wild type of D39 and its isogenic mutants were observed (Fig. 7H). Strikingly and in contrast to D39 infections, the acute pneumonia and sepsis infection models indicated a higher virulence potential of TIGR4 bacteria lacking HK08. In contrast, the loss of RR08 in the TIGR4 genetic background resulted in a significantly attenuated phenotype, leading to the survival of 50% of the infected mice. No differences were observed when both components of TCS08 were absent in TIGR4 (Fig. 7A, E, and G).

The impact of TCS08 on colonization and lung infection was further investigated in the competitive mouse infection assay using the intranasal infection route. Interestingly, the wild-type TIGR4 has a lower number of recovered bacteria than the *rr08* mutant, while having a significantly higher number in the nasopharynx or bronchoalveolar lavage fluid compared to the *hk08* mutant 24 and 48 h postinfection (Fig. S2). Taken together, it becomes clear that TCS08 and its individual components are essential for a balanced homeostasis, thereby maintaining pneumococcal fitness and robustness.

DISCUSSION

The role of a subset of pneumococcal TCS in competence, physiology, and virulence has been characterized, providing an initial understanding of their specific regulons (10, 12, 37). As such, TCS08 of *S. pneumoniae* has been initially identified and suggested to be important for virulence (11, 12, 37). Nevertheless, the mechanism underlying its effect on pathophysiological processes has not been elucidated before. A valid approach to estimate the regulons and effects of a TCS is to analyze the protein structures of its components. Unfortunately, only the structure of the pneumococcal RR11 and RR14 has been solved experimentally (38, 39). Nevertheless, it is possible to estimate the likely structural disposition of the remaining components by using bioinformatic tools. As such, according to the information obtained by the database SMART (Simpler

***Streptococcus pneumoniae pavB* and *Staphylococcus aureus saeP* upstream regions**

```
TIGR4    sp0082_pavB    GAACAGCGGA GCATCTGGCA -----AAAAA ACGCCAATTG TGGACCTATA TTCAGCAGAA
Newman   nwmn0677_saeP  CAAAAGGTTT ATAAATTTTA ATACCAAAAC TATTAAACAC TTCTGATATT CTTAGTTCAA
                         ** **        *  *   *       ****        **    *      ***   * **   **
                        \-314 bp
TIGR4    sp0082_pavB    AAATCCAGAA GTCTTTCAGG CTATTCGTAA GACCATGTTG AGCCGT---- TTGACCAAAC
Newman   nwmn0677_saeP  AATATCAGAA GTGTTTTATA GTGTTATCTA GTTCAGATAA ATATTTCCTT ACTTAAAAAA
                         **   ***** ** *** *    * **    * *  **  *   *    *           ***
                        \-254 bp
TIGR4    sp0082_pavB    ATTCTGTCTT GCCAGATCGC AAACTGTCCA ATGTCGTCTA TCAAATCACC AAATCTGTTT
Newman   nwmn0677_saeP  ACGCCCTCCT CTTATTTTGA CCCCTA---- -----TTTAT TTAAATCAGA CAATTATTTT
                         *   *   ** *    *  * *     **          *    * ******    ***   ***
                        \-194 bp
TIGR4    sp0082_pavB    ATGGATTTAA T-----TAAT ATAAGTGTTT TATAAGAGGG ATTTAAGAAA AATTTTAACT
Newman   nwmn0677_saeP  CATTTTCAAA TTATTCTTTC TTCAATATTA GTTAAGCGAT ATTTAAACGA AGTTAAGAAT
                           *  ** *      *     * * * **    **** *   ******   * * **   * *
                        \-134 bp
TIGR4    sp0082_pavB    TTTTCTTAGT CCTTTTTAAT TTCAGGAGAT TATACTAGAG TCATCAAATA AAGAAAGACT
Newman   nwmn0677_saeP  TAGTTAATGG CATATTATTT GCCTTCATTT TAAACTTAAC TTATCAAATT GAAGAAATGA
                         *   *     *  * * **   *   *   *  * ** ***  *  * *******   *  **
                        \-74 bp
TIGR4    sp0082_pavB    CTAAGGAGAA TCCT ATG
Newman   nwmn0677_saeP  GGAGTTAGC- ---- ATG
                           *    **
                        \-14 bp
45,45% identity
```

***Streptococcus pneumoniae pavB* and *Staphylococcus aureus fnbA* upstream regions**

```
TIGR4    sp0082_pavB    -GAACAGCGG AGCATCTGGC AAAAAAACGC CAATTGTGGA CCTATATTCA GCAGAAAAAT
Newman   nwmn2399_fnbA  TGTACAGGCG ATAATTATGA AACGTTTAGT ATATTGTTT- ------TAAA TTAGATAATG
                          * ****  * *  **   *  **       *    *****          *  *   *** **
                        \-341 bp
TIGR4    sp0082_pavB    CCAGAAGT-C TTTCAGGCTA TTCGTAAGAC CATGTTGAGC CGTTTGACCA AACATTCTGT
Newman   nwmn2399_fnbA  ATTAATTTAA TTTAAAAAAA TAAGTATAAA AAATACAAGC CTTGTGTGAC AAGGGTTTC-
                           *  *    *** *    * *  ***  *   *     *** * * **     **   * *
                        \-281 bp
TIGR4    sp0082_pavB    CTTGCCAGAT CGCAAACTGT CCAATGTCGT CTATCAAATC ACCAAATCTG TTTATGGATT
Newman   nwmn2399_fnbA  ---------- ---------- -TGATGACTT GAA------- -----TACAA TTTATAGGTA
                                              *** * *   *          *    ***** * *
                        \-221 bp
TIGR4    sp0082_pavB    TAATT----- AATATAAGTG TTTTATAAGA GGGATTTAAG AAAAATTTTA ACTTTTTCTT
Newman   nwmn2399_fnbA  TATTTCAAAT AATAAAATTA TCAATTAACA TAAAATTAAT GACAATCTTA ACTTTTCATT
                         ** **      **** ** *  *    *** *    * ****   * *** *** ******  **
                        \-161 bp
TIGR4    sp0082_pavB    AGTCCTTTTT AATTTCAGGA GATTA----- ----TACTAG AGTCATCAAA TA--------
Newman   nwmn2399_fnbA  AACTCGCTTT TTTGTATTGC TTTTAAAAAC CGAACAATAT AGACTTGCAT TTATTAAGTT
                         *   *  *** *  *  *   ***      * **  ** * *  *  *
                        \-101 bp
TIGR4    sp0082_pavB    ---------A A----GAAAG ACTCTAAGGA GA-ATCCT-- - ATG
Newman   nwmn2399_fnbA  TAAAAAATTA ATGAATTTTG CATTTAAAGG GAGATATTAT A GTG
                                 * *         *   * *** *  ** **  *
                        \-41 bp
50,97 % identity
```

FIG 6 Sequence comparison of upstream regions from the genes *pavB*, *saeP*, and *fnbA*. An *in silico* alignment was performed using 300 bp upstream of the pneumococcal *pavB* and the staphylococcal *saeP* and *fbnA* genes. The arrows indicate the distance upstream from the starting ATG. The bold letters in the gray boxes highlight the SaeR binding motifs in all sequences. The alignment was done using the Clustal Omega tool from the EMBL-EBI. The DNA sequences were retrieved from the Kyoto Encyclopedia for Genes and Genomes (KEGG). Asterisks indicate conserved base pairs.

Modular Architecture Research Tool, http://smart.embl-heidelberg.de/), the pneumococcal histidine kinase 08 can be classified as an intermembrane histidine kinase (IM-HK) due to its short extracellular loop. Members of this class of HKs are known to respond to membrane disturbances (26). Additionally, RR08 is classified as a member of the OmpR class of response regulators, known to bind to short tandem repeats of DNA (40). Both components share high homology and similar sequence features with the HK SaeS and RR SaeR from *S. aureus* (Fig. S4) (24). Altogether, it is plausible to hypothesize that the regulatory behavior of the pneumococcal TCS08 is similar to the global virulence regulatory system SaeRS of *Staphylococcus aureus*.

The staphylococcal SaeRS TCS is known to be essential for the virulence of *S. aureus* by regulating approximately 20 virulence genes such as the α-hemolysin gene (*hla*), the fibronectin binding protein A gene (*fbnA*), and its own SaePQRS operon, among others

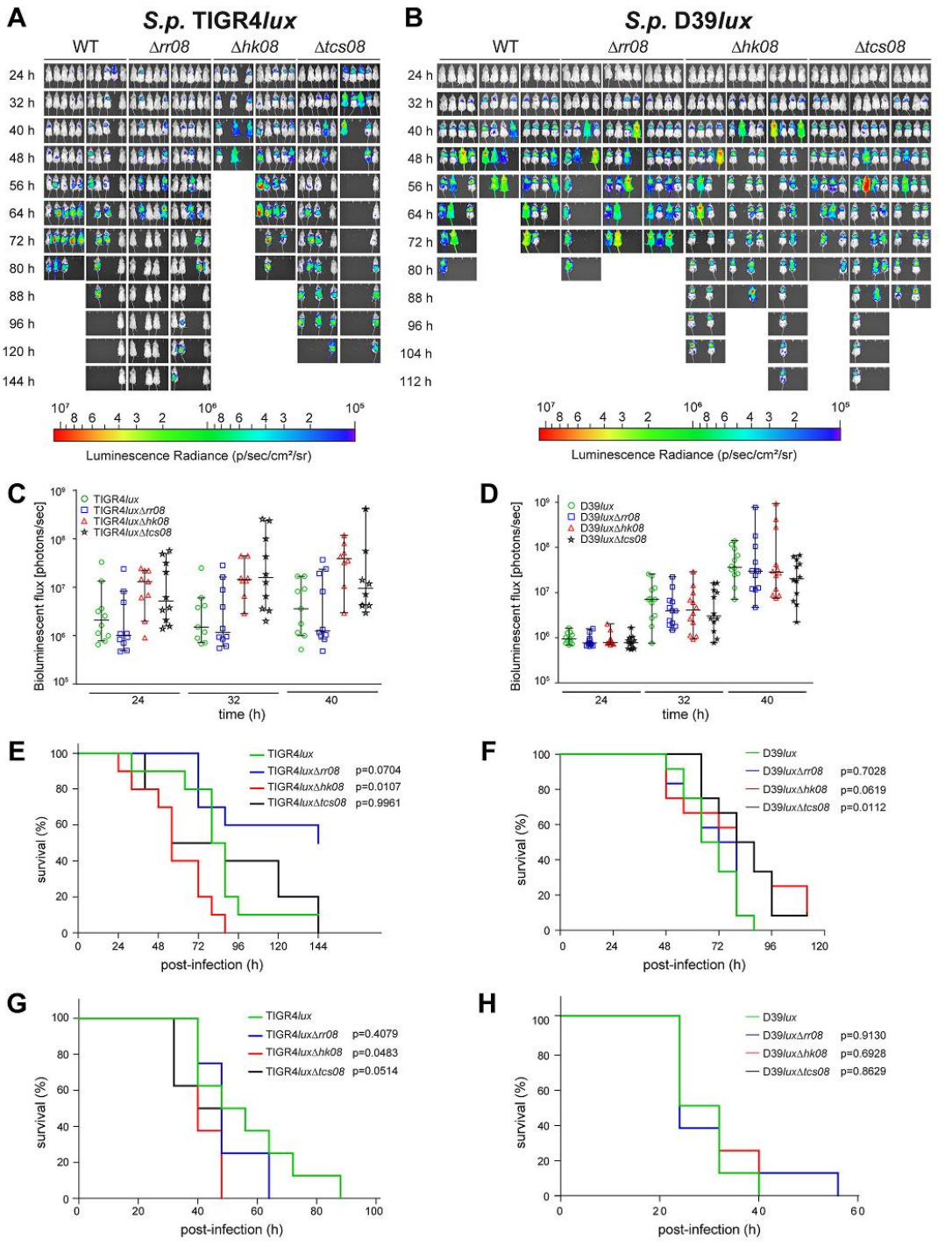
A
S.p. TIGR4lux
WT
Δrr08
Δhk08
Δtcs08
24 h
32 h
40 h
48 h
56 h
64 h
72 h
80 h
88 h
96 h
120 h
144 h
Luminescence Radiance (p/sec/cm²/sr)
B
S.p. D39lux
WT
Δrr08
Δhk08
Δtcs08
24 h
32 h
40 h
48 h
56 h
64 h
72 h
80 h
88 h
96 h
104 h
112 h
Luminescence Radiance (p/sec/cm²/sr)
C
Bioluminescent flux [photons/sec]
TIGR4lux
TIGR4luxΔrr08
TIGR4luxΔhk08
TIGR4luxΔtcs08
time (h)
D
Bioluminescent flux [photons/sec]
D39lux
D39luxΔrr08
D39luxΔhk08
D39luxΔtcs08
time (h)
E
survival (%)
post-infection (h)
TIGR4lux
TIGR4luxΔrr08 p=0.0704
TIGR4luxΔhk08 p=0.0107
TIGR4luxΔtcs08 p=0.9961
F
survival (%)
post-infection (h)
D39lux
D39luxΔrr08 p=0.7028
D39luxΔhk08 p=0.0619
D39luxΔtcs08 p=0.0112
G
survival (%)
post-infection (h)
TIGR4lux
TIGR4luxΔrr08 p=0.4079
TIGR4luxΔhk08 p=0.0483
TIGR4luxΔtcs08 p=0.0514
H
survival (%)
post-infection (h)
D39lux
D39luxΔrr08 p=0.9130
D39luxΔhk08 p=0.6928
D39luxΔtcs08 p=0.8629

(27). However, there are only a few reports regarding the control of staphylococcal fitness by the SaeRS system. One study investigated a negative regulatory effect of fatty acids on the phosphorylation of SaeS and the activation of the virulence factors controlled by SaeR (41). Our initial approach to investigate the regulatory roles of the pneumococcal TCS08 by transcriptomics discovered five main gene categories influenced by this TCS. Interestingly, we observed the most predominant regulation for genes participating in environmental information processing and intermediary metabolism (Fig. 2; Table S1). The genes grouped in these two categories are annotated as part of ABC transporters, phosphotransferase systems, and lipid biosynthesis and were found to be localized all along the pneumococcal genome (Fig. S3). The genes found to be regulated by TCS08 share an important feature, namely, their localization and/or activity in the pneumococcal membrane. Additionally, several of the different PTS and ABC transporters regulated by TCS08 are involved in the fitness and virulence of this pathogen. Hence, the effect of TCS08 is more pronounced in the colonization phase of the pneumococcal life cycle. This is, for example, the case for the neuraminidase NanA, lipoprotein PsaA, and arginine deiminase system (ADS) (31, 42–44). Moreover, the observed regulation of the complete *fab* operon encoding enzymes for fatty acid biosynthesis creates an important connection between TCS08 and sensing and responding to membrane instability (19, 45). The transporter systems affected by TCS08 are mostly essential during colonization under nutrient-limiting conditions but also in the initial stages of the diseases to take up nutrients and ensure pneumococcal fitness (Fig. 2 and 3) (46, 47).

In addition to the gene expression analysis of *tcs08* mutants, we further investigated the changes on the protein level for selected candidate proteins. Our immunoblot analyses demonstrated differences for PsaA and the arginine deiminase ArcA. Remarkably, compared to the respective wild-type strains ArcA occurred at higher protein levels in all mutants of D39 and the TIGR4 mutant lacking both HK08 and RR08 (2-fold), while ArcA had lower protein levels in the TIGR4 mutants lacking either HK08 or RR08 (2-fold). However, only the opposite effect of deletion of *hk08* on the ArcA level was statistically significant. This is a further proof that the ADS in D39 and TIGR4 is differentially regulated, as has been shown before for the stand-alone regulator ArgR2. There, the *arc* operon showed a constitutive expression in D39, while in TIGR4 gene expression was upregulated by ArgR2 (31).

It is essential that pneumococci activate their metabolic inventory when colonizing their host to ensure adaptation and fitness. As such, our results point to a role of TCS08 in the fine-tuning of colonization and metabolic homeostasis as exemplified by the level of change in the expression of *pavB* and the genes of the *pilus-1*, *fab*, and *arc* operons.

pavB belongs to a group of genes regulated by TCS08 which are strongly involved in colonization by its interactions with host proteins (32, 33). This group of genes codes mostly for surface-exposed proteins associated with peptidoglycan metabolism and adherence to host cells. These genes are found grouped clockwise mostly in the first quarter of the pneumococcal genome, and transcription and replication proceed into the same direction (Fig. S3). Interestingly, the regulation of the adhesin PI-1 and PavB proteins by the pneumococcal TCS08 illustrates the high homology between the staphylococcal SaeRS and pneumococcal TCS08. Differences in gene expression of the PI-1 component genes were detected by microarray analysis (Fig. 2) and qPCR (Fig. 3) in the TIGR4 TCS08 mutants. Similarly, protein levels were also affected in the TCS08 mutants, especially in the absence of both components of TCS08, in which strong

FIG 7 Influence of the TCS08 components on pneumococcal pathogenesis. CD-1 mice were used in the acute pneumonia model to determine the impact of the TCS08 components on virulence. Infection doses of 1×10^7 and 7×10^7 bacteria were applied for *S. pneumoniae* D39 and TIGR4, respectively. (A and B) Bioluminescent (*lux*) strains were used to monitor the progression of the disease *in vivo*. The results are shown as photon flux change (C and D) and analyzed by a Kaplan-Meier plot (E and F). For the sepsis model (G and H), 1×10^3 bacteria were used as the infection dose for both wild-type strains and corresponding mutants. A log rank test was used for the statistical test with a group size of $n = 12$ (D39) or $n = 10$ (TIGR4), and the error bars indicate the standard deviations.

downregulation was detected (Fig. 4A and 5A). Our findings correlate to some extent with a previous study showing the regulation of PI-1 by the pneumococcal TCS08 (28). For the adhesin PavB, inconsistent results were obtained for gene expression and protein abundance in the D39 strain. A minor but significant differential *pavB* gene expression was measured by microarray analysis and qPCR for TIGR4 (Fig. 2 and 3). In contrast, PavB protein levels were significantly affected in all mutants, with a 2-fold increase in the absence of HK08 and a decrease in PavB in mutants lacking either RR08 or both components of TCS08 as shown by immunoblotting and flow cytometry (Fig. 4 and 5).

The staphylococcal fibronectin binding protein FbnA is weakly regulated by the SaeRS system of *S. aureus* (48), which in pneumococci correlates with the link found between TCS08 and PavB/PI-1. A direct repeat sequence ($TTTAAN_7TTTAA$), similar to the imperfect SaeR binding site ($GTTAAN_6TTTAA$) (25), can be found directly upstream of *pavB* (Fig. 6), suggesting that RR08 binds directly to the *pavB* promoter region. A strong hint for *pavB* gene regulation by TCS08 is the higher abundance of PavB in the absence of HK08. Surprisingly, a conserved repeat sequence, $TTTAAN_{14}GTTAA$, was found close to the *rlrA* operon and could indicate an indirect effect of TCS08 in the regulation of *pilus-1* via its positive regulator RlrA (Table S5). The *in silico* search for SaeR-like binding motifs among different TCS08-regulated genes indicated the presence of a variation of this binding sequence for the cellobiose and *arc* operons, while it was absent for the *psa* operon (Table S5). All of the genes carried in these operons have been reported to be under the regulation of CcpA-dependent stand-alone regulators (31, 45, 49, 50). Additionally, the *psa* operon has been also shown to be under the regulation of PsaR and TCS04 (PnpRS), which might be interplaying with TCS08 (51, 52). This suggests either a cooperative role or a collateral effect of TCS08, and we hypothesize that TCS08 acts as a membrane stability sensor system.

The staphylococcal SaeRS was further reported to regulate proteases and be involved in biofilm formation. Our microarray analysis showed an effect on the expression for genes encoding a putative protease domain (Fig. 2 and 3) such as the gene (*sp_0144*) possessing an Abi (abortive infective domain) with unknown function in pneumococci. Bioinformatic analysis revealed that pneumococcal *sp_0144* is highly homologous to *spdABC* genes of *S. aureus* Newman, featuring an Abi domain. Interestingly, the SpdA, SpdB, and SpdC proteins have been reported to be involved in the deposition and surface abundance of sortase-anchored proteins in *S. aureus* (53). The gene expression of *sp_0144* (TIGR4) presented an upregulation in the *hk08* mutant in TIGR4. It cannot be ruled out that the changes in SP_0144 also contribute to the protein abundance demonstrated for PavB or PI-1 when the strains lack components of TCS08 (Fig. 3). In turn, changes in surface abundance of colonization factors will interfere with the pneumococcal virulence and/or immune evasion. However, this hypothesis was not evaluated in this study and needs experimental proof in a follow-up study.

Nasopharyngeal colonization by pneumococci requires adherence to host cells and generates a foothold in the human host. Hence, the regulation of adhesins and ECM binding proteins like PavB or PI-1 represents a successful strategy of the pathogen to adapt to this host compartment. Similarly, the sensing of human neutrophil peptides and membrane disruption molecules is also essential to ensure a successful colonization and immune escape phenotype. Our *in vivo* studies using pneumonia and sepsis murine models confirmed the contribution of the pneumococcal TCS08 not only in colonization but also virulence (Fig. 7). However, the effect is strain dependent, highlighting the role and network of different stand-alone regulators and other regulatory systems of pneumococci in the overall regulation of pneumococcal fitness and pathophysiology. Such strain-dependent effects have been also shown for additional pneumococcal TCS such as PnpRS and TCS09 (ZmpRS) (51, 54). Remarkably, a more virulent phenotype was observed for the TIGR4 mutant lacking HK08, while the TIGR4 mutant deficient for RR08 displayed a decrease in virulence in the pneumonia model (Fig. 7A). In D39, the opposite effect with a slight increase in survival was observed in the absence of HK08 in the same infection model (Fig. 7B). Additionally, the loss of

function of both TCS08 components in strain D39 resulted in a significant reduction in virulence in the pneumonia model (Fig. 7B). Strikingly, this D39 attenuation was not observed in the sepsis model. Similarly, the TIGR4 *rr08* mutant was also as virulent as the wild type, despite being attenuated in the pneumonia model (Fig. 7G and H). In contrast, the TIGR4 Δ*hk08* mutant was significantly more virulent than the wild type in the sepsis model (Fig. 7G). As such, our results suggest that TCS08 is mostly involved in bacterial fitness and regulation of adhesins required for a successful colonization. Such striking differences between two representative pneumococcal strains may reflect their different genomic background and the overall versatility of pneumococci.

Interesting pathophenotypes were observed in competitive mouse infections, i.e., coinfections with the TIGR4 wild type and its *tcs08* isogenic mutants (Fig. S2). While the pneumonia model showed an avirulent phenotype in the absence of RR08, this mutant revealed a higher competitive index (CI) than its wild type in the coinfection assay in both the nasopharyngeal and bronchoalveolar lavage fluids, indicating lower numbers of the wild type in these host compartments. In addition, TIGR4 mutants lacking either HK08 or both components of TCS08 were apparently outcompeted by the wild type (Fig. S2) despite being more virulent than the wild type as indicated in the acute pneumonia model. A plausible explanation for this phenomenon might be that the TIGR4 mutant lacking HK08 is rapidly progressing from the nasopharynx and lungs into the blood and, hence, low numbers are present in the nasopharynx and lavage. Similarly, the absence of RR08 impairs progressing into the blood, and thus, higher numbers of the *rr08* mutant are found in the nasopharynx. Indeed, this pneumococcal behavior after nasopharyngeal infection can also be visualized in the bioluminescent images of the acute pneumonia model, in which the mice infected with the strain lacking HK08 rapidly developed pneumonia and sepsis (Fig. 7A).

It is also important to mention here the mild impact of TCS08 on gene expression alterations. This suggests a role for TCS08 as a fine-tuning and signal modulation system, which is dependent on additional regulators. This hypothesis is supported by the altered gene expression of other TCS such as CiaRH and ComDE (Fig. 2; Table S1). Such low impact on gene expression might also facilitate an explanation for the predominant role of HK08 in controlling gene expression in pneumococci. A similar regulatory strategy has been reported for CiaRH. This system is able to control directly the expression of the protease HtrA and specific small RNAs, which in turn modulate indirectly the activity of ComDE and additional regulators (55, 56). We therefore hypothesize that the stimulus received by HK08 modulates the activity of RR08 and probably other regulators. In *Staphylococcus aureus*, the SaeRS system is also dependent on additional auxiliary proteins SaePQ (57). These proteins have been reported to interact with SaeS in order to control its phosphorylation state (57). Such systems have not yet been detected for the homologous TCS08 of the pneumococci. However, a more thorough biochemical analysis would be needed to generate a comprehensive regulatory map within pneumococcal regulators.

In conclusion, this study identified five main groups of genes influenced by the pneumococcal TCS08 in a strain-specific manner. A high number of these genes encode proteins involved in environmental signal processing, intermediary metabolism, colonization, or genetic information processing. Furthermore, most of the TCS08-regulated proteins are membrane bound and involved in nutrient transport as well as fatty acid biosynthesis. Additionally, surface-exposed PavB and PI-1 islet proteins involved in adhesion to host components were confirmed to be controlled by TCS08. Thus, HK08 of TCS08 is probably sensing small molecules entering the membrane compartment of pneumococci and adapts thereby the pneumococcus to the specific environmental conditions during colonization.

MATERIALS AND METHODS

Bacterial strains and growth conditions. *S. pneumoniae* and *Escherichia coli* strains used in this study are listed in Table S2 in the supplemental material. Pneumococcal wild type and isogenic *tcs08* deletion mutants were grown on Columbia blood agar plates (Oxoid) containing selection antibiotics (kanamycin [Km; 50 μg/ml] and erythromycin [5 μg/ml] or spectinomycin [Spec; 100 μg/ml]) using an

incubator at 37°C, 5% CO_2. In liquid cultures, pneumococci were cultivated in Todd-Hewitt broth (Roth) supplemented with 0.5% yeast extract (THY) or chemically defined medium (CDM; RPMI 1640 plus 2 mM L-glutamine medium [HyClone GE Healthcare Life Sciences] supplemented with 30.5 mM glucose, 0.65 mM uracil, 0.27 mM adenine, 1.1 mM glycine, 0.24 mM choline chloride, 1.7 mM $NaH_2PO_4 \cdot H_2O$, 3.8 mM Na_2HPO_4, and 27 mM $NaHCO_3$) using a water bath at 37°C. Recombinant *E. coli* strains were inoculated on lysogeny broth (LB) medium (Roth) in the presence of kanamycin (Km; 50 μg/ml) at 37°C using an orbital shaker.

Molecular techniques. The oligonucleotides and plasmid constructs used in this study are listed in Tables S3 and S4. The isolation of pneumococcal chromosomal DNA was achieved by using the standard phenol-chloroform extraction protocol. Briefly, *S. pneumoniae* strains were cultured in blood agar for 6 h, transferred to new blood agar plates with antibiotics, and grown for 10 h at 37°C and 5% CO_2. After inoculation in THY liquid medium and culture until reaching an optical density at 600 nm (OD_{600}) of 0.6 in a water bath at 37°C, the bacteria were harvested by centrifugation. The supernatant was discarded, and the bacterial pellet was resuspended in Tris-EDTA sodium (TES) buffer for lysis and processing. Finally, the DNA was extracted using phenol and phenol-chloroform-isoamyl alcohol (25:24:1), washed with 96% ethanol, and stored in Tris-EDTA (TE) buffer at −20°C for further use. The DNA regions needed for mutant generation and for protein production were amplified by PCR using the *Pfu* proofreading polymerase (Stratagene, La Jolla, CA, USA) and specific primers (Eurofins MWG Operon, Germany) according to the manufacturer's instructions. The annealing and extension temperatures were defined by the primers and length of the DNA inserts, respectively. The PCR products and the plasmids were purified using the Wizard SV gel and PCR cleanup system (Promega, USA). The final constructs were confirmed by sequencing (Eurofins MWG).

***S. pneumoniae* mutant generation.** For mutant generation in D39 and TIGR4 (Δ*cps* and bioluminescent [*lux*] strains), the insertion-deletion strategy was applied by amplifying 5′ and 3′ flanking regions of *rr08*, *hk08*, and the full *rr08-hk08* operon via PCR with specific primers. The genomic fragments were cloned in a pGEM-T Easy vector, transformed into *E. coli* DH5α, and further processed by inverse PCR using primers to delete the desired target gene and replacing it with either spectinomycin (*aad9*) or erythromycin (Erm^r) resistance gene cassettes. To achieve the deletion of the desired regions, the inverse PCR products and antibiotic cassettes were digested using specific restriction enzymes (Table S3). Finally, the deleted gene fragments encompass the following regions in each mutant: bp 29 to 953 in Δ*hk08*, bp 100 to 644 in Δ*rr08*, and bp 128 of *rr08* to bp 348 of *hk08* in Δ*tcs08*. Pneumococcal strains were transformed as described previously (31; see also ref. 60) using competence-stimulating peptide 1 (CSP1) (D39) or CSP2 (TIGR4) and cultivated in the presence of the appropriate antibiotics: kanamycin (50 μg/ml) and erythromycin (5 μg/ml) or spectinomycin (10 μg/ml). Briefly, *S. pneumoniae* strains were cultured on blood agar plates for 8 h, and a second passage was done for 10 h in an incubator at 37°C and 5% CO_2. Later, the strains were inoculated in THY with an initial OD_{600} of 0.05 and grown in a water bath until reaching a final OD_{600} of 0.1. The corresponding CSP was added and incubated at 37°C for 15 min, followed by the addition of the plasmid for transformation and a heat shock treatment of 10 min on ice and 30 min at 30°C. Bacteria were allowed to grow for 2 h at 37°C and plated on blood agar plates with the corresponding antibiotics. The resulting *S. pneumoniae* D39 and TIGR4 *tcs08*-deficient mutants were screened by colony PCR and real-time PCR (qPCR) (Fig. S1B). Stocks were generated in THY supplemented with 20% glycerol and stored at −80°C. Individual mutants for *rr08* (*sp_0083*) and *hk08* (*sp_0084*) as well as a Δ*tcs08* (*sp_0083* + *sp_0084*) mutant were confirmed by colony PCR.

Transcription analysis by microarrays. For the analysis of the gene expression by microarray, TIGR4 Δ*cps* and its isogenic *rr*, *hk*, and *tcs08* mutants were grown in CDM until reaching an OD_{600} of 0.35 to 0.4 in triplicate. Bacterial cultures were then added to previously prepared tubes containing frozen killing buffer (20 mM Tris-HCl [pH 7.5], 5 mM $MgCl_2$, 20 mM NaN_3) and centrifuged for 5 min at 10,000 × *g*. The supernatant was completely removed, and the tubes containing the pellets were immediately flash frozen in liquid nitrogen and stored at −80°C until the next step. The pellets were processed for total RNA extraction using acid phenol-chloroform and DNase treatment to remove genomic DNA. The products were purified using the RNA cleanup and concentration kit (Norgen Biotek Corp.), the quality of the RNA was determined with an Agilent 2100 Bioanalyzer, and the amount was quantified using a NanoDrop ND-1000 spectrophotometer (Peqlab). Five micrograms of total RNA was subjected to cDNA synthesis as described by Winter et al. (58). One hundred nanograms of Cy3-labeled cDNA was hybridized to the microarray according to Agilent's hybridization, washing, and scanning protocol (One-Color microarray-based gene expression analysis, version 6.9.1). Data were extracted and processed using the Feature Extraction software (version 11.5.1.1). Further data analysis was performed using the GeneSpring software (version 14.8). A Student *t* test with a *P* value of <0.05, followed by a Benjamini and Hochberg false discovery rate correction with a *q* value of <0.05, was performed for the analysis.

Gene expression analysis by qPCR. D39 and TIGR4 Δ*cps* strains and their corresponding *tcs08* mutants were grown in triplicate in CDM until early log phase and harvested for RNA isolation using the EURx GeneMatrix universal RNA purification kit (Roboklon). The RNA was checked for quality and contamination by PCR and agarose gel electrophoresis. Next, cDNA synthesis was carried out using the Superscript III reverse transcriptase (Thermo Fisher) and random hexamer primers (Bio-Rad). The obtained cDNA was checked by PCR using the same specific primers designed for the qPCR studies (Table S3). The cDNA was measured by a NanoDrop spectrophotometer and stored at −20°C until further tests. For the qPCR experiments, a StepOnePlus thermocycler (Applied Biosystems) with a Syber Green master mix (Bio-Rad) was used according to the instructions for relative quantification to determine the efficiency of the primers, and as such, a reference curve was designed to be run for every gene with 5 points and concentrations ranging from 100 ng/μl to 0.01 ng/μl with 1:10 dilution steps. The StepOne

software (version 2.3; Life Technologies) and Microsoft Office Excel 2016 software (Microsoft) were used for the analysis. The final results are plotted as the threshold cycle ($\Delta\Delta C_T$) ($\log_2$ of the fold change of expression), with the wild-type value set to 0 and compared to its respective *tcs08* mutants. For normalization, the gene encoding the ribosomal protein S16 (*sp_0775*) was used. The results are plotted as box-whisker plots showing the median and 95% confidence intervals and as a heat map.

Protein expression by immunoblotting. *S. pneumoniae* D39 and TIGR4 strains and their isogenic mutants were grown in CDM, harvested at mid-log phase, and resuspended in phosphate-buffered saline buffer (PBS). A total of 2×10^8 cells were loaded and run on a 12% SDS-PAGE gel and further transferred into a nitrocellulose membrane. Mouse polyclonal antibodies generated against different pneumococcal proteins and a secondary fluorescence-labeled IRDye 800CW goat anti-mouse IgG antibody (1:15,000) were used to detect their expression in the wild type (WT) and its isogenic mutants using the Odyssey CLx scanner (Li-Cor). Rabbit polyclonal antibody against enolase (1:25,000) and fluorescence-labeled IRDye 680RD goat anti-rabbit IgG antibody (1:15,000) were used as loading controls for normalization. The quantification was performed using Image Studio software (Li-Cor), and the data are presented as the $\log_2$ of the fold change with the wild-type value set to 0 and compared to each mutant after normalization against enolase. The Student *t* test was used for the statistical analysis.

Surface abundance of proteins analyzed by flow cytometry. The expression and abundance of different surface proteins were analyzed by flow cytometry. To detect the antigens, specific primary antibodies were used in conjunction with fluorescence-tagged secondary antibodies. In brief, nonencapsulated bacteria (D39 Δ*cps* and TIGR4 Δ*cps*) and the isogenic *tcs08* mutants were used after growth in CDM until reaching a final OD_{600} of 0.35 to 0.4. Bacteria were washed with 5 ml PBS and finally resuspended in 1 ml PBS supplemented with 0.5% fetal calf serum (FCS). The bacterial cell density was adjusted to 1×10^7 cells/ml in 1 ml of PBS-0.5% FCS-1% paraformaldehyde (PFA), loaded into a 96-well microtiter plate (U bottom), and incubated for 1 h at 4°C. The plates were centrifuged at 3,200 × *g* for 6 min, the supernatant was removed, and bacteria were incubated for 45 min at 4°C with antigen-specific mouse antibodies (31, 32, 59). Samples were washed twice with PBS-0.5% FCS and incubated with goat anti-mouse Alexa 488 (1/1,000 dilution) antibody for 45 min. Thereafter, the plate was washed twice with PBS-0.5% FCS and fixed using 1% PFA in the dark at 4°C overnight (o/n). Fluorescence of the bacteria was measured using a BD FACSCalibur machine equipped with log forward and log side scatter plots. The measurement of the data was conducted with CellQuestPro software 6.0. (BD Biosciences), collecting 50,000 events and a gated region. The results were analyzed using the freeware Flowing software version 2.5.1 (Turku Centre for Biotechnology, University of Turku, Finland) and presented as the geometric mean fluorescence intensity (GMFI) of the analyzed bacterial population by the percentage of labeled bacteria.

Impact of TCS08 in murine pneumonia and sepsis models. Bioluminescence-expressing *S. pneumoniae* D39 *lux* and TIGR4 *lux* and their isogenic mutants were grown in THY supplemented with 10% heat-inactivated fetal calf serum (FCS) until reaching an OD_{600} of 0.35 to 0.4 and harvested via centrifugation at 3,270 × *g* for 6 min. The bacteria were resuspended in PBS, and the CFU were adjusted for an infection dose of 1×10^7 CFU in 10 μl or 5×10^3 CFU in 200 μl per mouse for the pneumonia and sepsis models, respectively. The infection process for pneumonia was carried out as follows: 8- to 10-week-old 10 to 12 CD-1 outbred mice were arranged in groups of 5 or 4 animals per cage, respectively, and anesthetized with an intraperitoneal injection of 200 μl of ketamine 10% (mg/ml) and 2% xylazine (Rompun) (dose is determined according to the weight of the animals). The mice were held facing upward, and 20 μl of infection dose (10 μl bacteria plus 10 μl hyaluronidase [90 U]) was pipetted carefully in the nostrils. Mice were allowed to inhale the drops and rest facing upward until the anesthesia wore off. The infection dose was controlled by plating in triplicate dilutions of the bacterial solution on blood agar plates and counting the colonies. The infection was monitored in real time using the IVIS Spectrum system and imaging software. Mice were monitored after the first 24 h and every 8 h from then on until the end of the experiment. For the sepsis model, 8- to 10-week-old CD-1 outbred mice ($n = 8$) were arranged in groups of 4 animals per cage and intraperitoneally infected with 200 μl containing 5×10^3 CFU. Mice were monitored 16 h postinfection and every 8 h from then on until the end of the experiment. The infection dose was confirmed by plating different dilutions of the infection dose. The results were annotated using GraphPad Prism version 7.02 software and presented in a Kaplan-Meier (KM) graph. The log rank test was used for the statistics.

Bioluminescent TIGR4 wild type and its corresponding *tcs08* mutants were applied in the coinfection assay. Briefly, an infection dose of 2.5×10^7 CFU of wild type and a single mutant (Δ*rr08*, Δ*hk08*, or Δ*tcs08*) was mixed (1:1 ratio) and mice ($n = 10$ CD-1) were intranasally infected. The infection dose was determined by plating serial dilutions of the infection mixture onto plates with kanamycin or kanamycin plus erythromycin/Spec to enumerate CFU of the wild type and mutant or CFU of the mutant. Mice were sacrificed after 24 and 48 h, and nasopharyngeal and bronchoalveolar lavages were performed using a tracheal cannula filled with 1 ml of sterile PBS. The recovered solution was diluted and plated on blood agar plates with appropriate antibiotics (see above). Colonies were counted, and recovered CFU of the wild type and mutant was determined. The competitive index (CI) was calculated as the mutant/wild-type ratio. Values higher than 1 indicate a higher ratio of mutant bacteria, while values below 1 indicate a higher ratio of wild-type bacteria. The results were annotated using GraphPad Prism version 7.02 software and presented as scatter plots where every dot indicates 1 mouse.

Ethics statement. All animal experiments were conducted according to the German regulations of the Society for Laboratory Animal Science (GV-SOLAS) and the European Health Law of the Federation of Laboratory Animal Science Associations (FELASA). All experiments were approved by the Landesamt für Landwirtschaft, Lebensmittelsicherheit und Fischerei, Mecklenburg-Vorpommern (LALLFV M-V, Rostock, Germany, permit no. 7221.3-1-056/16).

Accession number(s). Data obtained from the microarray analysis have been uploaded to the National Center for Biotechnology Information (NCBI) at the Gene Expression Omnibus (GEO) ArrayExpress databases (https://www.ncbi.nlm.nih.gov/geo) under accession number GSE108874.

SUPPLEMENTAL MATERIAL

Supplemental material for this article may be found at https://doi.org/10.1128/mSphere.00165-18.

FIG S1, PDF file, 0.2 MB.
FIG S2, PDF file, 0.1 MB.
FIG S3, PDF file, 0.1 MB.
FIG S4, PDF file, 0.3 MB.
TABLE S1, XLS file, 0.2 MB.
TABLE S2, PDF file, 0.1 MB.
TABLE S3, PDF file, 0.1 MB.
TABLE S4, PDF file, 0.03 MB.
TABLE S5, PDF file, 0.1 MB.

ACKNOWLEDGMENTS

We acknowledge the technical work performed by Kristine Sievert-Giermann, Birgit Rietow, and Gerhard Burchhardt in this study.

This work was supported by a grant from the Deutsche Forschungsgemeinschaft (DFG GRK 1870; Bacterial Respiratory Infections) in Germany and by the Committee for Development of Research at the University of Antioquia (CODI, CIEMB-097-13) in Colombia.

A. Gómez-Mejia, G. Gámez, and S. Hammerschmidt conceived and designed the experiments. A. Gómez-Mejia, G. Gámez, S. Hirschmann, H. Rath, U. Mäder, F. Voss, L. Petruschka, S. Böhm, N. Kakar, and V. Kluger performed the experiments. A. Gómez-Mejia, G. Gámez, H. Rath, U. Mäder, and S. Hammerschmidt analyzed the data. A. Gómez-Mejia, G. Gámez, and S. Hammerschmidt wrote the manuscript. A. Gómez-Mejia, G. Gámez, H. Rath, U. Mäder, R. Brückner, U. Völker, and S. Hammerschmidt revised the manuscript.

REFERENCES

1. Balleza E, López-Bojorquez LN, Martínez-Antonio A, Resendis-Antonio O, Lozada-Chávez I, Balderas-Martínez YI, Encarnación S, Collado-Vides J. 2009. Regulation by transcription factors in bacteria: beyond description. FEMS Microbiol Rev 33:133–151. https://doi.org/10.1111/j.1574-6976.2008.00145.x.
2. Stock AM, Robinson VL, Goudreau PN. 2000. Two-component signal transduction. Annu Rev Biochem 69:183–215. https://doi.org/10.1146/annurev.biochem.69.1.183.
3. Miller MB, Bassler BL. 2001. Quorum sensing in bacteria. Annu Rev Microbiol 55:165–199. https://doi.org/10.1146/annurev.micro.55.1.165.
4. Beier D, Gross R. 2006. Regulation of bacterial virulence by two-component systems. Curr Opin Microbiol 9:143–152. https://doi.org/10.1016/j.mib.2006.01.005.
5. Hoch JA. 2000. Two-component and phosphorelay signal transduction. Curr Opin Microbiol 3:165–170. https://doi.org/10.1016/S1369-5274(00)00070-9.
6. Skerker JM, Prasol MS, Perchuk BS, Biondi EG, Laub MT. 2005. Two-component signal transduction pathways regulating growth and cell cycle progression in a bacterium: a system-level analysis. PLoS Biol 3:e334. https://doi.org/10.1371/journal.pbio.0030334.
7. Mitrophanov AY, Groisman EA. 2008. Signal integration in bacterial two-component regulatory systems. Genes Dev 22:2601–2611. https://doi.org/10.1101/gad.1700308.
8. Goulian M. 2010. Two-component signaling circuit structure and properties. Curr Opin Microbiol 13:184–189. https://doi.org/10.1016/j.mib.2010.01.009.
9. Jung K, Fried L, Behr S, Heermann R. 2012. Histidine kinases and response regulators in networks. Curr Opin Microbiol 15:118–124. https://doi.org/10.1016/j.mib.2011.11.009.
10. Lange R, Wagner C, de Saizieu A, Flint N, Molnos J, Stieger M, Caspers P, Kamber M, Keck W, Amrein KE. 1999. Domain organization and molecular characterization of 13 two-component systems identified by genome sequencing of *Streptococcus pneumoniae*. Gene 237:223–234. https://doi.org/10.1016/S0378-1119(99)00266-8.
11. Throup JP, Koretke KK, Bryant AP, Ingraham KA, Chalker AF, Ge Y, Marra A, Wallis NG, Brown JR, Holmes DJ, Rosenberg M, Burnham MK. 2000. A genomic analysis of two-component signal transduction in *Streptococcus pneumoniae*. Mol Microbiol 35:566–576. https://doi.org/10.1046/j.1365-2958.2000.01725.x.
12. Paterson GK, Blue CE, Mitchell TJ. 2006. Role of two-component systems in the virulence of *Streptococcus pneumoniae*. J Med Microbiol 55:355–363. https://doi.org/10.1099/jmm.0.46423-0.
13. Guenzi E, Hakenbeck R. 1995. Genetic competence and susceptibility to beta-lactam antibiotics in *Streptococcus pneumoniae* R6 are linked via a two-component signal-transducing system cia. Dev Biol Stand 85:125–128.
14. Håvarstein LS, Coomaraswamy G, Morrison DA. 1995. An unmodified heptadecapeptide pheromone induces competence for genetic transformation in *Streptococcus pneumoniae*. Proc Natl Acad Sci U S A 92:11140–11144. https://doi.org/10.1073/pnas.92.24.11140.
15. Håvarstein LS, Diep DB, Nes IF. 1995. A family of bacteriocin ABC transporters carry out proteolytic processing of their substrates concomitant with export. Mol Microbiol 16:229–240. https://doi.org/10.1111/j.1365-2958.1995.tb02295.x.
16. Giammarinaro P, Sicard M, Gasc AM. 1999. Genetic and physiological studies of the CiaH-CiaR two-component signal-transducing system involved in cefotaxime resistance and competence of *Streptococcus pneumoniae*. Microbiology 145:1859–1869. https://doi.org/10.1099/13500872-145-8-1859.
17. Mascher T, Zähner D, Merai M, Balmelle N, de Saizieu AB, Hakenbeck R. 2003. The *Streptococcus pneumoniae* cia regulon: CiaR target sites and

transcription profile analysis. J Bacteriol 185:60–70. https://doi.org/10.1128/JB.185.1.60-70.2003.
18. Cortes PR, Piñas GE, Cian MB, Yandar N, Echenique J. 2015. Stress-triggered signaling affecting survival or suicide of *Streptococcus pneumoniae*. Int J Med Microbiol 305:157–169. https://doi.org/10.1016/j.ijmm.2014.12.002.
19. Mohedano ML, Overweg K, de la Fuente A, Reuter M, Altabe S, Mulholland F, de Mendoza D, López P, Wells JM. 2005. Evidence that the essential response regulator YycF in *Streptococcus pneumoniae* modulates expression of fatty acid biosynthesis genes and alters membrane composition. J Bacteriol 187:2357–2367. https://doi.org/10.1128/JB.187.7.2357-2367.2005.
20. Ng WL, Tsui HC, Winkler ME. 2005. Regulation of the *pspA* virulence factor and essential *pcsB* murein biosynthetic genes by the phosphorylated VicR (YycF) response regulator in *Streptococcus pneumoniae*. J Bacteriol 187:7444–7459. https://doi.org/10.1128/JB.187.21.7444-7459.2005.
21. Gutu AD, Wayne KJ, Sham LT, Winkler ME. 2010. Kinetic characterization of the WalRKSpn (VicRK) two-component system of *Streptococcus pneumoniae*: dependence of WalKSpn (VicK) phosphatase activity on its PAS domain. J Bacteriol 192:2346–2358. https://doi.org/10.1128/JB.01690-09.
22. Ng WL, Robertson GT, Kazmierczak KM, Zhao J, Gilmour R, Winkler ME. 2003. Constitutive expression of PcsB suppresses the requirement for the essential VicR (YycF) response regulator in *Streptococcus pneumoniae* R6. Mol Microbiol 50:1647–1663. https://doi.org/10.1046/j.1365-2958.2003.03806.x.
23. Ng WL, Kazmierczak KM, Winkler ME. 2004. Defective cell wall synthesis in *Streptococcus pneumoniae* R6 depleted for the essential PcsB putative murein hydrolase or the VicR (YycF) response regulator. Mol Microbiol 53:1161–1175. https://doi.org/10.1111/j.1365-2958.2004.04196.x.
24. McKessar SJ, Hakenbeck R. 2007. The two-component regulatory system TCS08 is involved in cellobiose metabolism of *Streptococcus pneumoniae* R6. J Bacteriol 189:1342–1350. https://doi.org/10.1128/JB.01170-06.
25. Sun F, Li C, Jeong D, Sohn C, He C, Bae T. 2010. In the *Staphylococcus aureus* two-component system sae, the response regulator SaeR binds to a direct repeat sequence and DNA binding requires phosphorylation by the sensor kinase SaeS. J Bacteriol 192:2111–2127. https://doi.org/10.1128/JB.01524-09.
26. Liu Q, Cho H, Yeo WS, Bae T. 2015. The extracytoplasmic linker peptide of the sensor protein SaeS tunes the kinase activity required for staphylococcal virulence in response to host signals. PLoS Pathog 11:e1004799. https://doi.org/10.1371/journal.ppat.1004799.
27. Liu Q, Yeo WS, Bae T. 2016. The SaeRS two-component system of *Staphylococcus aureus*. Genes (Basel) 7(10):E81. https://doi.org/10.3390/genes7100081.
28. Song XM, Connor W, Hokamp K, Babiuk LA, Potter AA. 2009. The growth phase-dependent regulation of the pilus locus genes by two-component system TCS08 in *Streptococcus pneumoniae*. Microb Pathog 46:28–35. https://doi.org/10.1016/j.micpath.2008.10.006.
29. Pribyl T, Moche M, Dreisbach A, Bijlsma JJ, Saleh M, Abdullah MR, Hecker M, van Dijl JM, Becher D, Hammerschmidt S. 2014. Influence of impaired lipoprotein biogenesis on surface and exoproteome of *Streptococcus pneumoniae*. J Proteome Res 13:650–667. https://doi.org/10.1021/pr400768v.
30. Kloosterman TG, Kuipers OP. 2011. Regulation of arginine acquisition and virulence gene expression in the human pathogen *Streptococcus pneumoniae* by transcription regulators ArgR1 and AhrC. J Biol Chem 286:44594–44605. https://doi.org/10.1074/jbc.M111.295832.
31. Schulz C, Gierok P, Petruschka L, Lalk M, Mäder U, Hammerschmidt S. 2014. Regulation of the arginine deiminase system by ArgR2 interferes with arginine metabolism and fitness of *Streptococcus pneumoniae*. mBio 5:e01858-14. https://doi.org/10.1128/mBio.01858-14.
32. Jensch I, Gámez G, Rothe M, Ebert S, Fulde M, Somplatzki D, Bergmann S, Petruschka L, Rohde M, Nau R, Hammerschmidt S. 2010. PavB is a surface-exposed adhesin of *Streptococcus pneumoniae* contributing to nasopharyngeal colonization and airways infections. Mol Microbiol 77:22–43. https://doi.org/10.1111/j.1365-2958.2010.07189.x.
33. Kanwal S, Jensch I, Palm GJ, Brönstrup M, Rohde M, Kohler TP, Somplatzki D, Tegge W, Jenkinson HF, Hammerschmidt S. 2017. Mapping the recognition domains of pneumococcal fibronectin-binding proteins PavA and PavB demonstrates a common pattern of molecular interactions with fibronectin type III repeats. Mol Microbiol 105:839–859. https://doi.org/10.1111/mmi.13740.
34. LeMieux J, Hava DL, Basset A, Camilli A. 2006. RrgA and RrgB are components of a multisubunit pilus encoded by the *Streptococcus pneumoniae rlrA* pathogenicity islet. Infect Immun 74:2453–2456. https://doi.org/10.1128/IAI.74.4.2453-2456.2006.
35. Tettelin H, Nelson KE, Paulsen IT, Eisen JA, Read TD, Peterson S, Heidelberg J, DeBoy RT, Haft DH, Dodson RJ, Durkin AS, Gwinn M, Kolonay JF, Nelson WC, Peterson JD, Umayam LA, White O, Salzberg SL, Lewis MR, Radune D, Holtzapple E, Khouri H, Wolf AM, Utterback TR, Hansen CL, McDonald LA, Feldblyum TV, Angiuoli S, Dickinson T, Hickey EK, Holt IE, Loftus BJ, Yang F, Smith HO, Venter JC, Dougherty BA, Morrison DA, Hollingshead SK, Fraser CM. 2001. Complete genome sequence of a virulent isolate of *Streptococcus pneumoniae*. Science 293:498–506. https://doi.org/10.1126/science.1061217.
36. Hava DL, Camilli A. 2002. Large-scale identification of serotype 4 *Streptococcus pneumoniae* virulence factors. Mol Microbiol 45:1389–1406. https://doi.org/10.1046/j.1365-2958.2002.03106.x.
37. Gómez-Mejia A, Gámez G, Hammerschmidt S. 2017. *Streptococcus pneumoniae* two-component regulatory systems: the interplay of the pneumococcus with its environment. Int J Med Microbiol https://doi.org/10.1016/j.ijmm.2017.11.012.
38. Park AK, Moon JH, Oh JS, Lee KS, Chi YM. 2013. Crystal structure of the response regulator *spr1814* from *Streptococcus pneumoniae* reveals unique interdomain contacts among NarL family proteins. Biochem Biophys Res Commun 434:65–69. https://doi.org/10.1016/j.bbrc.2013.03.065.
39. Maule AF, Wright DP, Weiner JJ, Han L, Peterson FC, Volkman BF, Silvaggi NR, Ulijasz AT. 2015. The aspartate-less receiver (ALR) domains: distribution, structure and function. PLoS Pathog 11:e1004795. https://doi.org/10.1371/journal.ppat.1004795.
40. Nguyen MP, Yoon JM, Cho MH, Lee SW. 2015. Prokaryotic 2-component systems and the OmpR/PhoB superfamily. Can J Microbiol 61:799–810. https://doi.org/10.1139/cjm-2015-0345.
41. Ericson ME, Subramanian C, Frank MW, Rock CO. 2017. Role of fatty acid kinase in cellular lipid homeostasis and SaeRS-dependent virulence factor expression in *Staphylococcus aureus*. mBio 8:e00988-17. https://doi.org/10.1128/mBio.00988-17.
42. Brown JS, Gilliland SM, Ruiz-Albert J, Holden DW. 2002. Characterization of pit, a *Streptococcus pneumoniae* iron uptake ABC transporter. Infect Immun 70:4389–4398. https://doi.org/10.1128/IAI.70.8.4389-4398.2002.
43. Tseng HJ, McEwan AG, Paton JC, Jennings MP. 2002. Virulence of *Streptococcus pneumoniae*: PsaA mutants are hypersensitive to oxidative stress. Infect Immun 70:1635–1639. https://doi.org/10.1128/IAI.70.3.1635-1639.2002.
44. Kerr AR, Adrian PV, Estevão S, de Groot R, Alloing G, Claverys JP, Mitchell TJ, Hermans PW. 2004. The Ami-AliA/AliB permease of *Streptococcus pneumoniae* is involved in nasopharyngeal colonization but not in invasive disease. Infect Immun 72:3902–3906. https://doi.org/10.1128/IAI.72.7.3902-3906.2004.
45. Lu YJ, Rock CO. 2006. Transcriptional regulation of fatty acid biosynthesis in *Streptococcus pneumoniae*. Mol Microbiol 59:551–566. https://doi.org/10.1111/j.1365-2958.2005.04951.x.
46. Nobbs AH, Lamont RJ, Jenkinson HF. 2009. Streptococcus adherence and colonization. Microbiol Mol Biol Rev 73:407–450. https://doi.org/10.1128/MMBR.00014-09.
47. Richardson AR, Somerville GA, Sonenshein AL. 2015. Regulating the intersection of metabolism and pathogenesis in Gram-positive bacteria. Microbiol Spectr 3(3). https://doi.org/10.1128/microbiolspec.MBP-0004-2014.
48. Mainiero M, Goerke C, Geiger T, Gonser C, Herbert S, Wolz C. 2010. Differential target gene activation by the *Staphylococcus aureus* two-component system saeRS. J Bacteriol 192:613–623. https://doi.org/10.1128/JB.01242-09.
49. Kloosterman TG, Witwicki RM, van der Kooi-Pol MM, Bijlsma JJ, Kuipers OP. 2008. Opposite effects of Mn^{2+} and Zn^{2+} on PsaR-mediated expression of the virulence genes *pcpA*, *prtA*, and *psaBCA* of *Streptococcus pneumoniae*. J Bacteriol 190:5382–5393. https://doi.org/10.1128/JB.00307-08.
50. Shafeeq S, Kloosterman TG, Kuipers OP. 2011. CelR-mediated activation of the cellobiose-utilization gene cluster in *Streptococcus pneumoniae*. Microbiology 157:2854–2861. https://doi.org/10.1099/mic.0.051359-0.
51. McCluskey J, Hinds J, Husain S, Witney A, Mitchell TJ. 2004. A two-component system that controls the expression of pneumococcal sur-

face antigen A (PsaA) and regulates virulence and resistance to oxidative stress in *Streptococcus pneumoniae*. Mol Microbiol 51:1661–1675. https://doi.org/10.1111/j.1365-2958.2003.03917.x.

52. Johnston JW, Briles DE, Myers LE, Hollingshead SK. 2006. Mn^{2+}-dependent regulation of multiple genes in *Streptococcus pneumoniae* through PsaR and the resultant impact on virulence. Infect Immun 74:1171–1180. https://doi.org/10.1128/IAI.74.2.1171-1180.2006.
53. Frankel MB, Wojcik BM, DeDent AC, Missiakas DM, Schneewind O. 2010. ABI domain-containing proteins contribute to surface protein display and cell division in *Staphylococcus aureus*. Mol Microbiol 78:238–252. https://doi.org/10.1111/j.1365-2958.2010.07334.x.
54. Blue CE, Mitchell TJ. 2003. Contribution of a response regulator to the virulence of *Streptococcus pneumoniae* is strain dependent. Infect Immun 71:4405–4413. https://doi.org/10.1128/IAI.71.8.4405-4413.2003.
55. Laux A, Sexauer A, Sivaselvarajah D, Kaysen A, Brückner R. 2015. Control of competence by related non-coding csRNAs in *Streptococcus pneumoniae* R6. Front Genet 6:246. https://doi.org/10.3389/fgene.2015.00246.
56. Cassone M, Gagne AL, Spruce LA, Seeholzer SH, Sebert ME. 2012. The HtrA protease from *Streptococcus pneumoniae* digests both denatured proteins and the competence-stimulating peptide. J Biol Chem 287:38449–38459. https://doi.org/10.1074/jbc.M112.391482.
57. Jeong DW, Cho H, Jones MB, Shatzkes K, Sun F, Ji Q, Liu Q, Peterson SN, He C, Bae T. 2012. The auxiliary protein complex SaePQ activates the phosphatase activity of sensor kinase SaeS in the SaeRS two-component system of *Staphylococcus aureus*. Mol Microbiol 86:331–348. https://doi.org/10.1111/j.1365-2958.2012.08198.x.
58. Winter T, Winter J, Polak M, Kusch K, Mäder U, Sietmann R, Ehlbeck J, van Hijum S, Weltmann KD, Hecker M, Kusch H. 2011. Characterization of the global impact of low temperature gas plasma on vegetative microorganisms. Proteomics 11:3518–3530. https://doi.org/10.1002/pmic.201000637.
59. Kohler S, Voß F, Gómez Mejia A, Brown JS, Hammerschmidt S. 2016. Pneumococcal lipoproteins involved in bacterial fitness, virulence, and immune evasion. FEBS Lett 590:3820–3839. https://doi.org/10.1002/1873-3468.12352.
60. Hammerschmidt S, Agarwal V, Kunert A, Haelbich S, Skerka C, Zipfel PF. 2007. The host immune regulator factor H interacts via two contact sites with the PspC protein of *Streptococcus pneumoniae* and mediates adhesion to host epithelial cells. J Immunol 178:5848–5858. https://doi.org/10.4049/jimmunol.178.9.5848.

TABLES

Table S1: Gene expression change in TIGR4Δ*cps* and TCS08 mutants by microarray

TIGR4 Locus_Tag	*Gene Name*	Gene Product	General Function	Cellular or Metabolic Process	Metabolic Pathway or Specific Function	*TIGR4 wt vs TIGR4 Δrr08*				*TIGR4 wt vs TIGR4 Δhk08*				*TIGR4 wt vs TIGR4 Δtcs08*			
						p-value	Sig.	Regulation	Log FC	p-value	Sig.	Regulation	Log FC	p-value	Sig.	Regulation	Log FC
sp_0082	*pavB*	Surface-Exposed Protein	Colonization Factor	Cell Wall, Membrane Biogenesis	LPxTG Protein / Pneumococcal Adherence and Virulence Factor B	8,42E-01	n.s.	Up	0,07	1,26E-02	s	Up	0,84	5,89E-01	n.s.	Down	-0,21
sp_0083	*rr08*	Response Regulator	Environmental Information Processing	Signal Transduction	Two-Component Systems	4,67E-08	s	Down	-6,26	3,59E-04	s	Up	1,65	3,43E-08	s	Down	-2,49
sp_0084	*hk08*	Histidine Kinase	Environmental Information Processing	Signal Transduction	Two-Component Systems	1,72E-02	s	Up	0,78	3,42E-08	s	Down	-5,76	1,89E-06	s	Down	-2,84
sp_0085	*rpsD*	Ribosomal Protein	Genetic Information Processing	Translation	Ribosome	5,99E-01	n.s.	Up	0,16	6,26E-04	s	Up	1,34	4,93E-01	n.s.	Down	-0,21
sp_0090		ABC Transporter Permease	Environmental Information Processing	Membrane Transport	ABC Transporters	2,14E-01	n.s.	Down	-0,56	2,92E-02	s	Up	0,93	4,35E-01	n.s.	Down	-0,35
sp_0091		ABC Transporter Permease	Environmental Information Processing	Membrane Transport	ABC Transporters	7,74E-02	n.s.	Down	-0,73	3,15E-01	n.s.	Up	0,46	2,34E-01	n.s.	Up	0,54
sp_0092		ABC Transporter Substrate-Binding Protein	Environmental Information Processing	Membrane Transport	ABC Transporters	3,97E-03	s	Down	-1,10	3,35E-01	n.s.	Down	-0,23	2,00E-01	n.s.	Down	-0,42
sp_0101		Putative Transporter	Environmental Information Processing	Membrane Transport	ABC Transporters	7,69E-01	n.s.	Up	0,12	4,88E-02	s	Down	-1,02	4,15E-01	n.s.	Up	0,33
sp_0111		ABC Transporter ATP-Binding Protein	Environmental Information Processing	Membrane Transport	ABC Transporters	7,93E-01	n.s.	Down	-0,01	1,83E-02	s	Up	1,16	6,49E-01	n.s.	Up	0,09
sp_0112		ABC Transporter Substrate-Binding Protein	Environmental Information Processing	Membrane Transport	ABC Transporters	4,83E-01	n.s.	Up	0,27	7,32E-02	n.s.	Up	0,80	1,34E-01	n.s.	Up	0,45
sp_0144		CAAX Protease	Intermediary Metabolism	Lipid Metabolism	CAAX Protease	9,48E-01	n.s.	Down	-0,02	2,01E-02	s	Up	1,08	8,79E-01	n.s.	Down	-0,06
sp_0148		ABC Transporter Substrate-Binding Protein	Environmental Information Processing	Membrane Transport	ABC Transporters	5,62E-01	n.s.	Down	-0,16	1,04E-02	s	Up	1,01	1,93E-01	n.s.	Down	-0,40
sp_0198		Hypothetical Protein	Unknown Function	Unknown Function	Unknown Function	2,57E-01	n.s.	Down	-1,32	1,81E-02	s	Up	2,34	2,80E-01	n.s.	Down	-0,42
sp_0247		Transcriptional Regulator	Environmental Information Processing	Signal Transduction	Transcriptional Regulator	6,26E-01	n.s.	Down	-0,19	4,62E-03	s	Down	-1,09	6,99E-01	n.s.	Up	0,12
sp_0248		Cellobiose Phospho-Transfer System (PTS)	Environmental Information Processing	Membrane Transport	Phospho-Transferase System	2,76E-01	n.s.	Down	-0,43	6,87E-04	s	Down	-1,37	6,83E-01	n.s.	Up	0,14
sp_0249		Cellobiose Phospho-Transfer System (PTS)	Environmental Information Processing	Membrane Transport	Phospho-Transferase System	7,75E-01	n.s.	Up	0,10	1,02E-02	s	Down	-1,09	1,78E-01	n.s.	Up	0,44
sp_0250		Cellobiose Phospho-Transfer System (PTS)	Environmental Information Processing	Membrane Transport	Phospho-Transferase System	9,23E-01	n.s.	Down	-0,09	8,06E-03	s	Down	-0,68	2,81E-01	n.s.	Up	0,39
sp_0251		Acetyl Transferase	Intermediary Metabolism	Carbohydrate Metabolism	Propanoate, Butanoate and Pyruvate Metabolism	8,17E-01	n.s.	Up	0,07	1,25E-02	s	Down	-1,61	3,50E-01	n.s.	Up	0,27
sp_0278	*pepS*	Aminopeptidase	Intermediary Metabolism	Amino Acid Metabolism	Aminopeptidase	7,73E-01	n.s.	Up	0,08	6,25E-03	s	Down	-1,01	7,19E-01	n.s.	Up	0,11
sp_0317		Aldolase	Intermediary Metabolism	Carbohydrate Metabolism	Pentose Phosphate Pathway / Glyoxylate and Dicarboxylate Metabolism	6,49E-01	n.s.	Down	-0,23	8,37E-01	n.s.	Up	0,09	3,20E-02	s	Up	1,03
sp_0318		Carbohydrate Kinase	Intermediary Metabolism	Carbohydrate Metabolism	Pentose Phosphate Pathway	7,69E-01	n.s.	Down	-0,11	1,91E-02	s	Up	1,07	6,97E-02	n.s.	Up	0,82
sp_0319		Hypothetical Protein	Unknown Function	Unknown Function	Unknown Function	1,29E-01	n.s.	Down	-0,47	2,80E-03	s	Up	1,32	1,91E-02	s	Up	1,28
sp_0320		Oxidoreductase	Environmental Information Processing	Membrane Transport	Phospho-Transferase System	2,88E-01	n.s.	Down	-0,21	1,83E-03	s	Up	1,11	1,06E-02	s	Up	1,17
sp_0321		N-Acetylgalactosamine Phospho-Transfer System (PTS)	Environmental Information Processing	Membrane Transport	Phospho-Transferase System	2,44E-01	n.s.	Up	0,36	3,99E-01	n.s.	Up	0,17	2,84E-02	s	Up	1,11
sp_0322		Glucuronyl Hydrolase	Intermediary Metabolism	Carbohydrate Metabolism	Glucuronyl Hydrolase	8,10E-01	n.s.	Down	-0,08	3,82E-01	n.s.	Up	0,31	3,76E-02	s	Up	1,02
sp_0323		Phospho-Transfer System (PTS) - Transporter Subunit IIB	Environmental Information Processing	Membrane Transport	Phospho-Transferase System	4,85E-01	n.s.	Down	-0,33	3,92E-01	n.s.	Up	0,29	1,32E-02	s	Up	0,97
sp_0324		Phospho-Transfer System (PTS) - Transporter Subunit IIC	Environmental Information Processing	Membrane Transport	Phospho-Transferase System	1,25E-01	n.s.	Down	-0,46	6,04E-02	n.s.	Up	0,37	3,56E-02	s	Up	0,82
sp_0325		N-Acetylgalactosamine Phospho-Transfer System (PTS)	Environmental Information Processing	Membrane Transport	Phospho-Transferase System	7,38E-01	n.s.	Down	-0,15	1,89E-01	n.s.	Down	-0,51	8,92E-03	s	Up	1,32
sp_0369	*pbp1A*	Penicillin-Binding Protein	Colonization Factor	Cell Wall, Membrane Biogenesis	Peptidoglycan Biosynthesis	3,76E-01	n.s.	Down	-0,27	2,59E-02	s	Up	1,14	1,80E-01	n.s.	Down	-0,49
sp_0394	*mtlA*	Mannitol Phospho-Transfer System (PTS)	Environmental Information Processing	Membrane Transport	Phospho-Transferase System	3,98E-02	s	Down	-0,75	3,77E-01	n.s.	Up	0,21	1,01E-01	n.s.	Down	-0,58
sp_0395		Transcriptional Regulator	Environmental Information Processing	Signal Transduction	Transcriptional Regulator	1,78E-02	s	Down	-0,96	7,34E-01	n.s.	Up	0,06	3,84E-01	n.s.	Down	-0,48
sp_0396	*mtlF*	Mannitol Phospho-Transfer System (PTS)	Environmental Information Processing	Membrane Transport	Phospho-Transferase System	9,09E-01	n.s.	Up	0,06	3,05E-02	s	Up	1,23	1,75E-02	s	Up	1,11
sp_0397	*mtlD*	Mannitol-1-Phosphate 5-Dehydrogenase	Intermediary Metabolism	Carbohydrate Metabolism	Fructose and Mannose Metabolism	8,28E-02	n.s.	Down	-0,57	3,23E-02	s	Up	0,58	8,25E-01	n.s.	Up	0,07
sp_0415		Enoyl-CoA Hydratase	Intermediary Metabolism	Lipid Metabolism	Fatty Acid Biosynthesis	9,00E-02	n.s.	Down	-0,61	1,15E-02	s	Up	1,23	6,73E-01	n.s.	Down	-0,16

TABLES

Table S1: Gene expression change in TIGR4Δ*cps* and TCS08 mutants by microarray

TIGR4 Locus_Tag	*Gene Name*	Gene Product	General Function	Cellular or Metabolic Process	Metabolic Pathway or Specific Function	*TIGR4 wt vs TIGR4 Δrr08*				*TIGR4 wt vs TIGR4 Δhk08*				*TIGR4 wt vs TIGR4 Δtcs08*			
						p-value	Sig.	Regulation	Log FC	p-value	Sig.	Regulation	Log FC	p-value	Sig.	Regulation	Log FC
sp_0416		Transcriptional Regulator	Environmental Information Processing	Signal Transduction	Transcriptional Regulator	6,35E-01	n.s.	Down	-0,22	2,79E-02	s	Up	1,22	8,47E-01	n.s.	Up	0,08
sp_0417	*fabH*	3-Oxoacyl-Synthase	Intermediary Metabolism	Lipid Metabolism	Fatty Acid Biosynthesis	9,07E-01	n.s.	Down	-0,04	2,99E-02	s	Up	1,15	9,58E-01	n.s.	Down	-0,02
sp_0418	*acpP*	Acyl Carrier Protein	Intermediary Metabolism	Lipid Metabolism	Fatty Acid Biosynthesis	6,10E-01	n.s.	Down	-0,14	2,34E-01	n.s.	Up	0,22	7,59E-01	n.s.	Up	0,09
sp_0419	*fabK*	Enoyl-ACP Reductase	Intermediary Metabolism	Lipid Metabolism	Fatty Acid Biosynthesis	1,41E-01	n.s.	Down	-0,46	5,70E-01	n.s.	Up	0,13	7,38E-01	n.s.	Up	0,14
sp_0420	*fabD*	ACP S-Malonyl Transferase	Intermediary Metabolism	Lipid Metabolism	Fatty Acid Biosynthesis	2,25E-01	n.s.	Down	-0,39	4,46E-02	s	Up	0,83	2,52E-01	n.s.	Down	-0,36
sp_0421	*fabG*	3-Oxoacyl Reductase	Intermediary Metabolism	Lipid Metabolism	Fatty Acid Biosynthesis	3,85E-01	n.s.	Down	-0,42	2,21E-02	s	Up	1,40	5,19E-01	n.s.	Down	-0,30
sp_0422	*fabF*	3-Oxoacyl-ACP Synthase	Intermediary Metabolism	Lipid Metabolism	Fatty Acid Biosynthesis	4,08E-01	n.s.	Down	-0,32	3,74E-02	s	Up	0,86	3,94E-01	n.s.	Down	-0,21
sp_0423	*accB*	Acetyl-CoA Carboxylase	Intermediary Metabolism	Lipid Metabolism	Fatty Acid Biosynthesis	5,73E-01	n.s.	Down	-0,24	1,04E-02	s	Up	1,28	5,83E-01	n.s.	Down	-0,21
sp_0424	*fabZ*	3-Hydroxyacyl-Hydratase	Intermediary Metabolism	Lipid Metabolism	Fatty Acid Biosynthesis	4,60E-01	n.s.	Down	-0,32	5,81E-03	s	Up	1,37	7,24E-01	n.s.	Down	-0,14
sp_0425	*accC*	Acetyl-CoA Carboxylase	Intermediary Metabolism	Lipid Metabolism	Fatty Acid Biosynthesis	5,06E-01	n.s.	Down	-0,23	8,10E-02	n.s.	Up	0,57	4,48E-01	n.s.	Down	-0,30
sp_0426	*accD*	Acetyl-CoA Carboxylase	Intermediary Metabolism	Lipid Metabolism	Fatty Acid Biosynthesis	7,23E-01	n.s.	Down	-0,16	3,03E-02	s	Up	1,04	7,75E-01	n.s.	Up	0,13
sp_0427	*accA*	Acetyl-CoA Carboxylase	Intermediary Metabolism	Lipid Metabolism	Fatty Acid Biosynthesis	5,27E-01	n.s.	Down	-0,26	5,84E-02	n.s.	Up	0,75	2,99E-01	n.s.	Up	0,34
sp_0461	*rtrA*	Transcriptional Regulator	Genetic Information Processing	Transcription	Transcriptional Regulator	4,78E-01	n.s.	Down	-0,20	4,27E-02	s	Up	0,52	1,62E-05	s	Down	-2,44
sp_0462	*ngA*	Surface-Exposed Protein	Colonization Factor	Cell Wall, Membrane Biogenesis	LPxTG Protein / Pilus-1 Biogenesis / Pilus-1 Tip Protein (Adhesin)	4,49E-01	n.s.	Down	-0,23	6,69E-01	n.s.	Down	-0,10	1,06E-06	s	Down	-3,16
sp_0463	*ngB*	Surface-Exposed Protein	Colonization Factor	Cell Wall, Membrane Biogenesis	LPxTG Protein / Pilus-1 Biogenesis / Pilus-1 Backbone Protein	7,49E-01	n.s.	Up	0,02	3,38E-02	s	Down	-0,76	2,23E-06	s	Down	-3,05
sp_0464	*ngC*	Surface-Exposed Protein	Colonization Factor	Cell Wall, Membrane Biogenesis	LPxTG Protein / Pilus-1 Biogenesis / Pilus-1 Anchor Protein	4,32E-01	n.s.	Down	-0,26	7,32E-02	n.s.	Up	0,35	3,14E-06	s	Down	-3,13
sp_0465		Hypothetical Protein	Unknown Function	Unknown Function	Unknown Function	1,82E-03	s	Down	-1,40	5,16E-01	n.s.	Down	-0,16	5,17E-02	n.s.	Down	-0,71
sp_0466	*srtC-1*	Putative Sortase	Colonization Factor	Cell Wall, Membrane Biogenesis	Pilus-1 Biogenesis / Sortase	5,98E-01	n.s.	Down	-0,20	1,66E-01	n.s.	Up	0,12	8,92E-06	s	Down	-2,83
sp_0467	*srtC-2*	Putative Sortase	Colonization Factor	Cell Wall, Membrane Biogenesis	Pilus-1 Biogenesis / Sortase	7,97E-01	n.s.	Down	-0,12	3,00E-02	s	Up	0,97	3,86E-04	s	Down	-1,75
sp_0468	*srtC-3*	Putative Sortase	Colonization Factor	Cell Wall, Membrane Biogenesis	Pilus-1 Biogenesis / Sortase	3,35E-01	n.s.	Down	-0,16	2,69E-02	s	Down	-0,53	2,56E-06	s	Down	-2,61
SP_0476	*lacF-1*	Lactose Phospho-Transfer System (PTS)	Environmental Information Processing	Membrane Transport	Phospho-Transferase System	2,20E-01	n.s.	Up	0,37	5,60E-02	n.s.	Down	-0,66	5,34E-01	n.s.	Up	0,20
SP_0477	*lacG-1*	Lactose Phospho-Transfer System (PTS)	Environmental Information Processing	Membrane Transport	Phospho-Transferase System	3,33E-01	n.s.	Up	0,28	5,71E-02	n.s.	Down	-0,95	6,22E-01	n.s.	Up	0,26
sp_0478	*lacE-1*	Lactose Phospho-Transfer System (PTS)	Environmental Information Processing	Membrane Transport	Phospho-Transferase System	8,24E-01	n.s.	Up	0,08	6,24E-03	s	Down	-1,61	6,44E-01	n.s.	Up	0,16
sp_0479		Potassium Uptake Protein	Environmental Information Processing	Membrane Transport	Other Transporters	9,89E-01	n.s.	Down	0,00	1,68E-02	s	Up	1,05	6,94E-01	n.s.	Down	-0,15
sp_0480	*trkA*	Potassium Uptake Protein	Environmental Information Processing	Membrane Transport	Other Transporters	7,70E-01	n.s.	Down	-0,12	3,28E-02	s	Up	1,05	3,03E-01	n.s.	Down	-0,44
sp_0507		Type-I Restriction Enzyme	Genetic Information Processing	Restriction-Modification System	Type-I Endodeoxyribonuclease	4,24E-01	n.s.	Up	0,15	6,57E-03	s	Up	0,83	8,93E-04	s	Up	1,17
sp_0508	*hsdS*	Type-I Restriction Enzyme	Genetic Information Processing	Restriction-Modification System	Type-I Endodeoxyribonuclease	7,36E-04	s	Down	-1,35	5,97E-01	n.s.	Down	-0,10	7,61E-01	n.s.	Down	-0,04
sp_0516	*grpE*	Heat Shock Protein	Genetic Information Processing	Folding, Sorting and Degradation	Heat Shock Protein GrpE	5,70E-01	n.s.	Down	-0,44	2,34E-02	s	Down	-2,31	2,22E-01	n.s.	Up	0,46
sp_0517	*dnaK*	Molecular Chaperone	Genetic Information Processing	Folding, Sorting and Degradation	Molecular Chaperone DnaK	3,34E-01	n.s.	Down	-0,67	1,83E-02	s	Down	-2,62	1,76E-01	n.s.	Up	0,47
sp_0518		Hypothetical Protein	Unknown Function	Unknown Function	Unknown Function	6,99E-01	n.s.	Down	-0,32	1,32E-02	s	Down	-3,74	2,31E-01	n.s.	Up	0,77
sp_0519	*dnaJ*	Molecular Chaperone	Genetic Information Processing	Folding, Sorting and Degradation	Molecular Chaperone DnaJ	4,15E-01	n.s.	Down	-0,48	2,08E-02	s	Down	-2,87	2,71E-01	n.s.	Up	0,49
sp_0605	*fba*	Fructose Bi-Phosphate Aldolase	Intermediary Metabolism	Carbohydrate Metabolism	Fructose and Mannose Metabolism	5,29E-01	n.s.	Up	0,23	1,22E-02	s	Down	-1,24	9,34E-01	n.s.	Up	0,03
sp_0607		Amino Acid ABC Transporter Permease	Environmental Information Processing	Membrane Transport	ABC Transporters	1,45E-01	n.s.	Down	-0,40	8,69E-02	n.s.	Up	0,57	2,93E-01	n.s.	Down	-0,40
sp_0608		ABC Transporter Permease	Environmental Information Processing	Membrane Transport	ABC Transporters	9,55E-01	n.s.	Up	0,02	4,37E-02	s	Up	1,18	9,57E-01	n.s.	Up	0,02

TABLES

Table S1: Gene expression change in TIGR4Δ*cps* and TC508 mutants by microarray

TIGR4 Locus_Tag	*Gene Name*	Gene Product	General Function	Cellular or Metabolic Process	Metabolic Pathway or Specific Function	*TIGR4 wt vs TIGR4 Δrr08*				*TIGR4 wt vs TIGR4 Δhk08*				*TIGR4 wt vs TIGR4 Δtcs08*			
						p-value	Sig.	Regulation	Log FC	p-value	Sig.	Regulation	Log FC	p-value	Sig.	Regulation	Log FC
sp_0609		Amino Acid ABC Transporter Amino Acid-Binding Protein	Environmental Information Processing	Membrane Transport	ABC Transporters	1,83E-01	n.s.	Down	-0,56	2,42E-02	s	Up	1,00	5,95E-02	n.s.	Down	-0,77
sp_0611	*recJ*	Single-Stranded-DNA Exonuclease	Genetic Information Processing	Replication and Repair	Mismatch Repair	9,53E-01	n.s.	Down	-0,03	2,47E-02	s	Up	1,10	9,19E-01	n.s.	Up	0,05
sp_0620		Substrate-Binding Protein	Environmental Information Processing	Membrane Transport	ABC Transporters	2,81E-01	n.s.	Down	-0,53	7,86E-03	s	Up	1,22	2,71E-02	s	Down	-0,88
sp_0641	*prtA*	Serine Protease	Colonization Factor	Cell Wall, Membrane Biogenesis	LPXTG Protein / Cell Wall-Associated Serine Protease	6,93E-01	n.s.	Up	0,15	4,73E-03	s	Up	1,66	3,47E-01	n.s.	Up	0,28
sp_0646	*galB*	Galactose Phospho-Transfer System (PTS)	Environmental Information Processing	Membrane Transport	Phospho-Transferase System	3,91E-01	n.s.	Down	-0,32	2,41E-02	s	Down	-1,09	2,19E-01	n.s.	Down	-0,41
sp_0647	*galC*	Galactose Phospho-Transfer System (PTS)	Environmental Information Processing	Membrane Transport	Phospho-Transferase System	9,10E-01	n.s.	Down	-0,04	1,95E-02	s	Down	-1,28	8,36E-01	n.s.	Down	-0,10
sp_0668	*glcI*	Glucokinase	Intermediary Metabolism	Carbohydrate Metabolism	Glycolysis / Gluconeogenesis	8,14E-01	n.s.	Up	0,07	1,02E-02	s	Down	-1,07	4,99E-01	n.s.	Up	0,22
sp_0709		ATP-Binding Protein	Environmental Information Processing	Membrane Transport	ABC Transporters	2,39E-01	n.s.	Down	-0,32	4,53E-03	s	Up	1,35	1,71E-01	n.s.	Down	-0,42
sp_0710		ABC Transporter Permease	Environmental Information Processing	Membrane Transport	ABC Transporters	3,26E-01	n.s.	Down	-0,11	9,31E-03	s	Up	1,16	1,72E-01	n.s.	Down	-0,44
sp_0711		ABC Transporter	Environmental Information Processing	Membrane Transport	ABC Transporters	3,95E-01	n.s.	Down	-0,11	4,63E-04	s	Up	1,53	3,58E-01	n.s.	Down	-0,13
sp_0743		Transcriptional Regulator	Environmental Information Processing	Signal Transduction	Transcriptional Regulator	5,92E-01	n.s.	Up	0,19	2,44E-02	s	Down	-1,16	9,00E-02	n.s.	Up	0,62
sp_0783		Biotin Transport System	Environmental Information Processing	Membrane Transport	ABC Transporters	2,62E-01	n.s.	Down	-0,40	1,77E-02	s	Up	1,28	7,22E-01	n.s.	Down	-0,04
sp_0798	*ciaR*	Response Regulator	Environmental Information Processing	Signal Transduction	Two-Component Systems	4,22E-01	n.s.	Down	-0,14	2,42E-02	s	Up	1,30	7,07E-01	n.s.	Down	-0,09
sp_0799	*ciaH*	Histidine Kinase	Environmental Information Processing	Signal Transduction	Two-Component Systems	5,40E-01	n.s.	Down	-0,17	9,08E-02	n.s.	Up	1,01	5,72E-01	n.s.	Up	0,22
sp_0899		Hypothetical Protein	Unknown Function	Unknown Function	Unknown Function	8,13E-01	n.s.	Down	-0,07	2,92E-03	s	Down	-1,44	8,84E-01	n.s.	Up	0,04
sp_0912		ABC Transporter ATP-Binding Protein	Environmental Information Processing	Membrane Transport	ABC Transporters	3,47E-01	n.s.	Down	-0,38	1,76E-01	n.s.	Up	0,58	3,31E-01	n.s.	Down	-0,42
sp_0913		ABC Transporter Permease	Environmental Information Processing	Membrane Transport	ABC Transporters	8,53E-01	n.s.	Up	0,10	4,24E-02	s	Down	-1,16	3,09E-01	n.s.	Up	0,44
sp_0999	*ccdA2*	Cytochrome C-Type Biogenesis Protein	Environmental Information Processing	Membrane Transport	Other Transporters	3,47E-01	n.s.	Down	-0,35	1,14E-02	s	Up	1,15	6,22E-01	n.s.	Down	-0,17
sp_1032	*piaA*	ABC Transporter Substrate-Binding Protein	Environmental Information Processing	Membrane Transport	ABC Transporters	8,43E-01	n.s.	Down	-0,09	2,37E-02	s	Down	-1,00	6,01E-01	n.s.	Down	-0,24
sp_1033		Iron ABC Transporter Permease	Environmental Information Processing	Membrane Transport	ABC Transporters	8,59E-01	n.s.	Up	0,05	2,19E-01	n.s.	Down	-0,27	7,63E-01	n.s.	Up	0,10
sp_1034		Iron ABC Transporter Permease	Environmental Information Processing	Membrane Transport	ABC Transporters	7,27E-01	n.s.	Up	0,10	3,32E-02	s	Down	-0,57	3,38E-01	n.s.	Down	-0,29
sp_1035		ABC Transporter ATP-Binding Protein	Environmental Information Processing	Membrane Transport	ABC Transporters	6,22E-01	n.s.	Down	-0,17	1,37E-02	s	Down	-1,02	6,11E-01	n.s.	Down	-0,17
sp_1185	*lacE-2*	Phospho-Transfer System (PTS) - Lactose-Specific Transporter Subunit IIBC	Environmental Information Processing	Membrane Transport	Phospho-Transferase System	6,47E-01	n.s.	Up	0,15	1,89E-02	s	Up	0,96	6,41E-01	n.s.	Down	-0,15
sp_1186	*lacF-2*	Lactose Phospho-Transfer System (PTS)	Environmental Information Processing	Membrane Transport	Phospho-Transferase System	9,42E-01	n.s.	Down	-0,04	2,40E-02	s	Up	1,24	4,56E-01	n.s.	Down	-0,30
sp_1197		Galactose Phospho-Transfer System (PTS)	Environmental Information Processing	Membrane Transport	Phospho-Transferase System	5,84E-01	n.s.	Up	0,17	8,47E-03	s	Down	-1,15	9,32E-01	n.s.	Down	-0,01
sp_1198			Environmental Information Processing	Membrane Transport	Phospho-Transferase System	4,49E-01	n.s.	Down	-0,20	1,96E-01	n.s.	Down	-0,33	5,08E-02	n.s.	Down	-0,76
sp_1199		Hypothetical Protein	Unknown Function	Unknown Function	Unknown Function	7,22E-01	n.s.	Up	0,10	2,51E-01	n.s.	Down	-0,29	4,93E-01	n.s.	Down	-0,27
sp_1282		ABC Transporter ATP-Binding Protein	Environmental Information Processing	Membrane Transport	ABC Transporters	2,77E-03	s	Up	0,98	4,13E-04	s	Up	1,01	2,43E-01	n.s.	Up	0,08
sp_1315	*atpD*	V-Type Sodium ATP Synthase	Intermediary Metabolism	Energy Metabolism	Oxidative Phosphorylation	9,75E-04	s	Down	-1,53	7,96E-01	n.s.	Up	0,10	9,43E-03	s	Down	-1,36
sp_1316	*atpB*	V-Type ATP Synthase Subunit	Intermediary Metabolism	Energy Metabolism	Oxidative Phosphorylation	1,97E-01	n.s.	Down	-0,45	3,08E-01	n.s.	Up	0,29	7,47E-02	n.s.	Down	-0,79
sp_1317	*atpA*	V-Type ATP Synthase Subunit	Intermediary Metabolism	Energy Metabolism	Oxidative Phosphorylation	1,24E-01	n.s.	Down	-0,52	2,70E-01	n.s.	Up	0,32	6,91E-01	n.s.	Up	0,11
sp_1318	*ntpG*	V-Type ATP Synthase Subunit	Intermediary Metabolism	Energy Metabolism	Oxidative Phosphorylation	1,35E-01	n.s.	Down	-0,53	2,87E-01	n.s.	Up	0,34	2,96E-01	n.s.	Down	-0,44
sp_1319	*ntpC*	V-Type Sodium ATP Synthase	Intermediary Metabolism	Energy Metabolism	Oxidative Phosphorylation	8,42E-02	n.s.	Down	-0,68	3,38E-02	s	Up	0,86	3,56E-01	n.s.	Down	-0,45
sp_1320	*ntpE*	V-Type Sodium ATP Synthase	Intermediary Metabolism	Energy Metabolism	Oxidative Phosphorylation	1,08E-01	n.s.	Down	-0,62	1,34E-01	n.s.	Up	0,45	4,02E-01	n.s.	Down	-0,37

TABLES

Table S1: Gene expression change in TIGR4Δ*cps* and TCS08 mutants by microarray

TIGR4 Locus_Tag	*Gene Name*	Gene Product	General Function	Cellular or Metabolic Process	Metabolic Pathway or Specific Function	*TIGR4 wt vs TIGR4 Δrr08*				*TIGR4 wt vs TIGR4 Δhk08*				*TIGR4 wt vs TIGR4 Δtcs08*			
						p-value	Sig.	Regulation	Log FC	p-value	Sig.	Regulation	Log FC	p-value	Sig.	Regulation	Log FC
sp_1321	*ntpK*	V-Type ATP Synthase Subunit	Intermediary Metabolism	Energy Metabolism	Oxidative Phosphorylation	1,90E-02	s	Down	-0,89	1,01E-01	n.s.	Up	0,54	1,76E-01	n.s.	Down	-0,53
sp_1322	*ntpI*	V-Type ATP Synthase Subunit	Intermediary Metabolism	Energy Metabolism	Oxidative Phosphorylation	2,90E-01	n.s.	Up	0,30	2,67E-02	s	Up	0,65	2,53E-01	n.s.	Up	0,34
sp_1326	*nanA*	Neuraminidase	Colonization Factor	Cell Wall, Membrane Biogenesis	Glycan Degradation	1,26E-02	s	Down	-1,24	9,45E-01	n.s.	Down	-0,03	3,93E-02	s	Down	-1,13
sp_1341		ABC Transporter ATP-Binding Protein	Environmental Information Processing	Membrane Transport	ABC Transporters	5,42E-02	n.s.	Down	-0,63	1,33E-02	s	Down	-1,46	8,12E-01	n.s.	Up	0,06
sp_1342		ATP-Binding Cassette	Environmental Information Processing	Membrane Transport	ABC Transporters	4,83E-01	n.s.	Down	-0,31	3,39E-03	s	Down	-1,67	1,85E-01	n.s.	Up	0,37
sp_1346		CAAX Protease	Intermediary Metabolism	Lipid Metabolism	CAAX Protease	1,82E-02	s	Down	-1,01	7,65E-01	n.s.	Down	-0,07	1,01E-01	n.s.	Down	-0,67
sp_1434		ATP-Binding Cassette	Environmental Information Processing	Membrane Transport	ABC Transporters	8,10E-01	n.s.	Up	0,36	3,27E-02	s	Up	3,17	6,95E-01	n.s.	Up	0,43
sp_1435		ATP-Binding Protein	Environmental Information Processing	Membrane Transport	ABC Transporters	6,21E-01	n.s.	Up	0,52	3,23E-02	s	Up	2,48	6,45E-01	n.s.	Up	0,49
sp_1458	*trxB*	Thioredoxin Reductase	Intermediary Metabolism	Amino Acid Metabolism	Selenocompound Metabolism	6,22E-01	n.s.	Down	-0,15	1,06E-02	s	Up	1,07	8,81E-01	n.s.	Down	-0,06
sp_1459		Hypothetical Protein	Unknown Function	Unknown Function	Unknown Function	8,02E-02	n.s.	Up	0,63	1,18E-02	s	Up	0,94	2,36E-01	n.s.	Up	0,43
sp_1460		ABC Transporter ATP-Binding Protein	Environmental Information Processing	Membrane Transport	ABC Transporters	4,51E-01	n.s.	Up	0,22	1,59E-02	s	Up	1,18	9,79E-01	n.s.	Up	0,01
sp_1461		ABC Transporter Permease	Environmental Information Processing	Membrane Transport	ABC Transporters	7,62E-01	n.s.	Up	0,09	5,39E-03	s	Up	1,40	7,53E-01	n.s.	Down	-0,06
sp_1462		Arsenate Reductase	Environmental Information Processing	Arsenic Detoxification	Arsenate Reductase	4,12E-01	n.s.	Up	0,25	1,42E-02	s	Up	1,11	5,04E-01	n.s.	Up	0,19
sp_1492	*mucBP*	Surface-Exposed Protein	Colonization Factor	Cell Wall, Membrane Biogenesis	LPxTG Protein / Mucin-Binding Protein	1,84E-02	s	Down	-1,09	5,20E-01	n.s.	Down	-0,17	1,07E-01	n.s.	Down	-0,67
sp_1527	*aliB*	ABC Transporter Substrate-Binding Protein	Environmental Information Processing	Membrane Transport	ABC Transporters	9,94E-01	n.s.	Down	0,00	9,28E-03	s	Down	-2,39	5,04E-01	n.s.	Up	0,23
sp_1528		Hypothetical Protein	Unknown Function	Unknown Function	Unknown Function	1,92E-01	n.s.	Down	-0,42	1,34E-01	n.s.	Up	0,41	7,03E-02	n.s.	Up	0,81
sp_1647	*pepO*	Endopeptidase O	Colonization Factor	Physiological Processes	Endopeptidase	8,07E-01	n.s.	Down	-0,11	4,66E-02	s	Up	1,02	8,78E-01	n.s.	Down	-0,06
sp_1648	*psaB*	ABC Transporter ATP-Binding Protein	Environmental Information Processing	Membrane Transport	ABC Transporters	6,21E-01	n.s.	Up	0,32	9,88E-03	s	Up	1,57	9,59E-01	n.s.	Up	0,02
sp_1649	*psaC*	ABC Transporter Permease	Environmental Information Processing	Membrane Transport	ABC Transporters	3,31E-01	n.s.	Up	0,43	8,89E-03	s	Up	1,21	2,92E-01	n.s.	Up	0,31
sp_1650	*psaA*	ABC Transporter Substrate-Binding Protein	Environmental Information Processing	Membrane Transport	ABC Transporters	5,78E-01	n.s.	Up	0,34	7,95E-03	s	Up	1,50	7,03E-01	n.s.	Up	0,14
sp_1823		Putative Manganese Transporter	Environmental Information Processing	Membrane Transport	Other Transporters	2,87E-01	n.s.	Up	0,33	9,94E-03	s	Down	-1,13	8,04E-01	n.s.	Down	-0,09
sp_1824		ABC Transporter Permease	Environmental Information Processing	Membrane Transport	ABC Transporters	2,35E-01	n.s.	Down	-0,49	2,13E-01	n.s.	Up	0,36	8,96E-02	n.s.	Down	-0,69
sp_1825		ABC Transporter ATP-Binding Protein	Environmental Information Processing	Membrane Transport	ABC Transporters	1,82E-01	n.s.	Up	0,49	3,15E-03	s	Down	-1,21	2,22E-01	n.s.	Up	0,40
sp_1826		ABC Transporter Substrate-Binding Protein	Environmental Information Processing	Membrane Transport	ABC Transporters	3,46E-01	n.s.	Up	0,32	3,29E-02	s	Down	-1,14	9,11E-01	n.s.	Up	0,04
sp_1830	*phoU*	Transcriptional Regulator	Environmental Information Processing	Signal Transduction	Phosphate Transport System Regulatory Protein	9,13E-01	n.s.	Up	0,04	3,77E-03	s	Down	-1,14	5,67E-01	n.s.	Down	-0,21
sp_1856		Transcriptional Regulator	Environmental Information Processing	Signal Transduction	Transcriptional Regulator	2,63E-01	n.s.	Down	-0,47	1,65E-02	s	Up	1,04	7,57E-01	n.s.	Up	0,13
sp_1869		ABC Transporter Permease	Environmental Information Processing	Membrane Transport	ABC Transporters	1,57E-01	n.s.	Down	-0,57	3,72E-02	s	Up	1,24	1,80E-01	n.s.	Up	0,65
sp_1870		Iron ABC Transporter Permease	Environmental Information Processing	Membrane Transport	ABC Transporters	8,80E-02	n.s.	Down	-0,72	2,94E-02	s	Up	0,90	1,22E-01	n.s.	Up	0,80
sp_1871		ABC Transporter ATP-Binding Protein	Environmental Information Processing	Membrane Transport	ABC Transporters	9,22E-02	n.s.	Down	-0,77	3,43E-02	s	Up	1,17	4,14E-01	n.s.	Up	0,35
sp_1872	*piuA*	ABC Transporter Substrate-Binding Protein	Environmental Information Processing	Membrane Transport	ABC Transporters	8,07E-02	n.s.	Down	-0,72	2,09E-01	n.s.	Up	0,52	3,31E-01	n.s.	Up	0,43
sp_1884		Trehalose Phospho-Transfer System (PTS)	Environmental Information Processing	Membrane Transport	Phospho-Transferase System	3,09E-01	n.s.	Up	0,30	7,94E-01	n.s.	Up	0,09	2,99E-01	n.s.	Up	0,33
sp_1885	*treR*	Transcriptional Regulator	Environmental Information Processing	Signal Transduction	Transcriptional Regulator	7,64E-01	n.s.	Down	-0,18	8,39E-03	s	Down	-1,37	8,97E-01	n.s.	Up	0,06
sp_1894	*glfA*	Sucrose Phosphorylase	Intermediary Metabolism	Carbohydrate Metabolism	Starch and Sucrose Metabolism	8,67E-01	n.s.	Up	0,04	2,67E-03	s	Down	-1,12	1,55E-01	n.s.	Up	0,36
sp_1895	*ralG*	Sugar ABC Transporter Permease	Environmental Information Processing	Membrane Transport	ABC Transporters	4,94E-01	n.s.	Down	-0,21	3,66E-02	s	Down	-0,64	7,65E-01	n.s.	Down	-0,09

TABLES

Table S1: Gene expression change in TIGR4Δ*cps* and TCS08 mutants by microarray

TIGR4 Locus_Tag	*Gene Name*	Gene Product	General Function	Cellular or Metabolic Process	Metabolic Pathway or Specific Function	*TIGR4 wt vs TIGR4 Δrr08*				*TIGR4 wt vs TIGR4 Δhk08*				*TIGR4 wt vs TIGR4 Δtcs08*			
						p-value	Sig.	Regulation	Log FC	p-value	Sig.	Regulation	Log FC	p-value	Sig.	Regulation	Log FC
sp_1896	*ratF*	Sugar ABC Transporter Permease	Environmental Information Processing	Membrane Transport	ABC Transporters	5,83E-01	n.s.	Down	-0,22	9,42E-02	n.s.	Down	-0,72	6,43E-01	n.s.	Down	-0,16
sp_1897	*ratE*	ABC Transporter Substrate-Binding Protein	Environmental Information Processing	Membrane Transport	ABC Transporters	6,51E-01	n.s.	Up	0,18	1,27E-02	s	Down	-1,37	3,48E-01	n.s.	Up	0,37
sp_2006	*comX*	Transcriptional Regulator	Genetic Information Processing	Transcription	Transcriptional Regulator	2,92E-01	n.s.	Down	-0,50	2,40E-02	s	Down	-1,26	4,69E-01	n.s.	Down	-0,38
sp_2022		Phospho-Transfer System (PTS) - Transporter Subunit IIC	Environmental Information Processing	Membrane Transport	Phospho-Transferase System	6,66E-01	n.s.	Up	0,12	9,72E-02	n.s.	Down	-0,49	2,36E-01	n.s.	Up	0,38
sp_2023		Cellobiose Phospho-Transfer System (PTS)	Environmental Information Processing	Membrane Transport	Phospho-Transferase System	6,14E-01	n.s.	Down	-0,08	4,13E-03	s	Down	-1,14	3,78E-01	n.s.	Up	0,22
sp_2024		Phospho-Transfer System (PTS) - Transporter Subunit IIA	Environmental Information Processing	Membrane Transport	Phospho-Transferase System	9,69E-01	n.s.	Down	-0,01	4,53E-02	s	Down	-0,64	6,15E-01	n.s.	Up	0,18
sp_2106	*malP*	Glycogen Phosphorylase	Intermediary Metabolism	Carbohydrate Metabolism	Starch and Sucrose Metabolism	2,76E-01	n.s.	Down	-0,39	4,77E-02	s	Up	1,14	9,89E-01	n.s.	Down	-0,01
sp_2107	*malQ*	4-Alpha-Glucano-Transferase	Intermediary Metabolism	Carbohydrate Metabolism	Starch and Sucrose Metabolism	4,57E-01	n.s.	Down	-0,27	4,80E-02	s	Up	1,28	7,53E-01	n.s.	Up	0,10
sp_2108	*malX*	ABC Transporter Substrate-Binding Protein	Environmental Information Processing	Membrane Transport	ABC Transporters	9,68E-01	n.s.	Up	0,02	1,12E-02	s	Down	-1,31	4,99E-01	n.s.	Up	0,26
sp_2129	*ulaA*	Ascorbate Phospho-Transfer System (PTS)	Environmental Information Processing	Membrane Transport	Phospho-Transferase System	9,16E-01	n.s.	Up	0,04	2,41E-02	s	Down	-1,01	3,70E-01	n.s.	Up	0,33
sp_2130		Phospho-Transfer System (PTS) - Transporter Subunit IIB	Environmental Information Processing	Membrane Transport	Phospho-Transferase System	5,75E-01	n.s.	Up	0,17	1,99E-02	s	Down	-0,96	1,33E-01	n.s.	Up	0,48
sp_2136	*pcpA*	Choline-Binding Protein	Colonization Factor	Cell Wall, Membrane Biogenesis	Choline-Binding Protein (CBP)	5,39E-02	n.s.	Up	1,84	7,97E-04	s	Up	4,14	1,08E-01	n.s.	Up	0,81
sp_2148	*arcA*	Arginine Deiminase	Intermediary Metabolism	Amino Acid Metabolism	Arginine Biosynthesis	1,57E-03	s	Down	-2,16	1,82E-02	s	Up	1,19	2,43E-01	n.s.	Up	0,55
sp_2150	*arcB*	Ornithine Carbamoyl-Transferase	Intermediary Metabolism	Amino Acid Metabolism	Arginine Biosynthesis	1,84E-03	s	Down	-2,16	6,09E-03	s	Up	1,38	1,30E-01	n.s.	Up	0,62
sp_2151	*arcC*	Carbamate Kinase	Intermediary Metabolism	Amino Acid Metabolism	Arginine Biosynthesis	7,41E-04	s	Down	-2,06	7,13E-02	n.s.	Up	0,74	1,05E-01	n.s.	Up	0,83
sp_2152	*arcD*	Arginine-Ornithine Antiporter	Intermediary Metabolism	Amino Acid Metabolism	Arginine Biosynthesis	5,10E-03	s	Down	-1,50	2,04E-03	s	Up	1,32	5,03E-02	n.s.	Up	0,68
sp_2153	*arcT*	Putative Aminopeptidase	Intermediary Metabolism	Amino Acid Metabolism	Aminopeptidase	6,35E-03	s	Down	-1,14	4,10E-02	s	Up	0,92	1,85E-01	n.s.	Up	0,51
sp_2184	*glpF*	Glycerol Uptake Facilitator Protein	Environmental Information Processing	Membrane Transport	Other Transporters	6,39E-01	n.s.	Up	0,23	6,89E-03	s	Up	1,36	4,00E-01	n.s.	Up	0,31
sp_2185	*glpO*	Alpha-Glycero-Phosphate Oxidase	Intermediary Metabolism	Lipid Metabolism	Glycerophospholipid Biosynthesis	9,21E-01	n.s.	Down	-0,04	9,33E-03	s	Up	1,01	7,42E-01	n.s.	Down	-0,12
sp_2186	*glpK*	Glycerol Kinase	Intermediary Metabolism	Lipid Metabolism	Glycerophospholipid Biosynthesis	5,84E-01	n.s.	Up	0,23	1,32E-02	s	Up	1,05	9,61E-01	n.s.	Down	-0,02
sp_2235	*comE*	Response Regulator	Environmental Information Processing	Signal Transduction	Two-Component Systems	3,48E-01	n.s.	Down	-0,26	1,67E-01	n.s.	Down	-0,36	9,08E-01	n.s.	Up	0,03
sp_2236	*comD*	Histidine Kinase	Environmental Information Processing	Signal Transduction	Two-Component Systems	9,40E-01	n.s.	Up	0,03	2,70E-02	s	Down	-1,58	4,09E-01	n.s.	Up	0,41
sp_2237	*comC2*	Competence Stimulating Peptide 2	Environmental Information Processing	Membrane Transport	DNA Uptake / Competence Stimulator	9,39E-01	n.s.	Up	0,03	1,32E-02	s	Down	-1,06	3,34E-01	n.s.	Up	0,33

Table S2. Laboratory strains and mutants

***S. pneumoniae* strains**	**characteristics**	**reference**
PN111	D39Δ*cps*	Rennemeier et al., 2007
PN259	TIGR4Δ*cps*	Schulz et al., 2014
PN149	D39*lux*	Jensch et al., 2010
PN315	TIGR4*lux*	Schulz et al., 2014
***S. pneumoniae* mutants**	**characteristics**	**reference**
PN407	D39Δ*cps*Δ*rr08*	This study
PN412	D39Δ*cps*Δ*hk08*	This study
PN308	D39Δ*cps*Δ*tcs08*	This study
PN408	TIGR4Δ*cps*Δ*rr08*	This study
PN652	TIGR4Δ*cps*Δ*hk08*	This study
PN344	TIGR4Δ*cps*Δ*tcs08*	This study
PN409	D39*lux*Δ*rr08*	This study
PN414	D39*lux*Δ*hk08*	This study
PN372	D39*lux*Δ*tcs08*	This study
PN410	TIGR4*lux*Δ*rr08*	This study
PN415	TIGR4*lux*Δ*hk08*	This study
PN708	TIGR4*lux*Δ*tcs08*	This study
***E. coli* strains**	**characteristics**	**reference**
DH5α	Δ(*lac*)U169, *endA1*, *gyrA96*, *hsdR17*, Φ80Δ(*lacZ*)M15 recA1, relA1, supE44, thi-1	Novagen
BL21(DE3)	*E. coli B*, F- dcm *ompT hsdS gal λ* (DE3), T7 polymerase gene under control of the lacUV5 promoter	Stratagene

Table S3. Primers used in this study

Purpose	**Primer designation**	**Sequence (5'-3')**
		Insertion-deletion mutagenesis
Elongation of *hk08* gene	hk08_826	5`-GTGAGGTTCAATACTTATCACC-3`
	hk08_827	5`-CGTTATCCAAACGACGTTCC-3`
Inverse PCR of *hk08* cloned fragment	hk08_824	5`-CCGGGCTGCAGGTTAAGAGGGTTGAAATAATATAT-3`
	hk08_825	5`-CCGGCCTGCAGCCATCAATTGGGTGGGGAAATCA-3`
Elongation of *rr08* gene	rr08_249	5`-GCGCGCGGATCCCATCAGACACAGCAAATGGTTC-3`
	rr08_250	5`-GCGCGCCTGCAGGTGGACATCTCTTCTCTCCTG-3`
Inverse PCR of *rr08* cloned fragment	rr08_984	5`-TCATCGGGTACCCATGGGCTACCAAGACCTGA-3`
	rr08_985	5`-TCACTGCTCGAGTAAGACAGTTTGGGGGTTGG-3`
Elongation of *tcs08* genes	rr08_249	5`-GCGCGCGGATCCCATCAGACACAGCAAATGGTTC-3`
	rr08_250	5`-GCGCGCCTGCAGGTGGACATCTCTTCTCTCCTG-3`
Inverse PCR of *tcs08* cloned fragment	tcs08_252	5`-GCGCGCAAGCTTTTGAACAGCTCTAGCGCTTC-3`
	tcs08_253	5`-GCGCGCAAGCTTTGATTCCTTGGAAGAAAGC-3`
		Antibiotic cassette preparation
Spectinomycin (*aad9*)	spec_117	5'-AAAAAGCTTGAATTCGGATCCATCGATTTTCGTTCGTGAATAC3'
	spec_118	5'-AAAAAGCTTGCTAGCAATTAGAATGAATATTTCCC-3'
Erythromycin (*ermB*)	*ermpstI1_67*	5'-GCGCGCCTGCAGACGGTTCGTGTTCGTGCTG-3'
	Ermpst2_68	5'-GCGCGCCTGCAGCGTAGGCGCTAGGGACCTC-3'
Erythromycin (*ermB*)	*erm*_105	5'-GATGATGATGATCCCGGGTACCAAGCTTGAATTCACGGTTCGTGTTCGTGCTG-3'
	*erm*_106	5'-AGTGAGTGAGTCCCGGGCTCGAGAAGCTTGAATTCGTAGGCGCTAGGGACCTC-3'
		Real-Time PCR
arcA (sp_2148)	*arcA*RT_0611	5'-TGCCGGACTATCTTGAAAGG-3'
	*arcA*RT_1578	5'-GAGAGGTCAATGATTCAGCA-3'
arcD (sp_2152)	RT_*arcD*_F_1676	5'-GGGGCCTTTATAGAAGGTAT-3'
	RT_*arcD*_R_1677	5'-GGCTACATCAATCGCTGCG-3'
psaA (sp_1650)	RT_*psaA*_F_1680	5'-GCTACAAACTCAATCATCGC-3'
	RT_*psaA*_R_1681	5'-GAAAATCAAATTAGCCTCAGAA-3'
pavB (sp_0082)	*pavB*RT_1436	5'-CGGTGTTGCCTCAGTTGTTG-3'
	*pavB*RT_1437	5'-CCCTCAGGTTTCGCTTGAGT-3'
rrgB (sp_0463)	*rrgB*RT_1488	5'-AGCAGAAACGCCTGAAACCA-3'
	*rrgB*RT_1489	5'-CCTGTTTGCGCCTCTGTCC-3'
ribosomal protein S16 (sp_0775)	RT_16S_F	5'-CTACCGTATCAACGTAGCAG-3'
	RT_16S_R	5'-AGTTACTTGGTTTTCAGCAACA-3'
rr08 (sp_0083)	F_qRTPCR_RR08_1702	5'-AGGCAGGTTATCAGGTCTTG-3'
	R_qRTPCR_RR08_1703	5'-TTCACTGGTCTTAGCAGTAATA-3'
hk08 (sp_0084)	F_qRTPCR_HK08_1704	5'-AGGCGAGATTTACTTTTTGCT-3'
	R_qRTPCR_HK08_1705	5'-CTAATTGCTGAAATTCTACAGG-3'

Table S4. Plasmids used in this study

Plasmids	Features	Source
	Commercial plasmids	
pGEM-T Easy	Cloning Vector (3016bp), Amp^r	Promega
pSP72	Cloning Vector (2462bp), Amp^r	Promega
	Mutagenesis plasmids	
p927	pGEM-T Easy variant with *sp_0084* construct for mutagenesis	This study
p928	pGEM-T Easy variant with *sp_0083* construct for mutagenesis	This study
p896	pGEM-T Easy variant with *sp_0083+sp_0084* construct for mutagenesis	This study

Table S5. *In silico* search for RR08 binding motifs

TIGR4 Locus_Tag	TIGR4 new Locus_Tag	binding motif search (5'-3')	Genomic position (bp)
sp_0082	sp_rs00425	tataa-N6-tttaa-N7-tttaa-N16-tttaa	86,193
sp_0083	sp_rs00430	aaatt-N39-aattt-N32-aattt	88,916
sp_0084	sp_rs00435	ND	NA
sp_0085	sp_rs00440	ND	NA
sp_0090	sp_rs00460	ttaaa-N40-ttaaa-N159-tttaaa-N41-tttaa	92,642
sp_0091	sp_rs00465	ND	NA
sp_0092	sp_rs00475	ND	NA
sp_0101	sp_rs00510	aaatt-N67-tataa-N56-aaatt-N6-tataa	102,070
sp_0111	sp_rs00565	ttaaa-N8-ttaaa-N48-aaatt-N15-aaatt-N65-tttaa	112,758
sp_0112	sp_rs00570	atatt-N36-atatt-N28-tttaa-N8-aaatt-N2-aattt	113,913
sp_0144	sp_rs00740	tttaa-N104-gttaa	141,586
sp_0148	sp_rs00765	tttaa-N39-tataa-N21-gttaa	145,404
sp_0198	sp_rs00960	aaatt-N207-aaatt-N-48-aaatt-N5-aaatt-N13-aaatt	184,314
sp_0247	sp_rs01200	gttaa-N16-gttaa	216,720
sp_0248	sp_rs01205	tataa-N76-tttaa	217,791
sp_0249	sp_rs01210	tttaa-N6-aaatt-N55-ttaac	218,197
sp_0250	sp_rs01215	aaatt-N51-aaatt-N74-aaatt	218,354
sp_0251	sp_rs01220	gttaa-N29-gttaa-N10-gttaa	219,933
sp_0278	sp_rs01355	atatt-N37-caatt-N17-caatt	255,677
sp_0317	sp_rs01540	ND	NA
sp_0318	sp_rs01545	tttaa-N41-tttaa	293,621
sp_0319	sp_rs01550	ND	NA
sp_0320	sp_rs01555	gttaa-N8-tataa-N51-tataa-N48-ttaaa-N3-gttaa-N26-tttaa-N43-tataa	294,998
sp_0321	sp_rs01560	ttaaa-N3-gttaa-N26-tttaa-N43-tataa	295,120
sp_0322	sp_rs01565	tttaa-N106-gttaa-N44-gttaa	295,417
sp_0323	sp_rs01570	tttaa-N91-ttaaa-N22-tttaa-N64-tttaa	296,377
sp_0324	sp_rs01575	tttaa-N149-tttaa-N59-tttaa	297,163
sp_0325	sp_rs01580	tttaa-N18-aattt	297,811
sp_0369	sp_rs01800	gttaa-N10-ttaac-N115-ttaaa-N46-tttaa-N40-tataa-N155-ttaac-N82-gttaa	346,311
sp_0394	sp_rs01955	tataa-N2-tttaa-N63-tttaa-N5-tttaa-N16-tttaa	372,180
sp_0395	sp_rs01960	gttaa-N184-ttaac-N74-ttaac-N118-aaatt-N15-tttaa	373,521
sp_0396	sp_rs01965	tttaa-N37-ttata-N56-tttaa	375,922
sp_0397	sp_rs01970	aaatt-N7-aaatt-N31-ttaaa	376,387
sp_0415	sp_rs02050	tttaa-N92-tttaa-N45-tttaa-N40-ttata-N141-tttaa-N89-tttaa-N16-tataa-N6-tataa	393,858
sp_0416	sp_rs02055	tttaa-N81-ttaaa-N63-tttaa-N106-aaatt-N35-aattt-N3-tataa	394,847
sp_0417	sp_rs02060	tttaa-N8-tttaa-N43-tttaa-N121-aattt-N128-aaatt-N22-aattt-N34-aattt	395,249
sp_0418	sp_rs02065	tataa-N13-tttaa	396,656

sp_0419	sp_rs02070	ND	NA
sp_0420	sp_rs02075	gttaa-N177-ttaac-N183-tttaa-N60-ttaaa-N42-tttaa	397,298
sp_0421	sp_rs02080	ND	NA
sp_0422	sp_rs02085	ND	NA
sp_0423	sp_rs02090	ND	NA
sp_0424	sp_rs02095	ND	NA
sp_0425	sp_rs02100	tttaa-N133-gttaa	401,557
sp_0426	sp_rs02105	gttaa-N37-gttaa-N64-tttaa-N87-ttata-N239-tttaa-N3-tttaa	402,789
sp_0427	sp_rs02110	ND	NA
sp_0461	sp_rs02275	tttaa-N4-tataa-N38-aattt-N38-tttaa-N79-tataa-N41-tttaa-N15-gttaa-N62-tataa-N7-ttata-N29-ttaac-N83-ttaac-N18-ttaac	437,864
sp_0462	sp_rs02280	tttaa-N4-tataa-N38-aattt-N38-tttaa-N79-tataa-N41-tttaa-N15-gttaa-N62-tataa-N7-ttata-N29-ttaac-N83-ttaac-N18-ttaac	437,864
sp_0463	sp_rs02285	tttaa-N21-tttaa-N127-tttaa	441,046
sp_0464	sp_rs02290	ND	NA
sp_0465	#N/A	ND	NA
sp_0466	sp_rs02295	ND	NA
sp_0467	sp_rs02300	ND	NA
sp_0468	sp_rs02305	ND	NA
SP_0476	sp_rs02350	tttaa-N5-tttaa-N43-tttaa	455,401
SP_0477	sp_rs02355	ND	NA
sp_0478	sp_rs02360	tttaa-N5-tttaa	457,294
sp_0479	sp_rs02365	tttaa-N15-tttaa	459,076
sp_0480	sp_rs02370	ND	NA
sp_0507	sp_rs02490	ND	NA
sp_0508	sp_rs02495	ttaac-N41-ttaac-N18-tataa-N37-ttata	488,567
sp_0516	sp_rs02525	ND	NA
sp_0517	sp_rs02530	aattt-N123-aattt-N-106-ttaac	497,222
sp_0518	#N/A	ND	NA
sp_0519	sp_rs02540	tataa-N12-ttata-N5-tttaa-N12-gttaa-N144-tataa	499,680
sp_0605	sp_rs02975	gttaa-N54-tttaa	571,361
sp_0607	sp_rs02985	ND	NA
sp_0608	sp_rs02990	tttaa-N23-gttaa	574,859
sp_0609	sp_rs02995	ND	NA
sp_0611	sp_rs03005	tttaa-N41-tataa-N46-aaatt-N101-tataa-N5-tataa-N37-tataa-N	577,154
sp_0620	sp_rs03045	ND	NA
sp_0641	sp_rs03145	tttaa-N18-ttaac-N5-gttaa-N10-ttaaa-N4-tttaa-N31-ttatatataa-N42-tataa-N14-gttaa-N23-tataa-N12-ttaaa	603,681
sp_0646	sp_rs03160	ND	NA
sp_0647	sp_rs03165	ttaaa-N8-attaa-N14-gttaa	613,501
sp_0668	sp_rs03280	ttaac-N13-aaatt-N42-ttaac	643,880
sp_0709	sp_rs03470	ND	NA
sp_0710	sp_rs03475	ND	NA
sp_0711	sp_rs03480	ttaaa-N79-gttaa	675,224

2

sp_0743	sp_rs03640	gttaa-N21-gttaa-N63-aaatt-N15-ttata-N30-ttata	704,730
sp_0783	sp_rs03825	gttaa-N25-ttata-N28-tttaa-N79-aattt-N16-ttata-N	736,712
sp_0798	sp_rs03905	tttaa-N4-aattt-N3-tataa-N4-tttaa	751,915
sp_0799	sp_rs03910	ttaaa-N36-tttaa-N-31-gttaa-N16-gttaa	752,283
sp_0899	sp_rs04440	ttaaa-N6-ttaag-N43-ttaaa-N31-gttaa-N6-tttaa	854,511
sp_0912	sp_rs04505	ttata-N19-gttaa-N94-tttaa-N36-ttata-N28-ttaaa-N127-aaatt	864,298
sp_0913	sp_rs04510	ttaaa-N54-tttaa-N19-gttaa-N39-tataa-N14-aaatt-N26-gttaa-	864,932
sp_0999	sp_rs04955	ND	NA
sp_1032	sp_rs05120	tttaa-N43-tttaa-N46-tttaa-N132-gttaa-N18-tttaa-N34-ttata-N3-ttaaa-N59-tttaa	973,021
sp_1033	sp_rs05125	tttaa-N29-ttaaa-N32-aaatt-N112-ttaaa	974,106
sp_1034	sp_rs05130	tttaa-N16-tttaa-N26-aaatt-N108-tttaa-N41-gttaa-N1-gttaa-N86-ttata-N22-ttata-N37-ttata-N16-ttata-N5-tataa	974,902
sp_1035	sp_rs05135	tttaa-N16-tttaa-N65-aattt	976,158
sp_1185	sp_rs05830	ttaaa-N15-tttaa	1,124,503
sp_1186	sp_rs05835	ttata-N4-tttaa-N57-ttata-N75-tttaa	1,124,805
sp_1197	sp_rs05885	tttaa-N57-aattt-42-ttaac	1,131,638
sp_1198	sp_rs5890	ttaac-Ntataa-N1-tataa-N17-gttaa_N29-ttata-N12-ttata-N5-ttata	1,132,148
sp_1199	#N/A	ND	NA
sp_1282	sp_rs06285	aattt-N18-aattt-N2-ttaaa-N2-tataa-N0-tataa-N123-gttaa-N225-ttaaa-N2-tttaa	1,216,096
sp_1315	sp_rs06455	ttaaa-N47-tttaa-N67-ttata	1,239,170
sp_1316	sp_rs06460	tataa-N7-ttata-N49-tataa	1,240,544
sp_1317	sp_rs06465	tttaa-N7-tttaa	1,242,443
sp_1318	sp_rs06470	ND	NA
sp_1319	sp_rs06475	aattt-N14-aattt-N11-ttaac	1,243,725
sp_1320	sp_rs06480	gttaa-N11-ttaaa	1,244,620
sp_1321	sp_rs06485	ttaaa-N4-tttaa-N34-tttaa	1,245,601
sp_1322	sp_rs06490	ND	NA
sp_1326	sp_rs06510	tttaa-N27-tttaa-N18-tttaa	1,251,613
sp_1341	sp_rs06580	tttaa-N38-aattt-N23-ttata-N22-tttaa-N62-aattt-N15-aaatt	1,263,996
sp_1342	sp_rs11490	tataa-N23-tttaa-N11-ttaaa-N21-tttaa	1,264,708
sp_1346	sp_rs06600	tttaa-N19-gttaa-N19-ttaaa	1,271,721
sp_1434	sp_rs07035	attaa-N22-ttata-N38-attaa-N6-ttata-N12-attaa	1,352,482
sp_1435	sp_rs07040	ttaaa-N14-tttaa-N100-tttaa	1,353,934
sp_1458	sp_rs07165	ND	NA
sp_1459	sp_rs07170	tttaa-N45-ttata	1,375,544
sp_1460	sp_rs07175	ND	NA
sp_1461	sp_rs07180	aaatt-N64-ttata	1,377,196
sp_1462	sp_rs07185	ND	NA
sp_1492	sp_rs07345	ND	NA
sp_1527	sp_rs07525	tttaa-N12-ttata	1,439,510
sp_1528	#N/A	ND	NA
sp_1647	sp_rs08130	ttaac-N31-tttaa-N17-ttata-N61-tataa-N6-aattt-N42-tttaa-N12-ttaac-N16-tttaa	1,547,610

sp_1648	sp_rs08135	tttaa-N12-ttaac-N16-tttaa	1,547,791
sp_1649	sp_rs08140	ND	NA
sp_1650	sp_rs08145	ND	NA
sp_1823	sp_rs09045	gttaa-N6-gttaa-N2-tttaa	1,734,445
sp_1824	sp_rs09050	tttaa-20-ttaac-N2-tttaa	1,736,639
sp_1825	sp_rs09055	tttaa-N16-tttaa	1,736,936
sp_1826	sp_rs09060	aaatt-N3-gttaa	1,738,258
sp_1830	sp_rs09080	ttaac-N16-ttaac-N25-tttaa-N75-ttaaa-N11-ttaac-N55-ttaaa	1,742,145
sp_1856	sp_rs09210	tttaa-N66-ttata-N57-ttaac-N17-ttata-N18-aattt-N8-tttaa	1,764,323
sp_1869	sp_rs09270	ttaaa-N8-aattt-N29-ttata-N62-tttaa	1,774,413
sp_1870	sp_rs09275	ND	NA
sp_1871	sp_rs09280	ttata-N52-ttata-N27-ttaac	1,776,205
sp_1872	sp_rs09285	tttaa-N25-ttaaa	1,777,244
sp_1884	sp_rs09350	ttaaa-N16-tttaa-N30-tttaa	1,788,798
sp_1885	sp_rs09355	ttaaa-N16-tttaa-N30-tttaa	1,788,798
sp_1894	sp_rs09405	tttaa-N123-tttaa	1,800,976
sp_1895	sp_rs09415	ttaaa-N47-taatt-N48-tttaa-N9-tataa	1,802,243
sp_1896	sp_rs09420	gttaa-N43-ttaaa-N16-ttaat	1,803,475
sp_1897	sp_rs09425	gttaa-N52-ttata-N22-tttaa-N1-tttaa	1,804,532
sp_2006	sp_rs10155	ND	NA
sp_2022	sp_rs10230	tttaa-N22-gttaa	1,927,192
sp_2023	sp_rs10235	ttaac-N80-tttaa-N29-ttaat-N112-ttata-N46-tttaa-N42-ttata-N27-ttaaa-N94-gttaa-N29-gttaa	1,928,668
sp_2024	sp_rs10240	gttaa-N29-gttaa-N12-aattt-N38-gttaa	1,929,132
sp_2106	sp_rs10735	gttaa-N117-tttaa-N16-ttaat	2,018,567
sp_2107	sp_rs10740	gttaa-N46-ttata-N34-tttaa-N18-tttaa-N29-ttaaa	2,020,215
sp_2108	sp_rs10745	ttaaa-N37-ttaaa-N27-ttaaa-N5-tttaa	2,020,544
sp_2129	sp_rs10865	ttaaa-N65-tataa-N27-ttaat-N30-tttaa	2,041,877
sp_2130	sp_rs10870	tttaa-N18-tttaa-N7-tttaa-N24-ttaaa-N22-ttaaa-N6-gttaa-N13-tttaa	2,042,221
sp_2136	sp_rs10900	gttaa-N23-tttaa-N36-ttata-N16-ttata-N45-ttata-N34-tttaa-N2-tttaa-N11-ttaac-N4-tttaa-N7-tttaa-N5-gttaa-N8-ttaaa_N4-gttaa-N8-ttaac	2,048,492
sp_2148	sp_rs10955	tttaa-N7-ttata-N6-ttata-N43-tataa-N29-ttata-N15-ttata-N26-ttata-N43-tttaa	2,061,922
sp_2150	sp_rs10960	ND	NA
sp_2151	sp_rs10965	tataa-N16-ttaaa	2,064,541
sp_2152	sp_rs10970	tttaa-N45-tttaa	2,065,663
sp_2153	sp_rs10975	tataa-N32-tataa-N9-ttaaa-N18-ttaaa	2,067,274
sp_2184	sp_rs11155	ttaaa-N48-ttaaa-N58-tttaa	2,102,709
sp_2185	sp_rs11160	ND	NA
sp_2186	sp_rs11165	tttaa-N2-tttaa-N44-ttaac-N7-tttaa-N51-tttaa	2,106,284
sp_2235	sp_rs11425	ttaaa-N20-ttaaa-N85-tttaa	2,156,404
sp_2236	sp_rs11430	tataa-N29-ttaaa-N19-ttaaa	2,157,638
sp_2237	sp_rs11435	tttaa-N43-tttaa-N63-ttata-N66-tttaa	2,157,819

Figure S1

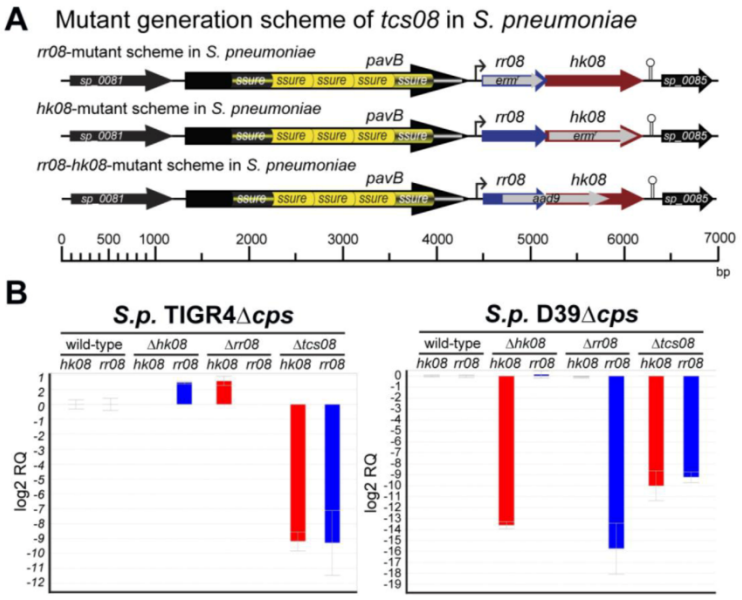

FIG S1: Generation of pneumococcal *tcs08* mutants. (A) Schematic model of the gene organization and insertion deletion mutagenesis by allelic replacement of the *tcs08* operon in *S. pneumoniae* TIGR4 as an example for all produced mutants. An *in silico* search for operon conformation identified the transcription start and terminator for the *tcs08* operon as indicated by the black arrow and lollipop, respectively. (B) Mutants were also confirmed by real-time PCR (qPCR). Specific primers were used for *rr08* and *hk08*. Additionally, the ribosomal protein S16 (*sp_0775*) was used as a control.

Figure S2

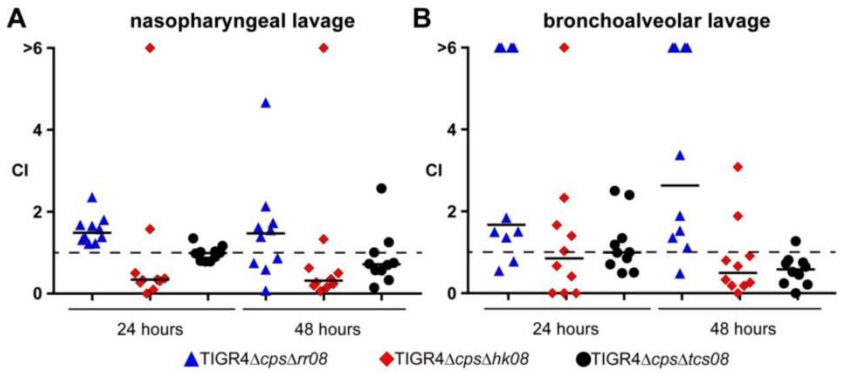

FIG S2: Coinfection assay with TIGR4 wild type and isogenic *tcs08* mutants. Competition assays between wild type and TCS08 mutants were carried out in *S. pneumoniae* TIGR4. CD-1 mice were intranasally inoculated with a mixture of bioluminescent TIGR4 and each *tcs08* mutant with an infection dose of 2.5 × 10^7 bacteria of each strain. Mice were sacrificed, and the samples were collected after 24 and 48 h. Colony determination data were plotted as the mutant/wild-type ratio to determine the CI for the nasopharyngeal (A) and bronchoalveolar (B) lavages. Results are displayed as scatter plots with each dot representing one mouse and the solid line indicating the median.

Figure S3

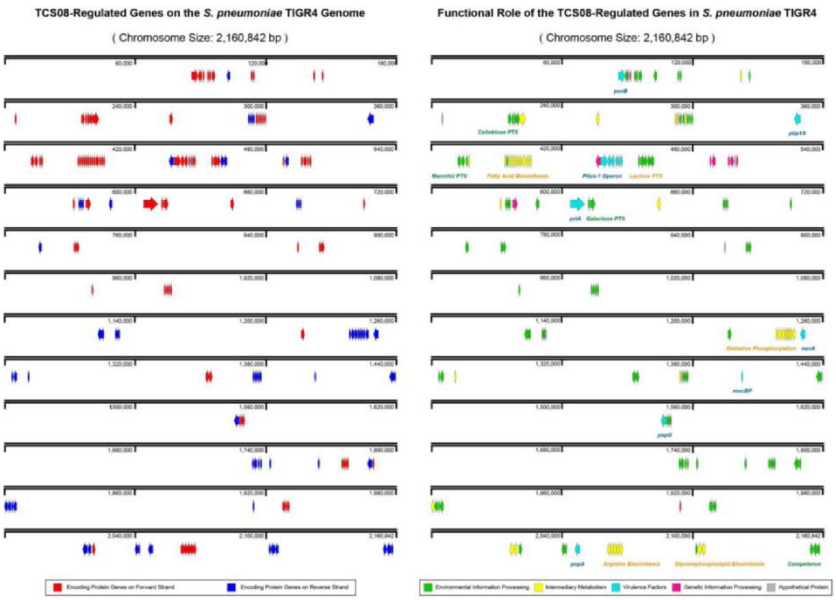

FIG S3: Localization, orientation, and grouping of the regulated genes (159 genes found by the microarray study) by the pneumococcal TCS08. Genes under regulation by the pneumococcal TCS08 are illustrated in a linear representation of the genome of *Streptococcus pneumoniae*. The left panel indicates the localization and orientation of each gene, where localization on the positive strand is indicated by red and that on the negative strand is indicated in blue. The right panel of the figure groups the genes in 5 different biochemical categories according to the characterization suggested by the databases KEGG (Kyoto Encyclopedia of Genes and Genomes) and BacMap (Bacterial Map genome atlas): green indicates environmental information processing (EIP), yellow indicates intermediary metabolism (IM), blue indicates colonization factors (CF), pink indicates genetic information processing (GIP), and gray indicates genes of unknown function (UF).

Figure S4

***Streptococcus pneumoniae* HK08 and *Staphylococcus aureus* SaeS protein sequence alignment**

```
TIGR4   SP0084_HK08      --MKLKSYIL VGYIISTLLT ------ILVV FWAVQKMLIA KGEIYFLLGM TIVASLVGAG  60 aa
Newman  NWMN0674_SaeS    MVLSIRSQII IGVVSSIPLT STILAIAYIL MWFNGHMTLT LT------LT TIITSCLTLL
                           :.::* *: :* : *  **          :: ::*   :* ::          **::* :
TIGR4   SP0084_HK08      ISLFLLLPVF TSLGKLKEHA KRVAAKDFPS N-LEVQGPVE FQQLGQTFNE MSHDLQVSFD 120 aa
Newman  NWMN0674_SaeS    ICSIFINPLI QKIKQFNIKT KQFANGNYAS NDKTFNSPKE IYELNQSFNK MASEITQQMN
                          *. ::: *::  .: ::: :: *:.*  :: * *    .:.* * : :*.*:**: *: ::  .::
TIGR4   SP0084_HK08      SLEESEREKG LMIAQLSHDI KTPITSIQAT VEGILDGIIK ESEQAHY-LA TIGRQTERLN 180 aa
Newman  NWMN0674_SaeS    QIKSEQQEKT ELIQNLADL KTPLASIISY SEGLRDGIIT KDHEIKESYD ILIKQANRLS
                          .::..::**   :* :*:**: ***::** :   **: ****. :..: :     : :*::**.
TIGR4   SP0084_HK08      KLVEELNF-L TLNTARNQVE TTSKDSIFLD KLLIECMSEF QFLIEQERRD VHLQVIPESA 240 aa
Newman  NWMN0674_SaeS    TLFDDMTHII TLNTG----K TYPPELIQLD QLLVSILQPY EQRIKHENRT LEVNFCNEID
                          .*.:::.. : ****.    : *   : * ** :**:. :. : :  *::*.*  :.::.  *
TIGR4   SP0084_HK08      RIEGDYAKLS RILVNLVDNA FKYSAPGTKL EVVA--KLEK DQLSISVTDE GQGIAPEDLE 300 aa
Newman  NWMN0674_SaeS    AFYQYRTPLE RILTNLLDNA LKFSNVGSRI DINISENEDQ DTIDIAISDE GIGIIPELQE
                           :    : *. ***.**:*** :*:*  *::: ::    : :: * :.*:::** * ** **  *
TIGR4   SP0084_HK08      NIFKRLYRVE TSRNMKTGGH GLGLAIAREL AHQLGGEITV SSQYGLGSTF TLVLNLSGSE 360 aa
Newman  NWMN0674_SaeS    RIFERTFRVE NSRNTKTGGS GLGLYIANEL AQQNNAKISV SSDIDVGTTM TVTLHKLDIT
                          .**:* :*** .*** ****  **** **.** *:* ..:*:* **: .:*:*: *:.*:  .
TIGR4   SP0084_HK08      NKA                                                              363 aa
Newman  NWMN0674_SaeS    S--
                          .
```

***Streptococcus pneumoniae* RR08 and *Staphylococcus aureus* SaeR protein sequence alignment**

```
TIGR4   SP0083_RR08      MGKTILLVDD EVEITDIHQR YLIQAGYQVL VAHDGLEALE LFKKKPIDLI ITDVMMPRMD  60 aa
Newman  NWMN0675_SaeR    -MTHLLIVDD EQDIVDICQT YFEYEGYKVT TTTSGKEAIS LLS-NDIDIM VLDIMMPEVN
                           . :*:*** * :*.** *  *:   **:*  .: .* **:. *:. : **:: : *:***.::
TIGR4   SP0083_RR08      GYDLISEVQY LSPEQPFLFI TAKTSEQDKI YGLSLGADDF IAKPFSPREL VLRVHNILRR 120 aa
Newman  NWMN0675_SaeR    GYDIVKEMKR QKLDIPFIYL TAKTQEHDTI YALTLGADDY VKKPFSPREL VLRINNLLTR
                          ***::.*::   . : **::: ****.*:*.* *.*:*****: : ******** ***::*:* *
TIGR4   SP0083_RR08      LHRGGET--E LISLGNLKMN HSSHEVQIGE EMLDLTVKSF ELLWILASNP ERVFSKTDLY 180 aa
Newman  NWMN0675_SaeR    MKKYHHQPVE QLSFDELTLI NLSKVVTVNG HEVPMRIKEF ELLWYLASRE NEVISKSELL
                          ::: .   *  :*:.:*.:  : *: * :.  . : : :*.* **** ***.  :.*:**::*
TIGR4   SP0083_RR08      EKIWKEDYVD DTNTLNVHIH ALRQELAKYS SDQTPTIKTV WGLGYKIEKP RGQT       234 aa
Newman  NWMN0675_SaeR    EKVWGYDYYE DANTVNVHIH RIREKLEKES -FTTYTITTV WGLGYKFERS R---
                          **:*  ** : *:**:*****  :*::* * *    * **.** ******:*:  *
```

FIG S4: Staphylococcal SaeRS and pneumococcal TCS08 sequence alignment. Amino acid sequence alignment between the histidine kinases and response regulators of the pneumococcal TCS08 and the staphylococcal SaeRS systems. The red residues indicate the reported histidine and aspartate residues for SaeS and SaeR, respectively. The sequence comparison was performed using the Clustal Omega tool from the EMBL-EBI, and the protein sequences were retrieved using the Kyoto Encyclopedia of Genes and Genomes (KEGG). The asterisk indicates a score of 1, the colon indicates a score of >0.5, and the single period indicates a score of >0 and <0.5.

5. Own Contributions to Publications

Publication 1

The Two-component System 09 Regulates Pneumococcal Carbohydrate Metabolism and Capsule Expression. **Stephanie Hirschmann**, Alejandro Gómez-Mejia, Ulrike Mäder, Julia Karsunke, Dominik Driesch, Manfred Rohde, Susanne Häussler, Gerhard Burchhardt and Sven Hammerschmidt

Microorganisms, 2021 Feb 24;9(3):468. doi: 10.3390/microorganisms9030468

Stephanie Hirschmann:	Design of the study; generation of pneumococcal mutants; growth analysis; RNA purification; RNA-seq Data analysis; qPCR analysis, electron microscopy sample preparation, CPS quantification by flow cytometry; visualization of pneumococcal colony phase variation; autolysis assay with Triton X-100; hydrogen peroxide toxicity test; Data Analysis; Data Visualization; Original Draft and Correction of the Manuscript
Alejandro Gómez-Mejia:	Generation of pneumococcal mutants; growth analysis; Editing Manuscript
Ulrike Mäder:	RNA-seq Data Analysis; Correction of the Manuscript
Julia Karsunke:	Generation of pneumococcal mutants
Dominik Driesch:	RNA-seq Data Analysis; Visualization of PCA and Volcano plots
Manfred Rohde:	Electron microscopy sample preparation and image analysis
Susanne Häussler:	RNA-sequencing and library preparation
Gerhard Burchhardt:	Generation of pneumococcal mutants
Sven Hammerschmidt:	Design of the study; Data Analysis; Original Draft and Correction of the Manuscript; Funding Acquisition; Project Administration, Supervision

Publication 2

The two-component system 09 of *Streptococcus pneumoniae* is important for metabolic fitness and resistance during dissemination in the host.
Stephanie Hirschmann, Alejandro Gómez-Mejia, Thomas P. Kohler, Franziska Voß, Manfred Rohde, Max Brendel and Sven Hammerschmidt
Microorganisms, submitted May 2021, Manuscript ID: microorganisms-1253919

Stephanie Hirschmann:	Design of the study; generation of pneumococcal mutants; growth analysis; protein expression analysis using LI-COR; electron microscopy sample preparation; infection of A549 cells with pneumococci and pneumococcal adherence analysis; infection of J774 cells with pneumococci and quantification of phagocytosed pneumococci; acute pneumonia infection model; systemic infection model; co-infection model; Data Analysis; Visualization; Original Draft of the Manuscript
Alejandro Gómez-Mejia:	Generation of pneumococcal mutants; growth analysis; protein expression analysis using LI-COR; acute pneumonia infection model; systemic infection model; Editing Manuscript
Thomas P. Kohler:	Co-infection model; Editing Manuscript
Franziska Voß:	Co-infection model; Editing Manuscript
Manfred Rohde:	Electron microscopy sample preparation and image analysis
Max Brendel:	Co-infection model
Sven Hammerschmidt:	Design of the study; Data Analysis; Original Draft of the Manuscript; Funding Acquisition; Project Administration, Supervision

Publication 3

Pneumococcal Metabolic Adaptation and Colonization Are Regulated by the Two-Component Regulatory System 08. Alejandro Gómez-Mejia, Gustavo Gámez, **Stephanie Hirschmann**, Viktor Kluger, Hermann Rath, Sebastian Böhm, Franziska Voss, Niamatullah Kakar, Lothar Petruschka, Uwe Völker, Reinhold Brückner, Ulrike Mäder and Sven Hammerschmidt

mSphere, 2018 May 16;3(3):e00165-18. doi: 10.1128/mSphere.00165-18

Alejandro Gómez-Mejia:	Design of the study; Sample Preparation; Investigation; Data Analysis; Visualization; Original Draft and Correction of the Manuscript
Gustavo Gámez:	Design of the study; Generation of pneumococcal mutants; Data Analysis; Correction of the Manuscript
Stephanie Hirschmann:	Protein expression analysis using LI-COR; acute pneumonia infection model; systemic infection model; co-infection model
Viktor Kluger:	Generation of pneumococcal mutants
Hermann Rath:	Microarray analysis; Correction of the Manuscript
Sebastian Böhm:	Generation of pneumococcal mutants
Franziska Voss:	Surface abundance of proteins by flow cytometry
Niamatullah Kakar:	Protein expression analysis using LI-COR
Lothar Petruschka:	Microarray analysis
Uwe Völker:	Correction of the Manuscript
Reinhold Brückner:	Development or design of methodology; creation of models; Correction of the Manuscript
Ulrike Mäder:	Microarray analysis; Correction of the Manuscript
Sven Hammerschmidt:	Design of the study; Data Analysis; Original Draft and Correction of the Manuscript; Funding Acquisition; Project Administration, Supervision

In Agreement (Publication 1 to 3)

Prof. Dr. Sven Hammerschmidt **Stephanie Hirschmann**

6. Results and Discussion

The pneumococcus is in general a harmless commensal of the URT but can also cause severe invasive disease such as pneumonia, septicemia, and meningitis. The ability of the pathogen to conquer a number of different host compartments and evade host immune defences is attributed to its versatile repertoire of fitness and virulence factors. The regulation of genes encoding these factors is required for pneumococcal adaptation to a specified host compartment and is vital for bacterial survival. *S. pneumoniae* has evolved different mechanisms including QS, ncRNA, stand-alone regulators and TCSs to enable a timely and spatial gene regulation. Thirteen TCSs and one orphan response regulator are encoded in the pneumococcal genome. While some of these TCSs have already been studied in detail, the impact of others with regard to virulence potential, the regulated gene repertoire and cross regulation between these systems is unknown. This study focused on the regulatory and pathophysiological impact of pneumococcal TCS09 in D39 (**Publication 1**) and TIGR4 (**Publication 2**) and TCS08 (**Publication 3**).

Publication 1: "The Two-Component System 09 Regulates Pneumococcal Carbohydrate Metabolism and Capsule Expression"

TCS09 is among the pneumococcal TCSs whose function and target genes are still incomplete described. Studies in the past focused mainly on the role of the RR09 and neglected the importance of the HK09 and both components, RR09 and HK09, which are directly interconnected. Initially, it was suggested that RR09 regulates the expression of the virulence factor ZmpB, but follow-up studies disproved this [369,408-410]. Using microarray analysis, it was reported that RR09 plays a role in metabolic processes as various PTS genes involved in carbon transport were found to be down-regulated in a RR09-deficient strain D39 [410]. In *in vivo* mice infection experiments *S. pneumoniae* strain D39 showed a complete avirulent phenotype in the absence of RR09 [411]. A recent study showed that the switch between opaque (O) and transparent (T) variants of pneumococci is regulated among others by RR09 [412]. Thus, TCS09 seems to play an important role in fitness and in phase variation, which could have a significant impact on virulence.

In the first study we investigated the role of the TCS09 on pneumococcal pathophysiology using *rr09*-, *hk09*- and *tcs09*-knock out mutants, electron microscopy, transcriptome analysis (RNA-seq and qPCR) and stress inducing assays. The use of deletion mutants targeting individual elements of TCS09 expands our knowledge regarding the regulatory behavior and virulence potential of this system. During host colonization and infection, pathogenic bacteria undergo several adaptive steps in their metabolism and virulence. As a consequence, pathogens adapt their metabolism to available nutrients in the host organism or host

compartment [419,420]. Since most human pathogenic bacteria are heterotrophic, they require at least one carbon source for energy production and for the production of catabolic intermediates. These intermediates are used for the production of anabolic monomers, which in turn are used to synthesize macromolecules such as proteins, nucleic acids, or cell wall components [419,421]. Furthermore, human pathogens possess host adapted metabolic pathways that enable them to colonize ecological niches in the host where they compete with the endogenous microflora [422]. The central carbon metabolism of *S. pneumoniae* is, compared to other human pathogenic bacteria, limited, indicating an adapted lifestyle in the human host.

Measured growth rates under nutrient defined conditions in chemically defined medium (CDM) with glucose as sole carbon source revealed that the deficiency of TCS09 did not impair growth of nonencapsulated mutant strains. Contrary, pneumococcal growth of D39Δ*hk09* is decelerated compared to the D39 wild-type. In CDM containing galactose as sole carbon source *hk09*- and *tcs09*-mutants of encapsulated and nonencapsulated D39 pneumococci showed clear growth defects supporting that TCS09 is linked to carbohydrate metabolism. Pneumococci ferment glucose primarily to lactate in a homofermentative manner, whereas galactose is metabolized to lactate, ethanol, acetate and formate [155,160,423,424]. As component of the mucine in the human nasopharynx galactose or galactosamine are imported by several ABC transporters as well as PTSs and metabolized in the tagatose pathway or Leloir pathway [155,157,158,306,423].

RNA-seq and qPCR analysis was conducted to explore whether genes involved in carbohydrate metabolism are differentially regulated in *tcs09*-mutants of D39. Pneumococci were recovered from CDM containing glucose as carbon source and several genes were monitored to be up- and downregulated, particularly in the *hk09*-mutant. This experimental setup revealed the repressor AgaR (17.5-fold downregulated) and its regulon the *aga* operon (*spd_0065* – *spd_0071*; upregulated), involved in galactose metabolism, as differentially regulated. The proteins encoded in this operon contribute to both, galactosamine transport and its further metabolic processing, and cleavage of Galβ1-3GlcNAc moiety of host receptors [425-427]. Thus, this operon contributes to carbohydrate utilization, adherence and transcellular migration of *S. pneumoniae* [426]. The contribution of RR09 to *gadVWEF* gene expression has been demonstrated earlier via its downregulation in complex media using a RR09 deficient strain in D39 [410]. Results of our study, performed in CDM, show the opposite effect for *gadVW* and *agaS* in D39Δ*rr09* indicating an important role for the used media and its composition. Thus, the availability of the nutrients and especially those in the host as shown by Aprianto *et al*. can influence gene regulation and complicating the analysis of regulatory pathways [428]. A previous study from 2003 showed a significant attenuation of pneumococcal *rr09*-mutants of D39 in the acute pneumonia and sepsis mouse models, but

the exact mechanism remains unknown [411]. The observed attenuation of the *rr09*-mutant in D39 seems not to rely on growth defects or diminished expression of crucial virulence factors such as pneumolysin, because our study found only *pspA* and *phtD* as differentially regulated virulence factors in the *hk09*-mutant. Future reinvestigation of *in vivo* mice infections studies are needed to decipher the impact of TCS09 on virulence and to provide meaningful insights for our understanding of the host pathogen interplay.

As we observed growth defects of *hk09*- and *tcs09*-mutants in CDM, we performed electron microscopic analysis to elucidate a possible role of the TCS09 on phenotypic and morphologic alterations. Studies on other pneumococcal TCSs, such as TCS02, indicated an altered morphological phenotype with its loss of function. The RR02 of TCS02, which is one of the essential response regulators in pneumococci, regulates genes involved in peptidoglycan biosynthesis, fatty acid synthesis, and cell division [370-372]. TCS02-deficient pneumococci showed clear defects in cell shape and in their cell division [371,373]. Our results revealed that a high number of nonencapsulated *hk09*- and *tcs09*-mutants showed a wrinkly and swollen surface with an increased number of outer membrane vesicles in the FESEM images. This already suggests an enhanced susceptibility to stress and lysis.

Additionally, microscopic images of LRR stained D39Δ*hk09* and D39Δ*tcs09* showed a higher amount of CPS and two populations varying in their capsule amount for D39Δ*rr09* and D39Δ*tcs09*. These two populations differ in their ability of capsule attachment, because some of the bacterial cells seem to detach their capsule from the peptidoglycan. The higher capsule content in *S. pneumoniae hk09*- and *tcs09*-mutants was confirmed by flow cytometry. Cultivation in CDM generally leads to a competition for energy vs central carbon metabolism (and thus capsule production) with final higher energy consumption and reduced growth rate [429]. A previous analysis of the amount of capsule produced by *S. pneumoniae* D39 revealed higher capsule production in galactose-containing medium compared to glucose-containing medium, which supports our data regarding the reduced growth of D39Δ*hk09* in CDM with galactose [306]. For D39Δ*rr09* and D39Δ*tcs09* we identified two populations, one with higher amounts of CPS and the other one with less CPS material. *S. pneumoniae* is known to exist in two colony opacity morphologies or phases (O = opaque and T = transparent), named according to their appearance when viewed under oblique, transmitted light on a clear solid medium. Both phases differ in their capsule amount (O: high; T: low) [113]. Pneumococci are able to spontaneously switch between phases. In animal models, T-variants of the same strain have an enhanced ability to colonize the nasopharynx, whereas O-variants are more likely to be isolated from deeper tissues such as the lungs, blood, or cerebrospinal fluid (CSF) [114,430]. Recently the contribution of RR09 and BgaC on phase variation towards the opaque type was described for the first time [412]. We also observed in our *rr09*-mutant a mixture of T- and O-variants with a higher proportion

of T-variants. *S. pneumoniae* D39Δ*hk09* showed exclusively O colonies and an upregulation of *bgaC*, which confirmed the results of the aforementioned studies. Thus, the TCS09 has a significant contribution on capsule expression.

Bacteria can release actively small vesicles from their surface containing own components such as lipids, membrane proteins, short-chain fatty acids, DNA and RNA and contributing to nutrient digestion, QS signaling or toxin transport [431-437]. However, vesicle formation can also happen passively by endolysin or autolysin production leading to peptidoglycan lysis and altered cell wall permeability as reported recently [438-440]. Due to the probably lower integrity of the cell membrane or cell wall of nonencapsulated *hk09*- and *tcs09*-mutants, our FESEM images showed more vesicles for these mutants. Loss of HK09 and the complete TCS09 also led to an increased Triton X-100 induced lysis and hydrogen peroxide induced toxicity in the nonencapsulated mutants, whereas the autolysis behavior of the nonencapsulated *rr09*-mutant is hardly affected. The *rr09*-mutant showed no membrane vesicles or altered cell morphology compared to the *hk09*-and *tcs09*-mutants confirming the link between an intact cell membrane and/or cell wall and resistance to stress induced lysis. Capsule expression is also important to resist lysis, as it reduces e.g., spontaneous and antibiotic induced lysis. Additionally, nonencapsulated mutants are in general more sensitive to lysis than their capsulated counterparts [106]. This was confirmed in our Triton X-100 induced lysis experiments. As *rr09*- and *tcs09*-mutants of encapsulated D39 showed two distinct populations with different capsule content and a higher number of transparent colonies, these two mutants are more susceptible to lysis. In conclusion, TCS09 of *S. pneumoniae* D39 does not directly influence capsule or virulence factor regulation, but it is involved in carbohydrate metabolism, maintenance of cell wall or cell membrane integrity in a yet unknown mechanism and therefore, TCS09 contributes to stress resistance. This can turn TCS09 to an important player during *in vivo* infections.

Publication 2: "The two-component system 09 of *Streptococcus pneumoniae* is important for metabolic fitness and resistance during dissemination in the host"

In this study we investigated the impact of the TCS09 on pneumococcal fitness using different carbon sources, protein expression, cell morphology and *in vivo* virulence by comparing TIGR4 and isogenic *tcs09*-mutants (Δ*rr09*, Δ*hk09* or Δ*tcs09*). *S. pneumoniae* has a large number of different carbohydrate transporter systems such as PTSs and ABC transporters, which can take up at least 12 different carbohydrates to maintain their energy and catabolite balance [14]. Glucose as the main carbon source for pneumococci is mainly available in the blood, but only limited in the nasopharynx [154]. Instead, pneumococci cleave glycoproteins via exoenzymes to release monosaccharides as well as disaccharides such as lactose and sucrose [139,149,151,152].

Pneumococcal growth of TIGR4Δ*cps* and isogenic *tcs09*-mutants was therefore investigated using lactose and sucrose. As we observed an extended lag phase under these growth conditions, an influence of the TCS09 on utilization of lactose and sucrose was assumed. These two disaccharides are taken up by specific PTSs (lactose: SP_0476, SP_0478, SP_1185, and SP_1186; sucrose: SP_1722) and phosphorylated to lactose-6-phosphate or sucrose-6-phosphate, respectively [139,423,441]. In further conversion steps, lactose enters glycolysis as glyceraldehyde-3-phosphate and dihydroxyacetone, whereas sucrose enters glycolysis as glucose-6-phosphate [157,306,441,442]. Together with the transcriptome and growth analysis of D39 and isogenic *tcs09*-mutants, the fundamental role of TCS09 in carbohydrate metabolism became more obvious.

In general, regulators or regulatory systems are localized in the proximity of their regulons but as already shown for the TCS09 in D39 and TCS08 in TIGR4, their regulated genes can be distributed throughout the whole pneumococcal genome [346,410,443]. A strain specific effect of the TCS09 on gene regulation was already reported, hence, different regulation pattern in TIGR4 and D39 were hypothesized [410]. In previous studies using mouse pneumonia models, *S. pneumoniae* TIGR4Δ*rr09* was attenuated and mainly the *rlrA* islet was identified to be regulated [369,410]. Therefore, we quantified the effect of TCS09-deletion on the abundance of individual selected virulence factors by immunoblotting. Virulence factors involved in oxidative stress response (Etrx1, Etrx2 and SodA) [234,444], nutrient transport (MetQ) [445], adherence or/and immune evasion (CbpL, Pce, PspA, PspC, PavB, RrgB and Ply) [188,189,193,226,230,446-450] were chosen. Loss of these proteins often results in an attenuated virulence behavior of *S. pneumoniae* as shown in experimental infection mouse models. Interestingly, only loss of HK09 reduced significantly expression of the pilus backbone RrgB, whereas the expression of the other investigated virulence factors was unaffected in all *tcs09*-mutants. Taken together, the investigated virulence factors are probably not causal for the observed attenuation of TIGR4Δ*rr09* in the studies of Hava and Camilli and Hendriksen [369,410].

Electron microscopic examination of D39 deficient in RR09, HK09 and TCS09 revealed changes in capsule content, surface structure, and membrane vesicle formation [443]. This finally led to increased stress susceptibility as described before. To investigate a similar effect of loss of TCS09 on pneumococcal morphology of TIGR4, FESEM and TEM images were prepared. All investigated *tcs09*-mutants showed no signs of an altered cell surface structure, septum formation, or capsule content, speculating that there is no impact of TCS09 on TIGR4 cell morphology. This further supports the findings regarding a strain specific influence of the TCS09 in *S. pneumoniae* [410,411].

To investigate the influence on adherence and phagocytosis, various *in vitro* cell culture-based infection experiments were performed with human A549 lung epithelial cells and

murine J774 macrophages. In *S. pneumoniae*, TCSs were shown to be essential for colonization and to mediate interaction with human epithelial cells. PspC, a major adhesion molecule, facilitates pneumococcal adhesion to respiratory epithelial cells via the secretory component of the polymeric Ig receptor [63,204,206] and is regulated by the TCS06 [385,451]. It was reported that deletion of RR06 and HK06 diminishes *S. pneumoniae* adherence to epithelial cells *in vitro* and survival and progression *in vivo* [385]. Additionally, TCS02 has an impact on positive regulation of PspA [372]. Despite a lower expression of the Pilus-1 component RrgB, we observed no reduced adherence of TIGR4 *tcs09*-mutants to lung epithelial cells. When colonizing the host, physical and chemical conditions undergo changes so that sensing and adapting of bacteria is of crucial importance for survival [254,338,452-455]. During phagocytosis, pathogens are confronted with several sources of stress, especially oxidative and acidic stress. These kind of stress can lead to loss of membrane stability and damaged proteins [456,457]. TCS05 is one of the key regulatory systems to control stress response by regulating HtrA, a protein with chaperone function [380,383,384]. HtrA expression is necessary for correct processing of proteins and degrading misfolded and non-functional proteins during growth and infection [383,458,459]. Furthermore, TCS05 and TCS12 control an acid response mechanism, in which among others, the activation of the autolysin LytA is repressed [460,461]. In our study pneumococcal uptake of the *tcs09*-mutants by mouse macrophages was unaffected. Contrary, we observed an effect on pneumococcal survival within macrophages with a higher killing rate of TIGR4Δ*cps*Δ*tcs09*. Several pneumococcal proteins contribute to survival in the phagolysosomes of macrophages after phagocytosis: i) to resist the low pH of up to 4.7, pneumococci produce ammonium by the arginine-deaminase-system (*arc*-operon) [310,462,463] and ii) to withstand ROS und thus misfolded proteins, pneumococci use an extracellular thioredoxin system (CcdA1/2-Etrx1/2-MsrAB2) [234], superoxide dismutase (SodA) [444], NADH oxidase [464], HtrA [459] and PsaBAC for manganese transport [465].

In our *in vivo* studies of acute pneumonia, sepsis and a competition assay, we investigated the impact of the TCS09 on pneumococcal virulence in detail. The *in vivo* studies in the mouse infection models of acute pneumonia and sepsis revealed no significant attenuation of the *tcs09*-mutants. In both infection models, survival of Δ*rr09*-, Δ*hk09*- or Δ*tcs09*-infected mice was not significantly increased or decreased. Previous studies using RR09-deficient pneumococci described a strain specific effect on virulence. Loss of RR09 in D39 resulted in an avirulent phenotype when administered intraperitoneal, intranasal and intravenous, whereas loss of RR09 in TIGR4 rendered the strain attenuated only when administered intranasal [369,410,411].

As the reported results could not be reproduced and to get a deeper insight into the *in vivo* role of TCS09, a competitive mouse infection model was applied. Co-infection experiments

indicated that the absence of the TCS09 reduced the fitness of TIGR4 during establishment of invasive infections, because the wild-type outcompeted TIGR4*lux*Δ*hk09* and TIGR4*lux*Δ*tcs09* in the lungs, blood, and brain. In contrast, colonization in the nasopharynx was unaffected by *tcs09*-deletion. Hence, the specific role of the TCS09 during *in vivo* virulence and the identification of regulated genes have to be further elucidated. Several studies have already addressed pneumococcal adaptation and its *in vivo* host compartment specific gene and protein expression using transcriptome and proteome analysis. These reports gave a hint for interesting gene and protein candidates in the respective compartments: i) *malX*, *comB* and other competence genes were upregulated during lung infection [466]; ii) NanA, NanB, and NanC cleave sialic acids from mucin to utilize carbohydrates and enable adherence to exposed receptors [151,152,467-469]; iii) capsule expression controlled among others by CcpA is necessary to withstand the immune system in the lungs [164,305]; iv) nutrient transporter coding genes *aliA*, *ilvH*, *cbiO* and the serine protease coding gene *prtA* were identified as upregulated in the blood [466,470] and v) *glnP* contributes for survival in the lungs, while *glnA* to survival in the blood [312]. In our co-infection experiment we were able to determine pneumococcal load in the brain. The reduced ability of TIGR4*lux*Δ*tcs09* to cross the blood-brain-barrier is probably linked to the higher killing rate by macrophages, as shown in the phagocytic survival experiment. In addition, it will be essential to analyze a possible impact of the TCS09 on interesting gene and protein candidates that are, in addition to pneumolysin, key players during meningitis. For example, *comDE*, which regulates indirectly via ComX the cell wall turnover proteins CbpD and LytA, was found as upregulated at transcriptome and protein level [248,428,471-473] and AliB, the oligopeptide transporter is higher expressed on protein level [248,471,472]. The complexity is even increased by compensatory mechanisms or crosstalk with other regulatory systems influencing the *in vivo* situation. For example TCS04 regulates TCS05, which in turn controls csRNA expression leading to reduced competence [335,336,377]. Furthermore, it has already been shown that bacterial metabolism *in vivo* is different from the *in vitro* situation [419]. In conclusion, TCS09 in TIGR4 is with the exception of pilus type 1 regulation, probably not directly involved in the regulation of essential virulence factors, but TCS09 has a pivotal role in carbohydrate metabolism to maintain pneumococcal fitness and resistance during dissemination and survival in the host. The complex regulatory network during *in vivo* infection and the specific impact of TCS09 has to be further elucidated.

Publication 3: "Pneumococcal Metabolic Adaptation and Colonization Are Regulated by the Two-Component Regulatory System 08"

In paper 3 we investigated the role of the TCS08 and its individual components in the metabolic and pathophysiological pathways and virulence of *S. pneumoniae*. TCS08 was

one of the first analyzed pneumococcal TCS and suggested to be important for virulence [174,345,367]. The RR08 is in the top 3 of highly conserved regulators in *S. pneumoniae* underlining its high impact on pneumococcal colonization and virulence and making it indispensable to unravel the mechanism of TCS08 [19]. Homologues are the SaeS and SaeR of *S. aureus*, which provides theoretically a hint regarding the regulatory effect of TCS08 [405,474]. The *S. aureus* pendant SaeRS was studied in extend in the past and among others genes coding for hemolysin and the fibronectin binding protein A were identified as regulons [475].

For our study we generated mutants lacking one or both components of the TCS08 in D39 and TIGR4 and performed microarray analysis followed up with an attempt to confirm these results by qPCR and immunoblotting. The main genes or operons changed by the TCS08 system in TIGR4 and analyzed therefore by complementary methods are involved in fatty acid biosynthesis (*fab* operon), arginine uptake (arginine deiminase system, ADS), PI-1 regulation, and the adhesin PavB. These regulated genes have in common their localization in the pneumococcal membrane and contribution to fitness, colonization and virulence [226,227,310,476,477]. This leads to the hypothesis that the TCS08 is involved in the fine-tuning of genes, especially in modulation of virulence factors needed for successful colonization and metabolic homeostasis. Because the HK08 was classified as intramembrane HK, which are known to respond to membrane disturbances [349,350], the identified regulated *fab* operon supports the link between TCS08 and sensing and responding to membrane instability [370,476]. Surprisingly, we observed strain-dependent regulatory effects with respect to the ADS with upregulation in D39 *tcs08*-mutants and downregulation in TIGR4 *rr08*- and *hk08*-mutants on protein level. Similar contradictory effects were reported earlier for ArgR2, which upregulates *arc* operon expression in TIGR4 but not in D39 due to ArgR2 absence [310]. The strain-dependent effects are not completely surprising taking into account the genetic variation across pneumococci. We found a downregulation on mRNA and protein level of PI-1 especially in the double mutant (Δ*tcs08*) correlating to some extent with a previous study demonstrating PI-1 regulation by TCS08 [406]. Together with the gene and protein expression data a direct regulation of TCS08 on PavB was supported by the fact that the staphylococcal fibronectin-binding protein FnbA is under the control of the homologous SaeRS in *S. aureus* [478]. Upstream of *pavB* a direct repeat sequence ($TTTAAN_7TTTAA$), which is similar to the conserved SaeR-like binding site ($GTTAAN_6TTTAA$), could be identified by *in silico* analysis [474]. This sequence region might act as binding site for RR08, which has to be proven. Similar repeat sequences were found close to the *rlrA* ($TTTAAN_{14}GTTAA$), cellobiose-specific PTSs and *arc* operon. Because several of the identified TCS08 regulated genes are under the control of CcpA [311],

RlrA [479], PsaR [480] or TCS04 [377,481], we cannot exclude an interplay causing the observed changes in gene expression.

Since the important adhesins PavB and PI-1 were found to be differentially regulated, *in vivo* studies using the acute pneumonia, sepsis and co-infection mouse model were used to assess the impact of TCS08 on colonization and virulence. We observed a strain dependent contribution of the TCS08 to colonization and virulence and elucidated striking differences between TIGR4 and D39. A simple reason for this effect might be the different network of stand-alone regulators, TCSs and ncRNAs interacting in concert in the serotypes. Several studies have previously reported strain-dependent effects by TCSs, such as TCS04 and TCS09, and other regulators in pneumococci [377,411]. Interestingly, TIGR4*lux*Δ*hk08* showed a more virulent behavior compared to TIGR4*lux*Δ*rr08*, which showed attenuation in the acute pneumonia model. In contrast, mice infected with the *hk08*- or *tcs08*-mutants of D39*lux* showed an increased survival time due to lower pneumococcal virulence. Using the sepsis mouse model of infection we observed no attenuation of all *tcs08*-mutants of D39, whereas the *hk08*-mutant of TIGR4*lux* was as virulent as in the pneumonia model. In connection with the gene and protein expression data TCS08 is mostly involved in pneumococcal fitness and adhesion regulation, both required for successful colonization. To analyze the impact of TCS08 in more detail, we performed co-infection experiments, infected mice with equal amount of wild-type and *rr08*-, *hk08*- or *tcs08*-mutants and determined the bacterial load in the nasopharynx and bronchi. Although the *rr08*-mutant of TIGR4*lux* was attenuated in the acute pneumonia model the mutant revealed a higher competitive index than the wild-type in the nasopharynx and bronchi. We observed the opposite for the HK08-deficient strain, which had lower bacterial loads in these two compartments, probably due to fast progression into the blood. In contrast, it is possible that the *rr08*-mutant was impaired in progression into the blood. In summary, we identified several regulated genes encoding membrane bound proteins involved in nutrient transport, fatty acid biosynthesis, and adhesion to host compartments. The TCS08 has in concert with additional regulators and TCSs (TCS05 and TCS12) a moderate impact on gene expression alteration and is thought to be involved in fine-tuning and signal modulation. Such complex network was already reported for the TCS05 (CiaRH), which controls directly csRNAs. These csRNAs modulate indirectly the activity of ComDE and additional regulators [336]. The predominant role of the TCS08 seems to be with the HK08, which probably senses small molecules entering the membrane compartment and finally modulates RR08 activity and possibly other regulators.

7. Outlook

In our studies, gene deletions of *tcs08* and *tcs09* and single components (*hk* or *rr*) were successfully generated in pneumococcal strains D39 and TIGR4. Bacterial fitness, possible morphological changes, differential gene expression pattern, abundance of selected virulence factor proteins, capsule content, stress resistance, and *in vivo* virulence of *tcs08*- and *tcs09*-deletion were investigated. We observed strain-specific effects for the TCS08 as well as for the TCS09 in *in vivo mouse* models. TIGR4*lux*Δ*hk08* showed a significantly increased virulence in the acute pneumonia model, whereas TIGR4*lux*Δ*hk09* and TIGR4*lux*Δ*tcs09* showed a reduced establishment in the respective host compartment during a competitive mouse infection model.

For both, HK08 and HK09, the external stimuli could not be identified yet. Via gene expression profiling the activity of HKs coding genes can be analyzed under various cultivation conditions. In this way, the signals for the HKs of TCS08 and TCS09 can be narrowed down. If this is successful, *in vitro* transcriptome and proteome analyses should be repeated using the respective signals to identify the direct targets of RR08 and RR09.

In future experiments, it is of crucial importance to identify and verify genes that are directly targeted and regulated by RR08 and RR09. For this purpose, it is mandatory to heterologously express and purify the recombinant proteins RR08 and RR09. RRs are known to be activated after phosphorylation of their aspartate residue in the REC domain leading to activation or repression of gene expression. But they can also act in the non-phosphorylated state, so that it is essential to analyze first binding activity of non-phosphorylated and phosphorylated RRs to their target genes and second, if phosphorylation leads to activation or repression of gene expression. Binding studies can be conducted as Electrophoretic Mobility Shift Assay (EMSA) or via Microscale Thermophoresis.

Another aspect of this work was to investigate the influence of TCS08 and TCS09 deficiency on pneumococcal virulence *in vivo*. In particular, for TCS09, previous studies demonstrating attenuation of *rr09*-mutants in D39 and TIGR4 could not be confirmed. The question still remains, which are the changes in the phenotype and how do these changes contribute to the limited establishment in the host of the *tcs09*-mutants in TIGR4 and the avirulent behavior of D39Δ*rr09* in the *in vivo* infection scenario. This leads to the assumption of a different regulatory network and gene expression pattern under *in vivo* conditions. Therefore, it will be necessary to investigate the *in vivo* transcriptome and proteome of *tcs08*- and *tcs09*-

mutants under infection relevant conditions in mouse compartments to get a better understanding of *in vivo* gene regulation and virulence.

Electron microscopic images of the *tcs09*-mutants in D39 suggest that the deficiency of TCS09 affects membrane integrity and permeability. In ongoing and future studies it is therefore of high interest to investigate this hypothesis. In this context, it will be also important to study the membrane composition or its fluidity in more detail.

In addition, the visualization of the morphologic alteration by electron microscopy and the flow cytometric analyses revealed that RR09 is probably involved in anchoring, attachment or preventing detachment of capsular polysaccharides, which has to be explored in more detail. Especially under infection relevant conditions (*in vivo* mice infection) loss or reduced amount of capsule of the *rr09*-mutant in D39 can lead to the discovered attenuation or even avirulence. A reinvestigation of the virulence behavior of TCS09 in the mouse models of acute pneumonia and sepsis using single (Δ*rr09* and Δ*hk09*) and double (Δ*tcs09*) mutants in D39 should be considered as well.

8. References

1. Spellberg, B. Dr. William H. Stewart: mistaken or maligned? *Clinical infectious diseases : an official publication of the Infectious Diseases Society of America* **2008**, *47*, 294, doi:10.1086/589579.
2. Jones, K.E.; Patel, N.G.; Levy, M.A.; Storeygard, A.; Balk, D.; Gittleman, J.L.; Daszak, P. Global trends in emerging infectious diseases. *Nature* **2008**, *451*, 990-993, doi:10.1038/nature06536.
3. Estimates of the global, regional, and national morbidity, mortality, and aetiologies of lower respiratory infections in 195 countries, 1990-2016: a systematic analysis for the Global Burden of Disease Study 2016. *The Lancet. Infectious diseases* **2018**, *18*, 1191-1210, doi:10.1016/s1473-3099(18)30310-4.
4. Sternberg, G.M. *A fatal form of septicaemia in the rabbit produced by the subcutaneous injection of human saliva: an experimental research*; John Murphy & Company: 1881.
5. Pasteur, L. Note sur la maladie nouvelle provoquée par la salive d'un enfant mort de la rage. *Bull acad med (Paris)* **1881**, *10*, 94-103.
6. Winslow, C.E.; Broadhurst, J.; Buchanan, R.E.; Krumwiede, C.; Rogers, L.A.; Smith, G.H. The Families and Genera of the Bacteria: Final Report of the Committee of the Society of American Bacteriologists on Characterization and Classification of Bacterial Types. *J Bacteriol* **1920**, *5*, 191-229, doi:10.1128/JB.5.3.191-229.1920.
7. Watson, D.A.; Musher, D.M.; Jacobson, J.W.; Verhoef, J. A brief history of the pneumococcus in biomedical research: a panoply of scientific discovery. *Clinical infectious diseases : an official publication of the Infectious Diseases Society of America* **1993**, *17*, 913-924, doi:10.1093/clinids/17.5.913.
8. Kawamura, Y.; Whiley, R.A.; Shu, S.E.; Ezaki, T.; Hardie, J.M. Genetic approaches to the identification of the mitis group within the genus *Streptococcus*. *Microbiology (Reading, England)* **1999**, *145 (Pt 9)*, 2605-2613, doi:10.1099/00221287-145-9-2605.
9. Griffith, F. The Significance of Pneumococcal Types. *J Hyg (Lond)* **1928**, *27*, 113-159, doi:10.1017/s0022172400031879.
10. Avery, O.T.; Macleod, C.M.; McCarty, M. STUDIES ON THE CHEMICAL NATURE OF THE SUBSTANCE INDUCING TRANSFORMATION OF PNEUMOCOCCAL TYPES : INDUCTION OF TRANSFORMATION BY A DESOXYRIBONUCLEIC ACID FRACTION ISOLATED FROM PNEUMOCOCCUS TYPE III. *J Exp Med* **1944**, *79*, 137-158, doi:10.1084/jem.79.2.137.
11. Lederberg, J. The transformation of genetics by DNA: an anniversary celebration of Avery, MacLeod and McCarty (1944). *Genetics* **1994**, *136*, 423-426.
12. Georgiev, V.S. *Streptococcus pneumoniae* (Pneumococcal) Disease. In *National Institute of Allergy and Infectious Diseases, NIH: Volume 2;Impact on Global Health*, Georgiev, V.S., Ed. Humana Press: Totowa, NJ, 2009; 10.1007/978-1-60327-297-1_11pp. 75-80.
13. Leifson, E. Types of Bacteria on Blood and Chocolate Agar and the Immediate Cause of These Types. *J Bacteriol* **1932**, *24*, 473-487, doi:10.1128/JB.24.6.473-487.1932.
14. Hoskins, J.; Alborn, W.E., Jr.; Arnold, J.; Blaszczak, L.C.; Burgett, S.; DeHoff, B.S.; Estrem, S.T.; Fritz, L.; Fu, D.J.; Fuller, W., et al. Genome of the bacterium *Streptococcus pneumoniae* strain R6. *J Bacteriol* **2001**, *183*, 5709-5717, doi:10.1128/jb.183.19.5709-5717.2001.
15. Tettelin, H.; Nelson, K.E.; Paulsen, I.T.; Eisen, J.A.; Read, T.D.; Peterson, S.; Heidelberg, J.; DeBoy, R.T.; Haft, D.H.; Dodson, R.J., et al. Complete genome sequence of a virulent isolate of *Streptococcus pneumoniae*. *Science (New York, N.Y.)* **2001**, *293*, 498-506, doi:10.1126/science.1061217.
16. Hiller, N.L.; Janto, B.; Hogg, J.S.; Boissy, R.; Yu, S.; Powell, E.; Keefe, R.; Ehrlich, N.E.; Shen, K.; Hayes, J., et al. Comparative genomic analyses of seventeen *Streptococcus pneumoniae* strains: insights into the pneumococcal supragenome. *J Bacteriol* **2007**, *189*, 8186-8195, doi:10.1128/jb.00690-07.
17. Hiller, N.L.; Ahmed, A.; Powell, E.; Martin, D.P.; Eutsey, R.; Earl, J.; Janto, B.; Boissy, R.J.; Hogg, J.; Barbadora, K., et al. Generation of genic diversity among *Streptococcus pneumoniae* strains via horizontal gene transfer during a chronic polyclonal pediatric infection. *PLoS pathogens* **2010**, *6*, e1001108, doi:10.1371/journal.ppat.1001108.
18. van Tonder, A.J.; Bray, J.E.; Jolley, K.A.; Quirk, S.J.; Haraldsson, G.; Maiden, M.C.J.; Bentley, S.D.; Haraldsson, Á.; Erlendsdóttir, H.; Kristinsson, K.G., et al. Heterogeneity among estimates of the core genome and pan-genome in different pneumococcal populations. *bioRxiv* **2017**, 10.1101/133991, 133991, doi:10.1101/133991.
19. Gámez, G.; Castro, A.; Gómez-Mejia, A.; Gallego, M.; Bedoya, A.; Camargo, M.; Hammerschmidt, S. The variome of pneumococcal virulence factors and regulators. *BMC genomics* **2018**, *19*, 10-10, doi:10.1186/s12864-017-4376-0.
20. Feil, E.J.; Smith, J.M.; Enright, M.C.; Spratt, B.G. Estimating recombinational parameters in *Streptococcus pneumoniae* from multilocus sequence typing data. *Genetics* **2000**, *154*, 1439-1450.
21. Dopazo, J.; Mendoza, A.; Herrero, J.; Caldara, F.; Humbert, Y.; Friedli, L.; Guerrier, M.; Grand-Schenk, E.; Gandin, C.; de Francesco, M., et al. Annotated draft genomic sequence from a *Streptococcus*

pneumoniae type 19F clinical isolate. *Microbial drug resistance (Larchmont, N.Y.)* **2001**, *7*, 99-125, doi:10.1089/10766290152044995.
22. Lanie, J.A.; Ng, W.L.; Kazmierczak, K.M.; Andrzejewski, T.M.; Davidsen, T.M.; Wayne, K.J.; Tettelin, H.; Glass, J.I.; Winkler, M.E. Genome sequence of Avery's virulent serotype 2 strain D39 of *Streptococcus pneumoniae* and comparison with that of unencapsulated laboratory strain R6. *J Bacteriol* **2007**, *189*, 38-51, doi:10.1128/jb.01148-06.
23. van der Poll, T.; Opal, S.M. Pathogenesis, treatment, and prevention of pneumococcal pneumonia. *Lancet (London, England)* **2009**, *374*, 1543-1556, doi:10.1016/s0140-6736(09)61114-4.
24. Obert, C.; Sublett, J.; Kaushal, D.; Hinojosa, E.; Barton, T.; Tuomanen, E.I.; Orihuela, C.J. Identification of a Candidate *Streptococcus pneumoniae* core genome and regions of diversity correlated with invasive pneumococcal disease. *Infect Immun* **2006**, *74*, 4766-4777, doi:10.1128/iai.00316-06.
25. Embry, A.; Hinojosa, E.; Orihuela, C.J. Regions of Diversity 8, 9 and 13 contribute to *Streptococcus pneumoniae* virulence. *BMC microbiology* **2007**, *7*, 80, doi:10.1186/1471-2180-7-80.
26. Oggioni, M.R.; Iannelli, F.; Pozzi, G. Characterization of cryptic plasmids pDP1 and pSMB1 of *Streptococcus pneumoniae*. *Plasmid* **1999**, *41*, 70-72, doi:10.1006/plas.1998.1364.
27. Henrichsen, J. Six newly recognized types of *Streptococcus pneumoniae*. *J Clin Microbiol* **1995**, *33*, 2759.
28. Bentley, S.D.; Aanensen, D.M.; Mavroidi, A.; Saunders, D.; Rabbinowitsch, E.; Collins, M.; Donohoe, K.; Harris, D.; Murphy, L.; Quail, M.A., et al. Genetic Analysis of the Capsular Biosynthetic Locus from All 90 Pneumococcal Serotypes. *PLOS Genetics* **2006**, *2*, e31, doi:10.1371/journal.pgen.0020031.
29. Geno, K.A.; Gilbert, G.L.; Song, J.Y.; Skovsted, I.C.; Klugman, K.P.; Jones, C.; Konradsen, H.B.; Nahm, M.H. Pneumococcal Capsules and Their Types: Past, Present, and Future. *Clinical microbiology reviews* **2015**, *28*, 871-899, doi:10.1128/cmr.00024-15.
30. Geno, K.A.; Saad, J.S.; Nahm, M.H. Discovery of Novel Pneumococcal Serotype 35D, a Natural WciG-Deficient Variant of Serotype 35B. *J Clin Microbiol* **2017**, *55*, 1416-1425, doi:10.1128/jcm.00054-17.
31. Watson, D.A.; Musher, D.M. Interruption of capsule production in *Streptococcus pneumoniae* serotype 3 by insertion of transposon Tn*916*. *Infect Immun* **1990**, *58*, 3135-3138, doi:10.1128/iai.58.9.3135-3138.1990.
32. Magee, A.D.; Yother, J. Requirement for capsule in colonization by *Streptococcus pneumoniae*. *Infect Immun* **2001**, *69*, 3755-3761, doi:10.1128/iai.69.6.3755-3761.2001.
33. File, T.M., Jr. *Streptococcus pneumoniae* and community-acquired pneumonia: a cause for concern. *The American journal of medicine* **2004**, *117 Suppl 3A*, 39s-50s, doi:10.1016/j.amjmed.2004.07.007.
34. Lynch, J.P., 3rd; Zhanel, G.G. *Streptococcus pneumoniae*: epidemiology and risk factors, evolution of antimicrobial resistance, and impact of vaccines. *Current opinion in pulmonary medicine* **2010**, *16*, 217-225, doi:10.1097/MCP.0b013e3283385653.
35. Feldman, C.; Anderson, R. Recent advances in our understanding of *Streptococcus pneumoniae* infection. *F1000Prime Rep* **2014**, *6*, 82-82, doi:10.12703/P6-82.
36. Bogaert, D.; De Groot, R.; Hermans, P.W. *Streptococcus pneumoniae* colonisation: the key to pneumococcal disease. *The Lancet. Infectious diseases* **2004**, *4*, 144-154, doi:10.1016/s1473-3099(04)00938-7.
37. O'Brien, K.L.; Wolfson, L.J.; Watt, J.P.; Henkle, E.; Deloria-Knoll, M.; McCall, N.; Lee, E.; Mulholland, K.; Levine, O.S.; Cherian, T. Burden of disease caused by *Streptococcus pneumoniae* in children younger than 5 years: global estimates. *Lancet (London, England)* **2009**, *374*, 893-902, doi:10.1016/s0140-6736(09)61204-6.
38. Isaacman, D.J.; McIntosh, E.D.; Reinert, R.R. Burden of invasive pneumococcal disease and serotype distribution among *Streptococcus pneumoniae* isolates in young children in Europe: impact of the 7-valent pneumococcal conjugate vaccine and considerations for future conjugate vaccines. *International journal of infectious diseases : IJID : official publication of the International Society for Infectious Diseases* **2010**, *14*, e197-209, doi:10.1016/j.ijid.2009.05.010.
39. Whitney, C.G.; Farley, M.M.; Hadler, J.; Harrison, L.H.; Bennett, N.M.; Lynfield, R.; Reingold, A.; Cieslak, P.R.; Pilishvili, T.; Jackson, D., et al. Decline in invasive pneumococcal disease after the introduction of protein-polysaccharide conjugate vaccine. *The New England journal of medicine* **2003**, *348*, 1737-1746, doi:10.1056/NEJMoa022823.
40. Henriques-Normark, B.; Tuomanen, E.I. The pneumococcus: epidemiology, microbiology, and pathogenesis. *Cold Spring Harbor perspectives in medicine* **2013**, *3*, doi:10.1101/cshperspect.a010215.
41. Rowe, H.M.; Karlsson, E.; Echlin, H.; Chang, T.-C.; Wang, L.; van Opijnen, T.; Pounds, S.B.; Schultz-Cherry, S.; Rosch, J.W. Bacterial Factors Required for Transmission of *Streptococcus pneumoniae* in Mammalian Hosts. *Cell Host & Microbe* **2019**, *25*, 884-891.e886, doi:https://doi.org/10.1016/j.chom.2019.04.012.

42. Cooper, V.S.; Honsa, E.; Rowe, H.; Deitrick, C.; Iverson, A.R.; Whittall, J.J.; Neville, S.L.; McDevitt, C.A.; Kietzman, C.; Rosch, J.W. Experimental Evolution *In Vivo* To Identify Selective Pressures during Pneumococcal Colonization. *mSystems* **2020**, *5*, e00352-00320, doi:10.1128/mSystems.00352-20.
43. García-Rodríguez, J.A.; Fresnadillo Martínez, M.J. Dynamics of nasopharyngeal colonization by potential respiratory pathogens. *The Journal of antimicrobial chemotherapy* **2002**, *50 Suppl S2*, 59-73, doi:10.1093/jac/dkf506.
44. Regev-Yochay, G.; Raz, M.; Dagan, R.; Porat, N.; Shainberg, B.; Pinco, E.; Keller, N.; Rubinstein, E. Nasopharyngeal carriage of *Streptococcus pneumoniae* by adults and children in community and family settings. *Clinical infectious diseases : an official publication of the Infectious Diseases Society of America* **2004**, *38*, 632-639, doi:10.1086/381547.
45. Smith, E.L.; Wheeler, I.; Adler, H.; Ferreira, D.M.; Sá-Leão, R.; Abdullahi, O.; Adetifa, I.; Becker-Dreps, S.; Esposito, S.; Farida, H., et al. Upper airways colonisation of *Streptococcus pneumoniae* in adults aged 60 years and older: A systematic review of prevalence and individual participant data meta-analysis of risk factors. *Journal of Infection* **2020**, *81*, 540-548, doi:https://doi.org/10.1016/j.jinf.2020.06.028.
46. Gray, B.M.; Converse, G.M., 3rd; Dillon, H.C., Jr. Serotypes of *Streptococcus pneumoniae* causing disease. *The Journal of infectious diseases* **1979**, *140*, 979-983, doi:10.1093/infdis/140.6.979.
47. Brugger, S.D.; Hathaway, L.J.; Mühlemann, K. Detection of *Streptococcus pneumoniae* strain cocolonization in the nasopharynx. *J Clin Microbiol* **2009**, *47*, 1750-1756, doi:10.1128/jcm.01877-08.
48. Austrian, R. Some aspects of the pneumococcal carrier state. *The Journal of antimicrobial chemotherapy* **1986**, *18 Suppl A*, 35-45, doi:10.1093/jac/18.supplement_a.35.
49. Orihuela, C.J.; Gao, G.; Francis, K.P.; Yu, J.; Tuomanen, E.I. Tissue-specific contributions of pneumococcal virulence factors to pathogenesis. *The Journal of infectious diseases* **2004**, *190*, 1661-1669, doi:10.1086/424596.
50. Cartwright, K. Pneumococcal disease in western Europe: burden of disease, antibiotic resistance and management. *European journal of pediatrics* **2002**, *161*, 188-195, doi:10.1007/s00431-001-0907-3.
51. McCullers, J.A.; Bartmess, K.C. Role of neuraminidase in lethal synergism between influenza virus and *Streptococcus pneumoniae*. *The Journal of infectious diseases* **2003**, *187*, 1000-1009, doi:10.1086/368163.
52. Steinfort, C.; Wilson, R.; Mitchell, T.; Feldman, C.; Rutman, A.; Todd, H.; Sykes, D.; Walker, J.; Saunders, K.; Andrew, P.W., et al. Effect of *Streptococcus pneumoniae* on human respiratory epithelium in vitro. *Infect Immun* **1989**, *57*, 2006-2013, doi:10.1128/IAI.57.7.2006-2013.1989.
53. AlonsoDeVelasco, E.; Verheul, A.F.; Verhoef, J.; Snippe, H. *Streptococcus pneumoniae*: virulence factors, pathogenesis, and vaccines. *Microbiological reviews* **1995**, *59*, 591-603.
54. Domon, H.; Oda, M.; Maekawa, T.; Nagai, K.; Takeda, W.; Terao, Y. *Streptococcus pneumoniae* disrupts pulmonary immune defence via elastase release following pneumolysin-dependent neutrophil lysis. *Scientific Reports* **2016**, *6*, 38013, doi:10.1038/srep38013.
55. Hyams, C.; Camberlein, E.; Cohen, J.M.; Bax, K.; Brown, J.S. The *Streptococcus pneumoniae* capsule inhibits complement activity and neutrophil phagocytosis by multiple mechanisms. *Infect Immun* **2010**, *78*, 704-715, doi:10.1128/iai.00881-09.
56. Mulks, M.H.; Kornfeld, S.J.; Plaut, A.G. Specific proteolysis of human IgA by *Streptococcus pneumoniae* and *Haemophilus influenzae*. *The Journal of infectious diseases* **1980**, *141*, 450-456, doi:10.1093/infdis/141.4.450.
57. Holmes, A.R.; McNab, R.; Millsap, K.W.; Rohde, M.; Hammerschmidt, S.; Mawdsley, J.L.; Jenkinson, H.F. The *pavA* gene of *Streptococcus pneumoniae* encodes a fibronectin-binding protein that is essential for virulence. *Molecular microbiology* **2001**, *41*, 1395-1408, doi:10.1046/j.1365-2958.2001.02610.x.
58. Pracht, D.; Elm, C.; Gerber, J.; Bergmann, S.; Rohde, M.; Seiler, M.; Kim, K.S.; Jenkinson, H.F.; Nau, R.; Hammerschmidt, S. PavA of *Streptococcus pneumoniae* modulates adherence, invasion, and meningeal inflammation. *Infect Immun* **2005**, *73*, 2680-2689, doi:10.1128/iai.73.5.2680-2689.2005.
59. Bergmann, S.; Lang, A.; Rohde, M.; Agarwal, V.; Rennemeier, C.; Grashoff, C.; Preissner, K.T.; Hammerschmidt, S. Integrin-linked kinase is required for vitronectin-mediated internalization of Streptococcus pneumoniae by host cells. *Journal of cell science* **2009**, *122*, 256-267, doi:10.1242/jcs.035600.
60. Voss, S.; Gámez, G.; Hammerschmidt, S. Impact of pneumococcal microbial surface components recognizing adhesive matrix molecules on colonization. *Molecular oral microbiology* **2012**, *27*, 246-256, doi:10.1111/j.2041-1014.2012.00654.x.
61. Gradstedt, H.; Iovino, F.; Bijlsma, J.J. *Streptococcus pneumoniae* invades endothelial host cells via multiple pathways and is killed in a lysosome dependent manner. *PLoS One* **2013**, *8*, e65626, doi:10.1371/journal.pone.0065626.
62. Yau, B.; Hunt, N.H.; Mitchell, A.J.; Too, L.K. Blood–Brain Barrier Pathology and CNS Outcomes in *Streptococcus pneumoniae* Meningitis. *Int J Mol Sci* **2018**, *19*, 3555, doi:10.3390/ijms19113555.

63. Elm, C.; Braathen, R.; Bergmann, S.; Frank, R.; Vaerman, J.P.; Kaetzel, C.S.; Chhatwal, G.S.; Johansen, F.E.; Hammerschmidt, S. Ectodomains 3 and 4 of human polymeric Immunoglobulin receptor (hpIgR) mediate invasion of *Streptococcus pneumoniae* into the epithelium. *The Journal of biological chemistry* **2004**, *279*, 6296-6304, doi:10.1074/jbc.M310528200.
64. Yamaguchi, M.; Terao, Y.; Mori-Yamaguchi, Y.; Domon, H.; Sakaue, Y.; Yagi, T.; Nishino, K.; Yamaguchi, A.; Nizet, V.; Kawabata, S. *Streptococcus pneumoniae* Invades Erythrocytes and Utilizes Them to Evade Human Innate Immunity. *PLOS ONE* **2013**, *8*, e77282, doi:10.1371/journal.pone.0077282.
65. Marks, L.R.; Parameswaran, G.I.; Hakansson, A.P. Pneumococcal interactions with epithelial cells are crucial for optimal biofilm formation and colonization *in vitro* and *in vivo*. *Infect Immun* **2012**, *80*, 2744-2760, doi:10.1128/IAI.00488-12.
66. Sanchez, C.J.; Hurtgen, B.J.; Lizcano, A.; Shivshankar, P.; Cole, G.T.; Orihuela, C.J. Biofilm and planktonic pneumococci demonstrate disparate immunoreactivity to human convalescent sera. *BMC microbiology* **2011**, *11*, 245, doi:10.1186/1471-2180-11-245.
67. Weiser, J.N.; Ferreira, D.M.; Paton, J.C. *Streptococcus pneumoniae*: transmission, colonization and invasion. *Nature reviews. Microbiology* **2018**, *16*, 355-367, doi:10.1038/s41579-018-0001-8.
68. Pikis, A.; Campos, J.M.; Rodriguez, W.J.; Keith, J.M. Optochin resistance in *Streptococcus pneumoniae*: mechanism, significance, and clinical implications. *The Journal of infectious diseases* **2001**, *184*, 582-590, doi:10.1086/322803.
69. Reller, L.B.; Weinstein, M.P.; Werno, A.M.; Murdoch, D.R. Laboratory Diagnosis of Invasive Pneumococcal Disease. *Clinical Infectious Diseases* **2008**, *46*, 926-932, doi:10.1086/528798.
70. Brito, D.A.; Ramirez, M.; de Lencastre, H. Serotyping *Streptococcus pneumoniae* by multiplex PCR. *J Clin Microbiol* **2003**, *41*, 2378-2384, doi:10.1128/jcm.41.6.2378-2384.2003.
71. Pai, R.; Gertz, R.E.; Beall, B. Sequential multiplex PCR approach for determining capsular serotypes of *Streptococcus pneumoniae* isolates. *J Clin Microbiol* **2006**, *44*, 124-131, doi:10.1128/jcm.44.1.124-131.2006.
72. da Gloria Carvalho, M.; Pimenta, F.C.; Jackson, D.; Roundtree, A.; Ahmad, Y.; Millar, E.V.; O'Brien, K.L.; Whitney, C.G.; Cohen, A.L.; Beall, B.W. Revisiting pneumococcal carriage by use of broth enrichment and PCR techniques for enhanced detection of carriage and serotypes. *J Clin Microbiol* **2010**, *48*, 1611-1618, doi:10.1128/jcm.02243-09.
73. Reinert, R.R. The antimicrobial resistance profile of *Streptococcus pneumoniae*. *Clinical microbiology and infection : the official publication of the European Society of Clinical Microbiology and Infectious Diseases* **2009**, *15 Suppl 3*, 7-11, doi:10.1111/j.1469-0691.2009.02724.x.
74. Klugman, K.; Goldstein, F.; Kohno, S.; Baquero, F. The role of fourth-generation cephalosporins in the treatment of infections caused by penicillin-resistant streptococci. *Clinical Microbiology and Infection* **1997**, *3*, S48-S60, doi:https://doi.org/10.1111/j.1469-0691.1997.tb00646.x.
75. Castanheira, M.; Gales, A.C.; Mendes, R.E.; Jones, R.N.; Sader, H.S. Antimicrobial susceptibility of *Streptococcus pneumoniae* in Latin America: results from five years of the SENTRY Antimicrobial Surveillance Program. *Clinical microbiology and infection : the official publication of the European Society of Clinical Microbiology and Infectious Diseases* **2004**, *10*, 645-651, doi:10.1111/j.1469-0691.2004.00872.x.
76. von Gottberg, A.; Klugman, K.P.; Cohen, C.; Wolter, N.; de Gouveia, L.; du Plessis, M.; Mpembe, R.; Quan, V.; Whitelaw, A.; Hoffmann, R., et al. Emergence of levofloxacin-non-susceptible *Streptococcus pneumoniae* and treatment for multidrug-resistant tuberculosis in children in South Africa: a cohort observational surveillance study. *Lancet (London, England)* **2008**, *371*, 1108-1113, doi:10.1016/s0140-6736(08)60350-5.
77. Kim, L.; McGee, L.; Tomczyk, S.; Beall, B. Biological and Epidemiological Features of Antibiotic-Resistant *Streptococcus pneumoniae* in Pre- and Post-Conjugate Vaccine Eras: a United States Perspective. *Clinical microbiology reviews* **2016**, *29*, 525-552, doi:10.1128/cmr.00058-15.
78. Croucher, N.J.; Harris, S.R.; Fraser, C.; Quail, M.A.; Burton, J.; van der Linden, M.; McGee, L.; von Gottberg, A.; Song, J.H.; Ko, K.S., et al. Rapid pneumococcal evolution in response to clinical interventions. *Science (New York, N.Y.)* **2011**, *331*, 430-434, doi:10.1126/science.1198545.
79. Kobayashi, M.; Bennett, N.M.; Gierke, R.; Almendares, O.; Moore, M.R.; Whitney, C.G.; Pilishvili, T. Intervals Between PCV13 and PPSV23 Vaccines: Recommendations of the Advisory Committee on Immunization Practices (ACIP). *MMWR. Morbidity and mortality weekly report* **2015**, *64*, 944-947, doi:10.15585/mmwr.mm6434a4.
80. Aliberti, S.; Mantero, M.; Mirsaeidi, M.; Blasi, F. The role of vaccination in preventing pneumococcal disease in adults. *Clinical microbiology and infection : the official publication of the European Society of Clinical Microbiology and Infectious Diseases* **2014**, *20 Suppl 5*, 52-58, doi:10.1111/1469-0691.12518.

81. Rose, M.A.; Schubert, R.; Strnad, N.; Zielen, S. Priming of immunological memory by pneumococcal conjugate vaccine in children unresponsive to 23-valent polysaccharide pneumococcal vaccine. *Clin Diagn Lab Immunol* **2005**, *12*, 1216-1222, doi:10.1128/CDLI.12.10.1216-1222.2005.
82. Pletz, M.W.; Maus, U.; Krug, N.; Welte, T.; Lode, H. Pneumococcal vaccines: mechanism of action, impact on epidemiology and adaption of the species. *International journal of antimicrobial agents* **2008**, *32*, 199-206, doi:10.1016/j.ijantimicag.2008.01.021.
83. Stein, K.E. Thymus-Independent and Thymus-Dependent Responses to Polysaccharide Antigens. *The Journal of infectious diseases* **1992**, *165*, S49-S52, doi:10.1093/infdis/165-Supplement_1-S49.
84. Papadatou, I.; Tzovara, I.; Licciardi, P.V. The Role of Serotype-Specific Immunological Memory in Pneumococcal Vaccination: Current Knowledge and Future Prospects. *Vaccines* **2019**, *7*, doi:10.3390/vaccines7010013.
85. Black, S.; Shinefield, H.; Fireman, B.; Lewis, E.; Ray, P.; Hansen, J.R.; Elvin, L.; Ensor, K.M.; Hackell, J.; Siber, G., et al. Efficacy, safety and immunogenicity of heptavalent pneumococcal conjugate vaccine in children. *The Pediatric infectious disease journal* **2000**, *19*, 187-195, doi:10.1097/00006454-200003000-00003.
86. Hicks, L.A.; Harrison, L.H.; Flannery, B.; Hadler, J.L.; Schaffner, W.; Craig, A.S.; Jackson, D.; Thomas, A.; Beall, B.; Lynfield, R., et al. Incidence of pneumococcal disease due to non-pneumococcal conjugate vaccine (PCV7) serotypes in the United States during the era of widespread PCV7 vaccination, 1998-2004. *The Journal of infectious diseases* **2007**, *196*, 1346-1354, doi:10.1086/521626.
87. Kaplan, S.L.; Barson, W.J.; Lin, P.L.; Stovall, S.H.; Bradley, J.S.; Tan, T.Q.; Hoffman, J.A.; Givner, L.B.; Mason, E.O. Serotype 19A Is the Most Common Serotype Causing Invasive Pneumococcal Infections in Children. *Pediatrics* **2010**, *125*, 429, doi:10.1542/peds.2008-1702.
88. Gruber, W.C.; Scott, D.A.; Emini, E.A. Development and clinical evaluation of Prevnar 13, a 13-valent pneumococcoccal CRM_{197} conjugate vaccine. *Annals of the New York Academy of Sciences* **2012**, *1263*, 15-26, doi:10.1111/j.1749-6632.2012.06673.x.
89. Wijmenga-Monsuur, A.J.; van Westen, E.; Knol, M.J.; Jongerius, R.M.; Zancolli, M.; Goldblatt, D.; van Gageldonk, P.G.; Tcherniaeva, I.; Berbers, G.A.; Rots, N.Y. Direct Comparison of Immunogenicity Induced by 10- or 13-Valent Pneumococcal Conjugate Vaccine around the 11-Month Booster in Dutch Infants. *PLoS One* **2015**, *10*, e0144739, doi:10.1371/journal.pone.0144739.
90. HogenEsch, H.; O'Hagan, D.T.; Fox, C.B. Optimizing the utilization of aluminum adjuvants in vaccines: you might just get what you want. *npj Vaccines* **2018**, *3*, 51, doi:10.1038/s41541-018-0089-x.
91. Ortqvist, A. Pneumococcal vaccination: current and future issues. *The European respiratory journal* **2001**, *18*, 184-195, doi:10.1183/09031936.01.00084401.
92. Voß, F.; Kohler, T.P.; Meyer, T.; Abdullah, M.R.; van Opzeeland, F.J.; Saleh, M.; Michalik, S.; van Selm, S.; Schmidt, F.; de Jonge, M.I., et al. Intranasal Vaccination With Lipoproteins Confers Protection Against Pneumococcal Colonisation. *Frontiers in immunology* **2018**, *9*, 2405, doi:10.3389/fimmu.2018.02405.
93. Voß, F.; van Beek, L.F.; Schwudke, D.; Ederveen, T.H.A.; van Opzeeland, F.J.; Thalheim, D.; Werner, S.; de Jonge, M.I.; Hammerschmidt, S. Lipidation of Pneumococcal Antigens Leads to Improved Immunogenicity and Protection. *Vaccines* **2020**, *8*, doi:10.3390/vaccines8020310.
94. Dochez, A.R.; Avery, O.T. THE ELABORATION OF SPECIFIC SOLUBLE SUBSTANCE BY PNEUMOCOCCUS DURING GROWTH. *Journal of Experimental Medicine* **1917**, *26*, 477-493, doi:10.1084/jem.26.4.477.
95. Heidelberger, M.; Avery, O.T. THE SOLUBLE SPECIFIC SUBSTANCE OF PNEUMOCOCCUS. *J Exp Med* **1923**, *38*, 73-79, doi:10.1084/jem.38.1.73.
96. Avery, O.T.; Heidelberger, M.; Goebel, W.F. THE SOLUBLE SPECIFIC SUBSTANCE OF FRIEDLANDER'S BACILLUS : PAPER II. CHEMICAL AND IMMUNOLOGICAL RELATIONSHIPS OF PNEUMOCOCCUS TYPE II AND OF A STRAIN OF FRIEDLANDER'S BACILLUS. *J Exp Med* **1925**, *42*, 709-725, doi:10.1084/jem.42.5.709.
97. van Dam, J.E.G.; Fleer, A.; Snippe, H. Immunogenicity and immunochemistry of *Streptococcus pneumoniae* capsular polysaccharides. *Antonie van Leeuwenhoek* **1990**, *58*, 1-47, doi:10.1007/BF02388078.
98. Yang, J.; Nahm, M.H.; Bush, C.A.; Cisar, J.O. Comparative structural and molecular characterization of *Streptococcus pneumoniae* capsular polysaccharide serogroup 10. *The Journal of biological chemistry* **2011**, *286*, 35813-35822, doi:10.1074/jbc.M111.255422.
99. Bush, C.A.; Yang, J.; Yu, B.; Cisar, J.O. Chemical structures of *Streptococcus pneumoniae* capsular polysaccharide type 39 (CPS39), CPS47F, and CPS34 characterized by nuclear magnetic resonance spectroscopy and their relation to CPS10A. *J Bacteriol* **2014**, *196*, 3271-3278, doi:10.1128/jb.01731-14.
100. Sørensen, U.B.; Henrichsen, J.; Chen, H.C.; Szu, S.C. Covalent linkage between the capsular polysaccharide and the cell wall peptidoglycan of *Streptococcus pneumoniae* revealed by immunochemical methods. *Microb Pathog* **1990**, *8*, 325-334, doi:10.1016/0882-4010(90)90091-4.

101. Ring, A.; Weiser, J.N.; Tuomanen, E.I. Pneumococcal trafficking across the blood-brain barrier. Molecular analysis of a novel bidirectional pathway. *The Journal of clinical investigation* **1998**, *102*, 347-360, doi:10.1172/JCI2406.
102. Kadioglu, A.; Taylor, S.; Iannelli, F.; Pozzi, G.; Mitchell, T.J.; Andrew, P.W. Upper and lower respiratory tract infection by *Streptococcus pneumoniae* is affected by pneumolysin deficiency and differences in capsule type. *Infect Immun* **2002**, *70*, 2886-2890, doi:10.1128/iai.70.6.2886-2890.2002.
103. Kim, J.O.; Romero-Steiner, S.; Sørensen, U.B.; Blom, J.; Carvalho, M.; Barnard, S.; Carlone, G.; Weiser, J.N. Relationship between cell surface carbohydrates and intrastrain variation on opsonophagocytosis of *Streptococcus pneumoniae*. *Infect Immun* **1999**, *67*, 2327-2333, doi:10.1128/IAI.67.5.2327-2333.1999.
104. Fine, D.P. Pneumococcal type-associated variability in alternate complement pathway activation. *Infect Immun* **1975**, *12*, 772-778, doi:10.1128/IAI.12.4.772-778.1975.
105. Wartha, F.; Beiter, K.; Albiger, B.; Fernebro, J.; Zychlinsky, A.; Normark, S.; Henriques-Normark, B. Capsule and D-alanylated lipoteichoic acids protect *Streptococcus pneumoniae* against neutrophil extracellular traps. *Cellular microbiology* **2007**, *9*, 1162-1171, doi:10.1111/j.1462-5822.2006.00857.x.
106. Fernebro, J.; Andersson, I.; Sublett, J.; Morfeldt, E.; Novak, R.; Tuomanen, E.; Normark, S.; Normark, B.H. Capsular expression in *Streptococcus pneumoniae* negatively affects spontaneous and antibiotic-induced lysis and contributes to antibiotic tolerance. *The Journal of infectious diseases* **2004**, *189*, 328-338, doi:10.1086/380564.
107. Nelson, A.L.; Roche, A.M.; Gould, J.M.; Chim, K.; Ratner, A.J.; Weiser, J.N. Capsule enhances pneumococcal colonization by limiting mucus-mediated clearance. *Infect Immun* **2007**, *75*, 83-90, doi:10.1128/iai.01475-06.
108. Skov Sørensen, U.B.; Blom, J.; Birch-Andersen, A.; Henrichsen, J. Ultrastructural localization of capsules, cell wall polysaccharide, cell wall proteins, and F antigen in pneumococci. *Infect Immun* **1988**, *56*, 1890-1896, doi:10.1128/iai.56.8.1890-1896.1988.
109. Hyams, C.; Yuste, J.; Bax, K.; Camberlein, E.; Weiser, J.N.; Brown, J.S. *Streptococcus pneumoniae* resistance to complement-mediated immunity is dependent on the capsular serotype. *Infect Immun* **2010**, *78*, 716-725, doi:10.1128/IAI.01056-09.
110. Austrian, R. Some observations on the pneumococcus and on the current status of pneumococcal disease and its prevention. *Reviews of infectious diseases* **1981**, *3 Suppl*, S1-17, doi:10.1093/clinids/3.supplement_1.s1.
111. McAllister, L.J.; Ogunniyi, A.D.; Stroeher, U.H.; Leach, A.J.; Paton, J.C. Contribution of serotype and genetic background to virulence of serotype 3 and serogroup 11 pneumococcal isolates. *Infect Immun* **2011**, *79*, 4839-4849, doi:10.1128/IAI.05663-11.
112. Hammerschmidt, S.; Wolff, S.; Hocke, A.; Rosseau, S.; Müller, E.; Rohde, M. Illustration of pneumococcal polysaccharide capsule during adherence and invasion of epithelial cells. *Infect Immun* **2005**, *73*, 4653-4667, doi:10.1128/iai.73.8.4653-4667.2005.
113. Kim, J.O.; Weiser, J.N. Association of Intrastrain Phase Variation in Quantity of Capsular Polysaccharide and Teichoic Acid with the Virulence of *Streptococcus pneumoniae*. *The Journal of infectious diseases* **1998**, *177*, 368-377, doi:10.1086/514205.
114. Weiser, J.N.; Austrian, R.; Sreenivasan, P.K.; Masure, H.R. Phase variation in pneumococcal opacity: relationship between colonial morphology and nasopharyngeal colonization. *Infect Immun* **1994**, *62*, 2582-2589, doi:10.1128/iai.62.6.2582-2589.1994.
115. Wen, Z.; Liu, Y.; Qu, F.; Zhang, J.-R. Allelic Variation of the Capsule Promoter Diversifies Encapsulation and Virulence In *Streptococcus pneumoniae*. *Scientific reports* **2016**, *6*, 30176-30176, doi:10.1038/srep30176.
116. Salter, S.J.; Hinds, J.; Gould, K.A.; Lambertsen, L.; Hanage, W.P.; Antonio, M.; Turner, P.; Hermans, P.W.M.; Bootsma, H.J.; O'Brien, K.L., et al. Variation at the capsule locus, *cps*, of mistyped and non-typable *Streptococcus pneumoniae* isolates. *Microbiology (Reading, England)* **2012**, *158*, 1560-1569, doi:10.1099/mic.0.056580-0.
117. Croucher, N.J.; Kagedan, L.; Thompson, C.M.; Parkhill, J.; Bentley, S.D.; Finkelstein, J.A.; Lipsitch, M.; Hanage, W.P. Selective and Genetic Constraints on Pneumococcal Serotype Switching. *PLOS Genetics* **2015**, *11*, e1005095, doi:10.1371/journal.pgen.1005095.
118. Beeby, M.; Gumbart, J.C.; Roux, B.; Jensen, G.J. Architecture and assembly of the Gram-positive cell wall. *Molecular microbiology* **2013**, *88*, 664-672, doi:10.1111/mmi.12203.
119. Barendt, S.M.; Sham, L.T.; Winkler, M.E. Characterization of mutants deficient in the L,D-carboxypeptidase (DacB) and WalRK (VicRK) regulon, involved in peptidoglycan maturation of *Streptococcus pneumoniae* serotype 2 strain D39. *J Bacteriol* **2011**, *193*, 2290-2300, doi:10.1128/jb.01555-10.
120. Abdullah, M.R.; Gutiérrez-Fernández, J.; Pribyl, T.; Gisch, N.; Saleh, M.; Rohde, M.; Petruschka, L.; Burchhardt, G.; Schwudke, D.; Hermoso, J.A., et al. Structure of the pneumococcal l,d-carboxypeptidase

DacB and pathophysiological effects of disabled cell wall hydrolases DacA and DacB. *Molecular microbiology* **2014**, *93*, 1183-1206, doi:10.1111/mmi.12729.
121. Fischer, H.; Tomasz, A. Peptidoglycan cross-linking and teichoic acid attachment in *Streptococcus pneumoniae*. *J Bacteriol* **1985**, *163*, 46-54, doi:10.1128/jb.163.1.46-54.1985.
122. Garcia-Bustos, J.F.; Chait, B.T.; Tomasz, A. Structure of the peptide network of pneumococcal peptidoglycan. *The Journal of biological chemistry* **1987**, *262*, 15400-15405.
123. Bui, N.K.; Eberhardt, A.; Vollmer, D.; Kern, T.; Bougault, C.; Tomasz, A.; Simorre, J.P.; Vollmer, W. Isolation and analysis of cell wall components from *Streptococcus pneumoniae*. *Analytical biochemistry* **2012**, *421*, 657-666, doi:10.1016/j.ab.2011.11.026.
124. Gisch, N.; Peters, K.; Zähringer, U.; Vollmer, W. Chapter 8 - The Pneumococcal Cell Wall. In *Streptococcus Pneumoniae*, Brown, J., Hammerschmidt, S., Orihuela, C., Eds. Academic Press: Amsterdam, 2015; https://doi.org/10.1016/B978-0-12-410530-0.00008-9pp. 145-167.
125. Schleifer, K.H.; Kandler, O. Peptidoglycan types of bacterial cell walls and their taxonomic implications. *Bacteriol Rev* **1972**, *36*, 407-477.
126. Sham, L.T.; Tsui, H.C.; Land, A.D.; Barendt, S.M.; Winkler, M.E. Recent advances in pneumococcal peptidoglycan biosynthesis suggest new vaccine and antimicrobial targets. *Current opinion in microbiology* **2012**, *15*, 194-203, doi:10.1016/j.mib.2011.12.013.
127. Zapun, A.; Philippe, J.; Abrahams, K.A.; Signor, L.; Roper, D.I.; Breukink, E.; Vernet, T. *In vitro* Reconstitution of Peptidoglycan Assembly from the Gram-Positive Pathogen *Streptococcus pneumoniae*. *ACS Chemical Biology* **2013**, *8*, 2688-2696, doi:10.1021/cb400575t.
128. Barreteau, H.; Kovač, A.; Boniface, A.; Sova, M.; Gobec, S.; Blanot, D. Cytoplasmic steps of peptidoglycan biosynthesis. *FEMS microbiology reviews* **2008**, *32*, 168-207, doi:10.1111/j.1574-6976.2008.00104.x.
129. van Heijenoort, J. Lipid Intermediates in Bacterial Peptidoglycan Biosynthesis. In *Handbook of Hydrocarbon and Lipid Microbiology*, Timmis, K.N., Ed. Springer Berlin Heidelberg: Berlin, Heidelberg, 2010; 10.1007/978-3-540-77587-4_31pp. 435-444.
130. Bouhss, A.; Trunkfield, A.E.; Bugg, T.D.H.; Mengin-Lecreulx, D. The biosynthesis of peptidoglycan lipid-linked intermediates. *FEMS microbiology reviews* **2008**, *32*, 208-233, doi:10.1111/j.1574-6976.2007.00089.x.
131. Sauvage, E.; Kerff, F.; Terrak, M.; Ayala, J.A.; Charlier, P. The penicillin-binding proteins: structure and role in peptidoglycan biosynthesis. *FEMS microbiology reviews* **2008**, *32*, 234-258, doi:10.1111/j.1574-6976.2008.00105.x.
132. Fleurie, A.; Manuse, S.; Zhao, C.; Campo, N.; Cluzel, C.; Lavergne, J.-P.; Freton, C.; Combet, C.; Guiral, S.; Soufi, B., et al. Interplay of the Serine/Threonine-Kinase StkP and the Paralogs DivIVA and GpsB in Pneumococcal Cell Elongation and Division. *PLOS Genetics* **2014**, *10*, e1004275, doi:10.1371/journal.pgen.1004275.
133. Vollmer, W.; Massidda, O.; Tomasz, A. The Cell Wall of *Streptococcus pneumoniae*. *Microbiology spectrum* **2019**, *7*, doi:10.1128/microbiolspec.GPP3-0018-2018.
134. Figueiredo, T.A.; Sobral, R.G.; Ludovice, A.M.; de Almeida, J.M.F.; Bui, N.K.; Vollmer, W.; de Lencastre, H.; Tomasz, A. Identification of Genetic Determinants and Enzymes Involved with the Amidation of Glutamic Acid Residues in the Peptidoglycan of *Staphylococcus aureus*. *PLoS pathogens* **2012**, *8*, e1002508, doi:10.1371/journal.ppat.1002508.
135. Mohammadi, T.; van Dam, V.; Sijbrandi, R.; Vernet, T.; Zapun, A.; Bouhss, A.; Diepeveen-de Bruin, M.; Nguyen-Distèche, M.; de Kruijff, B.; Breukink, E. Identification of FtsW as a transporter of lipid-linked cell wall precursors across the membrane. *The EMBO journal* **2011**, *30*, 1425-1432, doi:10.1038/emboj.2011.61.
136. Eberhardt, A.; Hoyland, C.N.; Vollmer, D.; Bisle, S.; Cleverley, R.M.; Johnsborg, O.; Håvarstein, L.S.; Lewis, R.J.; Vollmer, W. Attachment of capsular polysaccharide to the cell wall in *Streptococcus pneumoniae*. *Microbial drug resistance (Larchmont, N.Y.)* **2012**, *18*, 240-255, doi:10.1089/mdr.2011.0232.
137. Garcia-Bustos, J.; Tomasz, A. A biological price of antibiotic resistance: major changes in the peptidoglycan structure of penicillin-resistant pneumococci. *Proceedings of the National Academy of Sciences of the United States of America* **1990**, *87*, 5415-5419, doi:10.1073/pnas.87.14.5415.
138. Basavanna, S.; Khandavilli, S.; Yuste, J.; Cohen, J.M.; Hosie, A.H.F.; Webb, A.J.; Thomas, G.H.; Brown, J.S. Screening of *Streptococcus pneumoniae* ABC transporter mutants demonstrates that LivJHMGF, a branched-chain amino acid ABC transporter, is necessary for disease pathogenesis. *Infect Immun* **2009**, *77*, 3412-3423, doi:10.1128/IAI.01543-08.
139. Bidossi, A.; Mulas, L.; Decorosi, F.; Colomba, L.; Ricci, S.; Pozzi, G.; Deutscher, J.; Viti, C.; Oggioni, M.R. A Functional Genomics Approach to Establish the Complement of Carbohydrate Transporters in *Streptococcus pneumoniae*. *PLOS ONE* **2012**, *7*, e33320, doi:10.1371/journal.pone.0033320.

140. Brown, J.S.; Gilliland, S.M.; Holden, D.W. A *Streptococcus pneumoniae* pathogenicity island encoding an ABC transporter involved in iron uptake and virulence. *Molecular microbiology* **2001**, *40*, 572-585, doi:10.1046/j.1365-2958.2001.02414.x.
141. Culurgioni, S.; Harris, G.; Singh, A.K.; King, S.J.; Walsh, M.A. Structural Basis for Regulation and Specificity of Fructooligosaccharide Import in *Streptococcus pneumoniae*. *Structure (London, England : 1993)* **2017**, *25*, 79-93, doi:10.1016/j.str.2016.11.008.
142. Kohler, S.; Voß, F.; Gómez Mejia, A.; Brown, J.S.; Hammerschmidt, S. Pneumococcal lipoproteins involved in bacterial fitness, virulence, and immune evasion. *FEBS Lett* **2016**, *590*, 3820-3839, doi:10.1002/1873-3468.12352.
143. Bayle, L.; Chimalapati, S.; Schoehn, G.; Brown, J.; Vernet, T.; Durmort, C. Zinc uptake by *Streptococcus pneumoniae* depends on both AdcA and AdcAII and is essential for normal bacterial morphology and virulence. *Molecular microbiology* **2011**, *82*, 904-916, doi:10.1111/j.1365-2958.2011.07862.x.
144. Brown, J.S.; Gilliland, S.M.; Ruiz-Albert, J.; Holden, D.W. Characterization of Pit, a *Streptococcus pneumoniae* iron uptake ABC transporter. *Infect Immun* **2002**, *70*, 4389-4398, doi:10.1128/iai.70.8.4389-4398.2002.
145. Dintilhac, A.; Alloing, G.; Granadel, C.; Claverys, J.P. Competence and virulence of *Streptococcus pneumoniae*: Adc and PsaA mutants exhibit a requirement for Zn and Mn resulting from inactivation of putative ABC metal permeases. *Molecular microbiology* **1997**, *25*, 727-739, doi:10.1046/j.1365-2958.1997.5111879.x.
146. Johnston, J.W.; Myers, L.E.; Ochs, M.M.; Benjamin, W.H., Jr.; Briles, D.E.; Hollingshead, S.K. Lipoprotein PsaA in virulence of *Streptococcus pneumoniae*: surface accessibility and role in protection from superoxide. *Infect Immun* **2004**, *72*, 5858-5867, doi:10.1128/iai.72.10.5858-5867.2004.
147. McAllister, L.J.; Tseng, H.J.; Ogunniyi, A.D.; Jennings, M.P.; McEwan, A.G.; Paton, J.C. Molecular analysis of the *psa* permease complex of *Streptococcus pneumoniae*. *Molecular microbiology* **2004**, *53*, 889-901, doi:10.1111/j.1365-2958.2004.04164.x.
148. Hoyer, J.; Bartel, J.; Gómez-Mejia, A.; Rohde, M.; Hirschfeld, C.; Heß, N.; Sura, T.; Maaß, S.; Hammerschmidt, S.; Becher, D. Proteomic response of *Streptococcus pneumoniae* to iron limitation. *International journal of medical microbiology : IJMM* **2018**, *308*, 713-721, doi:10.1016/j.ijmm.2018.02.001.
149. Buckwalter, C.M.; King, S.J. Pneumococcal carbohydrate transport: food for thought. *Trends in microbiology* **2012**, *20*, 517-522, doi:10.1016/j.tim.2012.08.008.
150. Rose, M.C.; Voynow, J.A. Respiratory tract mucin genes and mucin glycoproteins in health and disease. *Physiological reviews* **2006**, *86*, 245-278, doi:10.1152/physrev.00010.2005.
151. Burnaugh, A.M.; Frantz, L.J.; King, S.J. Growth of *Streptococcus pneumoniae* on human glycoconjugates is dependent upon the sequential activity of bacterial exoglycosidases. *J Bacteriol* **2008**, *190*, 221-230, doi:10.1128/jb.01251-07.
152. King, S.J. Pneumococcal modification of host sugars: a major contributor to colonization of the human airway? *Molecular oral microbiology* **2010**, *25*, 15-24, doi:10.1111/j.2041-1014.2009.00564.x.
153. Hobbs, J.K.; Meier, E.P.W.; Pluvinage, B.; Mey, M.A.; Boraston, A.B. Molecular analysis of an enigmatic *Streptococcus pneumoniae* virulence factor: The raffinose-family oligosaccharide utilization system. *The Journal of biological chemistry* **2019**, *294*, 17197-17208, doi:10.1074/jbc.RA119.010280.
154. Krebs, H.A. Chemical Composition of Blood Plasma and Serum. *Annual review of biochemistry* **1950**, *19*, 409-430, doi:10.1146/annurev.bi.19.070150.002205.
155. Härtel, T.; Eylert, E.; Schulz, C.; Petruschka, L.; Gierok, P.; Grubmüller, S.; Lalk, M.; Eisenreich, W.; Hammerschmidt, S. Characterization of central carbon metabolism of *Streptococcus pneumoniae* by isotopologue profiling. *The Journal of biological chemistry* **2012**, *287*, 4260-4274, doi:10.1074/jbc.M111.304311.
156. Leonard, A.; Gierok, P.; Methling, K.; Gómez-Mejia, A.; Hammerschmidt, S.; Lalk, M. Metabolic inventory of *Streptococcus pneumoniae* growing in a chemical defined environment. *International journal of medical microbiology : IJMM* **2018**, *308*, 705-712, doi:10.1016/j.ijmm.2018.01.001.
157. Iskandar, C.F.; Cailliez-Grimal, C.; Borges, F.; Revol-Junelles, A.-M. Review of lactose and galactose metabolism in Lactic Acid Bacteria dedicated to expert genomic annotation. *Trends in Food Science & Technology* **2019**, *88*, 121-132, doi:https://doi.org/10.1016/j.tifs.2019.03.020.
158. Paixão, L.; Oliveira, J.; Veríssimo, A.; Vinga, S.; Lourenço, E.C.; Ventura, M.R.; Kjos, M.; Veening, J.-W.; Fernandes, V.E.; Andrew, P.W., et al. Host Glycan Sugar-Specific Pathways in *Streptococcus pneumonia*: Galactose as a Key Sugar in Colonisation and Infection. *PLOS ONE* **2015**, *10*, e0121042, doi:10.1371/journal.pone.0121042.
159. Neijssel, O.M.; Snoep, J.L.; Teixeira de Mattos, M.J. Regulation of energy source metabolism in streptococci. *Society for Applied Bacteriology symposium series* **1997**, *26*, 12s-19s.

160. Kandler, O. Carbohydrate metabolism in lactic acid bacteria. *Antonie van Leeuwenhoek* **1983**, *49*, 209-224, doi:10.1007/BF00399499.
161. Yesilkaya, H.; Spissu, F.; Carvalho, S.M.; Terra, V.S.; Homer, K.A.; Benisty, R.; Porat, N.; Neves, A.R.; Andrew, P.W. Pyruvate Formate Lyase Is Required for Pneumococcal Fermentative Metabolism and Virulence. *Infect Immun* **2009**, *77*, 5418, doi:10.1128/IAI.00178-09.
162. Al-Bayati, F.A.Y.; Kahya, H.F.H.; Damianou, A.; Shafeeq, S.; Kuipers, O.P.; Andrew, P.W.; Yesilkaya, H. Pneumococcal galactose catabolism is controlled by multiple regulators acting on pyruvate formate lyase. *Scientific reports* **2017**, *7*, 43587-43587, doi:10.1038/srep43587.
163. Hendriksen, W.T.; Bootsma, H.J.; Estevão, S.; Hoogenboezem, T.; de Jong, A.; de Groot, R.; Kuipers, O.P.; Hermans, P.W.M. CodY of *Streptococcus pneumoniae*: Link between Nutritional Gene Regulation and Colonization. *J Bacteriol* **2008**, *190*, 590, doi:10.1128/JB.00917-07.
164. Iyer, R.; Baliga, N.S.; Camilli, A. Catabolite Control Protein A (CcpA) Contributes to Virulence and Regulation of Sugar Metabolism in *Streptococcus pneumoniae*. *J Bacteriol* **2005**, *187*, 8340, doi:10.1128/JB.187.24.8340-8349.2005.
165. Stebbins, C.E.; Galán, J.E. Structural mimicry in bacterial virulence. *Nature* **2001**, *412*, 701-705, doi:10.1038/35089000.
166. Wilson, J.W.; Schurr, M.J.; LeBlanc, C.L.; Ramamurthy, R.; Buchanan, K.L.; Nickerson, C.A. Mechanisms of bacterial pathogenicity. *Postgraduate medical journal* **2002**, *78*, 216-224, doi:10.1136/pmj.78.918.216.
167. Bergmann, S.; Hammerschmidt, S. Versatility of pneumococcal surface proteins. *Microbiology (Reading, England)* **2006**, *152*, 295-303, doi:10.1099/mic.0.28610-0.
168. Kadioglu, A.; Weiser, J.N.; Paton, J.C.; Andrew, P.W. The role of *Streptococcus pneumoniae* virulence factors in host respiratory colonization and disease. *Nature reviews. Microbiology* **2008**, *6*, 288-301, doi:10.1038/nrmicro1871.
169. Mitchell, A.M.; Mitchell, T.J. *Streptococcus pneumoniae*: virulence factors and variation. *Clinical microbiology and infection : the official publication of the European Society of Clinical Microbiology and Infectious Diseases* **2010**, *16*, 411-418, doi:10.1111/j.1469-0691.2010.03183.x.
170. Hacker, J.; Ott, M.; Blum, G.; Marre, R.; Heesemann, J.; Tschäpe, H.; Goebel, W. Genetics of Escherichia coli uropathogenicity: Analysis of the O6:K15:H31 isolate 536. **1992**.
171. Klinkert, B.; Narberhaus, F. Microbial thermosensors. *Cellular and molecular life sciences : CMLS* **2009**, *66*, 2661-2676, doi:10.1007/s00018-009-0041-3.
172. Loh, E.; Dussurget, O.; Gripenland, J.; Vaitkevicius, K.; Tiensuu, T.; Mandin, P.; Repoila, F.; Buchrieser, C.; Cossart, P.; Johansson, J. A *trans*-acting riboswitch controls expression of the virulence regulator PrfA in *Listeria monocytogenes*. *Cell* **2009**, *139*, 770-779, doi:10.1016/j.cell.2009.08.046.
173. Heroven, A.K.; Böhme, K.; Rohde, M.; Dersch, P. A Csr-type regulatory system, including small non-coding RNAs, regulates the global virulence regulator RovA of *Yersinia pseudotuberculosis* through RovM. *Molecular microbiology* **2008**, *68*, 1179-1195, doi:10.1111/j.1365-2958.2008.06218.x.
174. Gómez-Mejia, A.; Gámez, G.; Hammerschmidt, S. *Streptococcus pneumoniae* two-component regulatory systems: The interplay of the pneumococcus with its environment. *International journal of medical microbiology : IJMM* **2018**, *308*, 722-737, doi:10.1016/j.ijmm.2017.11.012.
175. Kietzman, C.C.; Rosch, J.W. Chapter 6 - Regulatory Strategies of the Pneumococcus. In *Streptococcus Pneumoniae*, Brown, J., Hammerschmidt, S., Orihuela, C., Eds. Academic Press: Amsterdam, 2015; https://doi.org/10.1016/B978-0-12-410530-0.00006-5pp. 109-128.
176. Pérez-Dorado, I.; Galan-Bartual, S.; Hermoso, J.A. Pneumococcal surface proteins: when the whole is greater than the sum of its parts. *Molecular oral microbiology* **2012**, *27*, 221-245, doi:10.1111/j.2041-1014.2012.00655.x.
177. Patti, J.M.; Allen, B.L.; McGavin, M.J.; Höök, M. MSCRAMM-mediated adherence of microorganisms to host tissues. *Annual Reviews in Microbiology* **1994**, *48*, 585-617.
178. Hammerschmidt, S.; Rohde, M.; Preissner, K.T. Extracellular Matrix Interactions with Gram-Positive Pathogens. *Microbiology spectrum* **2019**, *7*, doi:10.1128/microbiolspec.GPP3-0041-2018.
179. Theocharis, A.D.; Skandalis, S.S.; Gialeli, C.; Karamanos, N.K. Extracellular matrix structure. *Advanced drug delivery reviews* **2016**, *97*, 4-27, doi:10.1016/j.addr.2015.11.001.
180. Tamkun, J.W.; DeSimone, D.W.; Fonda, D.; Patel, R.S.; Buck, C.; Horwitz, A.F.; Hynes, R.O. Structure of integrin, a glycoprotein involved in the transmembrane linkage between fibronectin and actin. *Cell* **1986**, *46*, 271-282, doi:10.1016/0092-8674(86)90744-0.
181. Binsker, U.; Kohler, T.P.; Krauel, K.; Kohler, S.; Schwertz, H.; Hammerschmidt, S. Pneumococcal adhesins PavB and PspC are important for the interplay with human thrombospondin-1. *Journal of Biological Chemistry* **2015**, *290*, 14542-14555.

182. Herrmann, M.; Suchard, S.J.; Boxer, L.A.; Waldvogel, F.A.; Lew, P.D. Thrombospondin binds to *Staphylococcus aureus* and promotes staphylococcal adherence to surfaces. *Infect Immun* **1991**, *59*, 279-288, doi:10.1128/iai.59.1.279-288.1991.
183. Kohler, T.P.; Gisch, N.; Binsker, U.; Schlag, M.; Darm, K.; Völker, U.; Zähringer, U.; Hammerschmidt, S. Repeating structures of the major staphylococcal autolysin are essential for the interaction with human thrombospondin 1 and vitronectin. *The Journal of biological chemistry* **2014**, *289*, 4070-4082, doi:10.1074/jbc.M113.521229.
184. Yanagisawa, N.; Li, D.-Q.; Ljungh, Å. The N-terminal of thrombospondin-1 is essential for coagulase-negative staphylococcal binding. *Journal of medical microbiology* **2001**, *50*, 712-719.
185. Hammerschmidt, S.; Bethe, G.; Remane, P.H.; Chhatwal, G.S. Identification of pneumococcal surface protein A as a lactoferrin-binding protein of *Streptococcus pneumoniae*. *Infect Immun* **1999**, *67*, 1683-1687.
186. Bergmann, S.; Rohde, M.; Chhatwal, G.S.; Hammerschmidt, S. α-Enolase of *Streptococcus pneumoniae* is a plasmin(ogen)-binding protein displayed on the bacterial cell surface. *Molecular microbiology* **2001**, *40*, 1273-1287, doi:10.1046/j.1365-2958.2001.02448.x.
187. Jedrzejas, M.J. Pneumococcal virulence factors: structure and function. *Microbiology and molecular biology reviews : MMBR* **2001**, *65*, 187-207 ; first page, table of contents, doi:10.1128/mmbr.65.2.187-207.2001.
188. Briles, D.E.; Yother, J.; McDaniel, L.S. Role of pneumococcal surface protein A in the virulence of *Streptococcus pneumoniae*. *Reviews of infectious diseases* **1988**, *10 Suppl 2*, S372-374, doi:10.1093/cid/10.supplement_2.s372.
189. Hammerschmidt, S.; Talay, S.R.; Brandtzaeg, P.; Chhatwal, G.S. SpsA, a novel pneumococcal surface protein with specific binding to secretory immunoglobulin A and secretory component. *Molecular microbiology* **1997**, *25*, 1113-1124, doi:10.1046/j.1365-2958.1997.5391899.x.
190. García, P.; González, M.P.; García, E.; López, R.; García, J.L. LytB, a novel pneumococcal murein hydrolase essential for cell separation. *Molecular microbiology* **1999**, *31*, 1275-1281, doi:10.1046/j.1365-2958.1999.01238.x.
191. Pérez-Dorado, I.; González, A.; Morales, M.; Sanles, R.; Striker, W.; Vollmer, W.; Mobashery, S.; García, J.L.; Martínez-Ripoll, M.; García, P., et al. Insights into pneumococcal fratricide from the crystal structures of the modular killing factor LytC. *Nature Structural & Molecular Biology* **2010**, *17*, 576-581, doi:10.1038/nsmb.1817.
192. Molina, R.; González, A.; Stelter, M.; Pérez-Dorado, I.; Kahn, R.; Morales, M.; Campuzano, S.; Campillo, N.E.; Mobashery, S.; García, J.L., et al. Crystal structure of CbpF, a bifunctional choline-binding protein and autolysis regulator from *Streptococcus pneumoniae*. *EMBO reports* **2009**, *10*, 246-251, doi:https://doi.org/10.1038/embor.2008.245.
193. Gutiérrez-Fernández, J.; Saleh, M.; Alcorlo, M.; Gómez-Mejía, A.; Pantoja-Uceda, D.; Treviño, M.A.; Voß, F.; Abdullah, M.R.; Galán-Bartual, S.; Seinen, J., et al. Modular Architecture and Unique Teichoic Acid Recognition Features of Choline-Binding Protein L (CbpL) Contributing to Pneumococcal Pathogenesis. *Scientific Reports* **2016**, *6*, 38094, doi:10.1038/srep38094.
194. Yother, J.; White, J.M. Novel surface attachment mechanism of the *Streptococcus pneumoniae* protein PspA. *J Bacteriol* **1994**, *176*, 2976-2985, doi:10.1128/jb.176.10.2976-2985.1994.
195. Gosink, K.K.; Mann, E.R.; Guglielmo, C.; Tuomanen, E.I.; Masure, H.R. Role of novel choline binding proteins in virulence of *Streptococcus pneumoniae*. *Infect Immun* **2000**, *68*, 5690-5695, doi:10.1128/iai.68.10.5690-5695.2000.
196. Hakenbeck, R.; Madhour, A.; Denapaite, D.; Brückner, R. Versatility of choline metabolism and choline-binding proteins in Streptococcus pneumoniae and commensal streptococci. *FEMS microbiology reviews* **2009**, *33*, 572-586, doi:10.1111/j.1574-6976.2009.00172.x.
197. Maestro, B.; Sanz, J.M. Choline Binding Proteins from *Streptococcus pneumoniae*: A Dual Role as Enzybiotics and Targets for the Design of New Antimicrobials. *Antibiotics (Basel, Switzerland)* **2016**, *5*, doi:10.3390/antibiotics5020021.
198. Ren, B.; Szalai, A.J.; Hollingshead, S.K.; Briles, D.E. Effects of PspA and antibodies to PspA on activation and deposition of complement on the pneumococcal surface. *Infect Immun* **2004**, *72*, 114-122, doi:10.1128/iai.72.1.114-122.2004.
199. Shaper, M.; Hollingshead, S.K.; Benjamin, W.H., Jr.; Briles, D.E. PspA protects *Streptococcus pneumoniae* from killing by apolactoferrin, and antibody to PspA enhances killing of pneumococci by apolactoferrin [corrected]. *Infect Immun* **2004**, *72*, 5031-5040, doi:10.1128/iai.72.9.5031-5040.2004.
200. Hammerschmidt, S.; Agarwal, V.; Kunert, A.; Haelbich, S.; Skerka, C.; Zipfel, P.F. The host immune regulator factor H interacts via two contact sites with the PspC protein of *Streptococcus pneumoniae* and mediates adhesion to host epithelial cells. *Journal of immunology (Baltimore, Md. : 1950)* **2007**, *178*, 5848-5858, doi:10.4049/jimmunol.178.9.5848.

201. Meinel, C.; Spartà, G.; Dahse, H.M.; Hörhold, F.; König, R.; Westermann, M.; Coldewey, S.M.; Cseresnyés, Z.; Figge, M.T.; Hammerschmidt, S., et al. *Streptococcus pneumoniae* From Patients With Hemolytic Uremic Syndrome Binds Human Plasminogen via the Surface Protein PspC and Uses Plasmin to Damage Human Endothelial Cells. *The Journal of infectious diseases* **2018**, *217*, 358-370, doi:10.1093/infdis/jix305.
202. Voss, S.; Hallström, T.; Saleh, M.; Burchhardt, G.; Pribyl, T.; Singh, B.; Riesbeck, K.; Zipfel, P.F.; Hammerschmidt, S. The choline-binding protein PspC of *Streptococcus pneumoniae* interacts with the C-terminal heparin-binding domain of vitronectin. *The Journal of biological chemistry* **2013**, *288*, 15614-15627, doi:10.1074/jbc.M112.443507.
203. Hammerschmidt, S.; Tillig, M.P.; Wolff, S.; Vaerman, J.P.; Chhatwal, G.S. Species-specific binding of human secretory component to SpsA protein of *Streptococcus pneumoniae* via a hexapeptide motif. *Molecular microbiology* **2000**, *36*, 726-736, doi:10.1046/j.1365-2958.2000.01897.x.
204. Zhang, J.R.; Mostov, K.E.; Lamm, M.E.; Nanno, M.; Shimida, S.; Ohwaki, M.; Tuomanen, E. The polymeric immunoglobulin receptor translocates pneumococci across human nasopharyngeal epithelial cells. *Cell* **2000**, *102*, 827-837, doi:10.1016/s0092-8674(00)00071-4.
205. Agarwal, V.; Hammerschmidt, S. Cdc42 and the phosphatidylinositol 3-kinase-Akt pathway are essential for PspC-mediated internalization of pneumococci by respiratory epithelial cells. *The Journal of biological chemistry* **2009**, *284*, 19427-19436, doi:10.1074/jbc.M109.003442.
206. Agarwal, V.; Asmat, T.M.; Dierdorf, N.I.; Hauck, C.R.; Hammerschmidt, S. Polymeric immunoglobulin receptor-mediated invasion of *Streptococcus pneumoniae* into host cells requires a coordinate signaling of SRC family of protein-tyrosine kinases, ERK, and c-Jun N-terminal kinase. *The Journal of biological chemistry* **2010**, *285*, 35615-35623, doi:10.1074/jbc.M110.172999.
207. Quin, L.R.; Carmicle, S.; Dave, S.; Pangburn, M.K.; Evenhuis, J.P.; McDaniel, L.S. In Vivo Binding of Complement Regulator Factor H by *Streptococcus pneumoniae*. *The Journal of infectious diseases* **2005**, *192*, 1996-2003, doi:10.1086/497605.
208. Howard, L.V.; Gooder, H. Specificity of the autolysin of *Streptococcus* (*Diplococcus*) *pneumoniae*. *J Bacteriol* **1974**, *117*, 796-804, doi:10.1128/jb.117.2.796-804.1974.
209. De Las Rivas, B.; García, J.L.; López, R.; García, P. Purification and polar localization of pneumococcal LytB, a putative endo-β-*N*-acetylglucosaminidase: the chain-dispersing murein hydrolase. *J Bacteriol* **2002**, *184*, 4988-5000.
210. Majcherczyk, P.A.; Langen, H.; Heumann, D.; Fountoulakis, M.; Glauser, M.P.; Moreillon, P. Digestion of *Streptococcus pneumoniae* cell walls with its major peptidoglycan hydrolase releases branched stem peptides carrying proinflammatory activity. *The Journal of biological chemistry* **1999**, *274*, 12537-12543, doi:10.1074/jbc.274.18.12537.
211. Fischetti, V.A.; Pancholi, V.; Schneewind, O. Conservation of a hexapeptide sequence in the anchor region of surface proteins from gram-positive cocci. *Molecular microbiology* **1990**, *4*, 1603-1605, doi:10.1111/j.1365-2958.1990.tb02072.x.
212. Schneewind, O.; Model, P.; Fischetti, V.A. Sorting of protein A to the staphylococcal cell wall. *Cell* **1992**, *70*, 267-281, doi:10.1016/0092-8674(92)90101-h.
213. Navarre, W.W.; Schneewind, O. Proteolytic cleavage and cell wall anchoring at the LPXTG motif of surface proteins in gram-positive bacteria. *Molecular microbiology* **1994**, *14*, 115-121, doi:10.1111/j.1365-2958.1994.tb01271.x.
214. Schneewind, O.; Fowler, A.; Faull, K.F. Structure of the cell wall anchor of surface proteins in *Staphylococcus aureus*. *Science (New York, N.Y.)* **1995**, *268*, 103-106, doi:10.1126/science.7701329.
215. Paterson, G.K.; Mitchell, T.J. The biology of Gram-positive sortase enzymes. *Trends in microbiology* **2004**, *12*, 89-95, doi:10.1016/j.tim.2003.12.007.
216. Kharat, A.S.; Tomasz, A. Inactivation of the *srtA* gene affects localization of surface proteins and decreases adhesion of *Streptococcus pneumoniae* to human pharyngeal cells in vitro. *Infect Immun* **2003**, *71*, 2758-2765, doi:10.1128/iai.71.5.2758-2765.2003.
217. Chen, S.; Paterson, G.K.; Tong, H.H.; Mitchell, T.J.; DeMaria, T.F. Sortase A contributes to pneumococcal nasopharyngeal colonization in the chinchilla model. *FEMS microbiology letters* **2005**, *253*, 151-154, doi:10.1016/j.femsle.2005.09.052.
218. Paterson, G.K.; Mitchell, T.J. The role of *Streptococcus pneumoniae* sortase A in colonisation and pathogenesis. *Microbes and infection* **2006**, *8*, 145-153, doi:10.1016/j.micinf.2005.06.009.
219. Paton, J.C.; Berry, A.M.; Lock, R.A. Molecular analysis of putative pneumococcal virulence proteins. *Microbial drug resistance (Larchmont, N.Y.)* **1997**, *3*, 1-10, doi:10.1089/mdr.1997.3.1.
220. Zähner, D.; Hakenbeck, R. The *Streptococcus pneumoniae* beta-galactosidase is a surface protein. *J Bacteriol* **2000**, *182*, 5919-5921, doi:10.1128/jb.182.20.5919-5921.2000.

221. Lock, R.A.; Paton, J.C.; Hansman, D. Purification and immunological characterization of neuraminidase produced by *Streptococcus pneumoniae*. *Microbial Pathogenesis* **1988**, *4*, 33-43, doi:https://doi.org/10.1016/0882-4010(88)90046-0.
222. Proctor, M.; Manning, P.J. Production of immunoglobulin A protease by *Streptococcus pneumoniae* from animals. *Infect Immun* **1990**, *58*, 2733-2737, doi:10.1128/IAI.58.9.2733-2737.1990.
223. Yamaguchi, M.; Terao, Y.; Mori, Y.; Hamada, S.; Kawabata, S. PfbA, a novel plasmin- and fibronectin-binding protein of *Streptococcus pneumoniae*, contributes to fibronectin-dependent adhesion and antiphagocytosis. *The Journal of biological chemistry* **2008**, *283*, 36272-36279, doi:10.1074/jbc.M807087200.
224. Berry, A.M.; Lock, R.A.; Thomas, S.M.; Rajan, D.P.; Hansman, D.; Paton, J.C. Cloning and nucleotide sequence of the *Streptococcus pneumoniae* hyaluronidase gene and purification of the enzyme from recombinant *Escherichia coli*. *Infect Immun* **1994**, *62*, 1101-1108, doi:10.1128/IAI.62.3.1101-1108.1994.
225. Löfling, J.; Vimberg, V.; Battig, P.; Henriques-Normark, B. Cellular interactions by LPxTG-anchored pneumococcal adhesins and their streptococcal homologues. *Cellular microbiology* **2011**, *13*, 186-197, doi:10.1111/j.1462-5822.2010.01560.x.
226. Jensch, I.; Gámez, G.; Rothe, M.; Ebert, S.; Fulde, M.; Somplatzki, D.; Bergmann, S.; Petruschka, L.; Rohde, M.; Nau, R., et al. PavB is a surface-exposed adhesin of *Streptococcus pneumoniae* contributing to nasopharyngeal colonization and airways infections. *Molecular microbiology* **2010**, *77*, 22-43, doi:10.1111/j.1365-2958.2010.07189.x.
227. Kanwal, S.; Jensch, I.; Palm, G.J.; Brönstrup, M.; Rohde, M.; Kohler, T.P.; Somplatzki, D.; Tegge, W.; Jenkinson, H.F.; Hammerschmidt, S. Mapping the recognition domains of pneumococcal fibronectin-binding proteins PavA and PavB demonstrates a common pattern of molecular interactions with fibronectin type III repeats. *Molecular microbiology* **2017**, *105*, 839-859, doi:10.1111/mmi.13740.
228. Bumbaca, D.; Littlejohn, J.E.; Nayakanti, H.; Rigden, D.J.; Galperin, M.Y.; Jedrzejas, M.J. Sequence analysis and characterization of a novel fibronectin-binding repeat domain from the surface of *Streptococcus pneumoniae*. *Omics : a journal of integrative biology* **2004**, *8*, 341-356, doi:10.1089/omi.2004.8.341.
229. Telford, J.L.; Barocchi, M.A.; Margarit, I.; Rappuoli, R.; Grandi, G. Pili in Gram-positive pathogens. *Nature Reviews Microbiology* **2006**, *4*, 509-519, doi:10.1038/nrmicro1443.
230. Barocchi, M.A.; Ries, J.; Zogaj, X.; Hemsley, C.; Albiger, B.; Kanth, A.; Dahlberg, S.; Fernebro, J.; Moschioni, M.; Masignani, V., et al. A pneumococcal pilus influences virulence and host inflammatory responses. *Proceedings of the National Academy of Sciences of the United States of America* **2006**, *103*, 2857-2862, doi:10.1073/pnas.0511017103.
231. Nelson, A.L.; Ries, J.; Bagnoli, F.; Dahlberg, S.; Fälker, S.; Rounioja, S.; Tschöp, J.; Morfeldt, E.; Ferlenghi, I.; Hilleringmann, M., et al. RrgA is a pilus-associated adhesin in *Streptococcus pneumoniae*. *Molecular microbiology* **2007**, *66*, 329-340, doi:10.1111/j.1365-2958.2007.05908.x.
232. Bagnoli, F.; Moschioni, M.; Donati, C.; Dimitrovska, V.; Ferlenghi, I.; Facciotti, C.; Muzzi, A.; Giusti, F.; Emolo, C.; Sinisi, A., et al. A second pilus type in *Streptococcus pneumoniae* is prevalent in emerging serotypes and mediates adhesion to host cells. *J Bacteriol* **2008**, *190*, 5480-5492, doi:10.1128/jb.00384-08.
233. Kovacs-Simon, A.; Titball, R.W.; Michell, S.L. Lipoproteins of bacterial pathogens. *Infect Immun* **2011**, *79*, 548-561, doi:10.1128/iai.00682-10.
234. Saleh, M.; Bartual, S.G.; Abdullah, M.R.; Jensch, I.; Asmat, T.M.; Petruschka, L.; Pribyl, T.; Gellert, M.; Lillig, C.H.; Antelmann, H., et al. Molecular architecture of *Streptococcus pneumoniae* surface thioredoxin-fold lipoproteins crucial for extracellular oxidative stress resistance and maintenance of virulence. *EMBO molecular medicine* **2013**, *5*, 1852-1870, doi:10.1002/emmm.201202435.
235. Novak, R.; Braun, J.S.; Charpentier, E.; Tuomanen, E. Penicillin tolerance genes of *Streptococcus pneumoniae*: the ABC-type manganese permease complex Psa. *Molecular microbiology* **1998**, *29*, 1285-1296, doi:10.1046/j.1365-2958.1998.01016.x.
236. Hermans, P.W.; Adrian, P.V.; Albert, C.; Estevão, S.; Hoogenboezem, T.; Luijendijk, I.H.; Kamphausen, T.; Hammerschmidt, S. The streptococcal lipoprotein rotamase A (SlrA) is a functional peptidyl-prolyl isomerase involved in pneumococcal colonization. *The Journal of biological chemistry* **2006**, *281*, 968-976, doi:10.1074/jbc.M510014200.
237. Yang, X.Y.; Li, N.; Xu, J.Y.; Sun, X.; He, Q.Y. Lipoprotein SPD_1609 of *Streptococcus pneumoniae* Promotes Adherence and Invasion to Epithelial Cells Contributing to Bacterial Virulence. *Frontiers in microbiology* **2019**, *10*, 1769, doi:10.3389/fmicb.2019.01769.
238. Cron, L.E.; Bootsma, H.J.; Noske, N.; Burghout, P.; Hammerschmidt, S.; Hermans, P.W.M. Surface-associated lipoprotein PpmA of *Streptococcus pneumoniae* is involved in colonization in a strain-specific manner. *Microbiology (Reading, England)* **2009**, *155*, 2401-2410, doi:10.1099/mic.0.026765-0.

239. Pribyl, T.; Moche, M.; Dreisbach, A.; Bijlsma, J.J.; Saleh, M.; Abdullah, M.R.; Hecker, M.; van Dijl, J.M.; Becher, D.; Hammerschmidt, S. Influence of impaired lipoprotein biogenesis on surface and exoproteome of *Streptococcus pneumoniae*. *Journal of proteome research* **2014**, *13*, 650-667, doi:10.1021/pr400768v.
240. Nakayama, H.; Kurokawa, K.; Lee, B.L. Lipoproteins in bacteria: structures and biosynthetic pathways. *The FEBS journal* **2012**, *279*, 4247-4268, doi:10.1111/febs.12041.
241. Zückert, W.R. Secretion of bacterial lipoproteins: through the cytoplasmic membrane, the periplasm and beyond. *Biochimica et biophysica acta* **2014**, *1843*, 1509-1516, doi:10.1016/j.bbamcr.2014.04.022.
242. van der Reest, J.; Lilla, S.; Zheng, L.; Zanivan, S.; Gottlieb, E. Proteome-wide analysis of cysteine oxidation reveals metabolic sensitivity to redox stress. *Nature Communications* **2018**, *9*, 1581, doi:10.1038/s41467-018-04003-3.
243. Sampson, J.S.; O'Connor, S.P.; Stinson, A.R.; Tharpe, J.A.; Russell, H. Cloning and nucleotide sequence analysis of *psaA*, the *Streptococcus pneumoniae* gene encoding a 37-kilodalton protein homologous to previously reported *Streptococcus* sp. adhesins. *Infect Immun* **1994**, *62*, 319-324, doi:10.1128/iai.62.1.319-324.1994.
244. Anderton, J.M.; Rajam, G.; Romero-Steiner, S.; Summer, S.; Kowalczyk, A.P.; Carlone, G.M.; Sampson, J.S.; Ades, E.W. E-cadherin is a receptor for the common protein pneumococcal surface adhesin A (PsaA) of *Streptococcus pneumoniae*. *Microb Pathog* **2007**, *42*, 225-236, doi:10.1016/j.micpath.2007.02.003.
245. Berry, A.M.; Paton, J.C. Sequence heterogeneity of PsaA, a 37-kilodalton putative adhesin essential for virulence of *Streptococcus pneumoniae*. *Infect Immun* **1996**, *64*, 5255-5262, doi:10.1128/iai.64.12.5255-5262.1996.
246. Marra, A.; Lawson, S.; Asundi, J.S.; Brigham, D.; Hromockyj, A.E. *In vivo* characterization of the *psa* genes from *Streptococcus pneumoniae* in multiple models of infection. *Microbiology (Reading, England)* **2002**, *148*, 1483-1491, doi:10.1099/00221287-148-5-1483.
247. Alloing, G.; de Philip, P.; Claverys, J.P. Three highly homologous membrane-bound lipoproteins participate in oligopeptide transport by the Ami system of the gram-positive *Streptococcus pneumoniae*. *Journal of molecular biology* **1994**, *241*, 44-58, doi:10.1006/jmbi.1994.1472.
248. Kerr, A.R.; Adrian, P.V.; Estevão, S.; de Groot, R.; Alloing, G.; Claverys, J.P.; Mitchell, T.J.; Hermans, P.W. The Ami-AliA/AliB permease of *Streptococcus pneumoniae* is involved in nasopharyngeal colonization but not in invasive disease. *Infect Immun* **2004**, *72*, 3902-3906, doi:10.1128/iai.72.7.3902-3906.2004.
249. Bergmann, S.; Wild, D.; Diekmann, O.; Frank, R.; Bracht, D.; Chhatwal, G.S.; Hammerschmidt, S. Identification of a novel plasmin(ogen)-binding motif in surface displayed α-enolase of *Streptococcus pneumoniae*. *Molecular microbiology* **2003**, *49*, 411-423.
250. Bergmann, S.; Rohde, M.; Hammerschmidt, S. Glyceraldehyde-3-phosphate dehydrogenase of *Streptococcus pneumoniae* is a surface-displayed plasminogen-binding protein. *Infect Immun* **2004**, *72*, 2416-2419, doi:10.1128/iai.72.4.2416-2419.2004.
251. Fulde, M.; Bernardo-García, N.; Rohde, M.; Nachtigall, N.; Frank, R.; Preissner, K.T.; Klett, J.; Morreale, A.; Chhatwal, G.S.; Hermoso, J.A., et al. Pneumococcal phosphoglycerate kinase interacts with plasminogen and its tissue activator. *Thrombosis and haemostasis* **2014**, *111*, 401-416, doi:10.1160/th13-05-0421.
252. Agarwal, V.; Hammerschmidt, S.; Malm, S.; Bergmann, S.; Riesbeck, K.; Blom, A.M. Enolase of *Streptococcus pneumoniae* binds human complement inhibitor C4b-binding protein and contributes to complement evasion. *Journal of immunology (Baltimore, Md. : 1950)* **2012**, *189*, 3575-3584, doi:10.4049/jimmunol.1102934.
253. Blom, A.M.; Bergmann, S.; Fulde, M.; Riesbeck, K.; Agarwal, V. *Streptococcus pneumoniae* phosphoglycerate kinase is a novel complement inhibitor affecting the membrane attack complex formation. *The Journal of biological chemistry* **2014**, *289*, 32499-32511, doi:10.1074/jbc.M114.610212.
254. Stock, A.M.; Robinson, V.L.; Goudreau, P.N. Two-component signal transduction. *Annual review of biochemistry* **2000**, *69*, 183-215, doi:10.1146/annurev.biochem.69.1.183.
255. Beier, D.; Gross, R. Regulation of bacterial virulence by two-component systems. *Current opinion in microbiology* **2006**, *9*, 143-152, doi:10.1016/j.mib.2006.01.005.
256. Hoch, J.A. Two-component and phosphorelay signal transduction. *Current opinion in microbiology* **2000**, *3*, 165-170, doi:10.1016/s1369-5274(00)00070-9.
257. Miller, M.B.; Bassler, B.L. Quorum sensing in bacteria. *Annual review of microbiology* **2001**, *55*, 165-199, doi:10.1146/annurev.micro.55.1.165.
258. Kleerebezem, M.; Quadri, L.E.; Kuipers, O.P.; de Vos, W.M. Quorum sensing by peptide pheromones and two-component signal-transduction systems in Gram-positive bacteria. *Molecular microbiology* **1997**, *24*, 895-904, doi:10.1046/j.1365-2958.1997.4251782.x.
259. Gray, K.M.; Garey, J.R. The evolution of bacterial LuxI and LuxR quorum sensing regulators. *Microbiology (Reading, England)* **2001**, *147*, 2379-2387, doi:10.1099/00221287-147-8-2379.

260. Lerat, E.; Moran, N.A. The evolutionary history of quorum-sensing systems in bacteria. *Molecular biology and evolution* **2004**, *21*, 903-913, doi:10.1093/molbev/msh097.
261. Nealson, K.H.; Platt, T.; Hastings, J.W. Cellular control of the synthesis and activity of the bacterial luminescent system. *J Bacteriol* **1970**, *104*, 313-322, doi:10.1128/JB.104.1.313-322.1970.
262. Rutherford, S.T.; Bassler, B.L. Bacterial quorum sensing: its role in virulence and possibilities for its control. *Cold Spring Harbor perspectives in medicine* **2012**, *2*, doi:10.1101/cshperspect.a012427.
263. Verbeke, F.; De Craemer, S.; Debunne, N.; Janssens, Y.; Wynendaele, E.; Van de Wiele, C.; De Spiegeleer, B. Peptides as Quorum Sensing Molecules: Measurement Techniques and Obtained Levels *In vitro* and *In vivo*. *Frontiers in Neuroscience* **2017**, *11*, 183.
264. Bassler, B.L. How bacteria talk to each other: regulation of gene expression by quorum sensing. *Current opinion in microbiology* **1999**, *2*, 582-587, doi:10.1016/s1369-5274(99)00025-9.
265. Sturme, M.H.J.; Kleerebezem, M.; Nakayama, J.; Akkermans, A.D.L.; Vaughan, E.E.; de Vos, W.M. Cell to cell communication by autoinducing peptides in gram-positive bacteria. *Antonie van Leeuwenhoek* **2002**, *81*, 233-243, doi:10.1023/A:1020522919555.
266. Papenfort, K.; Bassler, B.L. Quorum sensing signal–response systems in Gram-negative bacteria. *Nature Reviews Microbiology* **2016**, *14*, 576-588, doi:10.1038/nrmicro.2016.89.
267. Ng, W.L.; Bassler, B.L. Bacterial quorum-sensing network architectures. *Annual review of genetics* **2009**, *43*, 197-222, doi:10.1146/annurev-genet-102108-134304.
268. Bridges, A.A.; Bassler, B.L. The intragenus and interspecies quorum-sensing autoinducers exert distinct control over *Vibrio cholerae* biofilm formation and dispersal. *PLoS biology* **2019**, *17*, e3000429, doi:10.1371/journal.pbio.3000429.
269. Watve, S.; Barrasso, K.; Jung, S.A.; Davis, K.J.; Hawver, L.A.; Khataokar, A.; Palaganas, R.G.; Neiditch, M.B.; Perez, L.J.; Ng, W.-L. Parallel quorum-sensing system in *Vibrio cholerae* prevents signal interference inside the host. *PLoS pathogens* **2020**, *16*, e1008313, doi:10.1371/journal.ppat.1008313.
270. Swift, S.; Downie, J.A.; Whitehead, N.A.; Barnard, A.M.; Salmond, G.P.; Williams, P. Quorum sensing as a population-density-dependent determinant of bacterial physiology. *Advances in microbial physiology* **2001**, *45*, 199-270, doi:10.1016/s0065-2911(01)45005-3.
271. Abisado, R.G.; Benomar, S.; Klaus, J.R.; Dandekar, A.A.; Chandler, J.R. Bacterial Quorum Sensing and Microbial Community Interactions. *mBio* **2018**, *9*, e02331-02317, doi:10.1128/mBio.02331-17.
272. Yan, S.; Wu, G. Can Biofilm Be Reversed Through Quorum Sensing in *Pseudomonas aeruginosa*? *Frontiers in microbiology* **2019**, *10*, 1582.
273. Liu, X.; Bimerew, M.; Ma, Y.; Müller, H.; Ovadis, M.; Eberl, L.; Berg, G.; Chernin, L. Quorum-sensing signaling is required for production of the antibiotic pyrrolnitrin in a rhizospheric biocontrol strain of *Serratia plymuthica*. *FEMS microbiology letters* **2007**, *270*, 299-305, doi:10.1111/j.1574-6968.2007.00681.x.
274. de Kievit, T.R.; Iglewski, B.H. Bacterial quorum sensing in pathogenic relationships. *Infect Immun* **2000**, *68*, 4839-4849, doi:10.1128/iai.68.9.4839-4849.2000.
275. Perchat, S.; Talagas, A.; Poncet, S.; Lazar, N.; Li de la Sierra-Gallay, I.; Gohar, M.; Lereclus, D.; Nessler, S. How Quorum Sensing Connects Sporulation to Necrotrophism in *Bacillus thuringiensis*. *PLoS pathogens* **2016**, *12*, e1005779, doi:10.1371/journal.ppat.1005779.
276. von Bodman, S.B.; Bauer, W.D.; Coplin, D.L. QUORUM SENSING IN PLANT-PATHOGENIC BACTERIA. *Annual Review of Phytopathology* **2003**, *41*, 455-482, doi:10.1146/annurev.phyto.41.052002.095652.
277. Turkina, M.V.; Vikström, E. Bacteria-Host Crosstalk: Sensing of the Quorum in the Context of *Pseudomonas aeruginosa* Infections. *Journal of innate immunity* **2019**, *11*, 263-279, doi:10.1159/000494069.
278. González, J.E.; Marketon, M.M. Quorum Sensing in Nitrogen-Fixing Rhizobia. *Microbiology and Molecular Biology Reviews* **2003**, *67*, 574, doi:10.1128/MMBR.67.4.574-592.2003.
279. Montgomery, K.; Charlesworth, J.C.; LeBard, R.; Visscher, P.T.; Burns, B.P. Quorum sensing in extreme environments. *Life (Basel)* **2013**, *3*, 131-148, doi:10.3390/life3010131.
280. Blokesch, M. Natural competence for transformation. *Current biology : CB* **2016**, *26*, R1126-r1130, doi:10.1016/j.cub.2016.08.058.
281. Mell, J.C.; Redfield, R.J. Natural competence and the evolution of DNA uptake specificity. *J Bacteriol* **2014**, *196*, 1471-1483, doi:10.1128/jb.01293-13.
282. Cheng, Q.; Campbell, E.A.; Naughton, A.M.; Johnson, S.; Masure, H.R. The *com* locus controls genetic transformation in *Streptococcus pneumoniae*. *Molecular microbiology* **1997**, *23*, 683-692, doi:10.1046/j.1365-2958.1997.2481617.x.
283. Steinmoen, H.; Knutsen, E.; Håvarstein, L.S. Induction of natural competence in *Streptococcus pneumoniae* triggers lysis and DNA release from a subfraction of the cell population. *Proceedings of the National Academy of Sciences* **2002**, *99*, 7681, doi:10.1073/pnas.112464599.

284. Knutsen, E.; Ween, O.; Håvarstein, L.S. Two separate quorum-sensing systems upregulate transcription of the same ABC transporter in *Streptococcus pneumoniae*. *J Bacteriol* **2004**, *186*, 3078-3085, doi:10.1128/jb.186.10.3078-3085.2004.
285. Martin, B.; Granadel, C.; Campo, N.; Hénard, V.; Prudhomme, M.; Claverys, J.P. Expression and maintenance of ComD-ComE, the two-component signal-transduction system that controls competence of *Streptococcus pneumoniae*. *Molecular microbiology* **2010**, *75*, 1513-1528, doi:10.1111/j.1365-2958.2010.07071.x.
286. Pestova, E.V.; Håvarstein, L.S.; Morrison, D.A. Regulation of competence for genetic transformation in *Streptococcus pneumoniae* by an auto-induced peptide pheromone and a two-component regulatory system. *Molecular microbiology* **1996**, *21*, 853-862, doi:10.1046/j.1365-2958.1996.501417.x.
287. Hui, F.M.; Morrison, D.A. Genetic transformation in *Streptococcus pneumoniae*: nucleotide sequence analysis shows *comA*, a gene required for competence induction, to be a member of the bacterial ATP-dependent transport protein family. *J Bacteriol* **1991**, *173*, 372-381, doi:10.1128/jb.173.1.372-381.1991.
288. Ween, O.; Gaustad, P.; Håvarstein, L.S. Identification of DNA binding sites for ComE, a key regulator of natural competence in *Streptococcus pneumoniae*. *Molecular microbiology* **1999**, *33*, 817-827, doi:10.1046/j.1365-2958.1999.01528.x.
289. Peterson, S.; Cline, R.T.; Tettelin, H.; Sharov, V.; Morrison, D.A. Gene expression analysis of the *Streptococcus pneumoniae* competence regulons by use of DNA microarrays. *J Bacteriol* **2000**, *182*, 6192-6202, doi:10.1128/jb.182.21.6192-6202.2000.
290. Luo, P.; Li, H.; Morrison, D.A. Identification of ComW as a new component in the regulation of genetic transformation in *Streptococcus pneumoniae*. *Molecular microbiology* **2004**, *54*, 172-183, doi:10.1111/j.1365-2958.2004.04254.x.
291. Sung, C.K.; Morrison, D.A. Two Distinct Functions of ComW in Stabilization and Activation of the Alternative Sigma Factor ComX in *Streptococcus pneumoniae*. *J Bacteriol* **2005**, *187*, 3052, doi:10.1128/JB.187.9.3052-3061.2005.
292. Reid, S.D.; Hong, W.; Dew, K.E.; Winn, D.R.; Pang, B.; Watt, J.; Glover, D.T.; Hollingshead, S.K.; Swords, W.E. *Streptococcus pneumoniae* forms surface-attached communities in the middle ear of experimentally infected chinchillas. *The Journal of infectious diseases* **2009**, *199*, 786-794, doi:10.1086/597042.
293. Trappetti, C.; Potter, A.J.; Paton, A.W.; Oggioni, M.R.; Paton, J.C. LuxS mediates iron-dependent biofilm formation, competence, and fratricide in *Streptococcus pneumoniae*. *Infect Immun* **2011**, *79*, 4550-4558.
294. Vidal, J.E.; Ludewick, H.P.; Kunkel, R.M.; Zähner, D.; Klugman, K.P. The LuxS-dependent quorum-sensing system regulates early biofilm formation by *Streptococcus pneumoniae* strain D39. *Infect Immun* **2011**, *79*, 4050-4060, doi:10.1128/IAI.05186-11.
295. Stroeher, U.H.; Paton, A.W.; Ogunniyi, A.D.; Paton, J.C. Mutation of *luxS* of *Streptococcus pneumoniae* affects virulence in a mouse model. *Infect Immun* **2003**, *71*, 3206-3212, doi:10.1128/iai.71.6.3206-3212.2003.
296. Romao, S.; Memmi, G.; Oggioni, M.R.; Trombe, M.C. LuxS impacts on LytA-dependent autolysis and on competence in *Streptococcus pneumoniae*. *Microbiology (Reading, England)* **2006**, *152*, 333-341, doi:10.1099/mic.0.28406-0.
297. Hoover, S.E.; Perez, A.J.; Tsui, H.C.; Sinha, D.; Smiley, D.L.; DiMarchi, R.D.; Winkler, M.E.; Lazazzera, B.A. A new quorum-sensing system (TprA/PhrA) for *Streptococcus pneumoniae* D39 that regulates a lantibiotic biosynthesis gene cluster. *Molecular microbiology* **2015**, *97*, 229-243, doi:10.1111/mmi.13029.
298. McIver, K.S. Stand-alone response regulators controlling global virulence networks in *Streptococcus pyogenes*. *Contributions to microbiology* **2009**, *16*, 103-119, doi:10.1159/000219375.
299. Brennan, R.G.; Matthews, B.W. The helix-turn-helix DNA binding motif. *The Journal of biological chemistry* **1989**, *264*, 1903-1906.
300. Serror, P.; Sonenshein, A.L. CodY is required for nutritional repression of *Bacillus subtilis* genetic competence. *J Bacteriol* **1996**, *178*, 5910-5915, doi:10.1128/jb.178.20.5910-5915.1996.
301. den Hengst, C.D.; van Hijum, S.A.; Geurts, J.M.; Nauta, A.; Kok, J.; Kuipers, O.P. The *Lactococcus lactis* CodY regulon: identification of a conserved cis-regulatory element. *The Journal of biological chemistry* **2005**, *280*, 34332-34342, doi:10.1074/jbc.M502349200.
302. Molle, V.; Nakaura, Y.; Shivers, R.P.; Yamaguchi, H.; Losick, R.; Fujita, Y.; Sonenshein, A.L. Additional targets of the *Bacillus subtilis* global regulator CodY identified by chromatin immunoprecipitation and genome-wide transcript analysis. *J Bacteriol* **2003**, *185*, 1911-1922, doi:10.1128/jb.185.6.1911-1922.2003.
303. Levdikov, V.M.; Blagova, E.; Joseph, P.; Sonenshein, A.L.; Wilkinson, A.J. The structure of CodY, a GTP- and isoleucine-responsive regulator of stationary phase and virulence in gram-positive bacteria. *The Journal of biological chemistry* **2006**, *281*, 11366-11373, doi:10.1074/jbc.M513015200.

304. Stenz, L.; Francois, P.; Whiteson, K.; Wolz, C.; Linder, P.; Schrenzel, J. The CodY pleiotropic repressor controls virulence in gram-positive pathogens. *FEMS immunology and medical microbiology* **2011**, *62*, 123-139, doi:10.1111/j.1574-695X.2011.00812.x.
305. Giammarinaro, P.; Paton, J.C. Role of RegM, a homologue of the catabolite repressor protein CcpA, in the virulence of *Streptococcus pneumoniae*. *Infect Immun* **2002**, *70*, 5454-5461, doi:10.1128/iai.70.10.5454-5461.2002.
306. Carvalho, S.M.; Kloosterman, T.G.; Kuipers, O.P.; Neves, A.R. CcpA Ensures Optimal Metabolic Fitness of *Streptococcus pneumoniae*. *PLOS ONE* **2011**, *6*, e26707, doi:10.1371/journal.pone.0026707.
307. Miwa, Y.; Nakata, A.; Ogiwara, A.; Yamamoto, M.; Fujita, Y. Evaluation and characterization of catabolite-responsive elements (*cre*) of *Bacillus subtilis*. *Nucleic Acids Res* **2000**, *28*, 1206-1210, doi:10.1093/nar/28.5.1206.
308. Marciniak, B.C.; Pabijaniak, M.; de Jong, A.; Dűhring, R.; Seidel, G.; Hillen, W.; Kuipers, O.P. High- and low-affinity *cre* boxes for CcpA binding in *Bacillus subtilis* revealed by genome-wide analysis. *BMC genomics* **2012**, *13*, 401, doi:10.1186/1471-2164-13-401.
309. van Opijnen, T.; Bodi, K.L.; Camilli, A. Tn-seq: high-throughput parallel sequencing for fitness and genetic interaction studies in microorganisms. *Nature methods* **2009**, *6*, 767-772, doi:10.1038/nmeth.1377.
310. Schulz, C.; Gierok, P.; Petruschka, L.; Lalk, M.; Mäder, U.; Hammerschmidt, S. Regulation of the arginine deiminase system by ArgR2 interferes with arginine metabolism and fitness of *Streptococcus pneumoniae*. *mBio* **2014**, *5*, doi:10.1128/mBio.01858-14.
311. Kloosterman, T.G.; Kuipers, O.P. Regulation of arginine acquisition and virulence gene expression in the human pathogen *Streptococcus pneumoniae* by transcription regulators ArgR1 and AhrC. *The Journal of biological chemistry* **2011**, *286*, 44594-44605, doi:10.1074/jbc.M111.295832.
312. Hendriksen, W.T.; Kloosterman, T.G.; Bootsma, H.J.; Estevão, S.; de Groot, R.; Kuipers, O.P.; Hermans, P.W. Site-specific contributions of glutamine-dependent regulator GlnR and GlnR-regulated genes to virulence of *Streptococcus pneumoniae*. *Infect Immun* **2008**, *76*, 1230-1238, doi:10.1128/iai.01004-07.
313. Härtel, T.; Klein, M.; Koedel, U.; Rohde, M.; Petruschka, L.; Hammerschmidt, S. Impact of glutamine transporters on pneumococcal fitness under infection-related conditions. *Infect Immun* **2011**, *79*, 44-58, doi:10.1128/iai.00855-10.
314. Kloosterman, T.G.; Hendriksen, W.T.; Bijlsma, J.J.; Bootsma, H.J.; van Hijum, S.A.; Kok, J.; Hermans, P.W.; Kuipers, O.P. Regulation of glutamine and glutamate metabolism by GlnR and GlnA in *Streptococcus pneumoniae*. *The Journal of biological chemistry* **2006**, *281*, 25097-25109, doi:10.1074/jbc.M601661200.
315. Brekasis, D.; Paget, M.S. A novel sensor of NADH/NAD^+ redox poise in *Streptomyces coelicolor* A3(2). *The EMBO journal* **2003**, *22*, 4856-4865, doi:10.1093/emboj/cdg453.
316. Pagels, M.; Fuchs, S.; Pané-Farré, J.; Kohler, C.; Menschner, L.; Hecker, M.; McNamarra, P.J.; Bauer, M.C.; von Wachenfeldt, C.; Liebeke, M., et al. Redox sensing by a Rex-family repressor is involved in the regulation of anaerobic gene expression in *Staphylococcus aureus*. *Molecular microbiology* **2010**, *76*, 1142-1161, doi:10.1111/j.1365-2958.2010.07105.x.
317. Ruhland, B.R.; Reniere, M.L. Sense and sensor ability: redox-responsive regulators in *Listeria monocytogenes*. *Current opinion in microbiology* **2019**, *47*, 20-25, doi:10.1016/j.mib.2018.10.006.
318. Afzal, M.; Shafeeq, S.; Kuipers, O.P. NADH-Mediated Gene Expression in *Streptococcus pneumoniae* and Role of Rex as a Transcriptional Repressor of the Rex-Regulon. *Frontiers in microbiology* **2018**, *9*, 1300.
319. Sickmier, E.A.; Brekasis, D.; Paranawithana, S.; Bonanno, J.B.; Paget, M.S.; Burley, S.K.; Kielkopf, C.L. X-ray structure of a Rex-family repressor/NADH complex insights into the mechanism of redox sensing. *Structure (London, England : 1993)* **2005**, *13*, 43-54, doi:10.1016/j.str.2004.10.012.
320. Belenky, P.; Bogan, K.L.; Brenner, C. NAD^+ metabolism in health and disease. *Trends in biochemical sciences* **2007**, *32*, 12-19, doi:10.1016/j.tibs.2006.11.006.
321. Wang, E.; Bauer, M.C.; Rogstam, A.; Linse, S.; Logan, D.T.; von Wachenfeldt, C. Structure and functional properties of the *Bacillus subtilis* transcriptional repressor Rex. *Molecular microbiology* **2008**, *69*, 466-478, doi:10.1111/j.1365-2958.2008.06295.x.
322. Ravcheev, D.A.; Li, X.; Latif, H.; Zengler, K.; Leyn, S.A.; Korostelev, Y.D.; Kazakov, A.E.; Novichkov, P.S.; Osterman, A.L.; Rodionov, D.A. Transcriptional Regulation of Central Carbon and Energy Metabolism in Bacteria by Redox-Responsive Repressor Rex. *J Bacteriol* **2012**, *194*, 1145, doi:10.1128/JB.06412-11.
323. Zhang, L.; Nie, X.; Ravcheev, D.A.; Rodionov, D.A.; Sheng, J.; Gu, Y.; Yang, S.; Jiang, W.; Yang, C. Redox-responsive repressor Rex modulates alcohol production and oxidative stress tolerance in *Clostridium acetobutylicum*. *J Bacteriol* **2014**, *196*, 3949-3963, doi:10.1128/jb.02037-14.
324. Christensen, G.A.; Zane, G.M.; Kazakov, A.E.; Li, X.; Rodionov, D.A.; Novichkov, P.S.; Dubchak, I.; Arkin, A.P.; Wall, J.D. Rex (Encoded by DVU_0916) in *Desulfovibrio vulgaris* Hildenborough Is a

Repressor of Sulfate Adenylyl Transferase and Is Regulated by NADH. *J Bacteriol* **2015**, *197*, 29, doi:10.1128/JB.02083-14.
325. Bitoun, J.P.; Wen, Z.T. Transcription factor Rex in regulation of pathophysiology in oral pathogens. *Molecular oral microbiology* **2016**, *31*, 115-124, doi:10.1111/omi.12114.
326. Bitoun, J.P.; Liao, S.; Yao, X.; Xie, G.G.; Wen, Z.T. The redox-sensing regulator Rex modulates central carbon metabolism, stress tolerance response and biofilm formation by *Streptococcus mutans*. *PLoS One* **2012**, *7*, e44766, doi:10.1371/journal.pone.0044766.
327. Palazzo, A.F.; Lee, E.S. Non-coding RNA: what is functional and what is junk? *Frontiers in genetics* **2015**, *6*, 2, doi:10.3389/fgene.2015.00002.
328. Livny, J.; Waldor, M.K. Identification of small RNAs in diverse bacterial species. *Current opinion in microbiology* **2007**, *10*, 96-101, doi:10.1016/j.mib.2007.03.005.
329. Waters, L.S.; Storz, G. Regulatory RNAs in bacteria. *Cell* **2009**, *136*, 615-628, doi:10.1016/j.cell.2009.01.043.
330. Boisset, S.; Geissmann, T.; Huntzinger, E.; Fechter, P.; Bendridi, N.; Possedko, M.; Chevalier, C.; Helfer, A.C.; Benito, Y.; Jacquier, A., et al. *Staphylococcus aureus* RNAIII coordinately represses the synthesis of virulence factors and the transcription regulator Rot by an antisense mechanism. *Genes & development* **2007**, *21*, 1353-1366, doi:10.1101/gad.423507.
331. Zhang, A.; Wassarman, K.M.; Rosenow, C.; Tjaden, B.C.; Storz, G.; Gottesman, S. Global analysis of small RNA and mRNA targets of Hfq. *Molecular microbiology* **2003**, *50*, 1111-1124, doi:10.1046/j.1365-2958.2003.03734.x.
332. Acebo, P.; Martin-Galiano, A.J.; Navarro, S.; Zaballos, A.; Amblar, M. Identification of 88 regulatory small RNAs in the TIGR4 strain of the human pathogen *Streptococcus pneumoniae*. *RNA* **2012**, *18*, 530-546, doi:10.1261/rna.027359.111.
333. Mann, B.; van Opijnen, T.; Wang, J.; Obert, C.; Wang, Y.D.; Carter, R.; McGoldrick, D.J.; Ridout, G.; Camilli, A.; Tuomanen, E.I., et al. Control of virulence by small RNAs in *Streptococcus pneumoniae*. *PLoS pathogens* **2012**, *8*, e1002788, doi:10.1371/journal.ppat.1002788.
334. Sinha, D.; Zimmer, K.; Cameron, T.A.; Rusch, D.B.; Winkler, M.E.; De Lay, N.R. Redefining the Small Regulatory RNA Transcriptome in *Streptococcus pneumoniae* Serotype 2 Strain D39. *J Bacteriol* **2019**, *201*, doi:10.1128/jb.00764-18.
335. Halfmann, A.; Kovács, M.; Hakenbeck, R.; Brückner, R. Identification of the genes directly controlled by the response regulator CiaR in *Streptococcus pneumoniae*: five out of 15 promoters drive expression of small non-coding RNAs. *Molecular microbiology* **2007**, *66*, 110-126, doi:10.1111/j.1365-2958.2007.05900.x.
336. Laux, A.; Sexauer, A.; Sivaselvarajah, D.; Kaysen, A.; Brückner, R. Control of competence by related non-coding csRNAs in *Streptococcus pneumoniae* R6. *Frontiers in genetics* **2015**, *6*, 246, doi:10.3389/fgene.2015.00246.
337. Klumpp, S.; Krieglstein, J. Phosphorylation and dephosphorylation of histidine residues in proteins. *European journal of biochemistry* **2002**, *269*, 1067-1071, doi:10.1046/j.1432-1033.2002.02755.x.
338. Laub, M.T.; Goulian, M. Specificity in two-component signal transduction pathways. *Annual review of genetics* **2007**, *41*, 121-145, doi:10.1146/annurev.genet.41.042007.170548.
339. West, A.H.; Stock, A.M. Histidine kinases and response regulator proteins in two-component signaling systems. *Trends in biochemical sciences* **2001**, *26*, 369-376, doi:10.1016/s0968-0004(01)01852-7.
340. Lange, R.; Wagner, C.; de Saizieu, A.; Flint, N.; Molnos, J.; Stieger, M.; Caspers, P.; Kamber, M.; Keck, W.; Amrein, K.E. Domain organization and molecular characterization of 13 two-component systems identified by genome sequencing of *Streptococcus pneumoniae*. *Gene* **1999**, *237*, 223-234, doi:10.1016/s0378-1119(99)00266-8.
341. Ashby, M.K. Survey of the number of two-component response regulator genes in the complete and annotated genome sequences of prokaryotes. *FEMS microbiology letters* **2004**, *231*, 277-281, doi:10.1016/s0378-1097(04)00004-7.
342. Kiil, K.; Ferchaud, J.B.; David, C.; Binnewies, T.T.; Wu, H.; Sicheritz-Pontén, T.; Willenbrock, H.; Ussery, D.W. Genome update: distribution of two-component transduction systems in 250 bacterial genomes. *Microbiology (Reading, England)* **2005**, *151*, 3447-3452, doi:10.1099/mic.0.28423-0.
343. Mizuno, T. His-Asp phosphotransfer signal transduction. *The journal of biochemistry* **1998**, *123*, 555-563.
344. Shi, X.; Wegener-Feldbrügge, S.; Huntley, S.; Hamann, N.; Hedderich, R.; Søgaard-Andersen, L. Bioinformatics and experimental analysis of proteins of two-component systems in *Myxococcus xanthus*. *J Bacteriol* **2008**, *190*, 613-624, doi:10.1128/JB.01502-07.
345. Paterson, G.K.; Blue, C.E.; Mitchell, T.J. Role of two-component systems in the virulence of *Streptococcus pneumoniae*. *Journal of medical microbiology* **2006**, *55*, 355-363, doi:10.1099/jmm.0.46423-0.

346. Gómez-Mejia, A.; Gámez, G.; Hirschmann, S.; Kluger, V.; Rath, H.; Böhm, S.; Voss, F.; Kakar, N.; Petruschka, L.; Völker, U., et al. Pneumococcal Metabolic Adaptation and Colonization Are Regulated by the Two-Component Regulatory System 08. *mSphere* **2018**, *3*, doi:10.1128/mSphere.00165-18.
347. Khorchid, A.; Ikura, M. Bacterial histidine kinase as signal sensor and transducer. *The international journal of biochemistry & cell biology* **2006**, *38*, 307-312, doi:10.1016/j.biocel.2005.08.018.
348. Grebe, T.W.; Stock, J.B. The histidine protein kinase superfamily. *Advances in microbial physiology* **1999**, *41*, 139-227, doi:10.1016/s0065-2911(08)60167-8.
349. Mascher, T. Intramembrane-sensing histidine kinases: a new family of cell envelope stress sensors in Firmicutes bacteria. *FEMS microbiology letters* **2006**, *264*, 133-144, doi:10.1111/j.1574-6968.2006.00444.x.
350. Mascher, T.; Helmann, J.D.; Unden, G. Stimulus perception in bacterial signal-transducing histidine kinases. *Microbiology and molecular biology reviews : MMBR* **2006**, *70*, 910-938, doi:10.1128/MMBR.00020-06.
351. Surette, M.G.; Levit, M.; Liu, Y.; Lukat, G.; Ninfa, E.G.; Ninfa, A.; Stock, J.B. Dimerization is required for the activity of the protein histidine kinase CheA that mediates signal transduction in bacterial chemotaxis. *The Journal of biological chemistry* **1996**, *271*, 939-945, doi:10.1074/jbc.271.2.939.
352. Casino, P.; Rubio, V.; Marina, A. Structural insight into partner specificity and phosphoryl transfer in two-component signal transduction. *Cell* **2009**, *139*, 325-336, doi:10.1016/j.cell.2009.08.032.
353. Gao, R.; Bouillet, S.; Stock, A.M. Structural Basis of Response Regulator Function. *Annual review of microbiology* **2019**, *73*, 175-197, doi:10.1146/annurev-micro-020518-115931.
354. Birck, C.; Mourey, L.; Gouet, P.; Fabry, B.; Schumacher, J.; Rousseau, P.; Kahn, D.; Samama, J.P. Conformational changes induced by phosphorylation of the FixJ receiver domain. *Structure (London, England : 1993)* **1999**, *7*, 1505-1515, doi:10.1016/s0969-2126(00)88341-0.
355. Gao, R.; Mack, T.R.; Stock, A.M. Bacterial response regulators: versatile regulatory strategies from common domains. *Trends in biochemical sciences* **2007**, *32*, 225-234, doi:10.1016/j.tibs.2007.03.002.
356. Tierney, A.R.; Rather, P.N. Roles of two-component regulatory systems in antibiotic resistance. *Future microbiology* **2019**, *14*, 533-552, doi:10.2217/fmb-2019-0002.
357. Skerker, J.M.; Prasol, M.S.; Perchuk, B.S.; Biondi, E.G.; Laub, M.T. Two-component signal transduction pathways regulating growth and cell cycle progression in a bacterium: a system-level analysis. *PLoS biology* **2005**, *3*, e334, doi:10.1371/journal.pbio.0030334.
358. Agrawal, R.; Sahoo, B.K.; Saini, D.K. Cross-talk and specificity in two-component signal transduction pathways. *Future microbiology* **2016**, *11*, 685-697, doi:10.2217/fmb-2016-0001.
359. Procaccini, A.; Lunt, B.; Szurmant, H.; Hwa, T.; Weigt, M. Dissecting the Specificity of Protein-Protein Interaction in Bacterial Two-Component Signaling: Orphans and Crosstalks. *PLOS ONE* **2011**, *6*, e19729, doi:10.1371/journal.pone.0019729.
360. Rowland, M.A.; Deeds, E.J. Crosstalk and the evolution of specificity in two-component signaling. *Proceedings of the National Academy of Sciences* **2014**, *111*, 5550, doi:10.1073/pnas.1317178111.
361. López-Redondo, M.L.; Moronta, F.; Salinas, P.; Espinosa, J.; Cantos, R.; Dixon, R.; Marina, A.; Contreras, A. Environmental control of phosphorylation pathways in a branched two-component system. *Molecular microbiology* **2010**, *78*, 475-489, doi:10.1111/j.1365-2958.2010.07348.x.
362. Galperin, M.Y. Structural classification of bacterial response regulators: diversity of output domains and domain combinations. *J Bacteriol* **2006**, *188*, 4169-4182, doi:10.1128/jb.01887-05.
363. Martínez-Hackert, E.; Stock, A.M. Structural relationships in the OmpR family of winged-helix transcription factors. *Journal of molecular biology* **1997**, *269*, 301-312, doi:10.1006/jmbi.1997.1065.
364. Aravind, L.; Anantharaman, V.; Balaji, S.; Babu, M.M.; Iyer, L.M. The many faces of the helix-turn-helix domain: transcription regulation and beyond. *FEMS microbiology reviews* **2005**, *29*, 231-262, doi:10.1016/j.femsre.2004.12.008.
365. Rabin, R.S.; Stewart, V. Dual response regulators (NarL and NarP) interact with dual sensors (NarX and NarQ) to control nitrate- and nitrite-regulated gene expression in *Escherichia coli* K-12. *J Bacteriol* **1993**, *175*, 3259-3268, doi:10.1128/jb.175.11.3259-3268.1993.
366. Boudes, M.; Sanchez, D.; Graille, M.; van Tilbeurgh, H.; Durand, D.; Quevillon-Cheruel, S. Structural insights into the dimerization of the response regulator ComE from *Streptococcus pneumoniae*. *Nucleic Acids Res* **2014**, *42*, 5302-5313, doi:10.1093/nar/gku110.
367. Throup, J.P.; Koretke, K.K.; Bryant, A.P.; Ingraham, K.A.; Chalker, A.F.; Ge, Y.; Marra, A.; Wallis, N.G.; Brown, J.R.; Holmes, D.J., et al. A genomic analysis of two-component signal transduction in *Streptococcus pneumoniae*. *Molecular microbiology* **2000**, *35*, 566-576, doi:10.1046/j.1365-2958.2000.01725.x.
368. Reinoso-Vizcaíno, N.M.; Cian, M.B.; Cortes, P.R.; Olivero, N.B.; Hernandez-Morfa, M.; Piñas, G.E.; Badapanda, C.; Rathore, A.; Perez, D.R.; Echenique, J. The pneumococcal two-component system SirRH is

linked to enhanced intracellular survival of *Streptococcus pneumoniae* in influenza-infected pulmonary cells. *PLoS pathogens* **2020**, *16*, e1008761, doi:10.1371/journal.ppat.1008761.
369. Hava, D.L.; Camilli, A. Large-scale identification of serotype 4 *Streptococcus pneumoniae* virulence factors. *Molecular microbiology* **2002**, *45*, 1389-1406.
370. Mohedano, M.L.; Overweg, K.; de la Fuente, A.; Reuter, M.; Altabe, S.; Mulholland, F.; de Mendoza, D.; López, P.; Wells, J.M. Evidence that the essential response regulator YycF in *Streptococcus pneumoniae* modulates expression of fatty acid biosynthesis genes and alters membrane composition. *J Bacteriol* **2005**, *187*, 2357-2367, doi:10.1128/jb.187.7.2357-2367.2005.
371. Ng, W.L.; Robertson, G.T.; Kazmierczak, K.M.; Zhao, J.; Gilmour, R.; Winkler, M.E. Constitutive expression of PcsB suppresses the requirement for the essential VicR (YycF) response regulator in *Streptococcus pneumoniae* R6. *Molecular microbiology* **2003**, *50*, 1647-1663, doi:10.1046/j.1365-2958.2003.03806.x.
372. Ng, W.L.; Tsui, H.C.; Winkler, M.E. Regulation of the *pspA* virulence factor and essential *pcsB* murein biosynthetic genes by the phosphorylated VicR (YycF) response regulator in *Streptococcus pneumoniae*. *J Bacteriol* **2005**, *187*, 7444-7459, doi:10.1128/jb.187.21.7444-7459.2005.
373. Ng, W.L.; Kazmierczak, K.M.; Winkler, M.E. Defective cell wall synthesis in *Streptococcus pneumoniae* R6 depleted for the essential PcsB putative murein hydrolase or the VicR (YycF) response regulator. *Molecular microbiology* **2004**, *53*, 1161-1175, doi:10.1111/j.1365-2958.2004.04196.x.
374. Rosch, J.W.; Mann, B.; Thornton, J.; Sublett, J.; Tuomanen, E. Convergence of Regulatory Networks on the Pilus Locus of *Streptococcus pneumoniae*. *Infect Immun* **2008**, *76*, 3187, doi:10.1128/IAI.00054-08.
375. Eldholm, V.; Gutt, B.; Johnsborg, O.; Brückner, R.; Maurer, P.; Hakenbeck, R.; Mascher, T.; Håvarstein, L.S. The pneumococcal cell envelope stress-sensing system LiaFSR is activated by murein hydrolases and lipid II-interacting antibiotics. *J Bacteriol* **2010**, *192*, 1761-1773, doi:10.1128/jb.01489-09.
376. Haas, W.; Kaushal, D.; Sublett, J.; Obert, C.; Tuomanen, E.I. Vancomycin Stress Response in a Sensitive and a Tolerant Strain of *Streptococcus pneumoniae*. *J Bacteriol* **2005**, *187*, 8205, doi:10.1128/JB.187.23.8205-8210.2005.
377. McCluskey, J.; Hinds, J.; Husain, S.; Witney, A.; Mitchell, T.J. A two-component system that controls the expression of pneumococcal surface antigen A (PsaA) and regulates virulence and resistance to oxidative stress in *Streptococcus pneumoniae*. *Molecular microbiology* **2004**, *51*, 1661-1675, doi:10.1111/j.1365-2958.2003.03917.x.
378. Zheng, J.J.; Sinha, D.; Wayne, K.J.; Winkler, M.E. Physiological Roles of the Dual Phosphate Transporter Systems in Low and High Phosphate Conditions and in Capsule Maintenance of *Streptococcus pneumoniae* D39. *Front Cell Infect Microbiol* **2016**, *6*, 63, doi:10.3389/fcimb.2016.00063.
379. Guenzi, E.; Gasc, A.M.; Sicard, M.A.; Hakenbeck, R. A two-component signal-transducing system is involved in competence and penicillin susceptibility in laboratory mutants of *Streptococcus pneumoniae*. *Molecular microbiology* **1994**, *12*, 505-515, doi:10.1111/j.1365-2958.1994.tb01038.x.
380. Sebert, M.E.; Palmer, L.M.; Rosenberg, M.; Weiser, J.N. Microarray-based identification of *htrA*, a *Streptococcus pneumoniae* gene that is regulated by the CiaRH two-component system and contributes to nasopharyngeal colonization. *Infect Immun* **2002**, *70*, 4059-4067, doi:10.1128/iai.70.8.4059-4067.2002.
381. Ibrahim, Y.M.; Kerr, A.R.; McCluskey, J.; Mitchell, T.J. Control of virulence by the two-component system CiaR/H is mediated via HtrA, a major virulence factor of *Streptococcus pneumoniae*. *J Bacteriol* **2004**, *186*, 5258-5266, doi:10.1128/jb.186.16.5258-5266.2004.
382. Blanchette-Cain, K.; Hinojosa, C.A.; Akula Suresh Babu, R.; Lizcano, A.; Gonzalez-Juarbe, N.; Munoz-Almagro, C.; Sanchez, C.J.; Bergman, M.A.; Orihuela, C.J. *Streptococcus pneumoniae* biofilm formation is strain dependent, multifactorial, and associated with reduced invasiveness and immunoreactivity during colonization. *mBio* **2013**, *4*, e00745-00713, doi:10.1128/mBio.00745-13.
383. Cassone, M.; Gagne, A.L.; Spruce, L.A.; Seeholzer, S.H.; Sebert, M.E. The HtrA protease from *Streptococcus pneumoniae* digests both denatured proteins and the competence-stimulating peptide. *The Journal of biological chemistry* **2012**, *287*, 38449-38459, doi:10.1074/jbc.M112.391482.
384. Mascher, T.; Zähner, D.; Merai, M.; Balmelle, N.; de Saizieu, A.B.; Hakenbeck, R. The *Streptococcus pneumoniae cia* Regulon: CiaR Target Sites and Transcription Profile Analysis. *J Bacteriol* **2003**, *185*, 60, doi:10.1128/JB.185.1.60-70.2003.
385. Standish, A.J.; Stroeher, U.H.; Paton, J.C. The two-component signal transduction system RR06/HK06 regulates expression of *cbpA* in *Streptococcus pneumoniae*. *Proceedings of the National Academy of Sciences of the United States of America* **2005**, *102*, 7701, doi:10.1073/pnas.0409377102.
386. Standish, A.J.; Stroeher, U.H.; Paton, J.C. The pneumococcal two-component signal transduction system RR/HK06 regulates CbpA and PspA by two distinct mechanisms. *J Bacteriol* **2007**, *189*, 5591-5600, doi:10.1128/jb.00335-07.

387. Lau, G.W.; Haataja, S.; Lonetto, M.; Kensit, S.E.; Marra, A.; Bryant, A.P.; McDevitt, D.; Morrison, D.A.; Holden, D.W. A functional genomic analysis of type 3 *Streptococcus pneumoniae* virulence. *Molecular microbiology* **2001**, *40*, 555-571, doi:10.1046/j.1365-2958.2001.02335.x.
388. Andreassen, P.R.; Trappetti, C.; Minhas, V.; Nielsen, F.D.; Pakula, K.; Paton, J.C.; Jørgensen, M.G. Host-glycan metabolism is regulated by a species-conserved two-component system in *Streptococcus pneumoniae*. *PLoS pathogens* **2020**, *16*, e1008332, doi:10.1371/journal.ppat.1008332.
389. Novak, R.; Henriques, B.; Charpentier, E.; Normark, S.; Tuomanen, E. Emergence of vancomycin tolerance in *Streptococcus pneumoniae*. *Nature* **1999**, *399*, 590-593, doi:10.1038/21202.
390. Robertson, G.T.; Zhao, J.; Desai, B.V.; Coleman, W.H.; Nicas, T.I.; Gilmour, R.; Grinius, L.; Morrison, D.A.; Winkler, M.E. Vancomycin tolerance induced by erythromycin but not by loss of *vncRS*, *vex3*, or *pep27* function in *Streptococcus pneumoniae*. *J Bacteriol* **2002**, *184*, 6987-7000, doi:10.1128/jb.184.24.6987-7000.2002.
391. Haas, W.; Sublett, J.; Kaushal, D.; Tuomanen, E.I. Revising the role of the pneumococcal *vex-vncRS* locus in vancomycin tolerance. *J Bacteriol* **2004**, *186*, 8463-8471, doi:10.1128/JB.186.24.8463-8471.2004.
392. Lee, M.S.; Morrison, D.A. Identification of a new regulator in *Streptococcus pneumoniae* linking quorum sensing to competence for genetic transformation. *J Bacteriol* **1999**, *181*, 5004-5016, doi:10.1128/JB.181.16.5004-5016.1999.
393. Luo, P.; Li, H.; Morrison, D.A. ComX is a unique link between multiple quorum sensing outputs and competence in *Streptococcus pneumoniae*. *Molecular microbiology* **2003**, *50*, 623-633, doi:10.1046/j.1365-2958.2003.03714.x.
394. Tovpeko, Y.; Morrison, D.A. Competence for genetic transformation in *Streptococcus pneumoniae*: mutations in σ^A bypass the *comW* requirement. *J Bacteriol* **2014**, *196*, 3724-3734, doi:10.1128/jb.01933-14.
395. Zhu, L.; Lau, G.W. Inhibition of Competence Development, Horizontal Gene Transfer and Virulence in *Streptococcus pneumoniae* by a Modified Competence Stimulating Peptide. *PLoS pathogens* **2011**, *7*, e1002241, doi:10.1371/journal.ppat.1002241.
396. de Saizieu, A.; Gardès, C.; Flint, N.; Wagner, C.; Kamber, M.; Mitchell, T.J.; Keck, W.; Amrein, K.E.; Lange, R. Microarray-based identification of a novel *Streptococcus pneumoniae* regulon controlled by an autoinduced peptide. *J Bacteriol* **2000**, *182*, 4696-4703, doi:10.1128/jb.182.17.4696-4703.2000.
397. Son, M.R.; Shchepetov, M.; Adrian, P.V.; Madhi, S.A.; de Gouveia, L.; von Gottberg, A.; Klugman, K.P.; Weiser, J.N.; Dawid, S. Conserved Mutations in the Pneumococcal Bacteriocin Transporter Gene, *blpA*, Result in a Complex Population Consisting of Producers and Cheaters. *mBio* **2011**, *2*, e00179-00111, doi:10.1128/mBio.00179-11.
398. Dawid, S.; Roche, A.M.; Weiser, J.N. The *blp* Bacteriocins of *Streptococcus pneumoniae* Mediate Intraspecies Competition both In Vitro and In Vivo. *Infect Immun* **2007**, *75*, 443, doi:10.1128/IAI.01775-05.
399. Lux, T.; Nuhn, M.; Hakenbeck, R.; Reichmann, P. Diversity of Bacteriocins and Activity Spectrum in *Streptococcus pneumoniae*. *J Bacteriol* **2007**, *189*, 7741, doi:10.1128/JB.00474-07.
400. Ulijasz, A.T.; Andes, D.R.; Glasner, J.D.; Weisblum, B. Regulation of iron transport in *Streptococcus pneumoniae* by RitR, an orphan response regulator. *J Bacteriol* **2004**, *186*, 8123-8136, doi:10.1128/JB.186.23.8123-8136.2004.
401. Yesilkaya, H.; Andisi, V.F.; Andrew, P.W.; Bijlsma, J.J.E. *Streptococcus pneumoniae* and reactive oxygen species: an unusual approach to living with radicals. *Trends in microbiology* **2013**, *21*, 187-195, doi:https://doi.org/10.1016/j.tim.2013.01.004.
402. Maule, A.F.; Wright, D.P.; Weiner, J.J.; Han, L.; Peterson, F.C.; Volkman, B.F.; Silvaggi, N.R.; Ulijasz, A.T. The Aspartate-Less Receiver (ALR) Domains: Distribution, Structure and Function. *PLoS pathogens* **2015**, *11*, e1004795, doi:10.1371/journal.ppat.1004795.
403. Ulijasz, A.T.; Falk, S.P.; Weisblum, B. Phosphorylation of the RitR DNA-binding domain by a Ser-Thr phosphokinase: implications for global gene regulation in the streptococci. *Molecular microbiology* **2009**, *71*, 382-390, doi:10.1111/j.1365-2958.2008.06532.x.
404. Liu, Q.; Cho, H.; Yeo, W.-S.; Bae, T. The Extracytoplasmic Linker Peptide of the Sensor Protein SaeS Tunes the Kinase Activity Required for Staphylococcal Virulence in Response to Host Signals. *PLoS pathogens* **2015**, *11*, e1004799, doi:10.1371/journal.ppat.1004799.
405. McKessar, S.J.; Hakenbeck, R. The Two-Component Regulatory System TCS08 Is Involved in Cellobiose Metabolism of *Streptococcus pneumoniae* R6. *J Bacteriol* **2007**, *189*, 1342, doi:10.1128/JB.01170-06.
406. Song, X.M.; Connor, W.; Hokamp, K.; Babiuk, L.A.; Potter, A.A. The growth phase-dependent regulation of the pilus locus genes by two-component system TCS08 in *Streptococcus pneumoniae*. *Microb Pathog* **2009**, *46*, 28-35, doi:10.1016/j.micpath.2008.10.006.
407. Trappetti, C.; Ogunniyi, A.D.; Oggioni, M.R.; Paton, J.C. Extracellular Matrix Formation Enhances the Ability of *Streptococcus pneumoniae* to Cause Invasive Disease. *PLOS ONE* **2011**, *6*, e19844, doi:10.1371/journal.pone.0019844.

408. Novak, R.; Charpentier, E.; Braun, J.S.; Park, E.; Murti, S.; Tuomanen, E.; Masure, R. Extracellular targeting of choline-binding proteins in *Streptococcus pneumoniae* by a zinc metalloprotease. *Molecular microbiology* **2000**, *36*, 366-376, doi:10.1046/j.1365-2958.2000.01854.x.
409. Blue, C.E.; Paterson, G.K.; Kerr, A.R.; Bergé, M.; Claverys, J.P.; Mitchell, T.J. ZmpB, a novel virulence factor of *Streptococcus pneumoniae* that induces tumor necrosis factor alpha production in the respiratory tract. *Infect Immun* **2003**, *71*, 4925-4935, doi:10.1128/iai.71.9.4925-4935.2003.
410. Hendriksen, W.T.; Silva, N.; Bootsma, H.J.; Blue, C.E.; Paterson, G.K.; Kerr, A.R.; de Jong, A.; Kuipers, O.P.; Hermans, P.W.; Mitchell, T.J. Regulation of gene expression in *Streptococcus pneumoniae* by response regulator 09 is strain dependent. *J Bacteriol* **2007**, *189*, 1382-1389, doi:10.1128/jb.01144-06.
411. Blue, C.E.; Mitchell, T.J. Contribution of a response regulator to the virulence of *Streptococcus pneumoniae* is strain dependent. *Infect Immun* **2003**, *71*, 4405-4413, doi:10.1128/iai.71.8.4405-4413.2003.
412. Wang, J.; Li, J.-W.; Li, J.; Huang, Y.; Wang, S.; Zhang, J.-R. Regulation of pneumococcal epigenetic and colony phases by multiple two-component regulatory systems. *PLoS pathogens* **2020**, *16*, e1008417, doi:10.1371/journal.ppat.1008417.
413. Li, J.; Wang, J.; Ruiz-Cruz, S.; Espinosa, M.; Zhang, J.-R.; Bravo, A. *In vitro* DNA Inversions Mediated by the PsrA Site-Specific Tyrosine Recombinase of *Streptococcus pneumoniae*. *Frontiers in Molecular Biosciences* **2020**, *7*, 43.
414. Wyres, K.L.; Lambertsen, L.M.; Croucher, N.J.; McGee, L.; von Gottberg, A.; Liñares, J.; Jacobs, M.R.; Kristinsson, K.G.; Beall, B.W.; Klugman, K.P., et al. Pneumococcal capsular switching: a historical perspective. *The Journal of infectious diseases* **2013**, *207*, 439-449, doi:10.1093/infdis/jis703.
415. Briles, D.E.; Hollingshead, S.K.; Nabors, G.S.; Paton, J.C.; Brooks-Walter, A. The potential for using protein vaccines to protect against otitis media caused by *Streptococcus pneumoniae*. *Vaccine* **2000**, *19 Suppl 1*, S87-95, doi:10.1016/s0264-410x(00)00285-1.
416. Briles, D.E. Protection of the elderly from pneumococcal pneumonia with a protein-based vaccine? *Mechanisms of ageing and development* **2004**, *125*, 129-131, doi:10.1016/j.mad.2003.11.008.
417. Barrett, J.F.; Hoch, J.A. Two-component signal transduction as a target for microbial anti-infective therapy. *Antimicrobial agents and chemotherapy* **1998**, *42*, 1529-1536, doi:10.1128/aac.42.7.1529.
418. Gotoh, Y.; Eguchi, Y.; Watanabe, T.; Okamoto, S.; Doi, A.; Utsumi, R. Two-component signal transduction as potential drug targets in pathogenic bacteria. *Current opinion in microbiology* **2010**, *13*, 232-239, doi:10.1016/j.mib.2010.01.008.
419. Muñoz-Elías, E.J.; McKinney, J.D. Carbon metabolism of intracellular bacteria. *Cellular microbiology* **2006**, *8*, 10-22, doi:10.1111/j.1462-5822.2005.00648.x.
420. Ray, K.; Marteyn, B.; Sansonetti, P.J.; Tang, C.M. Life on the inside: the intracellular lifestyle of cytosolic bacteria. *Nature reviews. Microbiology* **2009**, *7*, 333-340, doi:10.1038/nrmicro2112.
421. Richardson, A.R.; Somerville, G.A.; Sonenshein, A.L. Regulating the Intersection of Metabolism and Pathogenesis in Gram-positive Bacteria. *Microbiology spectrum* **2015**, *3*, doi:10.1128/microbiolspec.MBP-0004-2014.
422. Hooper, L.V.; Midtvedt, T.; Gordon, J.I. How host-microbial interactions shape the nutrient environment of the mammalian intestine. *Annual review of nutrition* **2002**, *22*, 283-307, doi:10.1146/annurev.nutr.22.011602.092259.
423. Afzal, M.; Shafeeq, S.; Kuipers, O.P. LacR is a repressor of *lacABCD* and LacT is an activator of *lacTFEG*, constituting the lac gene cluster in *Streptococcus pneumoniae*. *Appl Environ Microbiol* **2014**, *80*, 5349-5358, doi:10.1128/AEM.01370-14.
424. Gaspar, P.; Al-Bayati, F.A.Y.; Andrew, P.W.; Neves, A.R.; Yesilkaya, H. Lactate dehydrogenase is the key enzyme for pneumococcal pyruvate metabolism and pneumococcal survival in blood. *Infect Immun* **2014**, *82*, 5099-5109, doi:10.1128/iai.02005-14.
425. Afzal, M.; Shafeeq, S.; Ahmed, H.; Kuipers, O.P. N-acetylgalatosamine-Mediated Regulation of the *aga* Operon by AgaR in *Streptococcus pneumoniae*. *Frontiers in Cellular and Infection Microbiology* **2016**, *6*, 101.
426. Jeong, J.K.; Kwon, O.; Lee, Y.M.; Oh, D.-B.; Lee, J.M.; Kim, S.; Kim, E.-H.; Le, T.N.; Rhee, D.-K.; Kang, H.A. Characterization of the *Streptococcus pneumoniae* BgaC protein as a novel surface beta-galactosidase with specific hydrolysis activity for the Galbeta1-3GlcNAc moiety of oligosaccharides. *J Bacteriol* **2009**, *191*, 3011-3023, doi:10.1128/jb.01601-08.
427. Andersson, B.; Dahmen, J.; Frejd, T.; Leffler, H.; Magnusson, G.; Noori, G.; Eden, C.S. Identification of an active disaccharide unit of a glycoconjugate receptor for pneumococci attaching to human pharyngeal epithelial cells. *J Exp Med* **1983**, *158*, 559-570.
428. Aprianto, R.; Slager, J.; Holsappel, S.; Veening, J.W. High-resolution analysis of the pneumococcal transcriptome under a wide range of infection-relevant conditions. *Nucleic Acids Res* **2018**, *46*, 9990-10006, doi:10.1093/nar/gky750.

429. Hathaway, L.J.; Brugger, S.D.; Morand, B.; Bangert, M.; Rotzetter, J.U.; Hauser, C.; Graber, W.A.; Gore, S.; Kadioglu, A.; Mühlemann, K. Capsule type of *Streptococcus pneumoniae* determines growth phenotype. *PLoS pathogens* **2012**, *8*, e1002574, doi:10.1371/journal.ppat.1002574.
430. Briles, D.E.; Novak, L.; Hotomi, M.; van Ginkel, F.W.; King, J. Nasal colonization with *Streptococcus pneumoniae* includes subpopulations of surface and invasive pneumococci. *Infect Immun* **2005**, *73*, 6945-6951, doi:10.1128/iai.73.10.6945-6951.2005.
431. Hoekstra, D.; van der Laan, J.W.; de Leij, L.; Witholt, B. Release of outer membrane fragments from normally growing *Escherichia coli*. *Biochimica et biophysica acta* **1976**, *455*, 889-899, doi:10.1016/0005-2736(76)90058-4.
432. Dorward, D.W.; Garon, C.F.; Judd, R.C. Export and intercellular transfer of DNA via membrane blebs of *Neisseria gonorrhoeae*. *J Bacteriol* **1989**, *171*, 2499-2505, doi:10.1128/jb.171.5.2499-2505.1989.
433. Horstman, A.L.; Kuehn, M.J. Bacterial Surface Association of Heat-labile Enterotoxin through Lipopolysaccharide after Secretion via the General Secretory Pathway*. *Journal of Biological Chemistry* **2002**, *277*, 32538-32545, doi:https://doi.org/10.1074/jbc.M203740200.
434. Mashburn, L.M.; Whiteley, M. Membrane vesicles traffic signals and facilitate group activities in a prokaryote. *Nature* **2005**, *437*, 422-425, doi:10.1038/nature03925.
435. Manning, A.J.; Kuehn, M.J. Contribution of bacterial outer membrane vesicles to innate bacterial defense. *BMC microbiology* **2011**, *11*, 258, doi:10.1186/1471-2180-11-258.
436. Elhenawy, W.; Debelyy, M.O.; Feldman, M.F. Preferential packing of acidic glycosidases and proteases into *Bacteroides* outer membrane vesicles. *mBio* **2014**, *5*, e00909-00914, doi:10.1128/mBio.00909-14.
437. Olaya-Abril, A.; Prados-Rosales, R.; McConnell, M.J.; Martín-Peña, R.; González-Reyes, J.A.; Jiménez-Munguía, I.; Gómez-Gascón, L.; Fernández, J.; Luque-García, J.L.; García-Lidón, C. Characterization of protective extracellular membrane-derived vesicles produced by *Streptococcus pneumoniae*. *Journal of proteomics* **2014**, *106*, 46-60.
438. Turnbull, L.; Toyofuku, M.; Hynen, A.L.; Kurosawa, M.; Pessi, G.; Petty, N.K.; Osvath, S.R.; Cárcamo-Oyarce, G.; Gloag, E.S.; Shimoni, R., et al. Explosive cell lysis as a mechanism for the biogenesis of bacterial membrane vesicles and biofilms. *Nat Commun* **2016**, *7*, 11220, doi:10.1038/ncomms11220.
439. Toyofuku, M.; Cárcamo-Oyarce, G.; Yamamoto, T.; Eisenstein, F.; Hsiao, C.C.; Kurosawa, M.; Gademann, K.; Pilhofer, M.; Nomura, N.; Eberl, L. Prophage-triggered membrane vesicle formation through peptidoglycan damage in *Bacillus subtilis*. *Nat Commun* **2017**, *8*, 481, doi:10.1038/s41467-017-00492-w.
440. Wang, X.; Thompson, C.D.; Weidenmaier, C.; Lee, J.C. Release of *Staphylococcus aureus* extracellular vesicles and their application as a vaccine platform. *Nature Communications* **2018**, *9*, 1379, doi:10.1038/s41467-018-03847-z.
441. Iyer, R.; Camilli, A. Sucrose metabolism contributes to *in vivo* fitness of *Streptococcus pneumoniae*. *Molecular microbiology* **2007**, *66*, 1-13, doi:10.1111/j.1365-2958.2007.05878.x.
442. Abranches, J.; Chen, Y.-Y.M.; Burne, R.A. Galactose Metabolism by *Streptococcus mutans*. *Appl Environ Microbiol* **2004**, *70*, 6047, doi:10.1128/AEM.70.10.6047-6052.2004.
443. Hirschmann, S.; Gómez-Mejia, A.; Mäder, U.; Karsunke, J.; Driesch, D.; Rohde, M.; Häussler, S.; Burchhardt, G.; Hammerschmidt, S. The Two-Component System 09 Regulates Pneumococcal Carbohydrate Metabolism and Capsule Expression. *Microorganisms* **2021**, *9*, doi:10.3390/microorganisms9030468.
444. Yesilkaya, H.; Kadioglu, A.; Gingles, N.; Alexander, J.E.; Mitchell, T.J.; Andrew, P.W. Role of manganese-containing superoxide dismutase in oxidative stress and virulence of *Streptococcus pneumoniae*. *Infect Immun* **2000**, *68*, 2819-2826, doi:10.1128/iai.68.5.2819-2826.2000.
445. Basavanna, S.; Chimalapati, S.; Maqbool, A.; Rubbo, B.; Yuste, J.; Wilson, R.J.; Hosie, A.; Ogunniyi, A.D.; Paton, J.C.; Thomas, G., et al. The effects of methionine acquisition and synthesis on *Streptococcus pneumoniae* growth and virulence. *PLoS One* **2013**, *8*, e49638, doi:10.1371/journal.pone.0049638.
446. Dave, S.; Brooks-Walter, A.; Pangburn, M.K.; McDaniel, L.S. PspC, a pneumococcal surface protein, binds human factor H. *Infect Immun* **2001**, *69*, 3435-3437, doi:10.1128/iai.69.5.3435-3437.2001.
447. Frolet, C.; Beniazza, M.; Roux, L.; Gallet, B.; Noirclerc-Savoye, M.; Vernet, T.; Di Guilmi, A.M. New adhesin functions of surface-exposed pneumococcal proteins. *BMC microbiology* **2010**, *10*, 190, doi:10.1186/1471-2180-10-190.
448. McDaniel, L.S.; Yother, J.; Vijayakumar, M.; McGarry, L.; Guild, W.R.; Briles, D.E. Use of insertional inactivation to facilitate studies of biological properties of pneumococcal surface protein A (PspA). *J Exp Med* **1987**, *165*, 381-394, doi:10.1084/jem.165.2.381.
449. Nishimoto, A.T.; Rosch, J.W.; Tuomanen, E.I. Pneumolysin: Pathogenesis and Therapeutic Target. *Frontiers in microbiology* **2020**, *11*, 1543.
450. Vollmer, W.; Tomasz, A. Identification of the teichoic acid phosphorylcholine esterase in *Streptococcus pneumoniae*. *Molecular microbiology* **2001**, *39*, 1610-1622, doi:10.1046/j.1365-2958.2001.02349.x.

451. Ma, Z.; Zhang, J.-R. RR06 activates transcription of *spr1996* and *cbpA* in *Streptococcus pneumoniae*. *J Bacteriol* **2007**, *189*, 2497-2509, doi:10.1128/JB.01429-06.
452. Duan, K.; Sibley, C.D.; Davidson, C.J.; Surette, M.G. Chemical interactions between organisms in microbial communities. *Bacterial sensing and signaling* **2009**, *16*, 1-17.
453. Lozada-Chávez, I.; Janga, S.C.; Collado-Vides, J. Bacterial regulatory networks are extremely flexible in evolution. *Nucleic Acids Res* **2006**, *34*, 3434-3445, doi:10.1093/nar/gkl423.
454. Nguyen, C.T.; Park, S.S.; Rhee, D.K. Stress responses in Streptococcus species and their effects on the host. *Journal of microbiology (Seoul, Korea)* **2015**, *53*, 741-749, doi:10.1007/s12275-015-5432-6.
455. Stock, J.B.; Stock, A.M.; Mottonen, J.M. Signal transduction in bacteria. *Nature* **1990**, *344*, 395-400, doi:10.1038/344395a0.
456. Ezraty, B.; Gennaris, A.; Barras, F.; Collet, J.-F. Oxidative stress, protein damage and repair in bacteria. *Nature Reviews Microbiology* **2017**, *15*, 385-396, doi:10.1038/nrmicro.2017.26.
457. Guan, N.; Liu, L. Microbial response to acid stress: mechanisms and applications. *Appl Microbiol Biotechnol* **2020**, *104*, 51-65, doi:10.1007/s00253-019-10226-1.
458. de Stoppelaar, S.F.; Bootsma, H.J.; Zomer, A.; Roelofs, J.J.; Hermans, P.W.; van 't Veer, C.; van der Poll, T. *Streptococcus pneumoniae* serine protease HtrA, but not SFP or PrtA, is a major virulence factor in pneumonia. *PLoS One* **2013**, *8*, e80062, doi:10.1371/journal.pone.0080062.
459. Ibrahim, Y.M.; Kerr, A.R.; McCluskey, J.; Mitchell, T.J. Role of HtrA in the virulence and competence of *Streptococcus pneumoniae*. *Infect Immun* **2004**, *72*, 3584-3591, doi:10.1128/IAI.72.6.3584-3591.2004.
460. Piñas, G.E.; Cortes, P.R.; Orio, A.G.A.; Echenique, J. Acidic stress induces autolysis by a CSP-independent ComE pathway in *Streptococcus pneumoniae*. *Microbiology (Reading, England)* **2008**, *154*, 1300-1308, doi:10.1099/mic.0.2007/015925-0.
461. Cortes, P.R.; Piñas, G.E.; Cian, M.B.; Yandar, N.; Echenique, J. Stress-triggered signaling affecting survival or suicide of *Streptococcus pneumoniae*. *International journal of medical microbiology : IJMM* **2015**, *305*, 157-169, doi:10.1016/j.ijmm.2014.12.002.
462. Casiano-Colón, A.; Marquis, R.E. Role of the arginine deiminase system in protecting oral bacteria and an enzymatic basis for acid tolerance. *Appl Environ Microbiol* **1988**, *54*, 1318-1324, doi:10.1128/aem.54.6.1318-1324.1988.
463. Ohkuma, S.; Poole, B. Fluorescence probe measurement of the intralysosomal pH in living cells and the perturbation of pH by various agents. *Proceedings of the National Academy of Sciences of the United States of America* **1978**, *75*, 3327-3331, doi:10.1073/pnas.75.7.3327.
464. Yu, J.; Bryant, A.P.; Marra, A.; Lonetto, M.A.; Ingraham, K.A.; Chalker, A.F.; Holmes, D.J.; Holden, D.; Rosenberg, M.; McDevitt, D. Characterization of the *Streptococcus pneumoniae* NADH oxidase that is required for infection. *Microbiology (Reading, England)* **2001**, *147*, 431-438, doi:10.1099/00221287-147-2-431.
465. Tseng, H.J.; McEwan, A.G.; Paton, J.C.; Jennings, M.P. Virulence of *Streptococcus pneumoniae:* PsaA mutants are hypersensitive to oxidative stress. *Infect Immun* **2002**, *70*, 1635-1639, doi:10.1128/iai.70.3.1635-1639.2002.
466. Ogunniyi, A.D.; Mahdi, L.K.; Trappetti, C.; Verhoeven, N.; Mermans, D.; Van der Hoek, M.B.; Plumptre, C.D.; Paton, J.C. Identification of genes that contribute to the pathogenesis of invasive pneumococcal disease by in vivo transcriptomic analysis. *Infect Immun* **2012**, *80*, 3268-3278, doi:10.1128/iai.00295-12.
467. King, S.J.; Hippe, K.R.; Weiser, J.N. Deglycosylation of human glycoconjugates by the sequential activities of exoglycosidases expressed by *Streptococcus pneumoniae*. *Molecular microbiology* **2006**, *59*, 961-974, doi:10.1111/j.1365-2958.2005.04984.x.
468. Tong, H.H.; Liu, X.; Chen, Y.; James, M.; Demaria, T. Effect of neuraminidase on receptor-mediated adherence of *Streptococcus pneumoniae* to chinchilla tracheal epithelium. *Acta oto-laryngologica* **2002**, *122*, 413-419, doi:10.1080/00016480260000111.
469. Yesilkaya, H.; Manco, S.; Kadioglu, A.; Terra, V.S.; Andrew, P.W. The ability to utilize mucin affects the regulation of virulence gene expression in *Streptococcus pneumoniae*. *FEMS microbiology letters* **2008**, *278*, 231-235, doi:10.1111/j.1574-6968.2007.01003.x.
470. Mahdi, L.K.; Van der Hoek, M.B.; Ebrahimie, E.; Paton, J.C.; Ogunniyi, A.D. Characterization of Pneumococcal Genes Involved in Bloodstream Invasion in a Mouse Model. *PLOS ONE* **2015**, *10*, e0141816, doi:10.1371/journal.pone.0141816.
471. Kowalko, J.E.; Sebert, M.E. The *Streptococcus pneumoniae* competence regulatory system influences respiratory tract colonization. *Infect Immun* **2008**, *76*, 3131-3140, doi:10.1128/iai.01696-07.
472. Schmidt, F.; Kakar, N.; Meyer, T.C.; Depke, M.; Masouris, I.; Burchhardt, G.; Gómez-Mejia, A.; Dhople, V.; Håvarstein, L.S.; Sun, Z., et al. *In vivo* proteomics identifies the competence regulon and AliB oligopeptide transporter as pathogenic factors in pneumococcal meningitis. *PLoS pathogens* **2019**, *15*, e1007987, doi:10.1371/journal.ppat.1007987.

473. Zhu, L.; Lin, J.; Kuang, Z.; Vidal, J.E.; Lau, G.W. Deletion analysis of *Streptococcus pneumoniae* late competence genes distinguishes virulence determinants that are dependent or independent of competence induction. *Molecular microbiology* **2015**, *97*, 151-165, doi:10.1111/mmi.13016.
474. Sun, F.; Li, C.; Jeong, D.; Sohn, C.; He, C.; Bae, T. In the *Staphylococcus aureus* two-component system sae, the response regulator SaeR binds to a direct repeat sequence and DNA binding requires phosphorylation by the sensor kinase SaeS. *J Bacteriol* **2010**, *192*, 2111-2127, doi:10.1128/jb.01524-09.
475. Liu, Q.; Yeo, W.S.; Bae, T. The SaeRS Two-Component System of *Staphylococcus aureus*. *Genes* **2016**, *7*, doi:10.3390/genes7100081.
476. Lu, Y.J.; Rock, C.O. Transcriptional regulation of fatty acid biosynthesis in *Streptococcus pneumoniae*. *Molecular microbiology* **2006**, *59*, 551-566, doi:10.1111/j.1365-2958.2005.04951.x.
477. Nobbs, A.H.; Lamont, R.J.; Jenkinson, H.F. Streptococcus adherence and colonization. *Microbiology and molecular biology reviews : MMBR* **2009**, *73*, 407-450, doi:10.1128/MMBR.00014-09.
478. Mainiero, M.; Goerke, C.; Geiger, T.; Gonser, C.; Herbert, S.; Wolz, C. Differential Target Gene Activation by the *Staphylococcus aureus* Two-Component System *saeRS*. *J Bacteriol* **2010**, *192*, 613, doi:10.1128/JB.01242-09.
479. Hava, D.L.; Hemsley, C.J.; Camilli, A. Transcriptional regulation in the *Streptococcus pneumoniae rlrA* pathogenicity islet by RlrA. *J Bacteriol* **2003**, *185*, 413-421, doi:10.1128/jb.185.2.413-421.2003.
480. Hendriksen, W.T.; Bootsma, H.J.; van Diepen, A.; Estevão, S.; Kuipers, O.P.; de Groot, R.; Hermans, P.W.M. Strain-specific impact of PsaR of *Streptococcus pneumoniae* on global gene expression and virulence. *Microbiology (Reading, England)* **2009**, *155*, 1569-1579, doi:10.1099/mic.0.025072-0.
481. Johnston, J.W.; Briles, D.E.; Myers, L.E.; Hollingshead, S.K. Mn^{2+}-dependent regulation of multiple genes in *Streptococcus pneumoniae* through PsaR and the resultant impact on virulence. *Infect Immun* **2006**, *74*, 1171-1180.
482. Rennemeier, C.; Hammerschmidt, S.; Niemann, S.; Inamura, S.; Zähringer, U.; Kehrel, B.E. Thrombospondin-1 promotes cellular adherence of gram-positive pathogens *via* recognition of peptidoglycan. *FASEB journal : official publication of the Federation of American Societies for Experimental Biology* **2007**, *21*, 3118-3132, doi:10.1096/fj.06-7992com.

9. List of Abbreviations

%	Percent
®	Registered
α	Alpha
β	Beta
ABC transporters	ATP-binding cassette transporters
ADS	Arginine deiminase system
AHL	Acyl homoserine lactone
AI	Autoinducer
AIP	Autoinducing peptide
Ala	Alanine
***arc* operon**	Arginine catabolism operon
AS	Amino acid
ATP	Adenosine triphosphate
BlpRH	Bacteriocin-like peptide operon
bp	Base pairs
CAP	Community-acquired pneumonia
CBP	Choline-binding protein
CcpA	Catabolite control protein A
CDM	Chemically-defined medium
cel	Cellobiose
CEM	CcdA-Etrx-MsrAB2
CFU	Colony forming units
CoA	Coenzyme A
CFU	Colony forming units
CiaRH	Competence induction and altered cefotaxime susceptibility
ComDE	Competence operon
CPS	Capsular polysaccharide
cre	Catabolite responsive element
CRM197	Cross reacting material, detoxified variant of the diphtheria toxin
CSF	Cerebrospinal fluid
CSP	Competence stimulating peptide
csRNA	Cia dependent small ribonucleic acid
D39	*Streptococcus pneumoniae* serotype 2
DNA	Deoxyribonucleic acid
ECM	Extracellular matrix
EMP	Embden-Meyerhof-Parnas
EMSA	Electrophoretic mobility shift assay
***fab* operon**	Fatty acid biosynthesis operon
FESEM	Field emission scanning electron microscopy
Glc*N*Ac	*N*-acetylglucosamine
h	hours
HIV	Human immunodeficiency viruses
HK	Histidine kinase
HTH	Helix-turn-helix
iC3b	inactivated C3b
IgA	Immunoglobulin A
iGln	Isoglutamine
IPD	Invasive pneumococcal disease
kb	Kilo base pair
LPxTG	Leucine-proline-any AS (x)-threonine-glycine
LRR	Lysine-ruthenium-red
Lys	Lysine

LytA, B, C	Autolysin A, B, C
Mbp	Millions of base pairs
mRNA	Messenger ribonucleic acid
MSCRAMMs	Microbial surface components recognizing adhesive matrix molecules
Mur*N*Ac	*N*-acetylmuramic acid
NADH	Nicotinamide adenine dinucleotide
NanA, B, C	Neuraminidase A, B, C
NET	Neutrophil extracellular trap
ncRNA	non-coding RNA
NCSP	Non-classical surface protein
NVT	Non-vaccine serotypes
PavA, B	Pneumococcal adherence and virulence factor A, B
PAI	Pathogenicity island
PBP	Penicillin-binding protein
PCR	Polymerase chain reaction
PCV	Pneumococcal conjugate vaccine
Pfl	Pyruvate formate lyase
PGN	Peptidoglycan
pH	Power of hydrogen
PI-1	Pilus-1
Pia	Pneumococcal iron acquisition
pIgR	Polymeric immunoglobulin receptor
Pit	Iron uptake ABC transporter
Piu	Pneumococcal iron uptake
Ply	Pneumolysin
PPP	Pentose phosphate pathway
PPV	Pneumococcal polysaccharide vaccine
PsaA, B, C	Pneumococcal surface antigen A, B, C
PspA, C	Pneumococcal surface protein A, C
PTS	Phosphotransferase system
qPCR	quantitative real-time PCR
QS	Quorum sensing
REC	CheY-like receiver domain
RNA	Ribonucleic acid
ROS	Reactive oxygen species
RR	Response regulator
RrgB	Pilus-1 backbone protein
S. pneumoniae	*Streptococcus pneumoniae*
SaeRS	*Staphylococcus aureus* exoprotein expression
Sc	Secretory component
sRNA	Small ribonucleic acid
SrtA	Sortase A
SSURE	Streptococcal surface repeats
TCA	Tri-carboxylic acid
TCS	Two-component regulatory system
TEM	Transmission electron microscopy
TIGR4	*Streptococcus pneumoniae* serotype 4
TM	Transmembrane
Tn-seq	Transposon insertion sequencing
TSP-1	Human thrombospondin 1
UDP	Uridine diphosphate
UMP	Uridine monophosphate
URT	Upper respiratory tract
WHO	World health organization

10. Pneumococcal strains

Table 1: Wild-type strains of *S. pneumoniae*

No.	Strain	Capsule Type	Resistance	Knockout genes	Reference
SP257	D39	2	-	-	NCTC 7466
SP261	TIGR4	4	-	-	[15]

Table 2: Mutant strains of *S. pneumoniae*

No.	Strain	Capsule Type	Resistance	Knockout genes	Reference
PN149	D39*lux*	2	-	-	[226]
PN315	TIGR4*lux*	4	Km^R	-	[310]
PN111	D39Δ*cps*	2	Km^R	*spd_0312 – spd_0333*	[482]
PN249	TIGR4Δ*cps*	4	Km^R	*sp_0343 – sp_0360*	[310]
TCS08					
PN409	D39*lux*Δ*rr08*	2	Km^R, Erm^R	*spd_0081*	This study
PN414	D39*lux*Δ*hk08*	2	Km^R, Erm^R	*spd_0082*	This study
PN372	D39*lux*Δ*tcs08*	2	Km^R, $Spec^R$	*spd_0081, spd_0082*	This study
PN407	D39Δ*cps*Δ*rr08*	2	Km^R, Erm^R	*spd_0312 – spd_0333, spd_0081*	This study
PN412	D39Δ*cps*Δ*hk08*	2	Km^R, Erm^R	*spd_0312 – spd_0333, spd_0082*	This study
PN308	D39Δ*cps*Δ*tcs08*	2	Km^R, $Spec^R$	*spd_0312 – spd_0333, spd_0081, spd_0082*	This study
PN410	TIGR4*lux*Δ*rr08*	4	Km^R, Erm^R	*sp_0083*	This study
PN415	TIGR4*lux*Δ*hk08*	4	Km^R, Erm^R	*sp_0084*	This study
PN708	TIGR4*lux*Δ*tcs08*	4	Km^R, $Spec^R$	*sp_0083, sp_0084*	This study
PN408	TIGR4Δ*cps*Δ*rr08*	4	Km^R, Erm^R	*sp_0343 – sp_0360, sp_0083*	This study
PN652	TIGR4Δ*cps*Δ*hk08*	4	Km^R, Erm^R	*sp_0343 – sp_0360, sp_0084*	This study
PN344	TIGR4Δ*cps*Δ*tcs08*	4	Km^R, $Spec^R$	*sp_0343 – sp_0360, sp_0083, sp_0084*	This study

No.	Strain	Capsule Type	Resistance	Knockout genes	Reference
TCS09					
PN507	D39Δ*rr09*	2	Erm^R	*spd_0574*	This study
PN513	D39Δ*hk09*	2	Erm^R	*spd_0575*	This study
PN624	D39Δ*tcs09*	2	Erm^R	*spd_0574, spd_0575*	This study
PN508	D39Δ*cps*Δ*rr09*	2	Km^R, Erm^R	*spd_0312 – spd_0333, spd_0574*	This study
PN625	D39Δ*cps*Δ*hk09*	2	Km^R, Erm^R	*spd_0312 – spd_0333, spd_0575*	This study
PN540	D39Δ*cps*Δ*tcs09*	2	Km^R, Erm^R	*spd_0312 – spd_0333, spd_0574, spd_0575*	This study
PN510	TIGR4Δ*rr09*	4	Erm^R	*sp_0661*	This study
PN627	TIGR4Δ*hk09*	4	Erm^R	*sp_0662*	This study
PN541	TIGR4Δ*tcs09*	4	Erm^R	*sp_0661, sp_0662*	This study
PN512	TIGR4*lux*Δ*rr09*	4	Km^R, Erm^R	*sp_0661*	This study
PN628	TIGR4*lux*Δ*hk09*	4	Km^R, Erm^R	*sp_0662*	This study
PN589	TIGR4*lux*Δ*tcs09*	4	Km^R, Erm^R	*sp_0661, sp_0662*	This study
PN511	TIGR4Δ*cps*Δ*rr09*	4	Km^R, Erm^R	*sp_0343 – sp_0360, sp_0661*	This study
PN629	TIGR4Δ*cps*Δ*hk09*	4	Km^R, Erm^R	*sp_0343 – sp_0360, sp_0662*	This study
PN630	TIGR4Δ*cps*Δ*tcs09*	4	Km^R, Erm^R	*sp_0343 – sp_0360, sp_0661, sp_0662*	This study

Erm, Erythromycin; Km, Kanamycin; Spec, Spectinomycin; R, Resistance

11. Eigenständigkeitserklärung

12. Curriculum Vitae

13. List of Publications

13.1. Publications included in this thesis

- **Hirschmann, S.**, Gómez-Mejia, A., Mäder, U., Karsunke, J., Driesch, D., Rohde, M., Häussler, S., Burchhardt, G. and Hammerschmidt, S. The Two-Component System 09 Regulates Pneumococcal Carbohydrate Metabolism and Capsule Expression. *Microorganisms, 2021 Feb 24;9(3):468. doi: 10.3390/microorganims9030468*

- **Hirschmann, S.**, Gómez-Mejia, A., Kohler, T. P., Voß, F., Rohde, M., Brendel, M. and Hammerschmidt, S. The two-component system 09 of *Streptococcus pneumoniae* is important for metabolic fitness and resistance during dissemination in the host.
  Microorganisms, submitted May 2021, Manuscript ID: microorganisms-1253919

- Gómez-Mejia, A., Gámez, G., **Hirschmann, S.**, Kluger, V., Rath, H., Böhm, S., Voss, F., Kakar, N., Petruschka, L., Völker, U., Brückner, R., Mäder, U. and Hammerschmidt, S. Pneumococcal Metabolic Adaptation and Colonization Are Regulated by the Two-Component Regulatory System 08.
  mSphere, 2018 May 16;3(3):e00165-18. doi: 10.1128/mSphere.00165-18

13.2. Publication not included in this thesis

- Abdullah, M. R., Batuecas, M. T., Jennert, F., Voß, F., Westhoff, P., Kohler, T. P., Molina, R., **Hirschmann, S.**, Lalk, M., Hermoso, J., A. and Hammerschmidt, S. Crystal Structure and Pathophysiological Role of the Pneumococcal Nucleoside-binding Protein PnrA. *Journal of Molecular Biology, 2021 Jan 22;433(2):166723. doi: 10.1016/j.jmb.2020.11.022*

14. Scientific Presentations

- **Hirschmann, S.**, Gómez-Mejia, A., Karsunke, J. and Hammerschmidt, S. Influence of the two-component regulatory system 09 on adaptive processes of *Streptococcus pneumoniae*.
  Rostock, poster presentation. 1st International Conference on Respiratory Pathogens 2017

- **Hirschmann, S.**, Gómez-Mejia, A., Karsunke, J. and Hammerschmidt, S. The pneumococcal two-component regulatory system 09 is involved in oxidative stress response.
  Berlin, poster presentation. 4th German Pneumococcal and Streptococcal Symposium 2018

- **Hirschmann, S.**, Gómez-Mejia, A., Mäder, U., Driesch, D., Karsunke, J., Häußler, S. and Hammerschmidt, S. Impact of the two-component regulatory system 09 on oxidative stress resistance of *Streptococcus pneumoniae*.
  Mainz, oral presentation. Annual Conference 2019 of the Association for General and Applied Microbiology

- **Hirschmann, S.**, Gómez-Mejia, A., Mäder, U., Driesch, D., Häußler, S. and Hammerschmidt, S. Impact of the two-component regulatory system 09 on the pathophysiology of *Streptococcus pneumoniae*.
  Greifswald, poster presentation. 14th European Meeting on the Molecular Biology of the Pneumococcus

Die Studien dieser Arbeit und damit verbunden die schriftliche Arbeit selbst, hätten nicht durchgeführt werden können, wenn nicht viele Personen auf vielfältige Weise dazu beigetragen hätten. Zunächst möchte ich meinem Betreuer, **Prof. Dr. Sven Hammerschmidt**, für die Möglichkeit danken, das interessante und vielversprechende Thema „TCS09 in Pneumokokken“ weiter als PhD Projekt bearbeiten zu dürfen. Seiner Unterstützung konnte ich mir stets sicher sein.

Ich möchte mich bei meinem zuverlässigem Kollegen und ehemaligem Betreuer meiner Masterarbeit **Dr. Alejandro Gómez-Mejia** für die nach wie vor wunderbare Zusammenarbeit bedanken. Auch während der Doktorandenzeit standest du mir mit Rat und Tat immer schnell zur Seite.

Ich möchte auch **Dr. Dominik Driesch** und **Prof. Dr. Susanne Häußler** für die Erhebung der Transkriptomdaten danken. Sie gaben mir die Grundlage für meine erste Publikation. Besonders hervorheben möchte ich zudem **Dr. Ulrike Mäder**. Ich möchte dir für deine geduldige Unterstützung bei der Auswertung und Diskussion der Transkriptomdaten danken.

Für die wunderbaren Mikroskopie Aufnahmen bedanke ich mich bei **Prof. Dr. Manfred Rohde** und seiner technischen Assistentin **Ina Schleicher**.

Besonders möchte ich **Dr. Thomas Kohler**, **Dr. Franziska Voß** und **Max Brendel** für die engagierte Hilfe bei der Koinfektion und den konstruktiven Ideen für meine zweite Publikation danken.

Der gesamten AG Hammerschmidt, der AG Siemens und dem technischen Personal, Birgit, Peggy, Kristine und Karsta, möchte ich vor Allem für nette, konstruktive Gespräche, Ratschläge, Anekdoten und Lebensweisheiten danken, die den Laboralltag um einiges lustiger gemacht haben.

Ein besonderer Dank gilt meinen ehemaligen und jetzigen Mitdoktoranden Lisa, Ali, Kristin, Lea, Richael, Antje, Surabhi, Fabian, Max und Patience! Danke für lustige Mittags- und Kaffeepausen, Spieleabende, konstruktive Diskussionen oder einfach nur zum Lachen bringen.

Darüber hinaus möchte ich mich bei meiner **Familie**, die sich mit mir gefreut, mit mir gelitten und aufgeatmet hat, bedanken. Danke für eure Geduld und eurer stets offenes Ohr. Schließlich hätte ich diese Dissertation nicht ohne die Unterstützung meiner Freunde fertigstellen können, die sowohl für anregende Diskussionen als auch für fröhliche Ablenkungen gesorgt haben. Vielen Dank an: Daniel, Julia, Julka, Mareike, Nico, Sarah, Luca, Madita, Magda, Julien, Dennis, Johanna, Kevin, Paula, Kathrin, Domi, Alex, und Lana.

Und ein ganz besonderer Dank gilt dir, lieber **Matthias**, für dein immerwährendes Verständnis, deine uneingeschränkte Unterstützung und deine schier endlose Geduld mit mir!